

**$^{40}\text{Ar}/^{39}\text{Ar}$ GEOCHRONOLOGY AND VOLCANIC EVOLUTION OF
THE TAOS PLATEAU VOLCANIC FIELD, NORTHERN NEW
MEXICO AND SOUTHERN COLORADO**

by
Robert M. Appelt

Submitted in Partial Fulfillment of the Requirements
for the Degree of Master of Science in Geochemistry
January, 1998

Department of Earth and Environmental Science
New Mexico Institute of Mining and Technology
Socorro, New Mexico

ACKNOWLEDGMENTS

Although my name is alone on the title page, it would not have been possible to complete it without help from numerous others. First, thanks go to New Mexico Bureau of Mines and Mineral Resources who provided funding, facilities, and vehicles which allowed for the broad scope of this project. Next is the New Mexico Geochronological Research Laboratory and staff who put up with my seemingly endless parade of samples. Then there are Dave Ennis, Sheila Hutchinson, Doug Jones, John Hall, Joe Stroud, Tim Pease, and Dan Miggins-who for the promise of food and a few microbrews endured my driving and assisted greatly in my field work. Also a special thanks to the ranchers of the Taos Plateau area, especially Tony Benson, without their permission and help there would have been no samples to collect. I would also like to thank Richard Chamberlin, Neila Dunbar, Matt Heizler, Thom Wilch, and Kurt Panter for their help in answering a wide range of questions. Thanks also to the members of my committee, Chuck Chapin and Phil Kyle, for their time and guidance. The final and most important thanks I have though is for Bill McIntosh, for six years of his time, patience, energy, guidance, and support without which none of this would have been possible. Thanks Bill.

TABLE OF CONTENTS

ACKNOWLEDGMENTS	i
TABLE OF CONTENTS	ii
LIST OF TABLES	iv
LIST OF FIGURES	v
ABSTRACT	vi
INTRODUCTION	1
GEOLOGIC SETTING	4
Regional Overview	4
Taos Plateau Volcanic Field	9
FIELD AND ANALYTICAL METHODS	15
RESULTS	19
Single-Crystal Total-Fusion Analyses	19
Furnace Step-Heating Analyses	20
Summary of Results	31
ERUPTIVE HISTORY	34
Servilleta Basalt	34
Pyroxene Dacites	38
Olivine Andesites	40
Basaltic Andesites	41
Other Lavas	42

Summary of Temporal and Spatial Trends in TPVF Volcanic Activity	43
Implications for Geochemical Modeling	46
Controls on Temporal and Spatial Trends in the TPVF	47
CONCLUSIONS	50
REFERENCES	52

APPENDICES

APPENDIX A	A-1
Explanation of Appendix A	A-1
$^{40}\text{Ar}/^{39}\text{Ar}$ analytical data	A-3
APPENDIX B	B-1
Explanation of Probability Distribution Plots	B-1
Probability Distribution Plots	B-3
Explanation of Age Spectra and Isochron Plots	B-7
Age Spectra and Isochron Plots	B-11

LIST OF TABLES

TABLE 1.	Summary of $^{40}\text{Ar}/^{39}\text{Ar}$ ages for Taos Plateau volcanic field, including location, composition, and confidence level.	21
TABLE 2.	Overview of criteria used to assign confidence levels to ages in this study.	25
TABLE A.	Irradiation information for samples.	A-2
TABLE B1.	Summary table of $^{40}\text{Ar}/^{39}\text{Ar}$ results for single-crystal laser analyses from No Agua volcanic center.	B-2
TABLE B2.	Summary table of $^{40}\text{Ar}/^{39}\text{Ar}$ results for step-heated samples, including total gas, plateau, isochron, and edited isochron ages.	B-8

LIST OF FIGURES

FIGURE 1.	Map showing location of study area, locations of other 10 m.y. and younger volcanic fields, and as selected geologic features.	5
FIGURE 2.	Distribution of volcanic lithologies and vents in the Taos Plateau volcanic field, sample locations and $^{40}\text{Ar}/^{39}\text{Ar}$ ages.	10
FIGURE 3.	Example spectra displaying variations used to determine quality and confidence of spectra for $^{40}\text{Ar}/^{39}\text{Ar}$ ages.	27
FIGURE 4.	Plot of K-Ar ages from previous studies versus $^{40}\text{Ar}/^{39}\text{Ar}$ ages for selected vents in the TPVF.	32
FIGURE 5.	Plot showing the distribution of Servilleta Basalt ages through time, including approximate age ranges for eruption of the Lower, Middle, and Upper members of the Servilleta Basalt as determined from sections collected in the Rio Grande gorge.	37
FIGURE 6.	Plot showing distribution of eruptive activity TPVF in time versus the composition of the erupted material.	39
FIGURE 7.	Map showing spatial distribution of ages for the TPVF lavas.	45

ABSTRACT

New $^{40}\text{Ar}/^{39}\text{Ar}$ ages provide a refined chronological framework for the Taos Plateau volcanic field (TPVF), northern New Mexico. The TPVF is the largest dominantly basaltic volcanic field erupted in relation to the reinitiation of extension in the Rio Grande rift in the middle to late Miocene. The lavas of the TPVF include the volumetrically dominant highly fluid olivine tholeiites of the Servilleta Basalt and lesser amounts of andesite, dacite, alkalic basalt, and basaltic andesite. Eighty-six $^{40}\text{Ar}/^{39}\text{Ar}$ ages were determined from 82 groundmass concentrates step-heated in a resistance furnace and 4 feldspar concentrates analyzed as single crystals with a CO₂ laser fusion.

The $^{40}\text{Ar}/^{39}\text{Ar}$ ages show that the TPVF erupted regularly from approximately 5.9-2.1 Ma, followed by a single small eruption at 1.1 Ma at the Mesita vent. Intermediate composition pyroxene dacite and olivine andesite lavas were erupted episodically from 5.4 - 2.1 Ma and 5.9 - 3.3 Ma respectively. These intermediate composition lavas include the oldest lavas to be erupted within the TPVF. The three members (lower, middle, and upper) of the Servilleta Basalt erupted from 4.8 - 2.6 Ma. The flows of the Servilleta Basalt represent the most regularly erupted lavas within the TPVF. The basaltic andesites and related alkalic basalts erupted primarily from 4.0 - 2.0, with an additional isolated eruption at 1.03 ± 0.01 Ma (Mesita vent).

The following table compiles the ages for prominent eruptive centers within the Taos Plateau volcanic field:

Eruptive Center	Age (Ma)±error (1 σ)
Cerro Montoso	5.88±0.18
Guadalupe Mtn.	5.34±0.08
Cerro Chiflo	5.32±0.08
Cerro de la Olla	4.97±0.06
Cerro de los Taoses	4.84±0.04
Cerro Negro	4.84±0.05
Tres Orejas	4.84±0.02
Los Mogotes	4.75±0.02
Cerro Mojino	4.32±0.03
No Agua Peak	4.06±0.05
Cerritos de los Cruz	3.94±0.05
Cerro del Aire	3.69±0.03
La Segita Peaks	3.53±0.09
San Antonio Mountain	3.05±0.05
Red Hill	2.91±0.01
Ute Mtn.	2.70±0.01
Pinebetoso Peaks	2.34±0.10
Mesita Vent	1.03±0.01

Eruptive activity in the TPVF generally tended to shift to the west and north with time. The 6-4 Ma volcanic rocks are exposed along the eastern boundary of the TPVF centered on the Red River gorge area. After 4 Ma the majority of the TPVF volcanism shifted to the western margin of the field in the Tres Piedras - San Antonio Mountain area. Two exceptions to this pattern are Ute Mountain and the Mesita vent which erupted after 3 Ma, but lie on the eastern margin of the TPVF, north of the 6-4 Ma lavas and eruptive centers. Two possible explanations for this shift in volcanism are migration of the zone of influx of new magma into the system with time, or, more probably, changing fault activity controlling the spatial distribution of the TPVF lavas.

INTRODUCTION

The Taos Plateau volcanic field (TPVF) is located in the southern end of the San Luis Basin of the Rio Grande rift in northern New Mexico and southernmost Colorado (Figure 1). The TPVF is largest of several, primarily basaltic volcanic fields in New Mexico associated with the reinitiation of rifting in the middle to late Miocene. The TPVF is geographically related to both the Rio Grande rift and the Jemez Lineament. The lavas of the TPVF are dominated by the tholeiitic Servilleta Basalts, but dacites, andesites, basaltic andesites, and alkalic basalts are also present in the field.

Previous geochemical studies [e.g. *Lipman and Mehnert, 1979; Zimmerman and Kudo, 1979; Dungan et al., 1984b; Dungan et al., 1986; McMillan and Dungan, 1986; McMillan and Dungan, 1993*], accompanied by limited amounts of K-Ar dating [*Ozima et al., 1967; Lipman and Mehnert, 1979; Manly, 1979; Baldridge et al., 1980*], have produced a large body of geochemical data on the lavas of the TPVF. This body of data has been used to develop a model [*Dungan et al., 1984b; Dungan et al., 1986; McMillan and Dungan, 1986; McMillan and Dungan, 1993*] for the development and eruption of the TPVF lavas over its history. This model suggests the presence of a complex plumbing system beneath the TPVF through which magma was distributed to the various eruptive centers following periodic influxes of new magma. It is believed that the Servilleta Basalt represents the parental magma in the system and that its eruptive activity conforms to the influx of new magma into the system. This has lead to the suggestion that the eruptive

history of the Servilleta Basalt can serve as a chronological basis for the eruptive history of the TPVF [Dungan *et al.*, 1984b].

The purpose of this study was to obtain more complete and precise geochronologic data from the lavas of the TPVF to provide increased resolution over the previous K-Ar studies, which are not sufficient to quantitatively model the geochemical evolution of the TPVF through time [Dungan *et al.*, 1984a]. This is in part due to the inability of the K-Ar method to provide the precision necessary to resolve the ages of the frequent eruptions within the study area. The K-Ar dating technique was also not able to address potential geochronological complications such as the presence of extraneous ^{40}Ar and possible xenocrystic contamination of the TPVF lavas [Ozima *et al.*, 1967; Lipman and Mehnert, 1979]. The $^{40}\text{Ar}/^{39}\text{Ar}$ dating with its demonstrated high precision is ideal for this type of study [e.g. Baski, 1987; Lanphere, 1988; McIntosh and Cather, 1994; Singer and Pringle, 1996; Singer *et al.*, 1997]. Additionally, the $^{40}\text{Ar}/^{39}\text{Ar}$ technique's ability to produce incremental heating age data can help to detect extraneous Ar and possible xenocrystic contamination, and in some cases, correct for them in the calculation of ages [Lanphere and Dalrymple, 1976; Fleck *et al.*, 1977 ; McDougall and Harrison, 1988].

The dates produced in this study have been used to construct a refined eruptive history for the TPVF lavas. This eruptive history illustrates the temporal relation between the production of the Servilleta Basalt and lavas of other compositions. This temporal relation, when combined with the existing geochemical data, may help to better establish the geochemical evolution of the TPVF lavas with time. These ages also illustrate the

migration of eruptive activity across the field, possibly tracking the movement of the magma source over time or indicating changing tectonic controls on volcanic activity.

GEOLOGIC SETTING

Regional Overview

The Rio Grande rift, a major intracontinental extensional structure in the North American Plate, extends from central Colorado through New Mexico and into northern Mexico and western Texas where it merges with the southern basin and range [Cordell, 1978]. The rift (Figure 1) is expressed topographically as a series of en echelon, fault-bounded basins resulting from middle and late Cenozoic extensional deformation. A well-defined series of axial grabens makes up the northern and central parts of the rift, which separates the stable platform of the Colorado Plateau from the craton of the Great Plains. The southern portion of the Rio Grande rift is the site of the earliest and greatest amount of crustal extension, becoming less distinct as it merges with the southern basin and range [Chapin, 1979; Cordell, 1982; Seager *et al.*, 1984; Perry *et al.*, 1987].

Geophysical studies of the Rio Grande rift have allowed the lithospheric structure underlying the rift to be inferred. These studies have shown that the crust of the Rio Grande rift is generally 30-35 km thick in north and 25-30 km thick in the southern half of the rift. This thickness is less than either that of the Great Plains (50 km) or the Colorado Plateau (40-45 km) [Keller *et al.*, 1979; Sinno *et al.*, 1986]. The lithospheric thickness for the Rio Grande rift region has been interpreted [Sinno *et al.*, 1986; Olsen *et al.*, 1987] as being the same as, or close to, the crustal thickness. This suggests that the asthenosphere is near to, or in direct contact with, the crust with little or no intervening

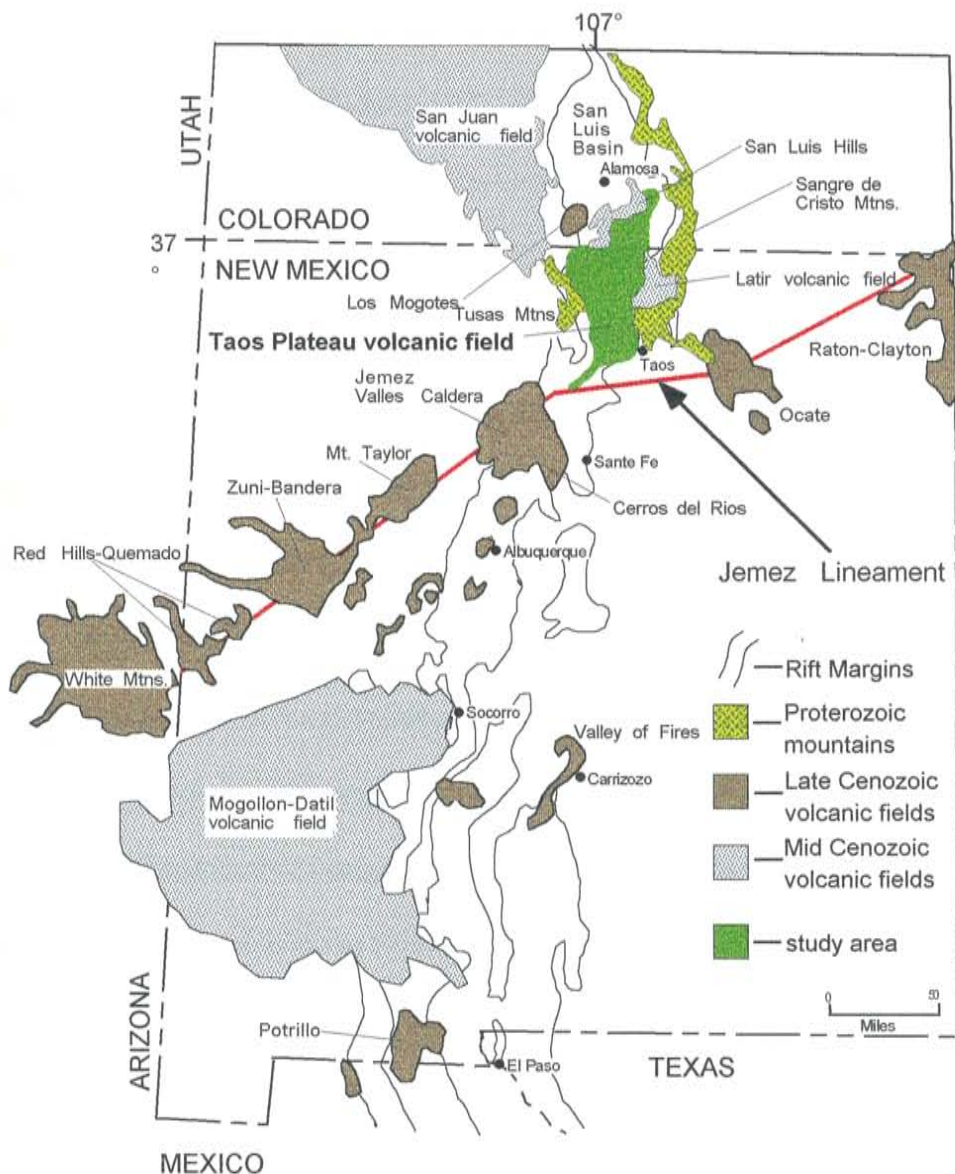


FIGURE 1. Generalized map of New Mexico showing the study area and its relation to other volcanic fields and geologic structures discussed in the text (Chapin, 1979; Gornitz, 1982; Baldridge et al., 1987; McMillan and Dungan, 1988; McIntosh et al., 1990; Thompson and McMillan, 1992).

lithospheric mantle. This indicates in anomalously high temperatures at depth in the upper mantle beneath the Rio Grande rift.

Tectonic activity associated with rifting began around 30 Ma and occurred in two major phases [*Chapin and Seager, 1975; Seager et al., 1984*]. The first was marked by a major phase of extensional deformation throughout the region. Broad basins formed bounded by low-angle faults with a pronounced NW trend. At around 20 Ma the tectonic activity associated with rifting lessened dramatically until around 16 Ma when rifting was reinitiated. This new phase of rifting was distinguished by development of N-trending, high-angle faults separating deep, narrow, asymmetric grabens [*Chapin and Seager, 1975; Seager et al., 1984; Cather et al., 1994*].

Volcanism in the region of the Rio Grande rift began as early as the Cretaceous and has continued into the Holocene. The Cretaceous magmatism consisted primarily of plutonism associated with the Laramide deformation [*Morgan and Golombek, 1984*]. The next regional phase of magmatism occurred during the Oligocene, with eruption of major silicic fields such as the Mogollon-Datil [*Chapin and Seager, 1975; Seager et al., 1984; McIntosh et al., 1990*] and the San Juan [*Lipman et al., 1970; Riciputi and Johnson, 1989*] volcanic fields. These fields are part of the Oligocene-Miocene “ignimbrite flare-up” and consist primarily of calc-alkaline compositions, and their activity continued well after the initiation of rifting [*Gornitz, 1982*]. These fields, however, are geochemically distinct [*Dungan et al., 1984b*] from the later Oligocene volcanism associated with the Rio Grande rift (Figure 1) in their lack of alkali-rich, high-

SiO_2 rhyolites such as those of the Questa caldera in the Latir volcanic field [*Johnson and Lipman, 1988; Czamanke et al., 1990*].

Volcanism directly associated with rifting occurred in two major pulses from 30-18 Ma and from around 10 Ma to the present. These two pulses are separated by a mid-Miocene lull in volcanism that coincides with the lull in tectonic activity within the rift [*Chapin and Seager, 1975; Baldridge et al., 1980; Gardner and Goff, 1984; Seager et al., 1984*]. The early 30-18 Ma pulse produced both silicic and mafic volcanism in southwestern and southern New Mexico [*Olsen et al., 1987*] and some intermediate to silicic volcanism such as the Latir volcanic field in northern New Mexico [*Johnson and Lipman, 1988; Czamanke et al., 1990*].

The majority of the volcanism associated with late stage Rio Grande rift extension is basaltic [*Olsen et al., 1987*], although the silicic Jemez and Mount Taylor volcanic fields are notable exceptions [*Luedke and Smith, 1987*]. The Mafic compositions include nephelinite, basanite, alkali olivine basalt, hawaiite, mugearite, and olivine tholeiite. Both tholeiitic and mildly alkalic lavas have been erupted within the rift axis and on its flanks, often occurring together within individual volcanic fields [*Laughlin et al., 1972, 1982; Stormer, 1972; Lipman and Mehnert, 1975, 1979; Aoki and Kudo, 1976; Baldridge, 1979; Baldridge et al., 1987*]. The compositions cannot be consistently correlated with the location of the field in relation to the rift structure, although the majority of alkalic compositions tend to occur in those fields on the shoulders of the rift axis [*Lipman and Mehnert, 1975; Dungan et al., 1983*]. This 16 Ma and younger volcanism is voluminous and widespread, and is temporally associated with tectonic rejuvenation of the rift.

The range of compositions in lavas of the late stage volcanic fields is believed to be the result of differing depths of generation for parental magmas beneath the rift [Perry *et al.*, 1987]. Differences in the geochemical signatures of the parental magmas indicates different sources of the melts within the underlying mantle, as well as varying amounts of crustal contamination or assimilation. It has been proposed that these correlations, both geochemical and spatial, were the result of progressive thinning of the crust and associated upwelling of the asthenosphere. This progressive upwelling resulted in changing temperatures at the depths the melts were generated, which in turn affected compositions of the erupted lavas within the volcanic fields [Perry *et al.*, 1987].

The distribution of volcanism is not controlled completely by the structure of the rift, but also by the Jemez lineament. The Jemez lineament (Figure 1) is an approximately 700 km long northeast trending zone of late Cenozoic volcanic fields extending from the San Carlos volcanic field of Arizona to the Rayton-Clayton volcanic field of northeastern New Mexico and onto the Great Plains [Laughlin *et al.*, 1976; Smith and Luedke, 1984]. The western part of the Jemez lineament broadly corresponds with the boundary that separates the extended and thinned lithosphere to the southeast, including the rift, from the core of the Colorado Plateau to the north [Baldridge and Olsen, 1989]. Structural studies in the Sangre de Cristo and Picuris mountains indicate that the lineament can be linked to a zone of Precambrian structural weakness [Nielson *et al.*, 1983].

Taos Plateau Volcanic Field

The Taos Plateau volcanic field (TPVF, Figure 1 and Figure 2) is located in the southern end of the San Luis Basin of the Rio Grande rift in northern New Mexico and southern Colorado. The TPVF is one of the largest and most compositionally diverse volcanic fields associated with late-stage Rio Grande rift extension during the last 16 m.y. [Thompson and McMillan, 1992]. The TPVF was defined initially by *Lipman and Mehnert* (1975, 1979) as a distinct volcanic feature within New Mexico. Previously, the lavas of the TPVF had been classified as the volcanic members of the Servilleta Formation by *Butler* (1946). The lavas of the TPVF cover approximately 15,000 km² of the San Luis Basin, an asymmetric, actively subsiding basin [Dungan et al., 1984; Thompson and McMillan, 1992]. The basin is bounded to the east by a major fault system against the Sangre de Cristo Mountains, and to the west by the Tusas Mountains which consist of Precambrian metamorphic rocks overlain by eastward-tilted early-and pre-rift volcanic and sedimentary units [Lipman and Mehnert, 1979; Dungan et al., 1984a; McMillan and Dungan, 1988].

Exposures of volcanic units that predate the eruption of the TPVF lavas are present within the TPVF. These older units were erupted prior to and during the initial phases of extension and are not directly related to the TPVF lavas [Thompson and McMillan, 1992]. They are dominated by 26 - 22 Ma calc-alkaline lavas and pyroclastic flows associated with the nearby Latir volcanic field. These outcrops are exposed within

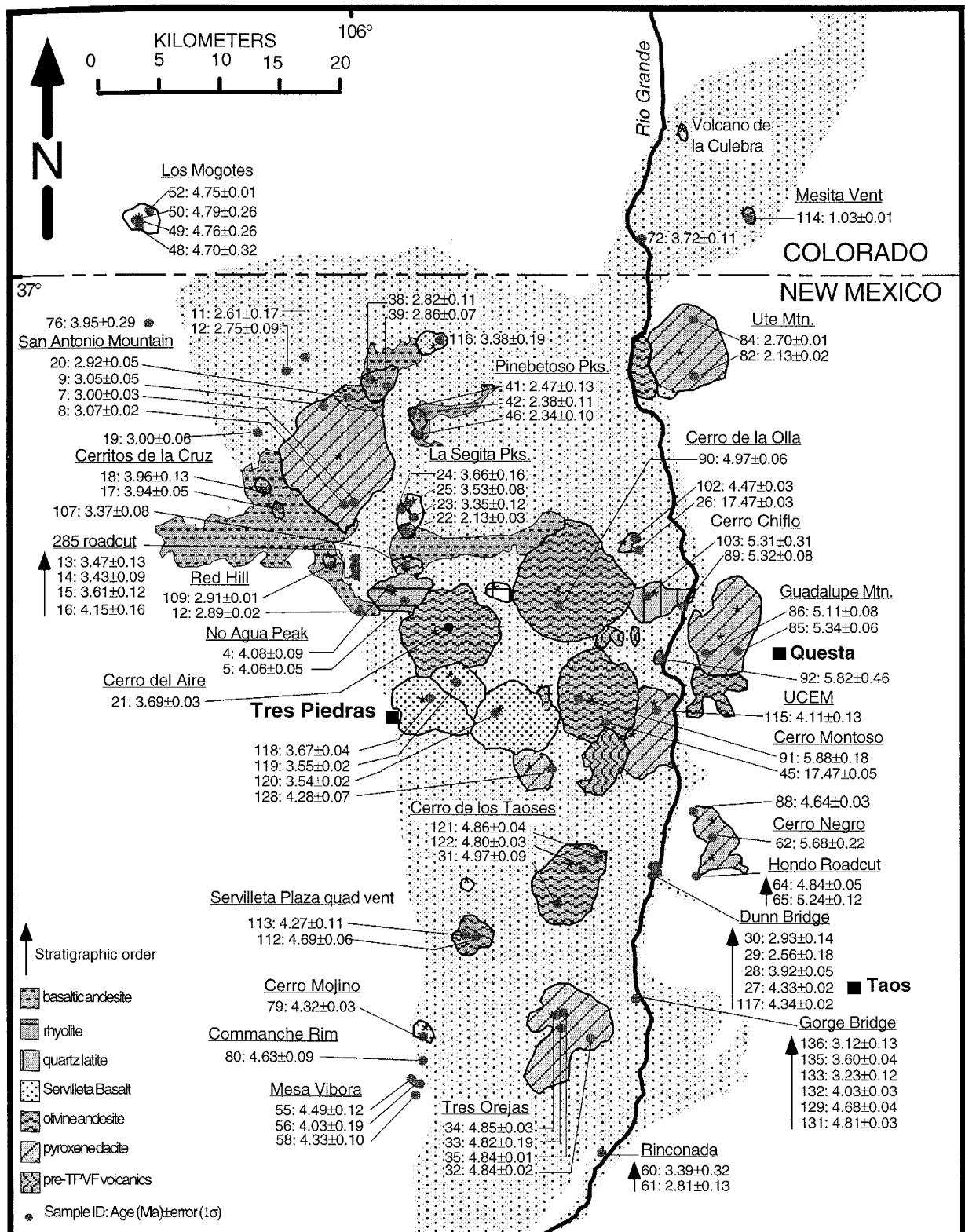


FIGURE 2. Distribution of vents and lithologies within the Taos Plateau volcanic field from Lipman and Mehnert (1979). Sample locations and ages are given for samples from this study.

the TPVF on intra-rift horsts at Brushy and Timber mountains (Figure 2) [Thompson *et al.*, 1986]. The time span from 20-10 Ma was marked by a mid-Miocene lull in both volcanic and tectonic activity in the northern Rio Grande rift. The few volcanic units erupted during this period include minor intrusions and lavas exposed on the flanks of the rifts from the nearby Tusas and Sangre de Cristo Mountains [Thompson and McMillan, 1992].

Plio-Pleistocene volcanic rocks within TPVF are volumetrically dominated by three lithologies, the tholeiitic Servilleta Basalts ($>200 \text{ km}^3$), pyroxene dacites (31 km^3), and olivine andesite (26 km^3) [Ozima *et al.*, 1967; Lipman and Mehnert, 1979; Thompson and McMillan, 1992]. Smaller amounts of silicic alkalic basalts, xenocrystic basaltic andesite, and rhyolite are also present [McMillan and Dungan, 1988]. Previous K-Ar studies of TPVF [Ozima *et al.*, 1967; Lipman and Mehnert, 1979; Baldridge *et al.*, 1980] have suggested that the field was active from 4.5 to 1.8 Ma and that the majority of the basaltic volcanism in the TPVF occurred during three major episodes that produced the three members (Upper, Middle, and Lower) of the Servilleta Basalt [Dungan *et al.*, 1984b; Dungan *et al.*, 1986] from 4.5 to 3.0 Ma [Ozima *et al.*, 1967; Lipman and Mehnert, 1979; Baldridge *et al.*, 1980].

The three pulses of Servilleta Basalt activity are defined by the eruptions of three major chemical varieties of basalts, the primitive LSKI (Low Silica, K_2O , Incompatible trace elements; Dungan *et al.*, 1986) basalts, more evolved tholeiitic basalts, and the San Cristobal lavas [Dungan *et al.*, 1984b; Dungan *et al.*, 1986; Thompson and McMillan, 1992]. The first of these, the LSKI are the most primitive compositions erupted in the

TPVF. The second type, the tholeiitic basalts, are slightly higher in SiO₂ and incompatible trace elements than the LSKI basalts. The San Cristobal lavas have the highest concentrations of incompatible trace elements, SiO₂, and K₂O of all the Servilleta Basalt compositions. The San Cristobal lavas have been modeled as mixtures between more typical Servilleta Basalts and magmas compositionally similar to the pyroxene dacites and olivine andesites of the TPVF [Dungan *et al.*, 1986; Thompson and McMillan, 1992]. The lower Servilleta Basalt consists of lava flows spanning compositions from LSKI to tholeiitic. The oldest lavas of the lower Servilleta Basalt are mostly LSKI in composition and become more tholeiitic with time. The middle Servilleta Basalt includes a few small flows of the LSKI and tholeiitic compositions, but is dominated by massive flows of the San Cristobal lavas. The upper Servilleta Basalts are similar to the lower Servilleta Basalts in compositional diversity.

Intermediate composition lavas (pyroxene dacites and olivine andesites) were also being erupted during the same interval as Servilleta Basalt activity. Stratigraphic relationships from the Red River and Rio Grande gorges [McMillan and Dungan, 1986] show that the eruption of intermediate lavas was contemporaneous with emplacement of the three members of the Servilleta Basalt. According to Lipman and Mehnert (1979) these intermediate lavas became more prevalent toward the end of each subsequent pulse of Servilleta activity, and continued on until 1.8 Ma, after the Servilleta basaltic activity ceased around 3.0 Ma. Minor amounts of silicic alkalic basalts and xenocrystic basaltic andesites were also erupted during the last stages of Servilleta activity and later as well. Two additional lava compositions erupted were the rhyolite of No Agua (3.9 Ma, K-Ar

by *Lipman and Mehnert*, 1979) and the quartz latite of Cerro Chiflo (5.32 Ma, this study). These two centers appear as isolated occurrences, with no similar lavas found elsewhere in the TPVF [*Thompson and McMillan*, 1992].

A crude, concentrically zoned distribution to the vents of the TPVF (Figure 2) was described by *Lipman and Mehnert* (1979). In this zoned pattern the basalt cones of the TPVF were erupted in a group of low shields along the western margin of the field, andesitic lava centers form a partial ring around the basalt vents, and the dacitic shields are located on the margins of the field. The largest of these dacitic shields (San Antonio, Ute, and Guadalupe Mountains) developed on older shields of olivine andesites. *Lipman and Mehnert* (1979) suggested that this distribution of vents, combined with existing dates and geochemical data, indicated a close genetic relationship among the TPVF lavas. *Lipman and Mehnert* (1979) suggested that the source of the TPVF lavas was an area of higher temperatures in the upper mantle underlying the TPVF that experienced partial melting, resulting in the formation of basaltic magmas. The more silicic magmas represent fractional crystallization of magmas that resided in chambers and also assimilated crustal material over time.

The contemporaneous production of varied TPVF lavas, the pattern of the vents, and the demonstrated mixing of parental LSKI basalt and dacite [*McMillan and Dungan*, 1986] are interpreted as indicating that the magmas of the TPVF evolved in a unified or interconnected magmatic system. Geochemical studies [*Lipman and Mehnert*, 1979; *Dungan et al.*, 1986; *McMillan and Dungan*, 1986] have shown the dacites erupted early in the history of the field do not significantly differ in geochemical or mineral

composition from those erupted late in the history of the TPVF activity. Also, the parental LSKI Servilleta basalts were erupted during all three basaltic pulses, which indicates that similar petrogenetic processes were active throughout the lifetime of the magmatic system. Thus *Dungan et al.* (1986) and *McMillan and Dungan* (1986) suggested that a complex system of interconnected magma chambers existed under the TPVF. This system received periodic recharge from the upper mantle, and crystal fractionation, assimilation of crustal material, and mixing within these chambers is responsible for the variation seen in the compositions of the TPVF lavas [*Thompson and McMillan*, 1992]. They also suggested that the distribution of the vents on the surface is related to clustering of chambers, and that the marginal vents that erupted silicic lavas were more isolated from the mafic magma source than the basaltic centers clustered in the center of the TPVF.

FIELD AND ANALYTICAL METHODS

A total of ninety-three samples for $^{40}\text{Ar}/^{39}\text{Ar}$ age analysis were collected from unweathered interiors of lava outcrops of the Taos Plateau volcanic field. Seventy-four samples were collected from eruptive centers, and nineteen samples were collected from lava flows not physically associated with locatable eruptive centers. These samples were collected to allow the inclusion of lavas erupted from sources that have been buried by younger lavas. Twelve of these samples were collected from flows of the Servilleta Basalt in four locations in the Rio Grande Gorge: near its northern end at Old State Bridge, Dunn Bridge at Arroyo Hondo, 1.6 miles south of the Rio Grande Gorge Bridge, and near the southern edge of the gorge at Rinconada.

$^{40}\text{Ar}/^{39}\text{Ar}$ age determinations were made on 89 groundmass concentrates and 4 feldspar mineral separates. Sample preparation began with crushing and then sieving to obtain material of the desired size. The groundmass concentrates were sized to one of three ranges: 850 to 500, 425 to 300, or 300 to 250 μm . The smaller sizes were used for samples with small phenocrysts or potential contamination from xenocrystic material. The feldspar concentrates were sized to the 425 to 300 μm range.

Both feldspar and groundmass concentrates were passed through a Frantz magnetic separator to remove any strongly magnetic material, and to remove noncrystalline material in the case of the feldspar separates. Next the samples were ultrasonically cleaned in a solution of 10% hydrochloric acid (groundmass) or 15% hydrofluoric acid (feldspar) and then rinsed in deionized water. The washing removed

any carbonate and clays that may have been present in the samples, as well as removing any glass or groundmass from the feldspars. After washing, the groundmass concentrates were evaluated under a binocular microscope and hand-picked to remove phenocrystic or xenocrystic material. Once washed, feldspar separates were processed in lithium metatungstate solutions to remove phases of unwanted densities, and finally hand-picked and inspected under a microscope.

Completed separates were packaged in aluminum disks and sealed into glass vials with Fish Canyon Tuff feldspar (FC-1, 27.84 Ma [*Deino and Potts, 1990*] relative to Mmhb-1 at 520.4 Ma [*Samson and Alexander, 1987*]) as a monitor of neutron flux (J-values), along with potassium and calcium salts for measuring interfering nuclear reactions produced during irradiation. Samples were irradiated at the research reactor facility at Texas A&M in four separate irradiations (Table A).

All ^{40}Ar / ^{39}Ar analyses were performed in the New Mexico Geochronological Research Laboratory at New Mexico Institute of Mining and Technology in Socorro, New Mexico. Isotopic ratios were measured by a Mass Analyzer Products (MAP) 215-50 mass spectrometer utilizing an electron multiplier with an effective gain of approximately 10,000, giving a net sensitivity approximately 2×10^{-17} moles/pA. The mass spectrometer was connected to a two-stage all-metal vacuum extraction line with two options for heating samples: a CO₂ laser and a Ta double vacuum resistance furnace capable of reaching 1750°C. The first stage of the extraction line contained a SAES AP-10 getter (later changed to a SAES GP-50) and the second stage a SAES GP-50 getter to remove reactive, non-noble gases from the sample gases.

Sample analysis was carried out using one of the two sample heating options based on the material being analyzed. The CO₂ laser was used to fuse single crystals of feldspar. The gas produced was passed through the second stage only and exposed to the SAE GP-50 getter for 3 minutes before being expanded into the mass spectrometer. The resistance furnace was used to heat 100 to 50 mg groundmass concentrate samples. Heating schedules for these samples consisted 9 to 15 steps and from 600 to 1750°C. The gas was held within the first stage getter for 6 minutes then expanded into the second stage and exposed to its getter for 5 minutes before being introduced into the mass spectrometer. Data for analysis was corrected for the extraction line blank. The ⁴⁰Ar, ³⁹Ar, ³⁸Ar, ³⁷Ar, and ³⁶Ar blanks for furnace analyses averaged 839.1, 4.1, 0.9, 1.9, 3.9 x 10⁻¹⁸ moles. The ⁴⁰Ar, ³⁹Ar, ³⁸Ar, ³⁷Ar, and ³⁶Ar blanks for laser analyses averaged 118.2, 2.6, 0.5, 1.9, 1.6 x 10⁻¹⁸ moles.

Irradiation parameters were calculated using the FC-1 monitor loaded in the aluminum disks with the samples. Six single crystals of the FC-1 monitor were taken from each monitor position and fused individually in the CO₂ laser to determine the J-values for each irradiation. These values were averaged, yielding standard deviations in J-value per monitor location typically less than ±0.25% (1σ). The J-values were calculated for each sample position around the circumference of the irradiation disk and applied to the appropriate samples during analysis.

All ⁴⁰Ar/³⁹Ar ages were determined using the decay constants recommended by *Steiger and Jager* (1977). Uncertainties in ages are reported at the 1σ level and include errors in J-values, isotope measurements, correction factors and background. All data is

shown in complete detail in Appendix A and as spectra and isochrons (step-heating) or probability distribution diagrams (laser) in Appendix B. Age spectra and ideograms are accompanied by plots of K/Ca (a function of measured $^{37}\text{Ar}/^{39}\text{Ar}$) and radiogenic yield (the percent of measured ^{40}Ar that cannot be attributed to trapped argon of atmospheric compositions, assumed $^{40}\text{Ar}/^{36}\text{Ar}=295.5$).

RESULTS

Single-Crystal Total-Fusion Analyses

Four feldspar separates from the No Agua Peaks rhyolite were analyzed by single-crystal total-fusion of twenty-five grains from each sample in the CO₂ laser extraction system (Appendix A). Probability distribution diagrams with auxiliary plots of K/Ca and radiogenic yield (Appendix B) were plotted to help evaluate the ages of individual analyses for a given sample. Analyses that varied significantly from the mean age and/or had anomalous K/Ca or radiogenic yield values were eliminated from the data set. Weighted mean ages were then calculated from the edited data set by weighting the individual analyses by the inverse of their variance [Samson and Alexander, 1987].

The main criteria used to eliminate analyses from the data set was radiogenic yield. Analyses with radiogenic yields greater than 100% or less than 60% were eliminated. Anomalously high yields were likely the result of inaccurate blank measurement and subsequent correction for atmospheric ⁴⁰Ar in the sample, causing the percent of radiogenic ⁴⁰Ar to be overestimated. Low yields resulted from samples that had low signal to blank ratios (low total gas yields) and high associated errors. K/Ca ratios for the overall data set of single-crystal analyses averaged approximately 0.27, with a few values as high as 9. The lower K/Ca values indicate that the samples consisted mostly of plagioclase, with rare sanidine or other high-potassium phases being present. The majority of the crystals with higher K/Ca ratios were eliminated because they often had low gas yields or problematic radiogenic yields (<60% or >100%).

Weighted mean ages for single-crystal total-fusion samples (Table 1) ranged from 3.51 - 4.22 Ma with 1σ errors from ± 0.05 - 0.14 Ma. The ages of two samples (RA-004 and RA-005) were within 1σ of each other, the remaining two samples (RA-001 and RA-003) have large errors and mean ages that differ by more than 1σ in age from the other two samples and each other. Ages for samples RA-004 and RA-005 are assigned moderate confidence levels and believed to be representative of eruption ages, whereas the ages for RA-001 and RA-003 were assigned low confidence levels and excluded from further discussion.

Furnace Step-Heating Analyses

Results for the eighty-nine samples (Appendix B) analyzed by step-heating in the resistance furnace were first plotted as spectra accompanied by auxiliary plots of radiogenic yield and K/Ca ratios. The spectra were then examined to see if they met the criteria for plateau selection. Plateaus in spectra were defined as three or more contiguous steps, totaling more than 50% of the ^{39}Ar released, that agreed within analytical error at the 95% confidence level (*Fleck et al.*, 1977). Plateau ages for the 61 samples that met plateau criteria were calculated by weighting of the steps in the plateau by the inverse of their variance. Next, preferred ages were calculated for fifteen of the remaining spectra by using steps that differed by slightly more than 2σ or that totaled somewhat less than 50% of the ^{39}Ar released. Preferred ages were calculated from the inverse-variance-weighted average of the selected heating steps. The remaining thirteen samples yielded highly disturbed spectra for which no plateau or preferred ages could be calculated.

TABLE 1. Summary table of $^{40}\text{Ar}/^{39}\text{Ar}$ ages (errors quoted at 1σ) for the Taos Plateau volcanic field. Table includes samples location, composition, type of age, and confidence level of the age.

Sample	Location	Composition	Age	Confidence	Age Type	Material	Latitude	Longitude
RA-001	No Agua Peaks	perlite	4.22±0.14*	low	mean	feldspar	36° 44' 26"	105° 57' 00"
RA-003	No Agua Peaks	perlite	3.51±0.12*	low	mean	feldspar	36° 45' 12"	105° 56' 26"
RA-004	No Agua Peaks	perlite	4.08±0.09*	moderate	mean	feldspar	36° 45' 12"	105° 56' 26"
RA-005	No Agua Peaks	perlite	4.06±0.05*	moderate	mean	feldspar	36° 45' 30"	105° 56' 54"
RA-007	San Antonio Mountain	pyroxene dacite	3.00±0.03	high	preferred	groundmass	36° 49' 45"	106° 00' 48"
RA-008	San Antonio Mountain	pyroxene dacite	3.07±0.02	high	edited iso.	groundmass	36° 49' 46"	106° 00' 56"
RA-009	San Antonio Mountain	pyroxene dacite	3.05±0.05	high	preferred	groundmass	36° 53' 19"	106° 01' 20"
RA-010	San Antonio Mountain area	Servilleta Basalt	2.75±0.09	moderate	edited iso.	groundmass	36° 53' 55"	106° 02' 47"
RA-011	San Antonio Mountain area	Servilleta Basalt	2.61±0.17	low	isochron	groundmass	36° 54' 42"	106° 02' 34"
RA-012	No Agua roadcut	basaltic andesite	2.89±0.02	high	plateau	groundmass	36° 44' 57"	105° 58' 51"
RA-013	285 roadcut	Servilleta Basalt	3.47±0.13	high	isochron	groundmass	36° 46' 06"	105° 58' 53"
RA-014	285 roadcut	Servilleta Basalt	3.43±0.09	high	isochron	groundmass	36° 46' 07"	105° 58' 53"
RA-015	285 roadcut	Servilleta Basalt	3.61±0.12	low	plateau	groundmass	36° 46' 09"	105° 58' 53"
RA-016	285 roadcut	Servilleta Basalt	4.15±0.16	low	edited iso.	groundmass	36° 46' 10"	105° 58' 53"
RA-017	Cerritos de la Cruz	basaltic andesite	3.94±0.05	high	preferred	groundmass	36° 49' 23"	106° 04' 03"
RA-018	Cerritos de la Cruz	basaltic andesite	3.96±0.13	low	plateau	groundmass	36° 49' 51"	106° 04' 35"
RA-019	San Antonio Mountain area	Servilleta Basalt	3.00±0.06	high	edited iso.	groundmass	36° 51' 25"	106° 04' 20"
RA-020	San Antonio Mountain	andesite	2.92±0.05	high	plateau	groundmass	36° 53' 16"	106° 00' 29"
RA-021	Cerro del Aire	olivine andesite	3.69±0.03	high	plateau	groundmass	36° 43' 19"	105° 54' 48"
RA-022	La Segita Peaks	basaltic andesite	2.13±0.03	high	preferred	groundmass	36° 48' 04"	105° 57' 06"
RA-023	La Segita Peaks	Servilleta Basalt	3.35±0.12	low	plateau	groundmass	36° 48' 42"	105° 57' 08"
RA-024	La Segita Peaks	Servilleta Basalt	3.66±0.16	low	plateau	groundmass	36° 48' 51"	105° 57' 22"
RA-025	La Segita Peaks	Servilleta Basalt	3.53±0.08	low	plateau	groundmass	36° 49' 01"	105° 57' 20"
RA-026	Cerro de la Olla area	basaltic andesite	17.47±0.03	high	edited iso.	groundmass	36° 47' 06"	105° 44' 09"
RA-027	Dunn Bridge section	Servilleta Basalt	4.33±0.02	high	plateau	groundmass	36° 32' 07"	105° 42' 32"
RA-028	Dunn Bridge section	Servilleta Basalt	3.92±0.05	high	plateau	groundmass	36° 32' 00"	105° 42' 38"
RA-029	Dunn Bridge section	Servilleta Basalt	2.56±0.18	low	isochron	groundmass	36° 32' 06"	105° 42' 38"
RA-030	Dunn Bridge section	Servilleta Basalt	2.93±0.14	moderate	edited iso.	groundmass	36° 32' 43"	105° 42' 28"
RA-031	Cerro de los Taoses	olivine andesite	4.97±0.09	high	plateau	groundmass	36° 30' 34"	105° 48' 01"
RA-032	Tres Orejas	pyroxene dacite	4.84±0.02	high	plateau	groundmass	36° 25' 10"	105° 46' 39"
RA-033	Tres Orejas	pyroxene dacite	4.82±0.19	low	plateau	groundmass	36° 24' 43"	105° 48' 30"

Sample	Location	Composition	Age	Confidence	Age Type	Material	Latitude	Longitude
RA-034	Tres Orejas	pyroxene dacite	4.85±0.03	high	preferred	groundmass	36°25'08"	105°48'42"
RA-035	Tres Orejas	pyroxene dacite	4.84±0.01	high	preferred	groundmass	36°25'04"	105°48'38"
RA-038	San Antonio Mountain	basaltic andesite	2.82±0.11	moderate	edited iso.	groundmass	36°54'05"	105°59'13"
RA-039	San Antonio Mountain	basaltic andesite	2.86±0.07	moderate	plateau	groundmass	36°54'11"	105°59'25"
RA-041	Pinebetoso Peaks	basaltic andesite	2.47±0.13	low	edited iso.	groundmass	36°53'25"	105°56'23"
RA-042	Pinebetoso Peaks	basaltic andesite	2.38±0.11	low	preferred	groundmass	36°53'23"	105°56'19"
RA-045	Cerro Montosa	basaltic andesite	17.47±0.05	high	edited iso.	groundmass	36°38'45"	105°45'24"
RA-046	Pinebetoso Peaks	basaltic andesite	2.34±0.10	moderate	edited iso.	groundmass	36°53'13"	105°56'11"
RA-047	Los Mogotes	tholeiitic basalt	none	none	N/A	groundmass	37°04'39"	106°10'15"
RA-048	Los Mogotes	tholeiitic basalt	4.70±0.32	low	edited iso.	groundmass	37°04'39"	106°10'14"
RA-049	Los Mogotes	tholeiitic basalt	4.76±0.26	low	isochron	groundmass	37°04'33"	106°10'14"
RA-050	Los Mogotes	tholeiitic basalt	4.79±0.26	low	isochron	groundmass	37°04'26"	106°10'10"
RA-051	Los Mogotes	tholeiitic basalt	none	none	N/A	groundmass	37°04'52"	106°10'23"
RA-052	Los Mogotes	tholeiitic basalt	4.75±0.01	high	plateau	groundmass	37°04'50"	106°09'55"
RA-055	Mesa Vibora	basalt	4.49±0.12	low	plateau	groundmass	36°18'43"	105°59'33"
RA-056	Mesa Vibora	basalt	4.03±0.19	moderate	edited iso.	groundmass	36°18'45"	105°59'33"
RA-058	Mesa Vibora	basalt	4.33±0.10	low	plateau	groundmass	36°18'18"	105°59'30"
RA-060	Rinconada	Servilleta Basalt	3.39±0.32	low	isochron	groundmass	36°14'47"	105°51'00"
RA-061	Rinconada	Servilleta Basalt	2.81±0.13	moderate	isochron	groundmass	36°14'48"	105°51'01"
RA-062	Cerro Negro	pyroxene dacite	5.68±0.22	low	plateau	groundmass	36°34'02"	105°38'41"
RA-064	Hondo roadcut	pyroxene dacite	4.84±0.05	high	preferred	groundmass	36°32'56"	105°38'41"
RA-065	Hondo roadcut	pyroxene dacite	5.24±0.12	low	plateau	groundmass	36°32'56"	105°40'15"
RA-072	northern Rio Grande gorge	Servilleta Basalt	3.72±0.11	moderate	edited iso.	groundmass	37°03'55"	105°46'06"
RA-076	Bighorn Peak area	tholeiitic basalt	3.95±0.29	moderate	edited iso.	groundmass	36°57'55"	106°07'45"
RA-079	Cerro Mojino	Servilleta Basalt	4.32±0.03	high	preferred	groundmass	36°55'16"	105°24'06"
RA-080	Comanche Rim	Servilleta Basalt	4.63±0.09	high	isochron	groundmass	36°20'45"	105°53'53"
RA-082	Ute Mountain	pyroxene dacite	2.13±0.02	high	edited iso.	groundmass	36°54'43"	105°40'02"
RA-083	Ute Mountain	olivine andesite	none	none	N/A	groundmass	36°56'45"	105°42'15"
RA-084	Ute Mountain	pyroxene dacite	2.70±0.01	high	plateau	groundmass	36°57'55"	105°39'57"
RA-085	Guadalupe Mountain	pyroxene dacite	5.34±0.06	high	plateau	groundmass	36°41'47"	105°38'17"
RA-086	Guadalupe Mountain	pyroxene dacite	5.11±0.08	high	N/A	groundmass	36°41'39"	105°39'27"
RA-087	Guadalupe Mountain	pyroxene dacite	none	none	edited iso.	groundmass	36°42'51"	105°40'00"
RA-088	Cerro Negro roadcut	pyroxene dacite	4.77±0.03	high	quartz latite	groundmass	36°35'04"	105°39'43"
RA-089	Cerro Chiflo	quartz latite	5.32±0.08	high	preferred	groundmass	36°44'33"	105°41'01"

Sample	Location	Composition	Age	Confidence	Age Type	Material	Latitude	Longitude
RA-090	Cerro del Olla	olivine andesite	4.97±0.06	high	plateau	groundmass	36° 44' 11"	105° 47' 38"
RA-091	Cerro Montoso	olivine andesite	5.88±0.18	low	plateau	groundmass	36° 40' 14"	105° 47' 03"
RA-092	Cerro Montoso area	pyroxene dacite	5.82±0.46	low	edited iso.	groundmass	36° 40' 16"	105° 49' 32"
RA-093	Cerro Montoso area	pyroxene dacite	none	none	N/A	groundmass	36° 40' 16"	105° 49' 32"
RA-102	Cerro del Olla area	pyroxene dacite	4.47±0.03	high	edited iso.	groundmass	36° 47' 34"	105° 44' 28"
RA-103	Cerro Chiflo	quartz latite	5.31±0.31	moderate	preferred	groundmass	36° 44' 53"	105° 43' 37"
RA-104	Cerro Chiflo	quartz latite	none	none	N/A	groundmass	36° 44' 17"	105° 42' 51"
RA-107	No Agua Peaks area	olivine andesite	3.37±0.08	moderate	edited iso.	groundmass	36° 46' 06"	105° 56' 45"
RA-109	Red Hill	basaltic andesite	2.91±0.01	high	isochron	groundmass	36° 46' 31"	106° 00' 57"
RA-112	Servilleta Plaza quad vent	pyroxene dacite	4.69±0.06	high	plateau	groundmass	36° 29' 01"	105° 53' 30"
RA-113	Servilleta Plaza quad vent	pyroxene dacite	4.27±0.11	moderate	edited iso.	groundmass	36° 29' 10"	105° 53' 52"
RA-114	Mesita vent	basaltic andesite	1.03±0.01	high	plateau	groundmass	37° 06' 20"	105° 38' 03"
RA-115	UCEM	pyroxene dacite	4.11±0.13	moderate	plateau	groundmass	36° 39' 55"	105° 42' 37"
RA-116	NE of San Antonio Mountain	Servilleta Basalt	3.38±0.19	moderate	edited iso.	groundmass	36° 56' 55"	105° 54' 48"
RA-117	Dunn Bridge section	Servilleta Basalt	4.34±0.02	high	plateau	groundmass	36° 32' 03"	105° 42' 25"
RA-118	Cerro del Aire area	Servilleta Basalt	3.67±0.04	high	edited iso.	groundmass	36° 40' 06"	105° 54' 49"
RA-119	Cerro del Aire area	Servilleta Basalt	3.55±0.02	high	plateau	groundmass	36° 41' 04"	105° 53' 58"
RA-120	Cerro del Aire area	Servilleta Basalt	3.54±0.02	high	plateau	groundmass	36° 31' 11"	105° 53' 13"
RA-121	Cerro de los Taoses	olivine andesite	4.86±0.04	high	plateau	groundmass	36° 31' 11"	105° 46' 42"
RA-122	Cerro de los Taoses	olivine andesite	4.80±0.03	high	plateau	groundmass	36° 32' 13"	105° 47' 04"
RA-123	Cerro de los Taoses	olivine andesite	none	none	N/A	groundmass	36° 32' 07"	105° 47' 23"
RA-128	San Cristobal Ranch	pyroxene dacite	4.28±0.07	high	isochron	groundmass	36° 36' 42"	105° 48' 33"
RA-129	Gorge Bridge section	Servilleta Basalt	4.68±0.04	high	plateau	groundmass	36° 27' 10"	105° 43' 40"
RA-131	Gorge Bridge section	Servilleta Basalt	4.81±0.03	high	plateau	groundmass	36° 27' 10"	105° 43' 42"
RA-132	Gorge Bridge section	Servilleta Basalt	4.03±0.03	high	plateau	groundmass	36° 27' 10"	105° 43' 44"
RA-133	Gorge Bridge section	Servilleta Basalt	3.23±0.12	low	plateau	groundmass	36° 27' 10"	105° 43' 44"
RA-135	Gorge Bridge section	Servilleta Basalt	3.60±0.04	high	edited iso.	groundmass	36° 27' 10"	105° 43' 46"
RA-136	Gorge Bridge section	Servilleta Basalt	3.12±0.13	moderate	edited iso.	groundmass	36° 27' 10"	105° 43' 48"

* Denotes samples analyzed by laser fusion, all others analyzed by furnace step-heating.

Inverse isochrons were also plotted for all the samples analyzed by step-heating, and accompany the appropriate spectra in Appendix B. Inverse isochrons are plots of the $^{36}\text{Ar}/^{40}\text{Ar}$ versus the $^{39}\text{Ar}/^{40}\text{Ar}$ ratios of a sample and offer an alternative means to calculate ages from the step-heating data, as well evaluating whether the trapped argon component has a atmospheric composition ($^{40}\text{Ar}/^{36}\text{Ar}=295.5$), an assumption implicit in the age spectrum plot. The isochron ages (Table-B, Appendix B) are assigned errors at the $\pm 1\sigma$ level and are accompanied by values for MSWD and $^{40}\text{Ar}/^{36}\text{Ar}$ intercept. MSWD or mean standard weighted deviation is a measure of the closeness of fit of the individual data points to a linear regression line. An MSWD cut-off of 10 was selected as the minimum acceptable level for the data sets to compensate for possible under estimation of error in correction factors. This is seen in the relatively small associated error ellipses for the individual data points resulting in artificially high MSWDs to apparent linear data sets. Initial $^{40}\text{Ar}/^{36}\text{Ar}$ intercepts values for many of the spectra were greater than 300. After editing the data by removing steps that appeared to have high associated errors due to low gas yield or other complicating factors, the average $^{40}\text{Ar}/^{36}\text{Ar}$ intercept more closely approach the atmospheric value of 295.5. MSWD values in the initial plots ranged from around 600 to 1, with the majority falling between 20 and 1. After editing, MSWD values tended to decrease, dropping the average range to approximately 10 to less than 1.

Eruption ages (Table 1) for the step-heated samples were assigned one of four confidence levels (high, moderate, low, and none) as indicators of their accuracy and precision. The confidence levels were assigned on the basis of several properties of the spectra and isochrons for each sample(Table 2). These factors include agreement between

TABLE 2. General factors used in the evaluation and assignment of confidence levels to ages in this study. Note that criteria are general and not all had to be met by a sample to be assigned a particular confidence levels. In some cases samples fit criteria of more than one group and were assigned to confidence level with which they shared the most similarities.

Properties	High	Moderate	Low	None
Spectra	generally flat, minor disturbances at low and high temperatures	slightly disturbed, but generally flat, disturbances at low and high temperatures	saddle shapes seen, increases or decreases slightly from low to high temperature	highly disturbed, or noticeably saddle shaped
plateau or preferred age	yes	yes in most cases	not always	seldom, often to disturbed spectra and isochron ages
relation of spectra age to isochron age	spectra age agrees with isochron age within 1 sigma	spectra ages agrees with isochron age within 1 sigma	spectra and isochron ages agree within 2 sigma	spectra and isochron ages agree at greater then 2 sigma
relation of isochron age to edited isochron age	agree at 1 sigma	agree within 2 sigma	agree within 2 sigma	agree at greater then 2 sigma
errors on individual heating steps	low average error per heating step	moderate average error per heating step	moderate to high average error per heating step	high average error per heating step
K/CA ratio	fairly constant	some minor variation	increases or decreases noticeably	disturbed
% Radiogenic yield	high (>60%)	moderate (>30%)	low (>15%)	extremely low (<15%)
MSWDs	<10	<10	<15	>15

spectra and isochron ages, behavior of radiogenic yields and K/Ca ratios, relative errors of the steps used in calculating plateau and preferred ages for spectra, error on the final ages, $^{40}\text{Ar}/^{36}\text{Ar}$ intercept, and MSWD values. The cited confidence levels are used in this study as a tool for weighting the relative worth of a particular eruption age in the creation of a more detailed eruptive history for the TPVF.

Forty-eight of the eighty-nine step-heated sample ages were assigned a high confidence level (Figure 3A-E). Greater than 90% of these samples had both spectrum (plateau or preferred) and isochron ages that agreed within 2σ of each other. All had uniformly high radiogenic yields (>60%) and relatively constant K/Ca ratios. Samples that yielded preferred ages in some cases had K/Ca ratios that decreased by an order of magnitude from their lowest to highest temperature heating step. Most of the ages had associated errors that were $\pm 2\text{-}5\%$ at the 1σ level. Two samples that were assigned high confidence levels failed to yield plateau or preferred ages, but did yield isochron ages that had acceptable MSWDs (<10) and errors from 2-5% at the 1σ level. These samples on average had $^{40}\text{Ar}/^{36}\text{Ar}$ ratios that indicated a high trapped component (>295.5), uniformly distributed throughout the sample. The remaining high confidence level samples had MSWD values averaging less than 10, with $^{40}\text{Ar}/^{36}\text{Ar}$ ratios that were within 2σ of the atmospheric value of 295.5.

Fourteen of the eighty-nine step-heated sample ages were assigned a confidence level of moderate (Figure 3F-G). These samples had spectra that showed higher average errors than the high confidence samples, typically around 10% at the 1σ level. The radiogenic yields for these samples were also not as high, typically ranging from 10-40%

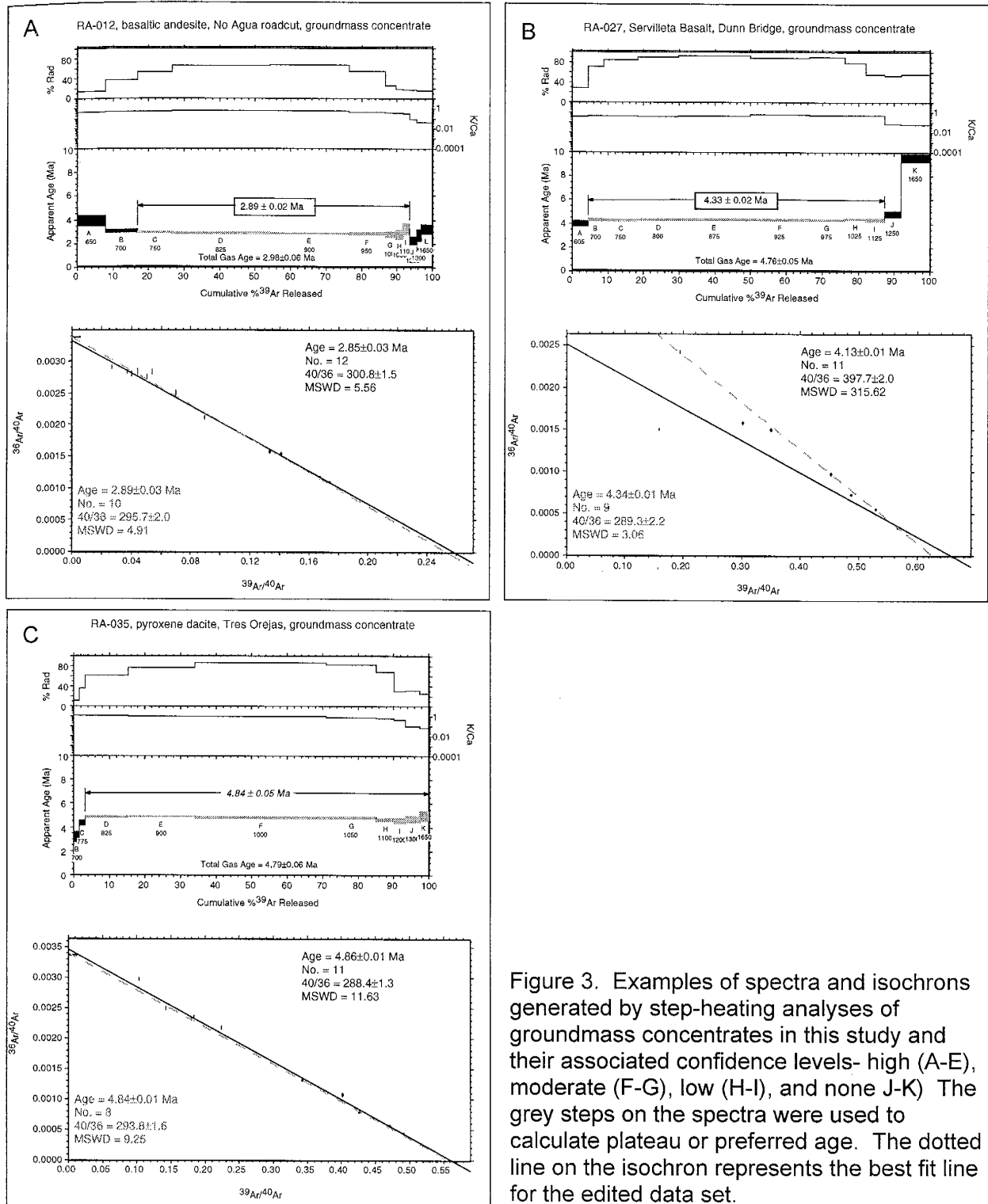
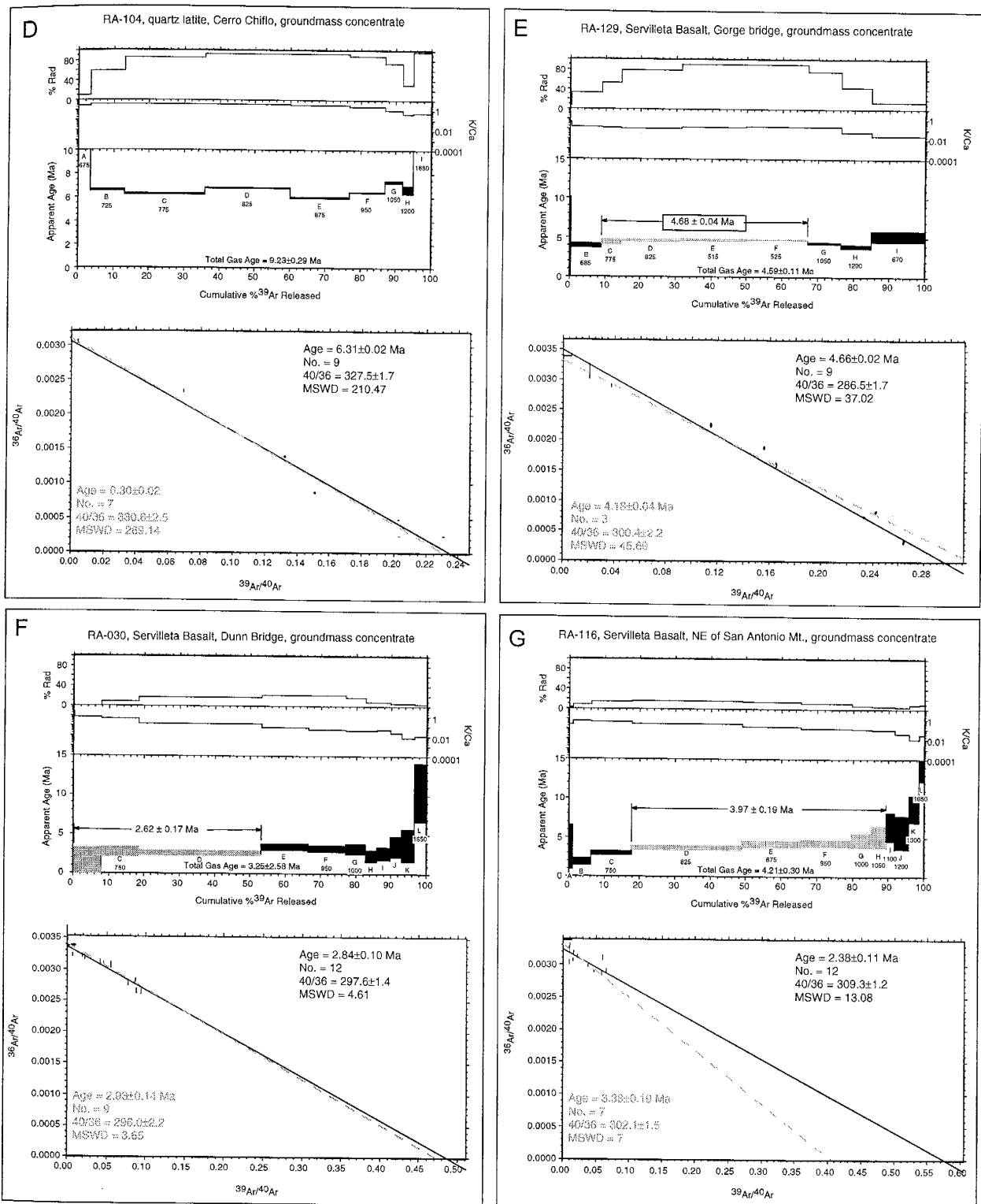
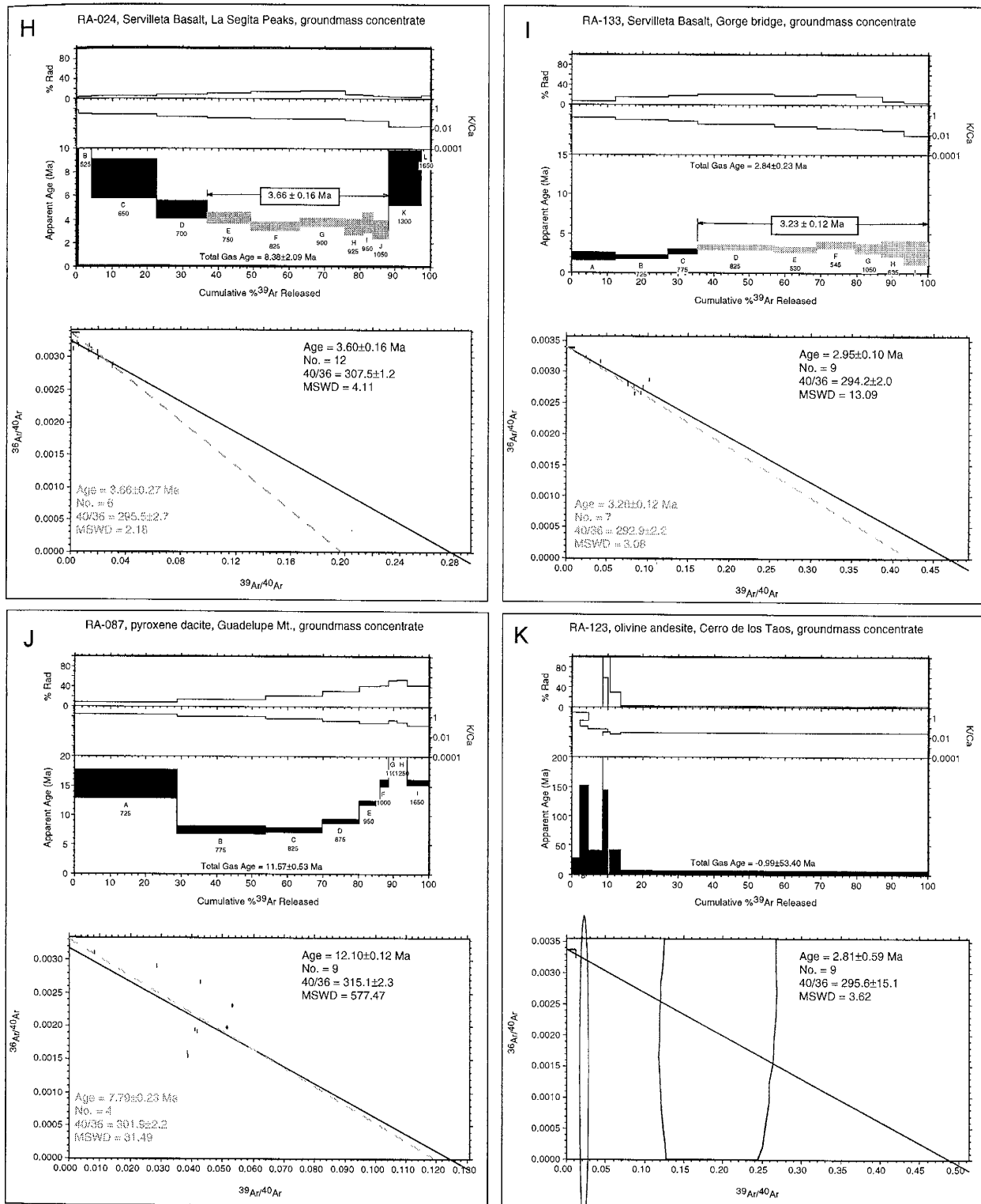


Figure 3. Examples of spectra and isochrons generated by step-heating analyses of groundmass concentrates in this study and their associated confidence levels- high (A-E), moderate (F-G), low (H-I), and none J-K) The grey steps on the spectra were used to calculate plateau or preferred age. The dotted line on the isochron represents the best fit line for the edited data set.





overall. The final MSWD values for these samples were closer to the cutoff value of 10 than those of the high confidence level. The $^{40}\text{Ar}/^{36}\text{Ar}$ intercept ratios were also higher, typically ranging from 300-320 after editing. The spectra and isochron ages were generally within 2σ of each other. The eruptive ages, except for two, are isochron or edited isochron ages, because the $^{40}\text{Ar}/^{36}\text{Ar}$ intercept values indicated that the assumption of a trapped atmospheric component of $^{40}\text{Ar}/^{36}\text{Ar} = 295.5$ implicit in the construction of the age spectrum was incorrect.

Twenty of the remaining sample ages were assigned a low confidence level (Figure 3H-I). These samples typically had low radiogenic yields (<15%) and analytical errors of 10-15% at the 1σ level. The plateau or preferred ages and isochron ages were generally not within 2σ of each other. The MSWDs of these samples were close to or higher than the cut-off value of 10 even after editing. The $^{40}\text{Ar}/^{36}\text{Ar}$ intercepts generally ranged from 300-330 after editing. The plateau or preferred ages were chosen as the eruptive age if the isochron ages agreed within 2σ . The uniformly low radiogenic yield caused the points to form tight clusters on the gas isochron plots. Because of this clustering due to low radiogenic yield and large analytical errors, ages and $^{40}\text{Ar}/^{36}\text{Ar}$ values for these samples are strongly affected by any editing of the data sets.

The remaining seven sample ages were assigned a confidence level of none (Figure 3J-K). These samples did not yield a plateau or preferred age and had isochron ages with associated errors greater $\pm 20\%$. The MSWD values for these samples were generally greater than 30-40 even after editing. The $^{40}\text{Ar}/^{36}\text{Ar}$ intercepts for these samples varied from 295 to 327. Radiogenic yields for these samples were typically

around 10%, but in some cases as low as 5%. The low radiogenic yields of these samples may reflect alteration of interstitial glass. The high MSWD and varying $^{40}\text{Ar}/^{36}\text{Ar}$ intercepts may indicate that these samples contain variable trapped components that are not homogeneously distributed in the sample.

Summary of Results

A total of ninety-three samples (See Figure 2) were analyzed, 4 feldspar separates by single crystal laser fusion and furnace step-heating of 89 groundmass concentrates, producing 86 acceptable $^{40}\text{Ar}/^{39}\text{Ar}$ ages for the Taos Plateau volcanic field. Ages were calculated using weighted means for samples analyzed by single-crystal total-fusion, and from isochron plots and age spectra of the step-heated samples. These ages range from 17.54 to 1.03 Ma, primarily falling between 5.88 and 2.10 Ma. Errors at the 1σ level for these samples range from ± 0.01 to ± 0.46 Ma, but most are less than ± 0.15 Ma. A complete summary of ages is given in Tables 1.

A comparison of ages produced by previous K-Ar studies (Figure 4) shows that the $^{40}\text{Ar}/^{39}\text{Ar}$ ages for this study tend to be older, and show considerably less error at the 1σ level. The ages from the two techniques however fall on the 1:1 line at the 1σ level, except for Cerro de la Olla, Guadalupe Mountain, San Antonio Mountain and Cerro Chiflo. The ages for Guadalupe and San Antonio Mountains lie close enough to the 1:1 line to allow them to be grouped with the other samples. The age for Cerro Chiflo is significantly younger than the previous K-Ar and most likely is the result of better correction for extraneous argon that may have been present in the sample that the K-Ar

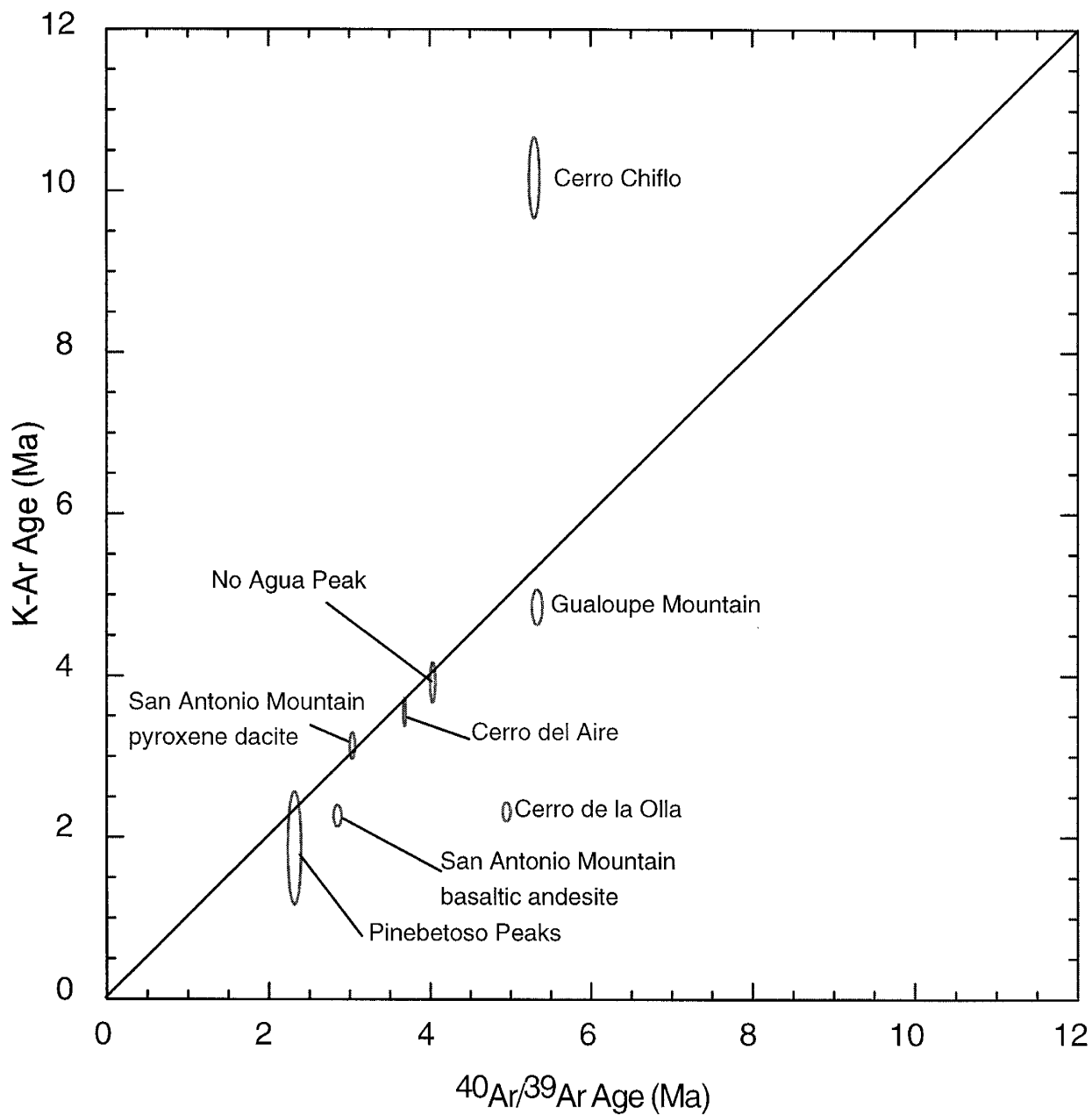


FIGURE 4. Comparison of selected $^{40}\text{Ar}/^{39}\text{Ar}$ ages versus K-Ar ages from previous studies (*Lipman and Mehnert, 1979*). Ellipses depict range of ages with error, diagonal line is 1:1 ratio.

technique was unable to compensate for in its age calculation. The significantly older age for Cerro de la Olla, however, is not due to the same factor. If it was the K-Ar would be older, not younger as is the case. It is possible that some analytical correction made in the $^{40}\text{Ar}/^{39}\text{Ar}$ technique either allowed a better estimation of the age, or else artificially increased the ^{40}Ar radiogenic used to calculate the sample age in the sample. It is also possible that this may also be affecting the ages for San Antonio and Guadalupe Mountains.

ERUPTIVE HISTORY

Servilleta Basalt

Lavas of the Servilleta Basalt are volumetrically dominant erupted in the TPVF and cover the largest portions of the study area. Previous workers [*Ozima et al.*, 1967; *Lipman and Mehnert*, 1979; *Dungan et al.*, 1984b] based the bulk of their interpretations of the eruptive history of the Servilleta Basalt upon the thick sections of flows exposed within the Rio Grande gorge. Early K-Ar dates from the Dunn Bridge area by *Ozima et al.* (1967) indicated an eruptive age range for Servilleta Basalt of approximately 4.5 - 3.6 Ma. Geochemical analysis of the flows of the Servilleta Basalt by *Lipman and Mehnert* (1979) and later by *Dungan et al.* (1984b) showed that the lower, middle, and upper members of the Servilleta Basalt were erupted in three distinct geochemical pulses. All the known vents of the Servilleta Basalt and the volumetric majority of its flows, however, occur outside the immediate vicinity of the Rio Grande Gorge and are generally ignored in most discussions of the eruptive history of the Servilleta Basalt. One goal of this study is to expand the record of eruptive history of the Servilleta Basalt to include these vents and lavas, and not restrict it to samples collected from within the gorge as in previous studies.

Stratigraphically distributed samples from the Rio Grande Gorge were collected at four locations and correlated with the sections described by *Dungan et al.* (1984b). The four locations sampled were at the northern end of the gorge near the Old State Bridge in Colorado, the Dunn Bridge at Arroyo Hondo, 1.6 miles south of the Rio Grande Gorge

Bridge, and west of Rinconada at the southern end of the gorge. The sample collected from the Old State Bridge produced an age of 3.72 ± 0.11 Ma. Four samples were collected from flows along the road from Dunn Bridge to the western rim of the gorge. One of these samples (RA-029) did not yield a usable age. The remaining three samples had ages of 4.33 ± 0.02 (base of the gorge-middle Servilleta), 3.92 ± 0.05 (approximately half way between the rim and base-middle Servilleta), and 2.93 ± 0.14 Ma (rim-upper Servilleta). Six samples were collected from the Rio Grande Gorge Bridge location from the upper and lowest flows for each member of the Servilleta Basalt at this location. The Lower Servilleta ages here were 4.81 ± 0.03 and 4.68 ± 0.04 Ma for the highest and lowest flows respectively. The middle Servilleta lava produced an age of 4.03 ± 0.03 Ma for the lowest flow at this location, the upper flow (RA-133) produced an age of 3.23 ± 0.12 Ma. This age has a low confidence level and violated stratigraphy by being younger than the overlying upper Servilleta flow; it is not considered accurate. The upper Servilleta lavas sampled produced ages of 3.60 ± 0.04 and 3.12 ± 0.13 Ma. The two samples collected near Rinconada yielded ages of 3.39 ± 0.32 and 2.81 ± 0.13 Ma. These ages show a range of activity for the Servilleta Basalt within the gorge area of approximately 4.8 - 2.8 Ma.

Samples collected from flows outside the immediate vicinity of the gorge, however, show a much narrower range of ages of approximately 3.7 - 2.6 Ma. This indicates that the majority of the exposed flows of the Servilleta basalt erupted after approximately 3.7 Ma, probably covering older vents and flows. The youngest dated Servilleta flows are in the area around San Antonio Mountain (2.61 ± 0.17 , 2.75 ± 0.09 , and 3.00 ± 0.06 Ma). A sequence of flows near No Agua Peaks have an age of 3.43 ± 0.09 Ma.

Ages for the Servilleta vents at La Segita Peaks (3.53 ± 0.09 Ma), San Antonio Mountain area (3.38 ± 0.19 Ma), and the Cerro del Aire area (3.67 ± 0.04 , 3.55 ± 0.02 , 3.54 ± 0.02 Ma) show a clustering in eruptive activity around 3.7 - 3.4 Ma. The remaining two Servilleta ages are the oldest for the Servilleta Basalt outside of the gorge. These two ages are at Comanche Rim (4.63 ± 0.09 Ma) and Cerro Mojino (4.32 ± 0.03 Ma), near the southern end of the TPVF.

The distribution of Servilleta Basalt ages indicates that the oldest exposed flows occur in the central area of the Rio Grande gorge and near the southern and eastern edges of the field. The youngest dated flows of the Servilleta Basalt, as well as all of the identified vents, are exposed along the western margin of the field in the San Antonio Mountain area. This distribution suggests that the center for eruptive activity of the Servilleta Basalt shifted to the west, away from the gorge and towards San Antonio Mountain, producing lavas that covered many of the earlier erupted flows. This apparent trend may have been aided by ponding of the earlier Servilleta basalts in the area of the present day Rio Grande gorge. The vents of the Servilleta Basalt in the western half of the field also appear to cluster not only in time, but also spatially along a linear north-south trend from the Cerro del Aire area to just northeast of San Antonio Mountain.

The ages for the Servilleta Basalt indicate a range of eruptions from approximately 4.8 - 2.6 Ma with no major hiatus in activity (Figure 5). Geochemical data from previous studies of Servilleta Basalt flows in the gorge indicate three distinct phases of lava production, interpreted as three distinct pulses of Servilleta activity. The $^{40}\text{Ar}/^{39}\text{Ar}$ ages (Figure 5) do not demonstrate any definite gaps in the eruptive history, although a

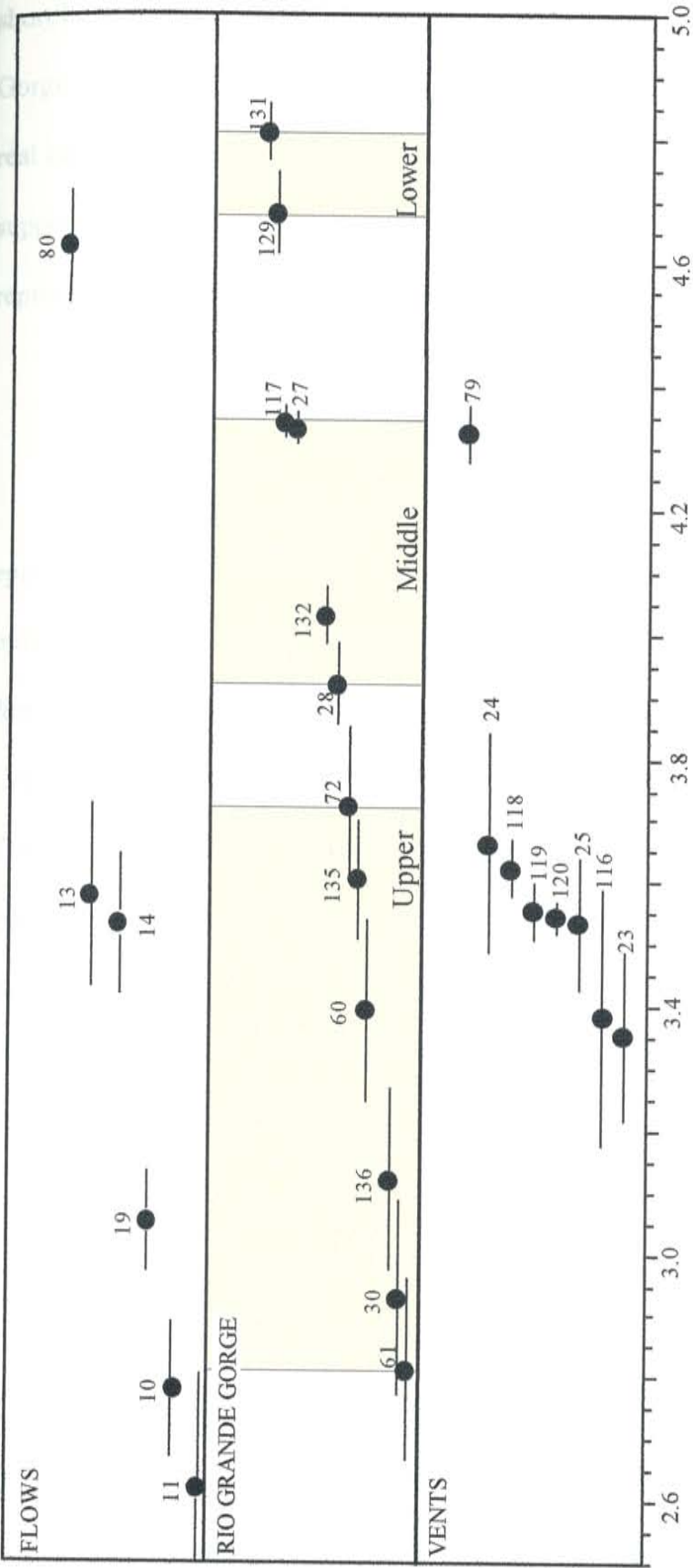


FIGURE 5. Distribution through time of Servilleta Basalt activity within the TPVF. Individual plots show age range for samples collected from flows (upper plot), sections in the Rio Grande Gorge (middle plot), and from identified vents of the Servilleta Basalt (lower plot). Ages are identified by sample number and depicted by symbol with 1-s error bars. Shaded areas on the middle plot depict approximate age ranges for the eruption of the three members of the Servilleta Basalt geochemically defined by Dungan *et al.* (1986).

short lull (0.3 m.y.) may have occurred between the lower and middle members at the Gorge Bridge section. This may simply be an artifact of the sampling however, and not a real hiatus in the eruption of Servilleta composition basalts. Thus, $^{40}\text{Ar}/^{39}\text{Ar}$ ages do not support the theory that the geochemically defined lower, middle, and upper members represent distinct temporal eruptive pulses.

Pyroxene Dacites

Ages for the eruption of pyroxene dacites lavas (Figure 6) in the TPVF show an episodic pattern, as opposed to the more regular Servilleta Basalt activity. Two distinct pulses of eruptions are seen in Figure 6, the first lasting from 5.4 - 4.1 Ma and the second from 3.0 - 2.1 Ma. The eruptions of the first pulse are concentrated along the Rio Grande Gorge in the central clustering of vents near the Red River Gorge. These vents include Tres Orejas (4.84 ± 0.02 Ma), Guadalupe Mountain (5.34 ± 0.08 Ma), UCEM (unnamed cerro east of Montosa, 4.11 ± 0.13 Ma), and Cerro Negro (4.84 ± 0.05 Ma). Additional early pyroxene dacites are found as small, low shields north of Cerro Chiflo in the Cerro de la Olla area (4.47 ± 0.03 Ma), the San Cristobal Ranch south of Cerro Montosa (4.28 ± 0.07 Ma), and in the Servilleta Plaza quad west of Tres Orejas (4.69 ± 0.06 and 4.27 ± 0.11 Ma). There appear to be no exposed pyroxene dacites lavas erupted within the TPVF from 4.1 Ma until around 3.0 Ma. The activity at 3.0 Ma is marked by the 3.0 - 2.9 Ma eruptions of lavas at San Antonio Mountain and the 2.7 and 2.1 Ma lavas of Ute Mountain.

The spatial distribution of the pyroxene dacite activity is similar to that of the Servilleta Basalts. The oldest pyroxene dacite lavas are in the vicinity of the gorge in the

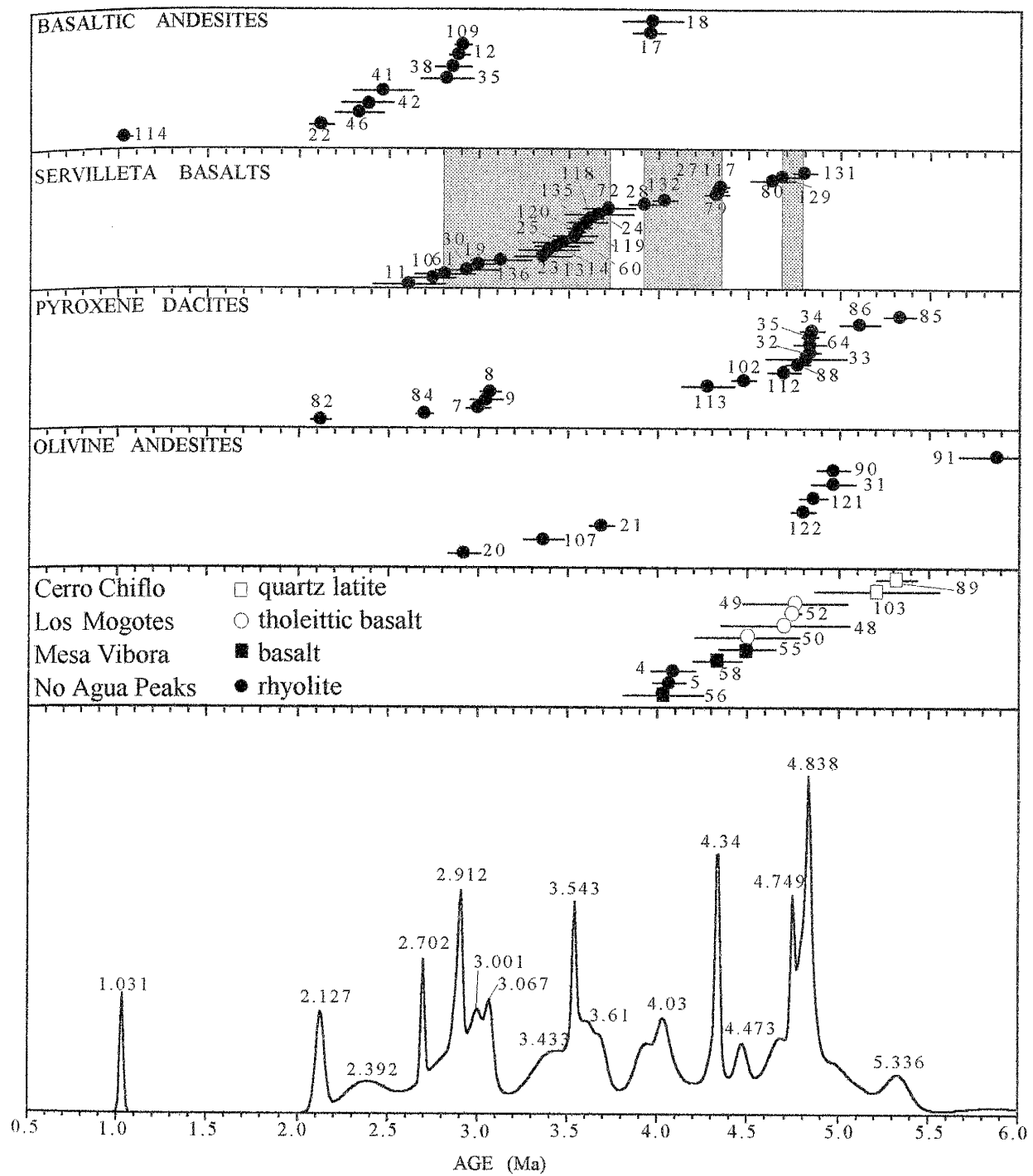


FIGURE 6. Distribution of activity versus time in the TPVF. Individual plots show age ranges for the general compositions of lavas. Other lavas is used as a catch all category for those lavas that do not fit into one of the primary compositions. Servilleta Basalt distribution includes approximate age ranges for the upper, middle, and lower members (shaded areas). Curve on lower plot represents relative level of activity in the field, height of the curve is proportional to the amount of volcanism recorded at a given time.

same area as the oldest Servilleta Basalt flows. The lavas of the younger pulse are exposed along the northwestern boundary of the field at San Antonio Mountain, as well as along the northeastern boundary at Ute Mountain. The oldest pulse of pyroxene dacite eruptions was prior to and concurrent with eruption of the lower Servilleta Basalt flows, then died out shortly after the beginning of the middle Servilleta Basalt eruptive period. The final episodes commenced near the end of upper Servilleta activity and continued until approximately 2.1 Ma, 0.4 m.y. later than the last dated Servilleta Basalt.

It is possible that the apparent distribution of ages of the pyroxene dacites is influenced by the eruption of Servilleta Basalt flows which buried earlier erupted pyroxene dacite lavas. However, sections from within the Rio Grande Gorge do not show significant interlayering of flows of intermediate composition lavas and Servilleta Basalt flows except within the Red River Gorge (*McMillan and Dungan, 1986; McMillan and Dungan, 1988*). The flows of intermediate lavas, such as the pyroxene dacites, apparently tended to form shield volcanoes, and not flow far from their sources. All of these cones appear to have had sufficient topographic relief to prevent burial by later Servilleta Basalt flows. If any pyroxene dacites erupted during the 4.2 - 3 Ma apparent hiatus, they were probably small in volume and very low in topographic relief, allowing burial by subsequent Servilleta lavas.

Olivine Andesites

The eruptive history of the olivine andesites (Figure 6) of the TPVF is also episodic, consisting of two pulses preceded by a single older event. The oldest olivine

andesite erupted is Cerro Montoso at 5.88 ± 0.18 Ma, marking the earliest eruptive activity in the TPVF. The two distinct pulses occurred from 5.0 - 4.8 Ma and 3.7 - 2.9 Ma. The first pulse consists of Cerro de los Taoses (4.84 ± 0.04 Ma) and Cerro de la Olla (4.97 ± 0.06 Ma) in the central cluster of vents near the Rio Grande Gorge. The second pulse consists of Cerro del Aire (3.69 ± 0.03 Ma), a vent just north of No Agua Peaks (3.37 ± 0.08 Ma), and an andesite on San Antonio Mountain (2.92 ± 0.05 Ma). No olivine andesite eruptions are recorded in the time between 5.8 and 5.0 Ma, between 4.8 - 3.7 Ma, or after 2.9 Ma.

The spatial distribution of olivine andesites versus their ages shows similar trends to those seen in the Servilleta Basalt and the pyroxene dacites. The oldest erupted lavas are within the clustering of vents near the Rio Grande Gorge. The youngest lavas were erupted to the northwest in the area of San Antonio Mountain and Tres Piedras. This distribution again suggests that the center of eruptive activity shifted during the eruptive history of the TPVF. The shift occurred during the 4.8 - 3.7 Ma hiatus between the two distinct pulses of olivine andesite activity. The initial olivine andesite activity predated the Servilleta Basalt. The older of the two distinct pulses occurred during the same time span as the eruption of lower Servilleta Basalt composition lavas, while the younger was coeval upper Servilleta Basalt.

Basaltic Andesites

The basaltic andesites and associated alkalic basalts of the TPVF erupted in four distinct pulses (Figure 6). The oldest basaltic andesites are those of the Cerritos de la

Cruz near San Antonio Mountain at 3.94 ± 0.05 Ma. From this point no additional basaltic andesites appear to have been erupted until around 2.9 - 2.8 at Red Hill (2.91 ± 0.01 Ma) and the northeastern flank of San Antonio Mountain (2.86 ± 0.07 and 2.82 ± 0.11 Ma). The next pulse of basaltic andesite activity occurred from 2.5 - 2.1 Ma at Pineteboso Peaks (2.47 ± 0.13 and 2.34 ± 0.10 Ma) and La Segita Peaks (2.13 ± 0.03). The final dated basaltic andesite event is the eruption of the Mesita vent (1.03 ± 0.01 Ma) which represents the youngest volcanic activity in the TPVF.

The spatial distribution of the basaltic andesites is primarily restricted to the area near San Antonio Mountain. The location of these vents agrees with the general trend of the less than 3.7 Ma lavas being erupted in the northwestern portion of the TPVF. The Mesita vent is an exception to this trend, instead being located north of Ute Mountain along the northeast margin of the TPVF. In relation to the eruption of the Servilleta Basalt, the first two pulses occurred near the end of the age ranges for the middle and upper Servilleta Basalts. The third pulse occurred after the cessation of Servilleta activity, but during the time-span of pyroxene dacite activity at Ute Mountain. The final eruption of the Mesita vent occurred almost 1 m.y. after the cessation of all other activity in the field.

Other Lava

A small number of lavas in the TPVF do not fall into one of the four major compositional categories discussed above. These lavas include the rhyolite of No Agua Peaks (4.06 ± 0.05 Ma), the quartz latite of Cerro Chiflo (5.32 ± 0.08 Ma), the tholeiitic

basalts of Los Mogotes (4.75 ± 0.02 Ma), the basalts of Mesa Vibora (4.49 ± 0.012 , 4.33 ± 0.10 , and 4.03 ± 0.19 Ma), and two older basaltic andesites (17.47 ± 0.03 Ma) exposed by faults in the Cerro de la Olla area and at Cerro Montosa. Only No Agua Peaks and Cerro Chiflo are classified as part of the TPVF by previous workers. The remaining vents have not previously been included in the TPVF because they lacked a common geochemical link with the other Plio-Pleistocene volcanic units of the area. Despite the geochemical differences, the geochronology and spatial distribution of these vents argues for their inclusion in the TPVF.

The age of Cerro Chiflo correlates with its position in the cluster of older vents in the Red River Gorge area on the eastern boundary of the TPVF. No Agua, however, is slightly older (4.1 Ma) than other lavas and vents on the western margin of the TPVF. All ages in the vicinity of No Agua are younger than 3.7 Ma with the exception of the Cerritos de la Cruz at 3.9 Ma. Geochemical data, however, indicates no strong petrogenetic link between the No Agua Peaks lavas and those of the rest of the TPVF, suggesting that while it was erupted during the time span of the TPVF, it may not be result of the same magma plumbing system that is believed to have produced the other TPVF lavas [Lipman and Mehnert, 1979].

Summary of Temporal and Spatial Trends in TPVF Volcanic Activity

The volcanic activity in the TPVF began with the eruption of Cerro Montoso at 5.9 Ma and continued with no major breaks in eruptive activity until 2.1 Ma (Figures 6 and 7). The final eruptive event occurred at 1.0 Ma at the Mesita vent after a lull of 1.1

million years. The geochronology of the TPVF indicates frequent eruptions of lavas during this time span. The olivine andesites, pyroxene dacites, and basaltic andesites display an episodic nature to their eruptions. In contrast, the Servilleta Basalt lavas display no episodic behavior, but instead have an almost uninterrupted eruptive history from 4.8 - 2.6 Ma.

The oldest lavas (5.9 -5.0 Ma) within the TPVF are the olivine andesites and pyroxene dacites clustered in the area of Cerro Chiflo along the Rio Grande Gorge. From 5 - 4 Ma the activity migrated (Figure 7) to the south and was dominated by the eruption of Servilleta Basalt and intermediate composition lavas. The activity subsequently migrated from the southern extent of the TPVF to the northwest where additional Servilleta Basalt, basaltic andesite, pyroxene dacite, and rhyolite were erupted from 4 - 2 Ma. The 2.7 and 2.1 Ma pyroxene dacites of Ute Mountain lie outside the migrational trend of the 4 -2 Ma lavas. Instead they were erupted along the northeastern margin of the TPVF, north of the clustering of older lavas around Cerro Chiflo. The final eruptive event at the Mesita vent occurred to the north of Ute Mountain at 1.1 Ma. Taken together the trends in migration of the vents of the TPVF yield a roughly spiral pattern to the age distributions.

Linear alignments are apparent in several groups of similar age vents in the TPVF. In the 6 -5 Ma lavas the linear alignment is along a west-northwest trend, paralleling trends in faults associated with the initial stages of rifting. The trends in alignment in the younger than 5 Ma lavas are north-south in orientation. Those include north-south linear alignments in the 5 - 4 Ma vents along the eastern edge of the TPVF. In the 4 - 2 Ma

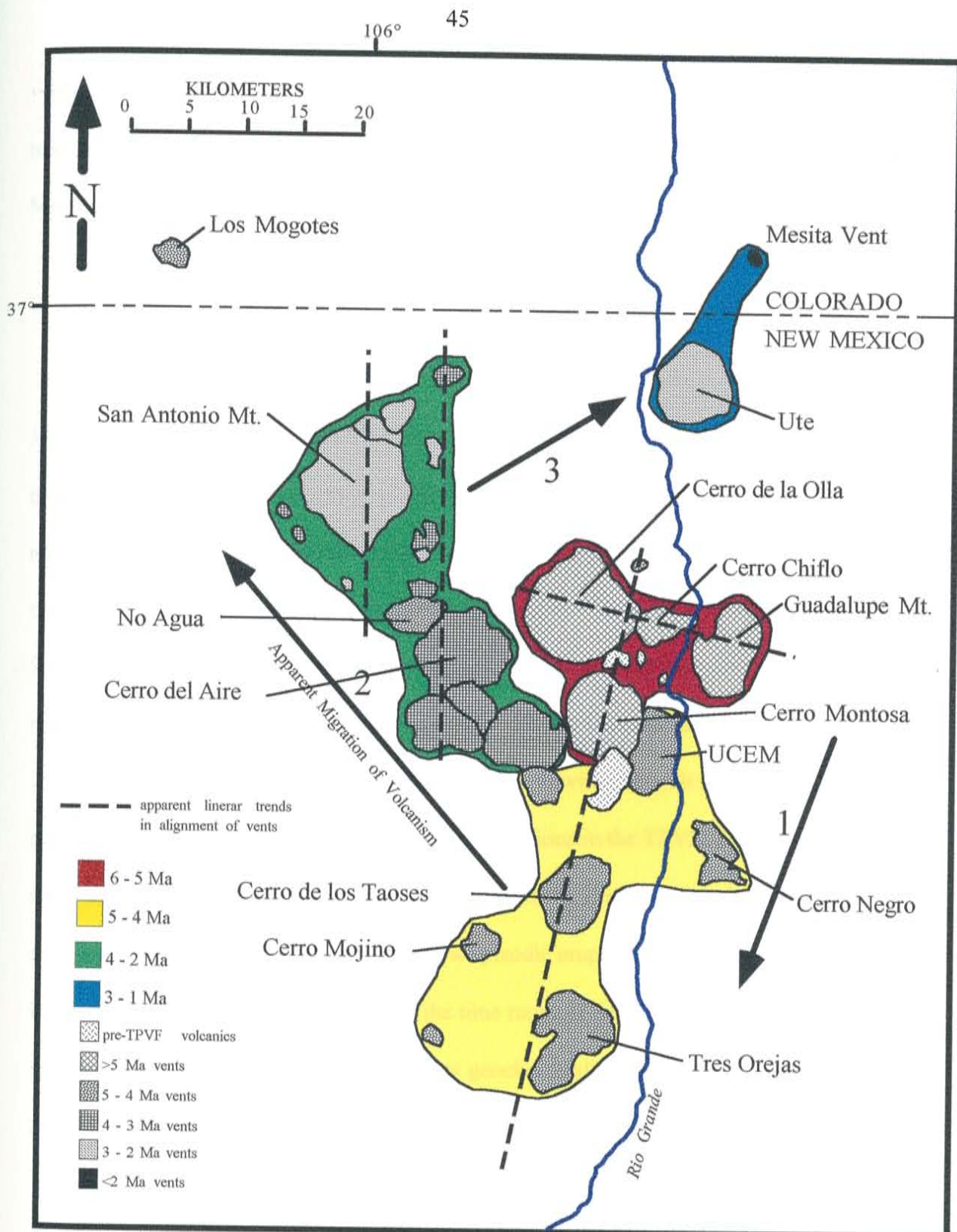


FIGURE 7. Distribution of ages of vents of the TPVF lavas illustrating trends seen in the data. Overall the distribution shows a migration (arrow) of activity towards the northwest with time as well as a linear appearing alignment (dashed lines) to vents of similar ages. Numbered arrows show generalized trends in migration for 5 - 4 Ma (1), 4 - 2 Ma (2), and 3 - 1 Ma (3).

vents, the north-south linear alignments are near San Antonio Mountain on the western margin of the field. A final north-south alignment exists between Ute Mountain and the Mesita vent on the eastern margin of the field.

Implications for Geochemical Modeling

Previous workers [*Dungan et al., 1984b; Dungan et al., 1986; Thompson and McMillan, 1992*] within the TPVF have suggested that the Servilleta Basalt represents the parental magma for the lavas of the TPVF. The intermediate composition lavas were modeled as the result of fractional crystallization of these melts and their interaction with the surrounding crustal material over time. According to this model eruptive pulses of the Servilleta Basalt would represent major influxes of magma and the intermediate lavas would tend to be erupted in the intervals between the Servilleta Basalt.

Factors other than the eruptive history of the Servilleta Basalt appear to have controlled the temporal distribution of lava compositions in the TPVF. Ages from this study show an almost continuous eruptive history for the Servilleta Basalt as opposed to an episodic one. The intermediate lavas show episodic eruptive histories producing the bulk of erupted material before and after the time range of Servilleta activity. This indicates that while the Servilleta Basalt may geochemically represent the parental magma source, its eruptive history is not an accurate guide to the history of the TPVF.

Controls on Temporal and Spatial Trends in the TPVF

Two possible explanations for the shift of volcanic activity are: migration of the magma source for the TPVF or changing tectonic controls on the eruption of TPVF lavas. Migration of the magma source for the TPVF lavas is suggested by the apparent trends (arrows on Figure 7) of the ages that decrease with distance from the older lavas clustered around Cerro Chiflo. These decreasing trends in age are most pronounced towards Tres Orejas to the south, and then to San Antonio Mountain to the northwest. These trends could be the result of a southern then northwestern migration of the heat source beneath the TPVF. One proposed model for this migration involves changing areas of influx within the complex system of magma chambers interpreted to exist under the TPVF [Dungan *et al.*, 1986; McMillan and Dungan, 1986]. According to this model, the chambers received periodic influxes of varying volumes of new magma. Variations in the amount of magma distributed to chambers in different areas of the field would have been responsible for the spatial trends in the volcanism. This would indicate that the initial influx of magma was to chambers in the east. Over time these chambers saw less influx of new magma as the chambers to the west began to receive more magma and became more active.

However, these migrational trends do not explain the ages for Ute Mountain and the Mesita vent. These two vents have ages that indicate a shift in volcanism, but one moving almost directly north from the central cluster of older vents. This migration would have had to have occurred simultaneously with the migration to the northwest. Also, the migrational model does not explain the apparent linear alignment of the vents (dashed

lines on Figure 7). The linear alignments of vents have a distinct north-south trend in the vents younger than 5 Ma. The vents older than 5 Ma have a roughly east-west trend that parallels the faults associated with the initial stages of rifting. Ages for vents along these alignments tend to be similar in age.

The second possible cause for the shifting center of eruptive activity is changing tectonic controls within the TPVF. Since the activity of the TPVF coincided with reinitiation of rifting in northern New Mexico, the distribution of volcanism could be linked to tectonic activity in the area. The linear alignment seen in the ages and distribution of the vents may reflect fault control on the distribution of vents. This is clearly seen in the east-west alignment of the 6-5 Ma TPVF vents around the horst blocks of Timber and Brushy Mountains. The 5-4 Ma vents also form linear groups that parallel the north-south fault that separates the Taos Plateau from the Sangre de Cristo Mountains and faults mapped along the Rio Grande Gorge (Figure 7). Many of the 4-2 Ma vents are aligned along north-south trends along the western margin of the field. This could indicate that tectonic activity in the area shifted from the eastern edge of the TPVF to a zone along the western area of the field and its boundary with the Tusas Mountains. Previous studies have suggested that a hinge structure may exist that dips to the east and may have been responsible for crustal weakening of the area. A final shift back to the east occurred along the faults separating the Taos Plateau from the Sangre de Cristo Mountains.

A combination of the these two models may offer a better explanation for the development of the TPVF. The complex magma plumbing system of *Dungan et al.*

(1986), may be the result of faulting in the area creating a variety of pathways for magma to reach the surface. Continued faulting could have caused pathways in some parts of the field to become more active while other pathways decreased in activity. This could explain the variable recharge of the *Dungan et al.* (1986) model, as well as the apparent migration of activity, while maintaining the linear alignments seen in the vents.

CONCLUSIONS

- The Taos Plateau volcanic field was active from approximately 5.9 - 1.0 Ma. The bulk of the eruptive activity occurred from around 5.9 - 2.1 Ma, followed by a hiatus in eruptive activity until the eruption of the Mesita vent at 1.0 Ma.
- The three members of the Servilleta Basalt (lower, middle, and upper) were erupted from approximately 4.8 - 2.6 Ma with no major gaps in the eruptive history. The age data do not define discernible temporal pulses that correlate with the geochemical divisions of the Servilleta Basalt as described by previous workers in the TPVF.
- Eruption of intermediate composition (pyroxene dacites and olivine andesites) and the more alkalic composition (basaltic andesites and associated alkalic basalts) were more episodic than the Servilleta Basalt. In many cases it appears that the bulk of the non-Servilleta Basalt lavas erupted prior to or after the major portion of Servilleta activity. This distribution relative to the Servilleta could be in part the result of burial by voluminous flows of the Servilleta Basalt.
- The locus for eruption of lavas in the TPVF has shifted from an area centered on Cerro Chiflo on the eastern margin of the TPVF south towards Tres Orejas, and finally northwestward towards San Antonio Mountain. These shift may be related to changes in the location of magma influx within the underlying plumbing system for

the TPVF described by previous workers in the area. Alternatively, part or all of the shift may be due to changing areas of faulting within the TPVF which provided pathways for magma migration to the surface.

REFERENCES

- Aoki, K. and A. M. Kudo, Major-element variations of late Cenozoic basalts of New Mexico, *Spec. Publ. N. M. Geol. Soc.*, 5, 82-88, 1976.
- Baldridge, W. S., Petrology and petrogenesis of Plio-Pleistocene basaltic rocks from the central Rio Grande rift, New Mexico and their relation to rift structure, in *Rio Grande Rift: Tectonics and Magmatism*, edited by R. E. Riecker, pp. 323-353, AGU, Washington, D. C., 1979.
- Baldridge, W. S., P. E. Damon, M. Shafiqullah, and R. J. Bridwell, Evolution of the Rio Grande rift, New Mexico: New potassium-argon ages, *Earth Planet. Sci. Lett.*, 51, 309-321, 1980.
- Baldridge, W. S., F. V. Perry, and M. Shafiqullah, Late Cenozoic volcanism of the southeastern Colorado Plateau I: Volcanic Geology of the Lucero area, New Mexico, *Geol. Soc. Am. Bull.*, 99, 463-470, 1987.
- Baldridge, W. S. and K. H. Olsen, The Rio Grande rift, *Am. Sci.*, 77, 240-247, 1989.
- Baski, A. K., Critical evaluation of the age of the Deccan Traps, India: Implications for flood-basalt volcanism and faunal extinction, *Geology*, 15, 147-150, 1987.
- Butler, A. P., Jr., Tertiary and Quaternary geology of the Tusas-Tres Piedras area, New Mexico, Ph.D. dissertation, Harvard Univ., 188 p., 1946.
- Chapin, C. E. and W. R. Seager, Evolution of the Rio Grande rift in the Socorro and Las Cruces areas, *N. M. Geol. Soc. Guideb.*, 35, 297-321, 1975.
- Chapin, C. E., Evolution of the Rio Grande rift - A summary, in *Rio Grande Rift*:

Tectonics and Magmatism, edited by R. E. Riecker, pp. 1-5, AGU,
Washington, D. C., 1979.

Chapin, C. E. and S. M. Cather, Tectonic setting of the axial basins of the northern
and central Rio Grande rift, in *Basins of the Rio Grande Rift: Structure,
Stratigraphy, and Tectonic Setting*, *Geol. Soc. Am. Spec. Paper 291*, pp. 5-25
edited by Keller, G. R. and S. M. Cather, Boulder, CO, 1994

Cordell, L., Regional geophysical setting of the Rio Grande rift, *Geol. Soc. Am. Bull.*,
89, 1073-1090, 1978.

Cordell, L., Extension in the Rio Grande rift, *J. Geophys. Res.*, 87, 8561-8569, 1982.

Czamanske, G. K., K. A. Foland, F. A. Kubacher, and J. C. Allen, The $^{40}\text{Ar}/^{39}\text{Ar}$
chronology of caldera formation, intrusive activity and Mo-ore deposition near
Questa, New Mexico, *N. M. Geol. Soc. Guideb.*, 41, 355-358, 1990.

Deino, A. and R. Potts, Single-crystal $^{40}\text{Ar}/^{39}\text{Ar}$ dating of the Olorgesailie Formation,
Southern Kenya Rift, *J. Geophys. Res.*, 95, 8453-8470, 1990.

Dungan, M. A., R. L. Nielsen, and D. Phelps, Spatial and temporal variation patterns in
late Cenozoic basaltic volcanism, NE Jemez lineament, northern New Mexico,
Geol. Soc. Am. Abstr. Programs, 15, 379, 1983.

Dungan, M. A., W. R. Muehlberger, L. Leininger, C. Peterson, N. J. McMillan, G.
Gunn, M. M. Lindstrom, and L. Haskin, Volcanic and sedimentary stratigraphy of
the Rio Grande gorge and the late Cenozoic geologic evolution of the southern
San Luis Valley, Rio Grande Rift: Northern New Mexico, *Field Conf. Guideb. N.
M. Geol. Soc.*, 35, 157-170, 1984a.

Dungan, M. A., M. M. Lindstrom, and L. A. Haskin, The petrology and geochemistry of
the Servilleta olivine tholeiites, Taos Plateau volcanic field, northern New

Mexico, in *Proceedings of the Conference on Open Magmatic Systems*, edited by M. A. Dungan, T. L. Grove, and W. Hildreth, pp. 43-45, Institute for the Study of Earth and Man, Dallas, Tex., 1984b.

Dungan, M. A., M. M. Lindstrom, N. J. McMillan, S. Moorbath, J. Hoefs, and L. A. Haskin, Open system magmatic evolution of the Taos Plateau volcanic field, northern New Mexico: 1. The petrology and geochemistry of the Servilleta Basalt, *J. Geophys. Res.*, 91, 5999-6028, 1986.

Fleck, R. J., J. F. Sutter, and D. H. Elliot, Interpretation of discordant $^{40}\text{Ar}/^{39}\text{Ar}$ age spectra of Mesozoic tholeiites from Antarctica, *Geochem. Cosmochim. Acta.*, 41, 15-32, 1977.

Gardner, J. N. and F. Goff, Potassium-argon dates from the Jemez volcanic field: Implications for tectonic activity in the north-central Rio Grande rift, *N. M. Geol. Soc. Guideb.*, 35, 75-81, 1984.

Gornitz, V., Volcanism and the tectonic development of the Rio Grande Rift and environs, New Mexico-Colorado, from analysis of petrochemical data, *The Mountain Geologist*, 19, 41-58, 1982.

Johnson, C. M. and P. W. Lipman, Origin of metaluminous and alkaline volcanic rocks of the Latir volcanic field, northern Rio Grande rift, New Mexico, *Contrib. Mineral Petrol.*, 100, 107-128, 1988.

Keller, G. R., L. W. Braile, and J. W. Schlue, Regional crustal structure of the Rio Grande rift from surface wave dispersion measurements, in *Rio Grande Rift: Tectonics and Magmatism*, edited by R. E. Riecker, pp. 115-126, AGU, Washington, D. C., 1979.

Lanphere, M. A. and G. B. Dalrymple, Identification of excess ^{40}Ar by the $^{40}\text{Ar}/^{39}\text{Ar}$ age spectrum technique, *Earth Planet. Sci. Lett.*, 32, 141-148, 1976.

Lanphere, M. A., High-resolution $^{40}\text{Ar}/^{39}\text{Ar}$ geochronology of Oligocene volcanic rocks, San Juan Mountains, Colorado, *Geochem Cosmochim Acta*, 52, 1425-1434, 1988.

Laughlin, A. W., D. G. Brookins, and J. D. Causey, Late Cenozoic basalts from the Bandera lava field, Valencia County, New Mexico, *Geol. Soc. Am. Bull.*, 83, 1543-1551, 1972.

Laughlin, A. W., D. G. Brookins, and J. D. Causey, Late Cenozoic basaltic volcanism along the Jemez zone of New Mexico and Arizona, *Geol. Soc. Am. Abstr. Programs*, 8, 598, 1976.

Laughlin, A. W., M. J. Aldrich, Jr., M. E. Ander, G. H. Heiken, D. T. Vaniman, Tectonic setting and history of late Cenozoic in west-central New Mexico, *Field Conf. Guideb. N. M. Geol. Soc.*, 33, 279-284, 1982.

Lipman, P. W. and H. H. Mehnert, Late Cenozoic basaltic volcanism and development of the Rio Grande depression the southern Rocky Mountains, *Mem. Geol. Soc. Am.*, 144, 119-154, 1975.

Lipman, P. W., T. A. Steven, and H. H. Mehnert, Volcanic history of the San Juan Mountains, Colorado, as indicated by potassium-argon dating, *Geol. Soc. Am. Bull.*, 81, 2329-2352, 1970.

Lipman, P. W. and H. H. Mehnert, The Taos Plateau volcanic field, northern Rio Grande rift, New Mexico, in *Rio Grande Rift: Tectonics and Magmatism*, edited by R. E. Riecker, pp. 289-311, AGU, Washington, D. C., 1979.

Luedke, R. G. and R. L. Smith, Map showing distributions, composition, and age of late Cenozoic volcanic centers in Arizona and New Mexico, scale 1:1,000,000, U.S. *Geol. Surv. Misc. Invest. Ser.*, Map I-1091-A, 1987.

Manley, K., The late Cenozoic history of the Espanola Basin, New Mexico, Ph.D. dissertation, University of Colorado, 171 pp., 1979.

McDougall, I. and T. M. Harrison, *Geochronology and Thermochronology by the $^{40}\text{Ar}/^{39}\text{Ar}$ Method*, Oxford University Press, New York, 1988.

McIntosh, W. C., J. F. Sutter, C. E. Chapin, and L. L. Kedzie, High-precision $^{40}\text{Ar}/^{39}\text{Ar}$ sanidine geochronology of ignimbrites in the Mogollon-Datil volcanic field, southwestern New Mexico, *Bull. Volcanol.*, 52, 584-601, 1990.

McIntosh, W. C. and S. M. Cather, $^{40}\text{Ar}/^{39}\text{Ar}$ geochronology of basaltic rocks and constraints on Late Cenozoic stratigraphy and landscape development in the Red Hill-Quemado area, New Mexico, *Field Conf. Guideb. N. M. Geol. Soc.*, 45, 209-224, 1994.

McMillan, N. J. and M. A. Dungan, Magma mixing as a petrogenetic process in the development of the Taos Plateau volcanic field, New Mexico, *J. Geophys. Res.*, 91, 6029-6045, 1986.

McMillan, N. J. and M. A. Dungan, Open system magmatic evolution of the Taos Plateau volcanic field, northern New Mexico: 3, Petrology and geochemistry of andesite and dacite, *J. Petr.*, 29, 527-557, 1988.

Morgan, P. and M. P. Golembek, Factors controlling the phases and styles of extension in the northern Rio Grande rift, *N. M. Geol. Soc. Guideb.*, 35, 13-19, 1984.

Nielsen, K. C., D. A. Bell, and M. D. Norman, Precambrian basement fabrics near the northeast-trending Jemez lineament, north-central New Mexico, *EOS*, 64, 857.

Olsen, K. H., W. S. Baldridge, and J. F. Callender, Rio Grande rift: An Overview, *Tectonophysics*, 143, 1987.

- Ozima, M., M. Kono, I. Kaneoka, H. Kinoshita, T. Nagata, E. E. Larson, and D. W. Strangway, Paleomagnetism and potassium-argon ages of some volcanic rocks from the Rio Grande gorge, New Mexico, *J. Geophys. Res.*, 72, 2615-2622, 1967.
- Perry, F. V., W. S. Baldridge, and D. J. DePaolo, Role of Athenosphere and Lithosphere in the genesis of late Cenozoic basaltic rocks from the Rio Grande rift and adjacent regions of the southwestern United States, *J. Geophys. Res.*, 92, 9193-9213, 1987.
- Riciputi, L. R. and C. M. Johnson, Relations between ash-flow magmatism and crust modification in the San Juan volcanic field, Colorado, *N. M. Bur. Mines & Min. Res., Bull.* 131, pp.223, 1989.
- Samson, S. D. and E. C. Alexander, Jr., Calibration of the interlaboratory $^{40}\text{Ar}/^{39}\text{Ar}$ dating standard, Mmhb-1, *Chem. Geol. Isot. Geoci.*, 66, 27-34, 1987.
- Seager, W. R., M. Shafiqullah, J. W. Hawley, and R. F. Marion, New K-Ar dates from basalts and the evolution of the southern Rio Grande rift, *Geol. Soc. Am. Bull.*, 95, 87-99, 1984.
- Singer, B. S. and M. S. Pringle, Age and duration of the Matuyama-Brunhes geomagnetic polarity reversal from $^{40}\text{Ar}/^{39}\text{Ar}$ incremental heating analysis of lavas, *Earth Planet. Sci. Letts.*, 139, 47-61, 1996.
- Singer, B. S., R. A. Thompson, M. A. Dungan, T. C. Freeley, S. T. Nelson, J. C. Pickens, L. L. Brown, A. W. Wulff, J. P. Davidson, and J. Metzger, Volcanism and erosion during the past 930 k.y. at the Tatara-San Pedro Complex, Chilean Andes, *Geol. Soc. Am. Bull.*, 109, 127-142, 1997.
- Sinno, Y. A., P. H. Dagget, G. R. Keller, P. Morgan, and S. H. Harder, Crustal structure of the southern Rio Grande rift determined from seismic refraction profiling,

J. Geophys. Res., 91, 6143-6156, 1986.

Smith, R. L. and R. G. Luedke, Potentially active volcanic lineaments and loci in western conterminous United States, in *Explosive Volcanism: Inception, Evolution, and Hazards*, pp. 47-66, National Academy Press, Washington, D. C., 1984.

Steiger, R. H. and E. Jager, Subcommission on geochronology: Convention on the use of decay constants in geo- and cosmochronology, *Earth and Planet. Sci. Lett.*, 36, pp. 359-362, 1977.

Stormer, J. C., Jr., Mineralogy and Petrology of the Rayton-Clayton volcanic field, northeastern New Mexico, *Geol. Soc. Am. Bull.*, 83, 3299-3322, 1972.

Taylor, J. R., *An Introduction to Error Analysis*, University Science Books, Mill Valley, California, 1982.

Thompson, R. A., M. A. Dungan, P.W. Lipman, Multiple differentiation processes in early-rift calc-alkaline volcanics, northern Rio Grande rift, New Mexico, *J. Geop. Res.*, 91, 6046-6058, 1986.

Thompson, R. A. and N. J. McMillan, A geologic overview and one-day field guide of the Taos Plateau volcanic field, Taos County, New Mexico, *U.S. Geol. Surv. Open-file Report 92-528*, 1992.

York, D., Least squares fitting of a straight line with correlated errors, *Earth Planet. Sci. Lett.*, 5, 320-324, 1969.

Zimmerman, C. and A. M. Kudo, Geochemistry of andesites and related rocks, Rio Grande rift, New Mexico, in *Rio Grande Rift: Tectonics and Magmatism*, edited by R. E. Riecker, pp. 355-381, AGU, Washington, D. C., 1979.

APPENDIX A

EXPLANATION OF APPENDIX A

Appendix A contains all of the $^{40}\text{Ar}/^{39}\text{Ar}$ analytical data for the 4 feldspar and 89 groundmass concentrates for lavas of the TPVF analyzed in this study. The information for the individual samples includes sample number, samples name, lava type, lab ID number, J-value, and irradiation ID number. The irradiation ID numbers can be correlated with the information in Table A to determine nuclear interference correction factors and mass spectrometer discriminations for individual samples. The isotopic ratios are calculated and corrected for as described in the Field and Analytical Methods section of this study. All errors are quoted at the 1σ level and propagate errors in J-value, mass discrimination, and system blank measurements. The four ages given for each sample are the total gas age, plateau or preferred age, isochron age, and edited isochron age. Also listed for these are the number of steps used to calculate them, and in the case of the isochrons MSWD and $^{40}\text{Ar}/^{36}\text{Ar}$ intercepts for the respective gas correlation diagrams. The bold faced age is the final selected age quoted in the text for a given sample.

TABLE A. Nuclear interference correction factors and mass spectrometer discrimination values listed by irradiation number and laboratory identification number.

Irradiatio n	Lab I.D. No.'s	Discrimination (1 amu)	$(^{39}\text{Ar}/^{37}\text{Ar})_{\text{Ca}}$	$(^{36}\text{Ar}/^{37}\text{Ar})_{\text{Ca}}$	$(^{38}\text{Ar}/^{39}\text{Ar})_{\text{K}}$	$(^{40}\text{Ar}/^{39}\text{Ar})_{\text{K}}$
NM34	5262 to 5279	1.00650	0.00070	0.00020	0.01190	0.00020
NM40	5704 to 5733	1.00700	0.00070	0.00020	0.01190	0.00020
NM44	6090 to 6152	1.00600	0.00070	0.00020	0.01190	0.00020
NM54	6966 to 6999	1.00820	0.00070	0.00020	0.01190	0.00020

D	$^{40}\text{Ar}/^{39}\text{Ar}$	$^{37}\text{Ar}/^{39}\text{Ar}$	$^{36}\text{Ar}/^{39}\text{Ar}$ ($\times 10^{-3}$)	$^{39}\text{Ar}_{\text{K}}$ ($\times 10^{-15}$ mol)	K/Ca	C/K ($\times 10^{-3}$)	% $^{40}\text{Ar}^*$	Age (Ma)	$\pm 1\sigma$ (Ma)
RA-001, feldspar concentrate, J=0.00084044±0.24%, Lab#=6086 (NM-44)									
No Aqua Peaks - perlite									
13	2.971	1.924	5.326	0.160	0.27	1.3	52.0	2.34	0.63
24	3.153	1.941	5.270	0.093	0.26	2.4	55.3	2.65	0.99
25	2.919	1.794	3.763	0.204	0.28	1.2	66.6	2.95	0.50
18	2.961	1.847	3.899	0.076	0.28	2.3	65.9	2.96	1.23
22	2.862	1.828	1.657	0.141	0.28	0.27	87.8	3.81	0.64
06	2.855	1.815	1.600	0.279	0.28	0.099	88.3	3.82	0.32
21	2.859	1.822	1.307	0.209	0.28	-0.160	91.4	3.96	0.49
11	3.071	1.815	1.601	0.165	0.28	0.79	89.1	4.15	0.64
10	5.013	1.932	8.176	0.200	0.26	1.8	54.8	4.16	0.54
23	2.787	1.869	0.5386	0.213	0.27	1.3	99.4	4.20	0.39
16	2.845	1.710	0.6202	0.175	0.30	1.2	98.2	4.23	0.58
12	2.983	1.818	1.078	0.132	0.28	2.2	94.0	4.25	0.81
05	7.065	1.619	14.58	0.158	0.32	0.99	40.8	4.37	0.64
01	3.211	1.907	0.8672	0.264	0.27	-0.689	96.4	4.69	0.39
17	3.206	1.921	0.5455	0.120	0.27	2.1	99.6	4.84	0.90
14	3.197	1.718	0.0990	0.135	0.30	2.9	103.2	5.00	0.77
02	4.862	1.789	5.504	0.313	0.29	-0.179	69.4	5.11	0.38
03	3.245	1.827	0.0660	0.212	0.28	1.5	104.3	5.13	0.44
08	3.252	1.872	-0.0522	0.140	0.27	0.026	104.9	5.17	0.62
19	3.071	1.938	-1.0568	0.165	0.26	-0.087	115.0	5.36	0.57
04	4.485	1.834	3.489	0.161	0.28	0.45	80.2	5.45	0.57
09	4.049	1.922	1.831	0.233	0.27	0.86	90.3	5.54	0.40
15	2.966	1.777	-2.3553	0.105	0.29	2.6	128.1	5.76	0.88
20	3.315	1.884	-1.3631	0.183	0.27	0.048	116.7	5.86	0.53
07	3.517	1.908	-2.9263	0.083	0.27	1.2	128.7	6.86	1.25
mean \pm sdev									
mean \pm SEM									
weighted mean \pm Taylor err									
weighted mean \pm S & A err									
n=14					0.3	± 0.0		3.97	0.99
n=14					0.3	± 0.0		3.97	0.27
n=14					0.3	± 0.0		4.22	0.14
n=14					0.3	± 0.0		4.22	0.29

D	$^{40}\text{Ar}/^{39}\text{Ar}$	$^{37}\text{Ar}/^{39}\text{Ar}$	$^{36}\text{Ar}/^{39}\text{Ar}$ ($\times 10^{-3}$)	$^{39}\text{Ar}_{\text{K}}$ ($\times 10^{-15}$ mol)	K/Ca	C/K ($\times 10^{-3}$)	% $^{40}\text{Ar}^*$	Age (Ma)	$\pm \sigma$ (Ma)
RA-003, feldspar concentrate, J=0.0008411781±0.24%, Lab#=6087 (NM-44)									
No Ar gas Peaks - perlite									
19	264.3	0.0000	4233.0	0.000	-	-1790.806	%-373.3	-3.195.65	74.144.67
16	2.980	1.941	6.082	0.212	0.26	-0.251	44.7	2.02	0.51
11	2.868	1.766	5.361	0.164	0.29	0.88	49.5	2.15	0.53
05	3.096	1.827	4.797	0.142	0.28	1.1	58.7	2.76	0.75
08	3.886	1.855	7.033	0.133	0.27	0.76	50.2	2.96	0.76
23	3.227	1.949	4.631	0.226	0.26	-0.930	62.2	3.05	0.48
12	2.915	1.954	3.564	0.160	0.26	0.43	69.0	3.05	0.61
21	2.952	1.933	3.543	0.240	0.26	-0.564	69.6	3.12	0.42
20	3.125	1.886	3.810	0.244	0.27	-1.485	68.6	3.25	0.41
17	2.853	1.922	2.717	0.219	0.27	-0.170	77.0	3.34	0.39
22	3.023	2.012	3.009	0.174	0.25	-0.096	75.7	3.47	0.57
09	4.467	1.823	7.680	0.206	0.28	-0.604	52.3	3.55	0.48
18	2.941	1.791	2.491	0.221	0.28	-0.353	79.6	3.56	0.49
15	3.127	2.031	3.072	0.128	0.25	2.7	76.0	3.61	0.79
03	3.082	1.936	2.641	0.175	0.26	-1.931	79.5	3.72	0.57
25	3.285	1.878	3.300	0.384	0.27	-0.281	74.7	3.73	0.26
24	2.732	1.883	0.9377	0.340	0.27	0.92	95.1	3.95	0.29
13	2.659	0.0911	0.1760	1.93	5.6	0.23	98.3	3.96	0.06
04	2.772	0.3235	0.2674	1.06	1.6	0.16	98.0	4.12	0.11
14	2.870	1.932	0.8158	0.144	0.26	0.99	96.8	4.22	0.74
06	3.131	0.3092	1.231	0.557	1.6	0.16	89.1	4.23	0.19
07	3.149	0.0207	0.9218	2.47	24.7	0.44	91.4	4.36	0.05
10	8.338	1.898	18.26	0.249	0.27	0.68	37.0	4.69	0.43
02	3.013	1.855	-1.1804	0.219	0.28	-2.348	116.3	5.32	0.48
01	23.31	1.741	65.25	0.224	0.29	-0.263	17.9	6.31	0.66
mean \pm sdev									
n=14									
mean \pm SEM									
n=14									
weighted mean \pm Taylor err									
weighted mean \pm S & A err									
n=14									
n=14									
n=14									
n=14									
n=14									

mean \pm sdev
mean \pm SEM
weighted mean \pm Taylor err
weighted mean \pm S & A err

D	$^{40}\text{Ar}/^{39}\text{Ar}$	$^{37}\text{Ar}/^{39}\text{Ar}$	$^{36}\text{Ar}/^{39}\text{Ar}$ ($\times 10^{-3}$)	$^{39}\text{Ar}_{\text{K}}$ ($\times 10^{-15}$ mol)	K/Ca	C/K ($\times 10^{-3}$)	% $^{40}\text{Ar}^*$	Age (Ma)	$\pm 1\sigma$ (Ma)
RA-005, feldspar concentrate, J=0.00084002±0.24%, Lab#=5265 (NM-44)									
No Aguia Peaks - peralite									
17	2.993	1.919	5.415	0.146	0.27	3.0	51.5	2.34	0.67
09	6.842	0.2240	17.25	0.377	2.3	0.11	25.8	2.67	0.28
10	5.479	1.830	12.95	0.133	0.28	1.1	32.7	2.72	0.78
21	4.993	1.795	10.40	0.073	0.28	2.6	41.2	3.12	1.54
23	4.167	1.974	7.356	0.149	0.26	1.00	51.5	3.25	0.77
12	3.761	1.898	5.861	0.224	0.27	-0.063	57.8	3.30	0.58
08	11.86	1.313	32.40	0.116	0.39	0.68	20.1	3.62	0.79
04	9.096	0.8781	22.85	0.239	0.58	1.4	26.5	3.65	0.47
03	4.893	1.805	8.497	0.126	0.28	-0.240	51.5	3.82	0.81
24	3.530	1.908	3.643	0.119	0.27	1.8	73.6	3.94	0.85
11	4.629	1.770	7.322	0.147	0.29	1.2	56.2	3.94	0.84
01	2.795	0.1157	0.5196	1.12	4.4	0.39	94.8	4.01	0.09
22	3.683	1.809	3.890	0.098	0.28	2.0	72.6	4.05	1.20
02	2.827	0.0533	0.4562	1.34	9.6	0.21	95.4	4.08	0.07
07	7.551	0.4387	16.49	0.454	1.2	0.14	35.9	4.11	0.26
13	3.832	1.814	4.178	0.126	0.28	0.55	71.4	4.15	0.72
25	16.41	1.869	46.73	0.177	0.27	0.030	16.7	4.16	0.90
15	5.760	1.933	9.894	0.086	0.26	0.66	51.8	4.52	1.04
14	3.538	1.954	2.041	0.175	0.26	0.17	87.2	4.68	0.56
05	6.928	0.3584	13.08	0.324	1.4	-0.673	44.6	4.68	0.34
19	3.927	1.859	3.059	0.207	0.27	1.5	80.6	4.80	0.52
16	4.100	1.823	3.362	0.133	0.28	1.5	79.2	4.92	0.75
20	3.443	1.895	-1.4616	0.124	0.27	-0.690	116.8	6.09	0.77
06	8.448	1.447	12.59	0.115	0.35	2.4	57.3	7.33	0.76
18	7.850	1.923	10.22	0.094	0.27	-0.989	63.4	7.54	0.92
mean ± sdev									
mean ± SEM									
weighted mean ± Taylor err									
weighted mean ± S & A err									
n=19									
n=19									
n=19									
n=19									
n=19									

mean ± sdev

mean ± SEM

weighted mean ± Taylor err

weighted mean ± S & A err

ID	Temp (°C)	⁴⁰ Ar/ ³⁹ Ar	³⁷ Ar/ ³⁹ Ar (x 10 ⁻³)	³⁶ Ar/ ³⁹ Ar (x 10 ⁻³)	³⁹ Ar _K (x 10 ⁻¹⁶ mol)	K/Ca	Cl/K (x 10 ⁻³)	⁴⁰ Ar* (%)	³⁹ Ar (%)	Age (Ma)	±1σ (Ma)
RA-007, groundmass concentrate (85.1 mg), J=0.0004066155±0.98%, Lab#=5709 (NM-40)											
San Antonio Peak - pyroxene dacite											
A	600	288.2	0.4117	923.8	1.86	1.2	2.5	5.3	2.7	11.14	1.42
B	700	42.80	0.5323	127.4	4.87	0.96	0.51	12.2	9.7	3.82	0.20
C	750	25.76	0.5041	70.31	2.32	0.87	0.57	19.5	13.1	3.69	0.13
D	825	12.75	0.6622	28.42	13.4	0.77	0.16	34.5	32.5	3.23	0.05
E	900	10.66	0.5834	22.57	11.2	0.87	0.14	37.9	48.7	2.96	0.04
F	950	11.43	0.6178	24.90	8.40	0.83	0.36	36.0	60.8	3.02	0.05
G	1000	14.91	0.7079	36.42	4.16	0.72	0.41	28.2	66.9	3.08	0.07
H	1050	17.69	0.5271	46.07	4.46	0.97	0.51	23.3	73.3	3.02	0.09
I	1100	18.94	0.3546	50.21	4.56	1.4	0.32	21.8	79.9	3.03	0.09
J	1200	25.18	0.5510	69.12	4.71	0.93	0.36	19.0	86.7	3.51	0.12
K	1300	35.98	2.939	106.4	1.33	0.17	0.51	13.2	88.7	3.50	0.20
L	1650	26.20	2.114	72.22	7.84	0.24	0.51	19.2	100.0	3.69	0.12
total gas age	n=12			69.1	0.82					3.47	
preferred age	n=5			steps E-I	32.7	0.93		47.4	3.00	0.03	
isochron age	n=12			MSWD=3.51			40/36=307.8±1.3		2.81	0.47	
edited isochron age	n=6			MSWD=4.94			40/36=299.2±3.7		2.97	0.08	
RA-008, groundmass concentrate (52.3 mg), J=0.0008362995±0.24%, Lab#=6141 (NM-44)											
San Antonio Peak - pyroxene dacite											
A	675	58.86	0.4062	182.1	5.93	1.3	0.70	8.6	5.6	7.64	0.59
B	725	9.177	0.3710	22.16	8.69	1.4	0.11	28.9	13.8	4.00	0.09
C	775	5.239	0.3609	9.841	7.76	1.4	-0.10	45.0	21.1	3.56	0.05
D	825	3.546	0.3793	4.644	23.4	1.3	-0.076	62.1	43.3	3.32	0.02
E	875	3.312	0.4932	4.360	17.7	1.0	-0.055	62.2	60.0	3.11	0.03
F	950	4.571	0.7740	9.061	13.8	0.66	0.12	42.7	72.9	2.94	0.04
G	1050	10.26	1.048	29.17	8.44	0.49	0.25	16.7	80.9	2.59	0.11
H	1200	31.67	0.7141	100.8	8.51	0.71	0.39	6.1	88.9	2.90	0.33
I	1650	35.05	1.593	109.2	11.7	0.32	0.31	8.2	100.0	4.36	0.45
total gas age	n=9			105.9	0.97					3.57	
preferred age	n=6			steps D-I	83.5	0.87		40/36=302.5±1.2	3.18	0.08	
isochron age	n=9			MSWD=43.25			40/36=292.9±1.5	3.17	0.02		
edited isochron age	n=5			MSWD=13.32			40/36=299.2±3.7	3.07	0.02		

ID	Temp [°C]	$^{40}\text{Ar}/^{39}\text{Ar}$	$^{39}\text{Ar}/^{38}\text{Ar}$	$^{38}\text{Ar}/^{39}\text{Ar}$ ($\times 10^{-3}$)	$^{39}\text{Ar}_\text{K}$ ($\times 10^{-15}$ mol)	K/Ca	Cl/K ($\times 10^{-3}$)	$^{40}\text{Ar}^*$ (%)	^{39}Ar (%)	Age (Ma)	$\pm 1\sigma$ (Ma)
RA-009, groundmass concentrate (90.2 mg), J=0.001511643±0.13%, Lab#=5268 (NM-34)											
San Antonio Peak - pyroxene dacite											
A	600	6.940	0.5193	20.61	3.83	0.98	0.80	12.8	1.9	2.42	0.19
B	700	1.935	0.36657	2.655	23.9	1.4	0.069	60.9	13.9	3.21	0.02
C	750	1.470	0.33885	1.085	30.8	1.5	-0.079	79.9	29.3	3.20	0.02
D	825	1.302	0.3681	0.71112	54.4	1.4	-0.029	86.0	56.5	3.05	0.01
E	900	1.341	0.4053	0.9697	41.9	1.3	0.12	80.9	77.5	2.96	0.01
F	950	1.369	0.5192	1.131	16.4	0.98	0.16	78.5	85.7	2.93	0.02
G	1000	1.781	0.7234	2.626	7.63	0.71	0.080	59.5	89.6	2.89	0.04
H	1050	1.729	0.8414	2.602	5.11	0.61	0.35	59.3	92.1	2.79	0.05
I	1100	2.721	0.9360	6.273	2.77	0.55	0.41	34.5	93.5	2.56	0.10
J	1200	4.481	1.315	12.72	2.81	0.39	0.38	18.4	94.9	2.25	0.11
K	1300	5.133	1.705	14.23	1.26	0.30	0.45	20.6	95.5	2.89	0.18
L	1650	5.604	2.124	13.52	8.93	0.24	0.54	31.6	100.0	4.83	0.09
total gas age	n=12				199.7	1.2				3.10	0.03
preferred age	n=7				180.2	1.3				90.2	0.05
Isochron age	n=12									2.99	0.01
edited Isochron age	n=11									3.07	0.01
RA-010, groundmass concentrate (70.52 mg), J=0.0008390849±0.24%, Lab#=6096 (NM-44)											
San Antonio Peak area - Servilleta Basalt											
A	650	3487.9	0.2780	11086.0	0.169	1.8	17.7	6.1	0.3	295.43	64.88
B	700	309.5	0.3118	974.4	0.566	1.6	2.1	7.0	1.2	32.38	3.12
C	775	112.5	0.7006	352.6	1.94	0.73	1.8	7.4	4.5	12.58	0.89
D	825	32.64	1.115	98.30	14.2	0.46	0.44	11.3	28.6	5.57	0.21
E	875	14.47	1.644	40.37	11.0	0.31	0.42	18.4	47.4	4.03	0.09
F	950	11.92	2.794	32.93	10.9	0.18	0.40	20.2	65.8	3.65	0.08
G	1000	12.66	3.713	35.60	3.78	0.14	0.73	19.2	72.3	3.68	0.14
H	1100	12.24	2.706	34.84	5.37	0.19	0.50	17.6	81.4	3.26	0.12
I	1200	21.59	3.685	66.43	5.11	0.14	0.66	10.4	90.1	3.40	0.19
J	1300	21.20	17.01	67.34	4.06	0.030	0.49	12.3	97.0	3.99	0.19
K	1650	25.38	18.07	80.31	1.79	0.028	0.70	12.0	100.0	4.65	0.37
total gas age	n=11				58.9	0.29				5.59	0.40
plateau	none			N/A					N/A	N/A	
Isochron age	n=11									2.66	0.08
edited Isochron age	n=8									2.75	0.09

D	Temp [°C]	$^{40}\text{Ar}/^{39}\text{Ar}$	$^{37}\text{Ar}/^{39}\text{Ar}$	$^{36}\text{Ar}/^{39}\text{Ar}$	$^{38}\text{Ar}_K$ ($\times 10^{-3}$)	K/Ca	$^{40}\text{Ar}^*$ ($\times 10^{-3}$)	^{39}Ar (%)	Age (Ma)	$\pm 1\sigma$ (Ma)
RA-011, groundmass concentrate (58.4 mg), J=0.0008271003±0.24%, Lab#=6127 (NM-44)										
San Antonio Peak area - Servilleta Basalt										
A	675	539.4	0.5136	1694.8	1.91	0.99	2.1	7.2	4.8	56.74
B	725	67.20	0.7817	206.9	6.82	0.65	0.98	9.1	22.1	9.13
C	775	34.78	1.040	104.6	3.93	0.49	0.54	11.4	32.0	5.90
D	825	21.21	1.765	62.25	8.24	0.29	0.68	13.9	52.9	4.40
E	875	17.21	2.739	49.05	5.55	0.19	0.21	17.0	66.9	4.37
F	950	17.46	4.393	51.38	4.87	0.12	0.14	15.0	79.2	3.91
G	1050	21.01	5.850	61.73	2.73	0.087	0.82	15.3	86.1	4.82
H	1200	28.83	6.816	89.00	2.22	0.075	1.5	10.6	91.8	4.57
I	1650	66.06	22.38	210.4	3.26	0.023	1.2	8.5	100.0	8.47
total gas age		n=9			39.5	0.32			8.20	0.67
plateau		n=5		steps D-H	23.6	0.19			4.34	0.59
isochron age		n=9		MSWD=1.60			40/36=315.8±1.5		2.61	0.18
edited isochron age		n=5		MSWD=2.33			40/36=305.2±5.8		3.52	0.17
								59.7		0.47
RA-012, groundmass concentrate (96.4 mg), J=0.0004094255±0.98%, Lab#=5719 (NM-40)										
No Agua readcut - basaltic andesite										
A	650	37.00	1.117	107.6	3.95	0.46	0.23	14.3	7.8	3.92
B	700	11.15	1.055	23.87	4.63	0.48	0.24	37.5	16.9	3.08
C	750	7.482	0.9725	12.05	4.89	0.52	0.051	53.4	26.5	2.95
D	825	5.976	0.86658	7.217	14.0	0.59	0.14	65.4	54.1	2.89
E	900	5.739	0.84448	6.481	11.4	0.60	0.23	67.8	76.5	2.87
F	950	7.088	1.080	11.13	5.19	0.47	0.12	54.8	86.7	2.87
G	1000	14.23	1.365	35.88	1.51	0.37	0.61	26.2	89.7	2.76
H	1050	19.88	1.363	54.85	1.08	0.37	0.79	19.0	91.8	2.79
I	1100	24.92	1.504	69.93	0.922	0.34	1.0	17.5	93.6	3.23
J	1200	16.51	5.818	53.85	1.02	0.088	1.2	16.4	95.6	2.25
K	1300	22.45	12.49	66.82	0.630	0.041	1.8	16.3	96.9	2.73
L	1650	26.68	11.67	78.72	1.58	0.044	1.8	16.2	100.0	3.21
total gas age		n=12			50.7	0.50			2.98	0.06
plateau		n=7		steps C-I	38.9	0.55			76.7	2.89
isochron age		n=12		MSWD=5.56			40/36=300.8±1.5		2.85	0.02
edited isochron age		n=10		MSWD=4.91			40/36=295.7±2.0		2.89	0.03

D	Temp [°C]	$^{40}\text{Ar}/^{39}\text{Ar}$	$^{37}\text{Ar}/^{39}\text{Ar}$	$^{36}\text{Ar}/^{39}\text{Ar}$	$^{39}\text{Ar}_{\text{K}}$ ($\times 10^{-3}$)	K/Ca	Cl/K ($\times 10^{-3}$)	$^{40}\text{Ar}^*$ (%)	^{39}Ar (%)	Age (Ma)	$\pm 1\sigma$ (Ma)
RA-013, groundmass concentrate (115.1 mg), J=0.0004066195±0.98%, Lab#=5704 (NM-40)											
A	500	1147.5	0.3578	3734.4	0.179	1.4	9.0	3.8	1.6	32.04	10.83
B	600	195.9	0.9418	633.3	0.512	0.54	3.0	4.5	6.1	6.44	1.21
C	700	58.47	1.844	179.1	3.86	0.28	0.70	9.8	40.3	4.18	0.30
D	800	26.98	3.924	75.66	3.17	0.13	0.43	18.2	68.4	3.62	0.15
E	900	21.00	8.699	56.91	1.87	0.059	0.73	23.1	85.0	3.58	0.13
F	1000	24.85	13.20	67.36	0.930	0.039	-0.050	24.0	93.2	4.41	0.20
G	1100	34.59	12.52	101.5	0.283	0.041	1.2	16.1	95.7	4.12	0.48
H	1200	39.36	20.44	105.5	0.112	0.025	0.71	24.7	96.7	7.23	0.94
I	1300	71.91	91.66	253.7	0.112	0.006	1.6	5.5	97.7	3.11	1.32
J	1450	59.23	105.2	210.7	0.181	0.005	5.9	8.5	99.3	3.98	0.80
K	1650	114.3	57.72	389.6	0.081	0.009	4.9	3.2	100.0	2.75	2.32
total gas age		n=11		11.3	0.19					4.49	0.48
plateau		n=3		steps C-E	8.9	0.18				78.8	3.65
Isochron age		n=11		MSWD=3.86			40/36=301.9±1.8			3.47	0.13
edited Isochron age		n=9		MSWD=4.74			40/36=299.9±2.8			3.58	0.17
RA-014, groundmass concentrate (111.7 mg), J=0.0004063362±0.98%, Lab#=5712 (NM-40)											
A	650	151.4	1.228	489.1	1.13	0.42	1.2	4.6	11.0	5.09	0.80
B	700	78.90	1.161	249.4	0.552	0.44	-0.350	6.7	16.3	3.87	0.49
C	750	52.00	2.384	158.1	2.52	0.21	0.24	10.5	40.7	4.00	0.25
D	825	37.48	3.095	111.5	1.12	0.16	0.19	12.7	51.5	3.51	0.23
E	900	18.40	4.971	46.34	2.89	0.10	0.47	27.6	79.5	3.73	0.11
F	950	9.972	7.061	20.82	0.965	0.072	0.39	43.7	88.8	3.21	0.12
G	1000	11.28	9.351	23.06	0.363	0.056	0.45	46.0	92.4	3.82	0.24
H	1050	16.68	11.31	40.58	0.238	0.045	0.69	33.3	94.7	4.10	0.33
I	1100	26.11	9.782	70.99	0.107	0.052	0.41	22.5	95.7	4.34	0.75
J	1200	30.65	11.32	89.71	0.151	0.045	3.2	16.3	97.2	3.70	0.59
K	1300	95.68	84.81	338.6	0.040	0.006	2.0	2.2	97.5	1.66	2.94
L	1650	51.72	95.73	180.6	0.254	0.005	1.5	11.1	100.0	4.49	0.70
total gas age		n=12		steps B-E	10.3	0.18				68.5	3.91
plateau		n=4		MSWD=2.21						3.74	0.12
Isochron age		n=12		MSWD=2.39			40/36=300.1±1.4			3.43	0.09
edited Isochron age		n=10					40/36=299.9±1.5			3.43	0.09

D	Temp [°C]	$^{40}\text{Ar}/^{39}\text{Ar}$	$^{37}\text{Ar}/^{39}\text{Ar}$	$^{36}\text{Ar}/^{39}\text{Ar}$ ($\times 10^{-3}$)	$^{39}\text{Ar}_K$ ($\times 10^{-15}$ mol)	K/Ca	C/K ($\times 10^{-3}$)	$^{40}\text{Ar}^*$ (%)	^{39}Ar (%)	Age (Ma)	$\pm 1\sigma$ (Ma)
RA-015, groundmass concentrate (105.5 mg), J=0.0004066163±0.98%, Lab#=5708 (NM-40)											
285 roadcut - Servilleta Basalt											
A	600	325.7	1.279	1046.7	2.09	0.40	1.4	5.1	15.2	12.10	1.56
B	700	69.78	2.511	216.6	3.82	0.20	0.60	8.6	43.1	4.39	0.33
C	750	41.71	3.715	124.3	1.88	0.14	0.79	12.6	56.8	3.87	0.23
D	825	31.27	6.117	90.70	2.38	0.083	1.0	15.8	74.2	3.64	0.17
E	900	29.96	9.723	87.62	1.34	0.052	0.66	16.1	83.9	3.55	0.20
F	950	29.43	12.40	87.33	0.787	0.041	0.99	15.5	89.7	3.38	0.25
G	1000	32.18	13.83	96.28	0.386	0.037	-0.491	14.9	92.5	3.55	0.30
H	1050	41.61	13.32	134.4	0.224	0.038	-1.142	7.0	94.1	2.17	0.53
I	1100	52.49	12.57	166.6	0.111	0.041	-1.979	8.0	95.0	3.12	0.76
J	1200	65.24	25.05	206.9	0.195	0.020	-1.701	9.2	96.4	4.50	0.74
K	1300	40.63	72.41	147.6	0.241	0.007	2.7	6.3	98.1	1.98	0.55
L	1650	57.45	86.46	199.3	0.256	0.006	3.4	9.1	100.0	4.06	0.62
total gas age		n=12		13.7	0.16				5.11	0.49	
preferred age		n=5		steps C-G	6.8	0.08			3.61	0.12	
isochron age		n=12		MSWD=3.09			40/36=305.8±1.9		2.75	0.16	
edited isochron age		n=7		MSWD=2.10			40/36=294.7±7.2		3.61	0.45	
RA-016, groundmass concentrate (84.7 mg), J=0.00040661791±0.98%, Lab#=5706 (NM-40)											
285 roadcut - Servilleta Basalt											
A	600	699.7	1.190	2263.3	0.539	0.43	3.0	4.4	6.1	22.61	4.38
B	700	89.14	2.715	279.7	3.29	0.19	0.61	7.5	43.1	4.93	0.43
C	750	36.34	4.989	102.9	1.10	0.10	1.3	17.4	55.5	4.64	0.22
D	825	18.65	8.531	49.11	1.62	0.060	0.30	25.7	73.7	3.54	0.11
E	900	17.64	11.96	47.01	0.917	0.043	0.45	26.5	84.0	3.45	0.17
F	950	20.53	13.99	62.47	0.473	0.036	0.75	15.3	89.3	2.33	0.21
G	1000	26.89	14.84	82.42	0.230	0.034	1.4	13.7	91.9	2.72	0.40
H	1050	38.22	13.98	123.7	0.131	0.037	-0.587	7.2	93.4	2.04	0.82
I	1100	84.02	12.36	287.7	0.083	0.041	-5.403	0.0	94.3	-0.03	1.60
J	1200	87.94	46.33	305.7	0.114	0.011	5.2	1.3	95.6	0.88	1.28
K	1300	29.73	87.15	118.1	0.286	0.006	1.6	5.2	98.8	1.20	0.51
L	1650	43.27	88.07	157.9	0.108	0.006	1.1	7.8	100.0	2.64	1.09
total gas age		n=12		N/A	8.89	0.13			5.07	0.59	
plateau		none		N/A					N/A		
isochron age		n=12		MSWD=14.04			40/36=303.2±1.7		3.00	0.10	
edited isochron age		n=9		MSWD=6.49			40/36=272.1±3.6		4.15	0.16	

D	Temp (°C)	$^{40}\text{Ar}/^{39}\text{Ar}_\text{f}$	$^{37}\text{Ar}/^{39}\text{Ar}_\text{f}$ ($\times 10^{-3}$)	$^{36}\text{Ar}/^{39}\text{Ar}_\text{f}$ ($\times 10^{-3}$)	$^{39}\text{Ar}_\text{K}$ ($\times 10^{15}$ mol)	K/Ca	C/I/K ($\times 10^{-3}$)	$^{40}\text{Ar}_\text{f}^*$ (%)	$^{39}\text{Ar}_\text{f}$ (%)	Age (Ma)	$\pm 1\sigma$ (Ma)
RA-017, groundmass concentrate (104.6 mg), J=0.000409435±0.98%, Lab#=5718 (NM-40)											
Cerritos de la Cruz - basaltic andesite											
A	650	77.56	1.019	238.4	2.78	0.50	0.46	9.3	5.7	5.32	0.45
B	700	29.59	0.9632	79.51	2.99	0.53	0.34	20.8	11.8	4.55	0.16
C	750	17.24	0.8652	38.68	3.05	0.59	0.36	34.1	18.0	4.34	0.09
D	825	10.54	0.7162	17.23	8.06	0.71	0.046	52.2	34.5	4.06	0.04
E	900	9.062	0.5966	12.92	7.23	0.86	0.22	58.4	49.2	3.90	0.03
F	950	10.11	0.6958	16.45	4.38	0.73	0.056	52.5	58.2	3.92	0.05
G	1000	13.42	0.7981	28.04	1.92	0.64	0.26	38.7	62.1	3.83	0.08
H	1050	18.96	0.6733	47.63	1.55	0.76	0.30	26.0	65.2	3.65	0.15
I	1100	24.75	0.5622	67.14	1.88	0.91	0.39	20.0	69.1	3.65	0.15
J	1200	30.26	0.7885	85.22	2.58	0.65	0.35	17.0	74.4	3.79	0.17
K	1300	30.81	3.246	86.23	1.23	0.16	0.44	18.1	76.9	4.12	0.21
L	1650	29.00	2.064	79.19	11.3	0.25	0.40	19.9	100.0	4.25	0.15
total gas age	n=12			49.0	0.59					4.14	0.12
preferred age	n=4			21.6	0.76					4.41	0.05
isochron age	n=12					MSWD=5.66	40/36=300.4±1.3			3.89	0.05
edited isochron age	n=11					MSWD=6.06	40/36=299.4±1.5			3.91	0.05
RA-018, groundmass concentrate (105.7 mg), J=0.0004087698±0.98%, Lab#=5722 (NM-40)											
Cerritos de la Cruz - basaltic andesite											
A	450	1345.9	0.5007	4392.5	0.100	1.0	15.8	3.6	1.0	35.04	12.98
B	525	327.3	0.8899	1061.5	0.648	0.57	1.9	4.2	7.3	10.05	2.00
C	650	83.21	2.119	256.8	2.99	0.24	1.1	9.0	36.5	5.52	0.47
D	700	38.23	3.744	112.3	1.84	0.14	0.61	13.9	54.5	3.93	0.24
E	750	26.83	5.347	74.25	1.34	0.095	0.63	19.7	67.6	3.92	0.18
F	825	26.19	7.024	71.73	1.17	0.073	0.96	21.1	79.0	4.09	0.18
G	925	35.58	9.883	106.6	0.732	0.052	0.53	13.6	86.1	3.58	0.29
H	1025	57.06	11.72	177.3	0.385	0.044	1.4	9.8	89.9	4.15	0.52
I	1250	81.23	29.74	263.8	0.409	0.017	1.3	6.8	93.8	4.18	0.64
J	1650	104.1	40.82	341.2	0.630	0.012	2.7	6.2	100.0	4.85	0.75
total gas age	n=10			10.2	0.17					5.15	0.59
plateau	n=7			steps D-J	6.5	0.08				63.5	3.96
isochron age	n=10					MSWD=1.16	40/36=302.8±1.6			3.48	0.16
edited isochron age	n=6					MSWD=0.63	40/36=295.8±3.6			3.97	0.26

D	Temp (°C)	$^{40}\text{Ar}/^{39}\text{Ar}$	$^{39}\text{Ar}/^{38}\text{Ar}$	$^{36}\text{Ar}/^{39}\text{Ar}$	$^{39}\text{Ar}_{\text{K}}$ ($\times 10^{-3}$)	K/Ca	C/K ($\times 10^{-3}$)	$^{40}\text{Ar}^*$ (%)	^{39}Ar (%)	Age (Ma)	$\pm 1\sigma$ (Ma)
RA-019, groundmass concentrate (124.34 mg), J=0.001515469±0.13%, Lab#=5267 (NM-34)											
San Antonio Peak area - Servilleta Basalt											
A	700	1043.0	1.236	3494.9	0.453	0.41	0.27	1.0	1.0	28.01	23.72
B	775	57.11	0.9998	186.8	0.363	0.51	0.99	3.5	1.6	5.44	1.66
C	825	14.24	2.020	45.89	3.09	0.25	0.46	5.9	8.9	2.29	0.30
D	900	7.367	3.334	21.72	6.12	0.15	0.21	16.4	22.7	3.30	0.14
E	950	4.883	4.216	13.66	6.57	0.12	0.19	24.0	37.6	3.21	0.11
F	1000	3.680	5.370	9.949	4.82	0.095	0.19	31.3	48.5	3.16	0.11
G	1050	3.345	6.457	8.930	4.30	0.079	0.20	35.9	58.3	3.30	0.10
H	1100	3.523	6.513	9.744	2.64	0.078	0.28	32.5	64.2	3.14	0.14
I	1200	5.268	4.781	15.43	7.48	0.11	0.16	20.4	81.2	2.95	0.10
J	1300	5.570	12.31	17.74	4.53	0.041	0.47	22.9	91.4	3.51	0.13
K	1650	33.60	38.76	116.6	3.78	0.013	0.78	6.3	100.0	5.98	0.68
total gas age		n=11		44.1	0.11					3.65	0.49
plateau		n=7		36.5	0.10					3.19	0.08
isochron age		n=11				steps D-J	40/36=299.0±1.2			3.11	0.05
edited isochron age		n=8				MSWD=5.80	40/36=303.0±1.8			3.00	0.06
RA-020, groundmass concentrate (102.1 mg), J=0.0004063287±0.98%, Lab#=5710 (NM-40)											
San Antonio Peak - andesite											
A	600	196.1	0.3821	623.1	4.43	1.3	1.2	6.1	7.5	8.79	0.91
B	700	43.53	0.2790	131.8	10.5	1.8	0.56	10.6	25.3	3.36	0.20
C	750	22.86	0.2614	63.14	4.19	2.0	0.48	18.5	32.4	3.09	0.11
D	825	13.81	0.5709	33.50	21.3	0.89	0.37	28.6	68.6	2.90	0.06
E	900	9.817	0.9942	19.97	10.3	0.51	0.37	40.7	86.1	2.93	0.04
F	950	9.582	1.717	19.38	4.65	0.30	0.42	41.6	94.0	2.92	0.05
G	1000	12.44	2.188	30.54	1.11	0.23	0.87	28.8	95.8	2.63	0.12
H	1050	16.99	2.132	49.13	0.720	0.24	0.80	15.5	97.1	1.93	0.21
I	1100	22.14	1.961	70.04	0.383	0.26	0.96	7.2	97.7	1.17	0.27
J	1200	39.63	3.730	124.5	0.276	0.14	2.5	7.9	98.2	2.30	0.53
K	1300	95.95	37.48	318.6	0.107	0.014	5.5	4.9	98.4	3.52	1.22
L	1650	28.54	18.56	86.87	0.961	0.027	1.6	15.0	100.0	3.19	0.23
total gas age		n=12				steps B-G	40/36=301.6±1.3			3.42	0.16
plateau		n=6				MSWD=10.13	40/36=289.6±1.7			2.92	0.05
isochron age		n=12				MSWD=2.55	40/36=303.0±1.8			2.78	0.04
edited isochron age		n=4								3.00	0.10

D	Temp (°C)	$^{40}\text{Ar}/^{39}\text{Ar}_\text{f}$	$^{37}\text{Ar}/^{39}\text{Ar}_\text{f}$ ($\times 10^{-3}$)	$^{36}\text{Ar}/^{39}\text{Ar}_\text{f}$ ($\times 10^{-3}$)	$^{39}\text{Ar}_\text{K}$ ($\times 10^{15}$ mol)	K/Ca	C/K ($\times 10^{-3}$)	$^{40}\text{Ar}^*$ (%)	^{39}Ar (%)	Age (Ma)	$\pm 1\sigma$ (Ma)
RA-021, groundmass concentrate (103.2 mg), J=0.0004015138±1.00%, Lab#=5733 (NM-40)											
Cerro del Alire - olivine andesite											
A	450	2783.3	0.1562	9230.3	0.243	3.3	9.4	2.0	0.3	39.94	24.73
B	525	305.4	0.2191	1003.4	1.98	2.3	1.2	2.9	3.1	6.41	1.52
C	650	74.88	0.4217	235.0	11.5	1.2	0.26	7.3	19.1	3.95	0.33
D	700	34.17	0.6098	97.11	9.42	0.84	0.44	16.2	32.2	4.00	0.15
E	750	17.12	0.7500	39.80	9.10	0.68	0.40	31.6	44.9	3.92	0.07
F	825	9.561	0.7061	15.09	15.4	0.72	0.11	53.9	66.3	3.73	0.03
G	900	8.747	0.7264	12.77	13.0	0.70	0.19	57.5	84.4	3.64	0.03
H	925	11.31	0.8924	21.26	4.33	0.57	0.34	45.1	90.4	3.69	0.05
I	950	18.32	1.111	45.05	1.69	0.46	1.0	27.8	92.8	3.69	0.11
J	1050	34.74	1.317	99.95	2.07	0.39	0.52	15.3	95.6	3.84	0.18
K	1300	49.92	8.016	154.5	1.98	0.064	1.1	9.8	98.4	3.55	0.24
L	1650	49.28	17.89	152.0	1.16	0.029	1.8	11.6	100.0	4.20	0.28
total gas age		n=12								4.01	0.24
plateau		n=7								55.1	3.69
isochron age		n=12								3.65	0.04
edited isochron age		n=5								3.59	0.05
								40/36=299.0±0.9			
								40/36=303.9±3.0			
RA-022, groundmass concentrate (66.8 mg), J=0.0004066187±1.98%, Lab#=5705 (NM-40)											
La Segita Peaks - basaltic andesite											
A	500	1863.3	0.0000	6075.2	0.108	-	26.5	3.7	0.2	49.28	21.30
B	600	203.0	0.7929	643.6	0.366	0.64	-0.230	6.4	1.1	9.44	1.37
C	700	28.38	0.8437	84.04	5.25	0.60	0.36	12.7	12.7	2.65	0.15
D	800	8.796	0.7505	19.39	11.8	0.68	0.006	35.5	39.0	2.29	0.04
E	900	6.365	0.8201	11.88	13.1	0.62	0.12	45.8	68.3	2.14	0.03
F	1000	8.609	1.197	19.64	5.81	0.43	0.14	33.6	81.2	2.13	0.05
G	1100	13.40	1.390	36.40	1.60	0.37	0.50	20.6	84.8	2.02	0.12
H	1200	13.36	3.605	38.36	1.80	0.14	1.2	17.2	88.8	1.69	0.11
I	1300	16.21	7.406	49.56	0.780	0.069	0.65	13.2	90.5	1.57	0.15
J	1450	17.35	4.996	49.64	4.02	0.10	0.64	17.6	99.5	2.25	0.10
K	1650	29.46	7.810	90.30	0.245	0.065	1.1	11.5	100.0	2.49	0.48
total gas age		n=11								2.39	0.13
preferred age		n=3								2.13	0.03
isochron age		n=11								2.07	0.03
edited isochron age		n=9								2.13	0.04
								40/36=302.0±1.6			
								40/36=303.9±1.9			

D	Temp ({°C})	⁴⁰ Ar/ ³⁹ Ar	³⁷ Ar/ ³⁹ Ar	³⁶ Ar/ ³⁹ Ar (x 10 ⁻³)	³⁹ Ar _K (x 10 ⁻¹⁵ mol)	K/Ca	C/K (x 10 ⁻³)	⁴⁰ Ar*	³⁹ Ar (%)	Age (Ma)	±1σ (Ma)
RA-023, groundmass concentrate (124.5 mg), J=0.0004015447±1.00%, Lab#=5729 (NM-40)											
La Segilla Peaks - Servilleta Basalt											
A	450	4837.9	1.003	16095.2	0.089	0.51	12.5	1.7	0.6	58.40	79.58
B	525	4677.8	1.243	1534.9	0.718	0.41	1.8	3.1	5.0	10.36	2.32
C	650	94.57	2.564	303.1	4.02	0.20	0.48	5.5	30.0	3.77	0.44
D	700	49.41	4.107	152.4	2.83	0.12	0.40	9.5	47.6	3.39	0.24
E	750	39.90	6.163	120.8	2.07	0.083	0.32	11.7	60.5	3.39	0.20
F	825	35.18	8.097	106.2	2.40	0.063	0.36	12.5	75.4	3.21	0.18
G	900	44.80	10.44	138.8	1.47	0.049	0.90	10.2	84.6	3.34	0.26
H	925	80.17	12.78	259.2	0.584	0.040	1.2	5.7	88.2	3.33	0.53
I	950	137.4	13.16	445.0	0.301	0.039	0.24	5.0	90.1	5.04	0.92
J	1050	193.2	11.74	637.6	0.385	0.043	4.1	2.9	92.4	4.13	1.19
K	1300	312.7	44.69	1043.3	0.598	0.011	4.8	2.5	96.2	5.82	1.80
L	1650	385.1	61.47	1261.9	0.617	0.008	5.7	4.4	100.0	12.77	2.18
total gas age		n=12		16.1		0.12				4.67	1.00
plateau		n=6		steps C-H		13.4				83.2	3.35
isochron age		n=12		MSWD=0.84						2.48	0.12
edited isochron age		n=9		MSWD=0.26						2.99	0.16
					40/36=301.5±1.1						0.19
					40/36=299.1±1.6						
RA-024, groundmass concentrate (124.4 mg), J=0.0004015371±1.00%, Lab#=5730 (NM-40)											
La Segilla Peaks - Servilleta Basalt											
A	450	14185.0	0.7153	46383.9	0.110	0.71	83.9	3.4	0.5	311.27	252.51
B	525	1130.2	1.643	3656.1	0.781	0.31	6.4	4.4	4.3	35.90	6.35
C	650	184.8	1.800	590.9	3.77	0.28	1.7	5.6	22.6	7.44	0.84
D	700	79.83	2.934	248.3	2.98	0.17	0.35	8.4	37.0	4.85	0.37
E	750	49.70	4.221	150.0	2.55	0.12	0.78	11.4	49.3	4.13	0.24
F	825	32.72	4.822	95.97	2.90	0.11	0.24	14.4	63.3	3.43	0.17
G	900	33.18	5.490	96.16	2.62	0.093	0.66	15.6	76.0	3.76	0.16
H	925	50.60	6.714	157.3	1.03	0.076	1.1	9.2	81.0	3.37	0.33
I	950	66.96	7.860	211.1	0.592	0.065	0.83	7.7	83.9	3.77	0.41
J	1050	74.55	7.968	239.5	0.921	0.064	0.90	5.9	88.3	3.19	0.40
K	1300	214.8	32.79	700.8	1.89	0.016	2.5	4.8	97.5	7.58	1.12
L	1650	509.0	28.25	1602.6	0.525	0.018	9.2	7.4	100.0	27.58	2.72
total gas age		n=12		steps E-J		20.7		0.14		8.38	2.09
plateau		n=6		MSWD=4.11		10.6		0.10		51.3	3.66
isochron age		n=12		MSWD=2.18						3.60	0.16
edited isochron age		n=6								3.66	0.27
				40/36=307.5±1.2						40/36=295.5±2.7	

D	Temp (°C)	$^{40}\text{Ar}/^{39}\text{Ar}$	$^{37}\text{Ar}/^{39}\text{Ar}$ ($\times 10^{-3}$)	$^{36}\text{Ar}/^{39}\text{Ar}$ ($\times 10^{-15}$ mol)	$^{39}\text{Ar}_\text{K}$ ($\times 10^{-15}$ mol)	K/Ca	C/K ($\times 10^{-3}$)	$^{40}\text{Ar}^*$ (%)	^{39}Ar (%)	Age (Ma)	$\pm 1\sigma$ (Ma)
RA-025, groundmass concentrate (60.9 mg), J=0.000040866844±0.98%, Lab#=5726 (NM-40)											
La Segita Peaks - Servilleta Basalt											
A	450	2397.9	1.480	7864.1	0.220	0.34	13.8	3.1	0.8	53.97	24.00
B	525	336.9	0.2372	1090.4	1.43	2.2	1.7	4.4	5.9	10.80	1.66
C	650	87.29	0.4705	277.6	6.72	1.1	0.71	6.1	30.0	3.90	0.40
D	700	48.83	0.8391	148.3	4.85	0.61	0.69	10.4	47.4	3.74	0.22
E	750	37.08	1.584	109.0	2.87	0.32	0.29	13.5	57.7	3.68	0.17
F	825	23.59	2.129	64.96	3.45	0.24	0.53	19.3	70.0	3.36	0.11
G	900	19.05	2.322	48.95	3.55	0.22	0.50	25.0	82.7	3.51	0.09
H	925	27.30	2.886	76.49	1.31	0.18	1.0	18.0	87.4	3.63	0.16
I	950	39.23	3.532	118.0	0.657	0.14	1.7	11.8	89.8	3.41	0.30
J	1050	48.98	3.706	146.8	0.768	0.14	-0.197	12.0	92.5	4.34	0.31
K	1300	89.07	10.94	283.0	0.992	0.047	0.88	7.1	96.1	4.67	0.51
L	1650	79.17	14.46	241.3	1.09	0.035	1.1	11.3	100.0	6.68	0.42
total gas age		n=12			27.9	0.59				4.61	0.51
plateau		n=7		steps C-I	23.4	0.56				3.53	0.08
isochron age		n=12		MSWD=3.93			40/36=304.5±1.2			3.07	0.09
edited isochron age		n=8		MSWD=1.33			40/36=301.8±1.4			3.19	0.10
RA-026, groundmass concentrate (104.31 mg), J=0.001515469±0.13%, Lab#=5265 (NM-34)											
Cerro de la Olla area - basaltic andesite											
A	700	2674.4	1.696	9053.2	0.029	0.30	15.8	0.0	0.0	-1.86	234.31
B	775	73.02	0.8622	246.3	0.049	0.59	2.5	0.4	0.0	0.85	5.70
C	825	10.77	0.5500	14.92	5.12	0.93	0.38	59.4	2.9	17.42	0.15
D	900	7.668	0.4592	4.387	12.6	1.1	0.14	83.5	9.8	17.44	0.06
E	950	7.120	0.4820	2.542	24.9	1.1	0.13	90.0	23.5	17.43	0.05
F	1000	7.071	0.4954	2.386	22.9	1.0	0.10	90.6	36.2	17.43	0.05
G	1050	7.102	0.5274	2.506	24.1	0.97	0.19	90.1	49.4	17.42	0.05
H	1100	7.238	0.5681	2.788	14.3	0.90	0.18	89.2	57.3	17.58	0.05
I	1200	8.909	0.6955	8.751	38.4	0.73	0.17	71.6	78.5	17.36	0.08
J	1300	17.17	2.509	37.51	16.3	0.20	0.52	36.6	87.5	17.12	0.22
K	1650	17.68	8.101	40.42	22.7	0.063	0.41	35.9	100.0	17.39	0.24
total gas age		n=11		steps C-K	181.4	0.76				100.0	17.45
plateau		n=9		MSWD=1.84	181.3	0.76				17.48	0.03
isochron age		n=11		MSWD=1.37			40/36=292.6±1.4			17.47	0.03
edited isochron age		n=9					40/36=293.1±1.4				

D	Temp [°C]	$^{40}\text{Ar}/^{39}\text{Ar}$	$^{37}\text{Ar}/^{39}\text{Ar}$	$^{38}\text{Ar}/^{39}\text{Ar}$ ($\times 10^{-3}$)	$^{39}\text{Ar}_K$ ($\times 10^{-15}$ mol)	K/Ca	C/K ($\times 10^{-3}$)	$^{40}\text{Ar}^*$ (%)	^{39}Ar (%)	Age (Ma)	$\pm 1\sigma$ (Ma)
RA-027, groundmass concentrate (122.1 mg), J=0.001511643±0.13%, Lab#=5269 (NM-34)											
Dunn Bridge Section - Servilleta Basalt											
A	600	5.145	1.456	12.84	5.79	0.35	0.19	28.4	4.4	3.99	0.10
B	700	2.205	1.128	2.436	6.04	0.45	0.048	71.3	8.9	4.28	0.04
C	750	1.887	1.220	1.362	12.5	0.42	0.14	83.6	18.3	4.30	0.02
D	800	1.763	1.377	0.9343	15.2	0.37	0.11	90.3	29.8	4.34	0.02
E	875	1.717	1.084	0.7013	26.6	0.47	0.17	92.8	49.8	4.34	0.01
F	925	1.781	0.8965	0.8920	22.0	0.57	0.21	89.1	66.4	4.32	0.02
G	975	1.754	1.011	0.8450	13.0	0.50	0.15	90.2	76.2	4.31	0.02
H	1025	2.051	1.030	1.756	7.76	0.50	0.26	78.5	82.1	4.39	0.03
I	1125	2.855	1.040	4.543	7.01	0.49	0.34	55.8	87.3	4.34	0.05
J	1250	3.295	6.765	6.953	6.11	0.075	0.33	53.4	91.9	4.82	0.07
K	1650	6.267	7.700	11.38	10.7	0.066	0.34	55.8	100.0	9.56	0.10
total gas age		n=11		132.8	0.42				4.76	0.05	
plateau		n=8		110.2	0.48			83.0	4.33	0.02	
isochron age		n=11		MSWD=315.62		40/36=397.7±2.0			4.13	0.01	
edited isochron age		n=9		MSWD=3.06		40/36=289.3±2.2			4.34	0.01	
RA-028, groundmass concentrate (121.7 mg), J=0.0015098±0.13%, Lab#=5279 (NM-34)											
Dunn Bridge Section - Servilleta Basalt											
A	600	34.58	4.481	114.6	0.806	0.11	0.62	3.0	1.7	2.86	0.81
B	700	4.008	3.478	9.087	4.43	0.15	0.068	39.7	11.2	4.34	0.11
C	750	2.481	3.451	4.068	5.87	0.15	0.066	62.2	23.8	4.21	0.06
D	825	1.948	3.654	2.552	10.5	0.14	0.16	75.7	46.2	4.02	0.04
E	900	1.847	2.976	2.137	8.72	0.17	0.18	78.2	64.9	3.94	0.03
F	950	1.906	2.701	2.323	4.82	0.19	0.26	74.9	75.2	3.89	0.05
G	1000	2.323	3.552	3.959	2.96	0.14	0.020	61.4	81.5	3.89	0.08
H	1050	2.447	4.704	4.677	2.25	0.11	0.26	58.3	86.4	3.89	0.12
I	1100	5.297	5.966	15.16	1.44	0.086	0.30	24.1	89.4	3.49	0.18
J	1200	4.223	10.46	12.62	1.18	0.049	0.90	30.7	92.0	3.55	0.18
K	1300	7.551	47.65	34.34	2.31	0.011	0.70	14.1	96.9	2.99	0.28
L	1650	15.88	38.05	58.60	1.44	0.013	0.55	9.4	100.0	4.16	0.47
total gas age		n=12		steps D-L	46.7	0.14			3.94	0.16	
plateau		n=9		MSWD=16.54	35.6	0.13		76.2	3.92	0.05	
isochron age		n=12		MSWD=13.81		40/36=289.7±1.2			4.00	0.01	
edited isochron age		n=8				40/36=300.9±2.2			3.95	0.01	

D	Temp (°C)	$^{40}\text{Ar}/^{39}\text{Ar}$	$^{37}\text{Ar}/^{39}\text{Ar}$	$^{38}\text{Ar}/^{39}\text{Ar}$ ($\times 10^{-3}$)	$^{39}\text{Ar}_K$ ($\times 10^{-15}$ mol)	K/Ca	Ci/K ($\times 10^{-3}$)	$^{40}\text{Ar}^*$ (%)	^{39}Ar (%)	Age (Ma)	$\pm 1\sigma$ (Ma)
RA-029, groundmass concentrate (94.0 mg), J=0.0004063401±0.98%, Lab#=5713 (NM-40)											
Dunn Bridge Section - Servilleta Basalt											
A	650	755.9	2.049	2408.8	0.541	0.25	6.9	5.9	7.0	32.22	4.48
B	700	200.6	2.644	629.1	0.835	0.19	7.4	17.7	10.93	1.09	1.01
C	750	124.0	3.135	388.7	0.289	0.16	-0.295	7.6	21.4	6.88	0.23
D	825	43.42	6.906	128.9	2.15	0.074	0.19	13.5	49.0	4.31	0.19
E	900	30.19	9.907	87.74	1.60	0.052	0.099	16.6	69.6	3.70	0.32
F	950	45.88	11.84	138.2	0.930	0.043	0.19	13.0	81.6	4.40	0.48
G	1000	66.21	14.46	199.4	0.463	0.035	0.054	12.7	87.6	6.20	0.48
H	1050	85.04	15.73	263.9	0.375	0.032	0.36	9.7	92.4	6.12	0.60
I	1100	183.2	17.05	579.9	0.158	0.030	-2.807	7.2	94.4	9.77	1.71
J	1200	158.73	29.15	5046.6	0.163	0.018	18.9	6.2	96.5	72.07	13.72
K	1300	62.1	161.0	2033.0	0.038	0.003	5.5	5.6	97.0	28.47	13.41
L	1650	832.6	146.3	2639.7	0.232	0.003	20.0	7.7	100.0	51.34	6.27
total gas age		n=12		7.77	0.085					10.19	1.30
plateau		n=3		steps D-F	4.68					4.03	0.26
Isochron age		n=12		MSWD=0.76	0.060					2.56	0.18
edited Isochron age		n=8		MSWD=1.14	40/36=314.4±1.4					2.53	0.31
RA-030, groundmass concentrate (50.64 mg), J=0.000766768±0.26%, Lab#=6986 (NM-54)											
Dunn Bridge Section - Servilleta Basalt											
A	550	1248.6	1	0.2196	41788.7	0.014	2.3	63.8	1.1	180.95	1,596.38
B	650	118.1	0.7301	397.7	0.777	0.70	0.59	0.6	7.9	0.92	1.15
C	750	21.66	1.021	66.89	1.04	0.50	0.097	9.1	18.4	2.73	0.29
D	825	11.44	3.233	33.14	3.49	0.16	0.41	16.5	53.4	2.62	0.13
E	875	11.28	7.566	31.92	1.32	0.067	0.27	21.5	66.6	3.37	0.19
F	950	10.55	10.84	30.65	1.07	0.047	-0.058	22.1	77.4	3.24	0.19
G	1000	12.79	12.73	38.94	0.554	0.040	0.37	17.7	82.9	3.16	0.30
H	1050	18.00	13.14	58.72	0.334	0.039	-0.147	9.2	86.3	2.31	0.37
I	1100	23.71	11.69	76.82	0.364	0.044	0.72	8.0	89.9	2.65	0.40
J	1200	43.92	22.49	146.1	0.335	0.023	1.5	5.6	93.3	3.48	0.61
K	1300	48.13	71.05	172.8	0.347	0.007	0.58	5.2	96.8	3.65	0.77
L	1650	153.4	46.66	506.8	0.323	0.011	0.85	4.7	100.0	10.38	1.75
total gas age		n=12		steps B-D	5.30	0.19				3.25	2.58
plateau		n=3		MSWD=4.61	0.30					2.62	0.17
Isochron age		n=12		MSWD=3.65	40/36=297.6±1.4					2.84	0.10
edited Isochron age		n=9		MSWD=3.65	40/36=296.0±2.2					2.93	0.14

D	Temp (°C)	$^{40}\text{Ar}/^{39}\text{Ar}$	$^{39}\text{Ar}/^{38}\text{Ar}$	$^{38}\text{Ar}/^{39}\text{Ar}$ ($\times 10^{-3}$)	$^{39}\text{Ar}_K$ ($\times 10^{-15}$ mol)	K/Ca	Ci/K ($\times 10^{-3}$)	$^{40}\text{Ar}^*$ (%)	^{39}Ar (%)	Age (Ma)	$\pm 1\sigma$ (Ma)
RA-031, groundmass concentrate (50.0 mg), J=0.0004094064±0.98%, Lab#=5721 (NM-40)											
<i>Cerro de los Taos - olivine andesite</i>											
A	450	961.0	0.2017	3186.3	0.125	2.5	0.71	2.0	0.6	14.30	10.86
B	525	226.3	0.2823	719.9	0.916	1.8	2.6	6.0	4.8	10.03	1.42
C	650	65.04	0.5060	196.9	5.02	1.0	0.29	10.6	28.2	5.08	0.35
D	700	33.69	0.7670	91.51	4.06	0.67	0.67	19.9	47.0	4.95	0.18
E	750	26.40	1.230	67.59	3.04	0.41	0.096	24.7	61.1	4.82	0.16
F	850	23.71	1.904	57.76	3.58	0.27	0.28	28.6	77.7	5.01	0.12
G	975	27.67	2.327	71.03	2.22	0.22	0.12	24.8	88.0	5.07	0.16
H	1150	36.48	2.770	107.7	0.792	0.18	1.2	13.4	91.7	3.61	0.29
I	1300	35.17	6.914	96.75	0.630	0.074	-0.549	20.2	94.6	5.27	0.27
J	1650	33.30	9.177	94.56	1.15	0.056	0.71	18.2	100.0	4.50	0.21
total gas age		n=10			21.5	0.59			5.19	0.33	
plateau		n=5		steps C-G	17.9	0.58			83.2	4.97	0.09
isochron age		n=10		MSWD=4.76			40/36=300.1±2.0		4.62	0.14	
edited isochron age		n=8		MSWD=4.73			40/36=292.6±3.2		5.04	0.19	
RA-032, groundmass concentrate (53.14 mg), J=0.0008382726±0.24%, Lab#=6110 (NM-44)											
<i>Tres Orejas - pyroxene dacite</i>											
A	675	79.94	1.436	251.3	0.782	0.36	0.72	7.3	1.0	8.76	1.04
B	725	11.75	1.433	29.36	2.91	0.36	0.026	27.1	4.9	4.81	0.16
C	775	7.301	1.304	14.16	3.38	0.39	0.11	44.1	9.3	4.86	0.08
D	825	5.083	1.042	6.489	13.4	0.49	0.24	63.8	27.1	4.90	0.03
E	875	3.972	0.7587	2.878	13.8	0.67	0.16	80.1	45.3	4.81	0.02
F	950	3.582	0.7194	1.431	15.8	0.71	0.15	89.7	66.2	4.86	0.02
G	1050	3.611	0.6886	1.614	15.3	0.74	0.20	88.2	86.3	4.81	0.02
H	1200	7.423	0.9173	15.00	5.29	0.56	0.41	41.2	93.3	4.63	0.08
I	1650	27.42	14.08	85.03	5.05	0.036	0.91	12.3	100.0	5.14	0.31
total gas age		n=9		steps B-G	75.7	0.58			4.89	0.07	
plateau		n=6		MSWD=4.25	64.6	0.63			85.3	4.84	0.02
isochron age		n=9		MSWD=3.80			40/36=298.5±1.4		4.82	0.01	
edited isochron age		n=7					40/36=294.7±2.0		4.84	0.02	

D	Temp (°C)	$^{40}\text{Ar}/^{39}\text{Ar}$	$^{37}\text{Ar}/^{39}\text{Ar}$	$^{36}\text{Ar}/^{39}\text{Ar}$ ($\times 10^{-3}$)	$^{39}\text{Ar}_K$ ($\times 10^{15}$ mol)	K/Ca ($\times 10^{-3}$)	Ci/K ($\times 10^{-3}$)	$^{40}\text{Ar}^*$ (%)	^{39}Ar (%)	Age (Ma)	$\pm 1\sigma$
RA-033, groundmass concentrate (84.7 mg), J=0.0004063324±0.98%, Lab#=5711 (NM-40)											
Tres Orijas - pyroxene dacite											
A	700	114.2	0.3793	356.1	8.86	1.3	1.1	7.9	22.7	6.63	0.65
B	800	39.62	0.6483	113.6	8.61	0.79	0.32	15.4	44.7	4.46	0.20
C	850	43.70	0.7380	126.9	6.40	0.69	0.48	14.3	61.0	4.59	0.22
D	925	49.85	0.8407	145.9	6.03	0.61	0.29	13.6	76.5	4.98	0.25
E	1000	62.73	0.9822	186.9	3.33	0.52	0.70	12.1	85.0	5.54	0.32
F	1050	92.89	1.169	291.4	1.30	0.44	0.57	7.4	88.3	5.03	0.53
G	1100	134.4	1.143	431.2	0.738	0.45	0.65	5.3	90.2	5.19	0.90
H	1150	131.9	0.9032	420.8	1.11	0.56	0.52	5.8	93.0	5.60	0.76
I	1200	98.48	1.358	307.9	1.01	0.38	0.89	7.7	95.6	5.58	0.61
J	1300	84.33	2.871	256.1	1.34	0.18	1.3	10.5	99.0	6.51	0.48
K	1400	76.07	8.464	228.0	0.260	0.060	0.50	12.3	99.7	6.88	0.60
L	1750	83.61	10.39	215.8	0.112	0.049	5.0	24.7	100.0	15.17	0.98
total gas age			n=12		39.1	0.78				5.36	0.39
plateau			n=8	steps B-I	28.5	0.65				4.82	0.19
isochron age			n=12	MSWD=12.80			40/36=306.7±1.9			3.76	0.20
edited isochron age			n=7	MSWD=2.25			40/36=304.1±1.9			3.94	0.23
RA-034, groundmass concentrate (93.8 mg), J=0.0004063484±0.98%, Lab#=5715 (NM-40)											
Tres Orijas - pyroxene dacite											
A	700	101.2	0.6373	304.8	7.26	0.80	1.1	11.1	14.1	8.20	0.53
B	800	9.931	0.4914	9.897	13.8	1.0	0.025	70.9	40.7	5.16	0.03
C	850	8.150	0.4412	4.983	10.2	1.2	0.008	82.3	60.4	4.91	0.02
D	925	7.897	0.4652	4.470	10.6	1.1	0.15	83.7	80.9	4.84	0.02
E	1000	8.830	0.6329	7.989	5.50	0.81	0.19	73.8	91.5	4.77	0.03
F	1050	11.20	1.061	16.36	1.70	0.48	0.24	57.6	94.8	4.72	0.06
G	1100	14.53	1.417	27.59	0.790	0.36	0.58	44.6	96.4	4.75	0.12
H	1150	19.81	1.662	47.43	0.353	0.31	0.21	29.9	97.0	4.34	0.23
I	1200	40.58	2.341	115.8	0.331	0.22	1.9	16.1	97.7	4.80	0.33
J	1300	44.78	7.531	129.9	0.486	0.068	2.2	15.5	98.6	5.12	0.32
K	1400	103.5	13.97	318.4	0.584	0.037	2.8	10.1	99.8	7.75	0.63
L	1750	282.7	13.27	886.1	0.125	0.038	5.4	7.8	100.0	16.16	3.40
total gas age			n=12		51.7	0.95				5.46	0.12
preferred age			n=5	steps C-G	28.8	1.01				4.85	0.03
isochron age			n=12	MSWD=17.88			40/36=305.8±1.4			4.86	0.05
edited isochron age			n=8	MSWD=31.98			40/36=304.7±3.4			4.86	0.05

D	Temp (°C)	$^{40}\text{Ar}/^{39}\text{Ar}$	$^{37}\text{Ar}/^{39}\text{Ar}$	$^{36}\text{Ar}/^{39}\text{Ar}$ ($\times 10^{-3}$)	$^{39}\text{Ar}_{\text{K}}$ ($\times 10^{15}$ mol)	K/Ca	C/K ($\times 10^{-3}$)	$^{40}\text{Ar}^+$ (%)	^{39}Ar (%)	Age (Ma)	$\pm 1\sigma$ (Ma)
RA-035, groundmass concentrate (87.19 mg), J=0.001515469±0.13%, Lab#=5262 (NM-34)											
Tres Orejas - pyroxene dacite											
A	600	2301.5	0.0000	7694.9	0.0008	-	-39.178	1.2	0.0	74.17	480.15
B	700	9.725	0.4060	29.06	3.27	1.3	0.43	12.0	1.7	3.19	0.22
C	775	4.464	0.4035	9.795	2.98	1.3	0.18	35.8	3.2	4.37	0.11
D	825	2.922	0.4272	3.961	23.3	1.2	0.045	61.1	15.2	4.87	0.04
E	900	2.346	0.5063	1.980	36.3	1.0	0.15	76.7	34.0	4.91	0.02
F	1000	2.035	0.5179	1.055	72.0	0.99	0.15	86.6	71.0	4.82	0.02
G	1050	2.123	0.6629	1.377	27.2	0.77	0.17	83.2	85.0	4.83	0.02
H	1100	2.489	0.8335	2.887	9.82	0.61	0.20	68.3	90.1	4.64	0.05
I	1200	5.461	1.153	13.14	6.55	0.44	0.28	30.5	93.5	4.56	0.10
J	1300	5.515	5.240	14.17	7.67	0.097	0.58	31.4	97.4	4.74	0.11
K	1650	6.990	7.535	19.49	4.98	0.068	0.52	25.9	100.0	4.97	0.16
total gas age	n=11				194.1	0.90				4.79	0.06
preferred age	n=6				steps B-G	165.1	0.99			85.0	4.84
Isochron age	n=11				MSWD=11.63			40/36=288.4±1.3		4.86	0.05
edited isochron age	n=8				MSWD=9.25			40/36=293.8±1.6		4.84	0.01
RA-036, groundmass concentrate (80.4 mg), J=0.0004094443±0.98%, Lab#=5717 (NM-40)											
San Antonio Peak - basaltic andesite											
A	650	63.14	0.2347	196.8	6.04	2.2	0.35	7.9	9.8	3.70	0.31
B	700	31.25	0.2846	93.20	5.96	1.8	0.62	12.0	19.5	2.76	0.15
C	750	24.97	0.3765	71.70	4.56	1.4	0.41	15.3	26.9	2.81	0.12
D	825	21.41	0.4774	60.17	11.9	1.1	0.37	17.1	46.2	2.71	0.10
E	900	20.97	0.5782	58.53	11.2	0.88	0.24	17.7	64.4	2.75	0.10
F	950	26.72	0.6639	78.16	7.02	0.77	0.28	13.8	75.8	2.72	0.13
G	1000	42.53	0.7337	133.4	3.54	0.70	0.14	7.5	81.5	2.34	0.22
H	1050	76.17	0.8261	246.6	2.44	0.62	-0.099	4.4	85.5	2.48	0.39
I	1100	131.5	0.8787	433.2	1.66	0.58	0.94	2.7	88.2	2.64	0.71
J	1200	447.5	1.630	1474.5	1.79	0.31	1.6	2.7	91.1	8.77	2.66
K	1300	443.5	2.664	1450.2	4.05	0.19	1.7	3.4	97.6	11.20	2.57
L	1650	260.5	6.404	847.6	1.46	0.080	3.0	4.0	100.0	7.79	1.57
total gas age	n=12				steps B-I	61.6	1.0			3.65	0.44
plateau	n=8				MSWD=2.40	48.3	1.0	40/36=239.9±1.1		2.72	0.06
Isochron age	n=12				MSWD=0.51			40/36=293.7±1.7		2.49	0.08
edited isochron age	n=8									2.82	0.11

D	Temp (°C)	$^{40}\text{Ar}/^{39}\text{Ar}$	$^{37}\text{Ar}/^{39}\text{Ar}$	$^{36}\text{Ar}/^{39}\text{Ar}$ ($\times 10^{-3}$)	$^{39}\text{Ar}_{\text{K}}$ ($\times 10^{15}$ mol)	K/Ca	C/K ($\times 10^{-3}$)	$^{40}\text{Ar}^*$ (%)	^{39}Ar (%)	Age (Ma)	$\pm 1\sigma$ (Ma)	
RA-042, groundmass concentrate (92.9 mg), J=0.0004066171±0.98%, Lab#=5707 (NM-40)												
A	600	347.8	0.7424	1120.6	1.59	0.69	2.2	4.8	5.2	12.22	1.67	
B	700	63.24	1.136	198.6	3.25	0.45	0.31	7.3	15.9	3.41	0.32	
C	750	39.26	1.500	121.4	2.04	0.34	0.64	8.9	22.7	2.57	0.21	
D	825	30.49	2.168	92.59	4.19	0.24	0.53	10.8	36.5	2.42	0.16	
E	900	33.08	2.937	102.6	3.16	0.17	0.34	9.0	46.9	2.20	0.18	
F	950	39.45	3.499	123.0	2.05	0.15	1.0	8.6	53.7	2.49	0.23	
G	1000	44.08	3.465	139.8	1.24	0.15	-0.069	6.8	57.7	2.22	0.27	
H	1050	43.50	3.490	140.9	0.937	0.15	0.59	4.9	60.8	1.56	0.30	
I	1100	48.44	3.080	153.9	0.730	0.17	0.16	6.6	63.2	2.34	0.37	
J	1200	72.01	5.457	231.1	10.8	0.093	0.69	5.7	98.8	3.03	0.35	
K	1300	66.48	17.22	209.5	0.261	0.030	1.8	8.9	99.7	4.37	0.63	
L	1650	126.6	21.36	372.3	0.098	0.024	-0.614	14.4	100.0	13.53	2.01	
total gas age		n=12			30.3	0.22				3.27	0.36	
preferred age		n=5			steps C-G	12.7	0.21			41.8	2.38	
isochron age		n=12			MSWD=4.24			40/36=309.1±1.8			0.11	
edited isochron age		n=8			MSWD=2.03			40/36=299.6±3.4			0.12	
									1.99	0.99		
RA-045, groundmass concentrate (53.8 mg), J=0.000833809710.24%, Lab#=6144 (NM-44)												
Cerro Montosa area - basaltic andesite												
A	675	165.8	0.7620	489.4	2.60	0.67	1.2	12.8	2.9	31.74	1.59	
B	725	23.90	0.7873	38.44	3.76	0.65	0.15	52.7	7.2	18.86	0.19	
C	775	16.02	0.7625	13.69	3.20	0.67	-0.041	75.1	10.8	18.02	0.10	
D	825	13.34	0.7515	5.010	12.7	0.68	0.12	69.3	25.2	17.85	0.06	
E	875	12.60	0.6863	3.452	12.3	0.74	0.11	92.3	39.2	17.42	0.05	
F	950	12.25	0.6793	2.711	23.9	0.75	0.078	93.9	66.2	17.22	0.05	
G	1050	12.78	0.7702	4.197	18.6	0.66	0.098	90.8	87.3	17.37	0.05	
H	1200	21.42	0.8120	34.56	9.14	0.63	0.19	52.6	97.7	16.89	0.14	
I	1650	72.26	26.30	218.5	2.06	0.019	1.7	13.5	100.0	14.84	0.81	
total gas age		n=9			steps E-G	88.3	0.68				17.81	0.13
plateau		n=3			MSWD=36.46	54.9	0.72			62.1	17.33	0.07
isochron age		n=9			MSWD=36.45			40/36=304.6±1.3			17.41	0.05
edited isochron age		n=8						40/36=298.4±1.6			17.47	0.05

ID	Temp (°C)	$^{40}\text{Ar}/^{39}\text{Ar}$	$^{37}\text{Ar}/^{39}\text{Ar}$	$^{36}\text{Ar}/^{39}\text{Ar}$ ($\times 10^{-3}$)	$^{39}\text{Ar}_{\text{K}}$ ($\times 10^{15}$ mol)	K/Ca	C/K ($\times 10^{-3}$)	$^{40}\text{Ar}^*$ (%)	^{39}Ar (%)	Age (Ma)	$\pm 1\sigma$ (Ma)
RA-046, groundmass concentrate (51.8 mg), J=0.0008271055±0.24%, Lab#=6126 (NM-44)											
Pinebeloso Peaks - basaltic andesite											
A	675	187.6	1.825	590.6	0.743	0.28	1.3	7.0	3.5	19.64	2.17
B	725	23.59	1.751	70.89	0.897	0.29	0.63	11.8	7.8	4.14	0.37
C	775	10.56	1.569	30.14	0.941	0.33	0.24	16.8	12.3	2.65	0.20
D	825	5.888	1.456	14.44	3.03	0.35	-0.017	29.4	26.8	2.59	0.10
E	875	5.069	1.256	11.99	3.25	0.41	0.32	32.0	42.3	2.42	0.09
F	950	6.683	1.187	16.93	4.67	0.43	0.34	26.5	64.7	2.65	0.09
G	1050	9.331	1.393	25.78	3.03	0.37	0.59	19.5	79.1	2.72	0.13
H	1200	25.74	2.250	80.03	1.37	0.23	0.25	8.8	85.7	3.38	0.44
I	1650	45.13	9.538	142.0	3.00	0.053	0.78	8.6	100.0	5.84	0.53
total gas age		n=9			20.9	0.32				3.79	0.28
plateau		n=6		steps C-H	16.3	0.38				2.58	0.08
isochron age		n=9		MSWD=1.14			40/36=312.8±1.6			2.14	0.07
edited isochron age		n=6		MSWD=0.55			40/36=304.8±3.7			2.34	0.10
RA-047, groundmass concentrate (114.17 mg), J=0.0008378725±0.24%, Lab#=6094 (NM-44)											
Los Mogotes - tholeiitic basalt											
A	650	5633.1	0.2902	18020.6	0.077	1.8	45.3	5.5	0.2	414.30	156.60
B	700	416.8	0.5996	1308.3	0.460	0.85	5.0	7.3	1.6	45.15	3.95
C	775	137.8	1.370	433.0	1.84	0.37	0.70	7.2	7.0	14.98	1.06
D	825	41.64	2.610	130.7	11.3	0.20	0.57	7.7	40.6	4.87	0.26
E	875	17.47	5.326	54.38	10.2	0.096	0.56	10.4	70.6	2.75	0.14
F	950	13.17	9.213	42.14	4.69	0.055	0.61	10.8	84.4	2.17	0.13
G	1000	16.24	10.34	53.37	1.37	0.049	0.49	7.8	88.5	1.93	0.22
H	1100	15.79	7.696	48.68	1.38	0.066	1.2	12.7	92.6	3.04	0.24
I	1200	27.79	31.68	95.62	1.21	0.016	1.4	7.1	96.1	3.04	0.40
J	1300	26.50	97.15	106.7	1.02	0.005	1.5	9.1	99.2	3.92	0.40
K	1650	30.27	62.86	111.9	0.287	0.008	0.32	6.7	100.0	3.22	0.95
total gas age		n=11			33.8	0.14				5.59	0.70
plateau		none		N/A			N/A			N/A	
isochron age		n=11		MSWD=2.72			40/36=316.5±1.2			0.91	0.10
edited isochron age		n=7		MSWD=4.47			40/36=314.0±3.1			1.06	0.16

D	Temp (°C)	$^{40}\text{Ar}/^{39}\text{Ar}$	$^{37}\text{Ar}/^{39}\text{Ar}$	$^{36}\text{Ar}/^{39}\text{Ar}$ ($\times 10^{-3}$)	$^{39}\text{Ar}_K$ ($\times 10^{-15}$ mol)	K/Ca	C/K ($\times 10^{-3}$)	$^{40}\text{Ar}^*$ (%)	^{39}Ar (%)	Age (Ma)	$\pm 1\sigma$ (Ma)
RA-048, groundmass concentrate (61.04 mg), J=0.000838266±0.24%, Lab#=6111 (NM-44)											
Los Mogotes - tholeiitic basalt											
A	675	1107.6	1.550	35397.5	0.040	0.33	43.2	5.6	0.1	752.36	597.76
B	725	282.7	2.480	874.9	1.55	0.21	2.1	8.6	4.3	36.51	2.85
C	775	118.5	2.535	369.5	0.533	0.20	2.3	8.0	5.7	14.30	1.41
D	825	33.80	2.433	98.19	4.79	0.21	0.34	14.7	18.5	7.51	0.34
E	875	23.96	2.270	66.98	4.68	0.22	0.095	18.1	31.1	6.57	0.24
F	950	23.04	2.038	63.97	7.26	0.25	0.35	18.6	50.5	6.49	0.22
G	1050	21.98	1.534	60.74	7.31	0.33	0.23	18.9	70.1	6.26	0.21
H	1200	38.14	1.522	111.7	8.02	0.34	0.74	13.7	91.6	7.92	0.36
I	1650	357.7	19.69	1113.5	3.12	0.026	4.0	8.4	100.0	45.66	3.95
total gas age		n=9			37.3	0.26				12.33	1.35
plateau		n=3		steps E-G	19.3	0.28		51.6	6.43	0.16	
isochron age		n=9		MSWD=0.67	40/36=318.3±1.5			4.22	0.21		
edited isochron age		n=6		MSWD=0.17	40/36=313.9±2.7			4.70	0.32		
RA-049, groundmass concentrate (107.22 mg), J=0.0008375459±0.24%, Lab#=6101 (NM-44)											
Los Mogotes - tholeiitic basalt											
A	650	90512.6	4.051	284509.7	0.049	0.13	628.1	7.1	0.1	3,351.55	3,980.66
B	700	1689.6	0.9002	5210.4	0.047	0.57	31.8	8.9	0.1	213.67	68.61
C	775	283.8	1.176	887.2	1.19	0.43	2.8	7.6	1.3	32.49	2.04
D	825	36.63	1.644	106.9	38.4	0.31	0.35	14.1	41.1	7.81	0.23
E	875	39.73	1.719	118.4	10.6	0.30	0.32	12.2	52.1	7.34	0.26
F	950	52.15	2.290	159.5	9.51	0.22	0.23	10.0	61.9	7.86	0.37
G	1000	68.70	2.727	214.0	4.38	0.19	0.14	8.3	66.4	8.56	0.52
H	1100	73.75	2.630	231.7	5.74	0.19	0.35	7.4	72.4	8.29	0.55
I	1200	181.4	2.645	578.4	9.90	0.19	0.99	5.9	82.6	16.03	1.18
J	1300	128.2	11.67	404.4	16.6	0.044	1.7	7.5	99.8	14.63	0.95
K	1650	309.2	21.93	996.2	0.151	0.023	1.5	5.3	100.0	25.20	6.68
total gas age		n=11			96.6	0.23				11.98	2.60
plateau		n=5		steps D-H	68.6	0.28			71.0	7.76	0.23
isochron age		n=11		MSWD=4.42	40/36=310.4±1.0			4.76	0.26		
edited isochron age		n=5		MSWD=0.96	40/36=299.8±2.4			6.87	0.50		

ID	Temp (°C)	$^{40}\text{Ar}/^{39}\text{Ar}$	$^{37}\text{Ar}/^{39}\text{Ar}$ ($\times 10^{-3}$)	$^{36}\text{Ar}/^{39}\text{Ar}$ ($\times 10^{-3}$)	$^{39}\text{Ar}_{\text{K}}$ ($\times 10^{-15}$ mol)	K/Ca	C/U ($\times 10^{-3}$)	$^{40}\text{Ar}^*$ (%)	^{39}Ar (%)	Age (Ma)	$\pm 1\sigma$ (Ma)
RA-050, groundmass concentrate (50.6 mg), J=0.0008270898±0.24%, Lab#=6129 (NM-44)											
Los Mogotes - tholeiitic basalt											
A	675	474.1	1.275	1510.9	0.556	0.40	-0.385	5.8	0.9	40.92	5.08
B	725	15.49	1.051	41.91	2.89	0.49	0.42	20.6	5.4	4.75	0.19
C	775	8.221	0.9148	17.11	1.11	0.56	0.048	39.3	7.1	4.82	0.14
D	825	5.583	0.8042	7.826	10.6	0.63	0.058	59.7	23.7	4.97	0.04
E	875	4.216	0.6226	3.401	11.8	0.82	0.11	77.3	42.2	4.86	0.03
F	950	3.807	0.6368	2.142	17.1	0.80	0.17	84.7	68.8	4.80	0.02
G	1050	4.041	0.8553	2.843	7.80	0.60	0.23	80.8	81.0	4.87	0.03
H	1200	6.077	1.338	10.18	9.37	0.38	0.15	52.2	95.7	4.73	0.06
I	1650	22.22	19.75	67.99	2.76	0.026	0.99	16.4	100.0	5.52	0.27
total gas age		n=9			63.9	0.63				5.18	0.10
plateau		n=4		steps E-H	46.0	0.69				4.93	0.03
isochron age		n=9		MSWD=6.15			40/36=304.0±1.4			4.79	0.26
edited isochron age		n=5		MSWD=6.80			40/36=300.8±3.6			4.81	0.50
RA-051, groundmass concentrate (51.4 mg), J=0.0008375772±0.24%, Lab#=6092 (NM-44)											
Los Mogotes - tholeiitic basalt											
A	675	399.6	2.411	1255.3	1.63	0.21	2.9	7.2	3.4	43.16	4.17
B	725	39.12	2.273	110.8	3.04	0.22	0.25	16.7	9.7	9.88	0.39
C	775	15.72	2.168	39.07	3.91	0.24	0.43	27.6	17.9	6.56	0.16
D	825	10.01	1.978	21.18	8.87	0.26	0.19	39.0	36.4	5.89	0.08
E	900	14.86	1.362	36.07	10.0	0.37	0.27	29.0	57.2	6.50	0.14
F	950	26.69	1.049	72.43	6.17	0.49	0.34	20.1	70.1	8.10	0.26
G	1050	24.27	1.179	64.51	6.11	0.43	0.41	21.8	82.8	7.99	0.24
H	1200	20.18	2.581	48.93	4.17	0.20	0.32	29.3	91.5	8.94	0.19
I	1650	108.4	18.93	329.7	4.10	0.027	1.3	11.4	100.0	18.87	1.18
total gas age		n=9			48.0	0.30				9.51	0.41
plateau		none		N/A			N/A			N/A	
isochron age		n=9		MSWD=13.81			40/36=324.2±1.4			5.15	0.09
edited isochron age		n=7		MSWD=1.86			40/36=321.0±1.6			5.19	0.10

D	Temp (°C)	$^{40}\text{Ar}/^{39}\text{Ar}$	$^{37}\text{Ar}/^{39}\text{Ar}$	$^{36}\text{Ar}/^{39}\text{Ar}$ ($\times 10^{-3}$)	$^{39}\text{Ar}_K$ ($\times 10^{-15}$ mol)	K/Ca	C/K ($\times 10^{-3}$)	$^{40}\text{Ar}^*$ (%)	^{39}Ar (%)	Age (Ma)	$\pm 1\sigma$ (Ma)
RA-052, groundmass concentrate (52.8 mg), J=0.00008363078±0.24%, Lab#=6140 (NM-44)											
A	675	27.73	0.9716	80.71	3.99	0.53	0.34	14.3	5.4	5.96	0.33
B	725	5.047	0.9422	6.753	5.30	0.54	0.014	61.9	12.6	4.71	0.04
C	775	4.164	0.8173	3.805	4.73	0.62	0.27	74.5	19.0	4.68	0.04
D	825	3.607	0.6820	1.720	17.6	0.75	0.29	87.4	43.0	4.75	0.02
E	875	3.406	0.5683	1.026	14.1	0.90	0.24	92.4	62.1	4.74	0.02
F	950	3.422	0.8295	1.116	14.8	0.62	0.18	92.2	82.2	4.76	0.02
G	1050	3.754	2.079	2.500	6.19	0.25	0.20	84.6	90.6	4.79	0.03
H	1200	6.753	1.8666	13.13	4.68	0.27	0.47	44.7	97.0	4.55	0.07
I	1650	27.59	30.50	87.31	2.22	0.017	1.1	15.0	100.0	6.37	0.37
total gas age		n=9			73.7	0.62				4.85	0.06
plateau		n=6		steps B-G	62.8	0.67				4.75	0.01
isochron age		n=9		MSWD=7.08			40/36=310.0±1.6			4.74	0.01
edited isochron age		n=8		MSWD=7.54			40/36=298.7±1.9			4.74	0.01
RA-055, groundmass concentrate (54.15 mg), J=0.00008296375±0.24%, Lab#=6119 (NM-44)											
Mesa Vibora - basalt											
A	675	88.79	0.4053	282.2	13.1	1.3	0.68	6.1	20.9	8.11	0.62
B	725	27.69	0.5902	83.79	14.2	0.86	0.41	10.8	43.7	4.45	0.19
C	775	20.52	1.009	59.38	10.3	0.51	0.52	14.8	60.1	4.55	0.15
D	825	17.30	1.731	48.50	10.9	0.29	0.54	17.9	77.4	4.64	0.12
E	875	18.05	2.249	52.13	5.74	0.23	0.19	15.6	86.6	4.22	0.15
F	950	23.36	2.448	70.79	3.35	0.21	0.29	11.3	91.9	3.95	0.21
G	1050	32.68	1.831	105.5	1.37	0.28	0.55	5.0	94.1	2.46	0.34
H	1200	62.10	2.362	201.5	1.67	0.22	0.30	4.4	96.8	4.08	0.61
I	1650	46.08	15.72	136.5	2.00	0.032	1.6	15.1	100.0	10.49	0.44
total gas age		n=9		steps B-E	62.6	0.64				5.36	0.28
plateau		n=4		MSWD=34.01	41.1	0.54				4.49	0.12
isochron age		n=9		MSWD=3.85			40/36=306.1±1.4			3.51	0.13
edited isochron age		n=5					40/36=291.8±3.7			4.75	0.31

D	Temp (°C)	$^{40}\text{Ar}/^{39}\text{Ar}$	$^{37}\text{Ar}/^{39}\text{Ar}$	$^{36}\text{Ar}/^{39}\text{Ar}$ ($\times 10^{-3}$)	$^{39}\text{Ar}_{\text{K}}$ ($\times 10^{15}$ mol)	K/Ca	Cl/K ($\times 10^{-3}$)	$^{40}\text{Ar}^*$ (%)	^{39}Ar (%)	Age (Ma)	$\pm 1\sigma$ (Ma)
RA-056, groundmass concentrate (54.6 mg), J=0.00008313663±0.24%, Lab#=6151 (NM-44)											
Mesa Vibora - basalt											
A	675	124.3	0.5802	394.3	5.50	0.88	0.95	6.3	8.3	11.75	1.28
B	725	32.48	0.7972	98.29	6.43	0.64	0.48	10.8	18.0	5.24	0.33
C	775	22.08	1.037	63.57	6.54	0.49	0.34	15.3	28.0	5.05	0.21
D	825	17.49	1.269	49.28	10.5	0.40	0.47	17.3	43.9	4.53	0.16
E	875	15.50	1.246	42.09	9.73	0.41	0.23	20.4	58.6	4.73	0.15
F	950	14.40	1.216	39.05	11.0	0.42	0.36	20.5	75.3	4.42	0.14
G	1050	18.83	1.165	53.77	6.89	0.44	0.46	16.1	85.7	4.55	0.20
H	1200	63.72	2.681	201.9	3.49	0.19	0.79	6.7	91.0	6.40	0.66
I	1650	75.87	4.773	160.8	5.93	0.11	0.71	37.9	100.0	42.71	0.57
total gas age		n=9			66.1	0.44				8.79	0.34
plateau		n=6			51.2	0.45				77.4	0.13
isochron age		n=9			MSWD=363.09		40/36=376.0±1.9			-1.10	0.02
edited isochron age		n=7			MSWD=0.83		40/36=303.8±2.3			4.03	0.19
RA-058, groundmass concentrate (55.42 mg), J=0.00008382953±0.24%, Lab#=6106 (NM-44)											
Mesa Vibora - basalt											
A	700	-93.1223	12.35	-635.1240	-0.001	0.041	-106.145	%-102.6	0.0	140.11	217.09
B	700	122.0	0.2926	387.6	6.52	1.7	0.82	6.1	8.5	11.29	0.82
C	775	25.20	0.4937	75.08	19.7	1.0	0.55	12.1	34.3	4.61	0.16
D	825	17.35	0.8010	49.25	13.3	0.64	0.42	16.5	51.7	4.32	0.12
E	875	16.55	0.9522	46.55	15.2	0.54	0.30	17.3	71.6	4.33	0.11
F	950	17.06	0.9151	48.82	10.3	0.56	0.19	15.8	85.1	4.09	0.12
G	1000	17.13	0.8499	48.15	4.34	0.60	0.15	17.3	90.8	4.49	0.16
H	1100	14.28	0.9753	40.28	1.85	0.52	0.58	17.2	93.2	3.71	0.20
I	1200	17.40	2.038	49.67	1.91	0.25	1.1	16.5	95.7	4.35	0.19
K	1650	18.07	7.510	43.41	3.27	0.068	1.3	32.2	100.0	8.83	0.13
total gas age		n=10			76.3	0.76				5.15	0.19
plateau		n=5			steps C-G	62.7	0.72			82.2	0.10
isochron age		n=10			MSWD=181.68		40/36=308.2±1.5			4.09	0.08
edited isochron age		n=7			MSWD=1.36		40/36=308.4±1.6			3.34	0.13

D	Temp (°C)	$^{40}\text{Ar}/^{39}\text{Ar}$	$^{37}\text{Ar}/^{39}\text{Ar}$	$^{36}\text{Ar}/^{39}\text{Ar}$ ($\times 10^{-3}$)	$^{39}\text{Ar}_{\text{K}}$ ($\times 10^{15}$ mol)	K/Ca	C/K ($\times 10^{-3}$)	$^{40}\text{Ar}^*$ (%)	^{39}Ar (%)	Age (Ma)	$\pm 1\sigma$ (Ma)
RA-060, groundmass concentrate (87.88 mg), J=0.0008298317±0.24%, Lab#=6120 (NM-44)											
Rinconada - Servilleta Basalt											
A	675	1670.6	1.404	5277.4	0.567	0.36	13.1	6.7	3.9	159.39	20.40
B	725	121.0	2.889	379.5	2.55	0.18	1.4	7.5	21.5	13.55	1.23
C	775	65.36	4.277	201.0	1.20	0.12	1.6	9.6	29.8	9.42	0.74
D	825	37.58	8.762	112.3	3.57	0.058	0.67	13.5	54.4	7.60	0.43
E	875	29.60	14.62	91.12	1.61	0.035	0.54	12.8	65.5	5.73	0.38
F	950	33.34	18.23	102.5	1.70	0.028	1.2	13.3	77.2	6.73	0.41
G	1050	39.35	20.29	124.5	1.22	0.025	0.47	10.5	85.6	6.25	0.49
H	1200	127.0	20.94	401.2	0.877	0.024	3.1	7.9	91.7	15.23	1.52
I	1650	300.6	83.96	961.4	1.21	0.006	5.5	7.6	100.0	36.17	3.40
total gas age		n=9			14.5	0.081				17.16	1.75
plateau		none			N/A	N/A				N/A	N/A
isochron age		n=9				MSWD=1.40	40/36=315.8±1.5			3.39	0.32
editted Isochron age		n=7				MSWD=1.72	40/36=314.1±2.2			3.69	0.41
RA-061, groundmass concentrate (52.1 mg), J=0.00083337798±0.24%, Lab#=6145 (NM-44)											
Rinconada - Servilleta Basalt											
A	675	103.1	1.600	322.8	4.05	0.32	0.65	7.6	26.7	11.79	1.07
B	725	30.17	2.718	89.25	2.87	0.19	0.55	13.3	45.6	6.03	0.32
C	775	18.89	4.751	54.44	1.76	0.11	0.70	16.7	57.1	4.77	0.26
D	825	13.20	8.026	36.81	1.70	0.064	0.70	22.2	68.3	4.43	0.25
E	875	10.24	11.74	30.41	1.13	0.043	0.69	21.1	75.8	3.27	0.20
F	950	10.03	14.35	29.12	1.15	0.036	0.37	25.2	83.4	3.83	0.19
G	1050	11.12	13.68	32.69	0.923	0.037	0.47	22.6	89.4	3.81	0.22
H	1200	21.53	16.23	65.77	0.587	0.031	-0.327	15.5	93.3	5.08	0.41
I	1650	38.07	57.25	126.7	1.02	0.009	1.1	13.2	100.0	7.87	0.60
total gas age		n=9			15.2	0.15				6.82	0.53
plateau		none			N/A	N/A				N/A	N/A
isochron age		n=9				MSWD=2.82	40/36=318.9±1.9			2.81	0.13
editted Isochron age		n=6				MSWD=2.65	40/36=324.5±5.4			2.55	0.26

D	Temp (°C)	$^{40}\text{Ar}/^{39}\text{Ar}$	$^{37}\text{Ar}/^{39}\text{Ar}$	$^{36}\text{Ar}/^{39}\text{Ar}$ ($\times 10^{-3}$)	$^{39}\text{Ar}_K$ ($\times 10^{-15}$ mol)	K/Ca	C/K ($\times 10^{-3}$)	$^{40}\text{Ar}^*$ (%)	^{39}Ar (%)	Age (Ma)	$\pm 1\sigma$ (Ma)
RA-062, groundmass concentrate (51.48 mg), J=0.00008362847±0.24%, Lab# =6108 (NM-44)											
Cerro Negro - pyroxene dacite											
A	675	125.8	0.3936	391.7	5.54	1.3	1.2	8.0	13.8	15.19	1.30
B	725	42.93	0.5213	129.4	5.32	0.98	0.64	11.0	27.1	7.16	0.44
C	775	32.39	0.7074	96.88	3.96	0.72	0.56	11.8	36.9	5.76	0.37
D	825	28.39	0.9135	82.77	6.06	0.56	0.62	14.1	52.0	6.05	0.29
E	875	28.56	1.006	84.92	5.38	0.51	0.26	12.4	65.4	5.36	0.28
F	950	28.80	1.086	85.27	5.55	0.47	0.45	12.8	79.2	5.58	0.29
G	1050	30.88	1.209	89.47	2.93	0.42	0.50	14.7	86.5	6.85	0.35
H	1200	53.40	1.324	165.5	1.97	0.39	1.2	8.6	91.5	6.96	0.61
/	1650	39.53	5.182	112.9	3.43	0.098	0.73	16.6	100.0	9.96	0.52
total gas age		n=9			40.1	0.66				7.71	0.50
plateau		n=4			steps C-F	21.0	0.55			52.2	0.22
isochron age		n=9			MSWD=7.59			40/36=316.3±2.5		3.29	0.29
edited isochron age		n=6			MSWD=2.62			40/36=300.3±4.4		4.07	0.55
RA-064, groundmass concentrate (57.96 mg), J=0.00008348983±0.24%, Lab# =6114 (NM-44)											
Hondo roadcut - pyroxene dacite											
A	675	38.49	0.2326	113.4	12.5	2.2	0.22	13.0	9.1	7.54	0.25
B	725	5.446	0.2238	7.021	15.1	2.3	0.068	62.2	20.1	5.10	0.03
C	775	4.224	0.2672	3.091	13.3	1.9	0.071	78.9	29.7	5.01	0.02
D	825	3.810	0.3568	2.189	25.3	1.4	0.11	83.7	48.1	4.80	0.01
E	875	3.696	0.5239	1.983	18.8	0.97	0.15	85.2	61.7	4.74	0.02
F	950	4.005	0.7702	2.904	16.6	0.66	0.24	80.0	73.7	4.83	0.02
G	1050	4.295	0.6668	4.151	13.2	0.77	0.30	72.6	83.3	4.69	0.03
H	1200	5.263	0.3055	6.770	18.3	1.7	0.26	62.4	96.6	4.94	0.04
/	1650	17.36	2.289	32.76	4.71	0.22	0.42	45.2	100.0	11.81	0.21
total gas age		n=9			steps B-H	137.9	1.4			5.34	0.05
preferred age		n=7			MSWD=130.72			40/36=332.1±1.5		4.84	0.05
isochron age		n=9			MSWD=39.30			40/36=323.7±8.5		4.67	0.01
edited isochron age		n=5								4.70	0.03

D	Temp (°C)	$^{40}\text{Ar}/^{39}\text{Ar}$	$^{37}\text{Ar}/^{39}\text{Ar}$	$^{36}\text{Ar}/^{39}\text{Ar}$ ($\times 10^{-3}$)	$^{39}\text{Ar}_{\text{K}}$ ($\times 10^{-15}$ mol)	K/Ca	Cu/K ($\times 10^{-3}$)	$^{40}\text{Ar}^*$ (%)	^{39}Ar (%)	Age (Ma)	t1σ (Ma)
RA-065, groundmass concentrate (51.4 mg), J=0.0008271108±0.24%, Lab#=6125 (NM-44)											
Hondo roadcut - pyroxene dacite											
A	675	82.66	0.2081	257.0	16.9	2.5	0.60	8.2	26.4	10.04	0.82
B	725	28.61	0.2804	83.83	15.5	1.8	0.52	13.5	50.6	5.75	0.27
C	775	19.52	0.4584	53.99	9.88	1.1	0.33	18.5	66.0	5.37	0.18
D	825	13.18	0.9549	33.29	12.4	0.53	0.52	25.9	85.4	5.10	0.12
E	875	9.268	1.900	20.04	5.39	0.27	0.41	37.8	93.8	5.24	0.10
F	950	8.071	3.658	17.40	2.26	0.14	0.30	39.8	97.3	4.80	0.12
G	1050	10.24	5.704	26.60	0.664	0.089	1.3	27.5	98.3	4.21	0.23
H	1200	7.601	5.952	22.14	0.468	0.086	1.2	19.9	99.1	2.27	0.36
I	1650	36.29	22.83	100.4	0.592	0.022	2.5	23.1	100.0	12.65	0.60
total gas age		n=9			64.0	1.4				6.64	0.35
plateau		n=4		steps B-E	MSWD=30.40	1.1				6.24	0.12
isochron age		n=9			MSWD=1.47		40/36=314.6±1.7			4.25	0.08
edited isochron age		n=4					40/36=299.8±2.5			5.03	0.14
RA-072, groundmass concentrate (54.83 mg), J=0.00077291±0.26%, Lab#=6990 (NM-54)											
northern Rio Grande gorge - Servilleta Basalt											
A	550	13.30	0.0000	40.76	0.551	-	0.90	9.4	1.3	1.74	0.25
B	650	6.682	0.1422	17.41	4.18	3.6	0.59	23.2	11.0	2.16	0.07
C	750	7.576	0.2348	18.76	6.12	2.2	0.37	27.0	25.3	2.85	0.07
D	825	9.017	0.5227	20.49	20.1	0.98	0.35	33.3	72.0	4.18	0.06
E	875	9.572	1.131	20.61	6.97	0.45	0.14	37.3	88.3	4.97	0.07
F	950	10.28	2.339	21.21	3.06	0.22	0.39	40.8	95.4	5.85	0.09
G	1000	13.88	3.211	31.90	0.682	0.16	0.45	33.9	97.0	6.56	0.21
H	1050	23.03	2.490	53.71	0.471	0.20	0.40	31.9	98.1	10.24	0.35
I	1100	34.78	1.901	92.67	0.271	0.27	1.9	21.7	98.7	10.51	0.56
J	1200	36.82	4.443	101.4	0.262	0.11	2.8	19.5	99.3	10.03	0.61
K	1300	34.37	23.02	113.8	0.079	0.022	2.9	7.3	99.5	3.56	1.15
L	1650	25.50	17.95	66.26	0.223	0.028	1.5	28.6	100.0	10.28	0.64
total gas age		n=12			43.0	1.2				4.22	0.08
plateau		none		N/A	N/A	N/A				N/A	N/A
isochron age		n=12			MSWD=122.33		40/36=412.1±3.9			0.65	0.02
edited isochron age		n=8			MSWD=24.83		40/36=354.3±3.6			3.72	0.11

D	Temp (°C)	$^{40}\text{Ar}/^{39}\text{Ar}$	$^{37}\text{Ar}/^{39}\text{Ar}$	$^{36}\text{Ar}/^{39}\text{Ar}$ ($\times 10^{-3}$)	$^{38}\text{Ar}_{\text{K}}$ ($\times 10^{-15}$ mol)	K/Ca	C/K ($\times 10^{-3}$)	$^{40}\text{Ar}^*$ (%)	$^{39}\text{Ar}_\text{f}$ (%)	Age (Ma)	$\pm 1\sigma$ (Ma)
RA-076, groundmass concentrate (54.80 mg), J=0.0008382902±0.24%, Lab#=6107 (NM-44)											
A	675	176.8	2.672	553.1	2.54	0.19	1.2	7.7	18.4	20.39	1.73
B	725	43.30	3.997	131.1	2.16	0.13	0.90	11.3	34.0	7.39	0.50
C	775	23.49	4.945	70.73	1.42	0.10	1.3	12.6	44.2	4.50	0.32
D	825	13.62	5.091	37.25	2.21	0.10	0.68	22.1	60.3	4.55	0.24
E	875	12.10	4.970	33.69	1.69	0.10	0.045	20.8	72.5	3.82	0.20
F	950	16.05	5.716	44.71	1.48	0.089	0.56	20.4	83.1	4.96	0.25
G	1050	31.64	8.204	99.14	0.658	0.062	0.12	9.4	87.9	4.51	0.50
H	1200	49.87	12.61	154.3	0.416	0.040	2.4	10.5	90.9	7.97	0.81
I	1650	92.17	40.83	288.8	1.26	0.012	2.6	10.8	100.0	15.47	1.32
total gas age		n=9	none	N/A	N/A	0.11				8.95	0.70
plateau		n=9	none	N/A	MSWD=4.92					N/A	N/A
isochron age		n=6	MSWD=4.48				40/36=317.0±1.6			2.98	0.65
edited isochron age							40/36=301.9±4.3			3.95	0.29
RA-079, groundmass concentrate (54.56 mg), J=0.000773038±0.26%, Lab#=6991 (NM-54)											
Cerro Mojino - Servilleta Basalt											
A	550	190.0	0.1239	622.6	0.147	4.1	0.70	3.2	0.3	8.36	3.10
B	650	15.80	0.3191	46.97	1.14	1.6	1.1	12.3	3.0	2.71	0.22
C	750	6.346	0.4008	12.50	2.34	1.3	0.26	42.3	8.4	3.74	0.07
D	825	4.365	0.8417	4.608	13.4	0.61	0.12	70.3	39.4	4.28	0.07
E	875	4.406	1.285	4.612	7.12	0.40	0.20	71.3	55.9	4.38	0.02
F	950	4.939	1.668	6.509	6.20	0.31	0.15	63.6	70.2	4.38	0.03
G	1000	6.400	1.856	11.46	2.11	0.27	0.27	49.3	75.1	4.40	0.08
H	1050	8.577	1.414	19.31	2.54	0.36	0.61	34.7	81.0	4.15	0.08
I	1100	11.79	1.245	29.78	2.57	0.41	0.44	26.2	86.9	4.30	0.11
J	1200	17.91	2.349	50.02	2.67	0.22	0.50	18.5	93.1	4.62	0.16
K	1300	13.13	11.43	37.10	1.74	0.045	0.29	23.2	97.1	4.27	0.14
L	1650	11.77	10.50	30.13	1.24	0.049	0.71	31.2	100.0	5.15	0.21
total gas age		n=12	steps D-I	43.2	0.50					4.30	0.08
prefered age		n=6	MSWD=17.67	33.9	0.45					4.32	0.03
isochron age		n=12	MSWD=6.69				40/36=293.7±1.2			4.33	0.02
edited isochron age		n=9	MSWD=6.69				40/36=297.7±1.5			4.32	0.02

D	Temp (°C)	$^{40}\text{Ar}/^{39}\text{Ar}$	$^{37}\text{Ar}/^{39}\text{Ar}$	$^{39}\text{Ar}/^{39}\text{Ar}_{\text{f}}$ ($\times 10^{-3}$)	$^{39}\text{Ar}/^{39}\text{Ar}_{\text{f}}$ ($\times 10^{-15}$ mol)	K/Ca	C/K ($\times 10^{-3}$)	$^{40}\text{Ar}^*$ (%)	$^{39}\text{Ar}_{\text{f}}$ (%)	Age (Ma)	$\pm \Delta$ (Ma)
RA-080, groundmass concentrate (63.86 mg), J=0.000773097±0.26%, Lab#=6992 (NM-54)											
A	550	-22:09.3100	7.816	-75184.8600	-0.010	0.065	-123.584	0.9	0.0	-290.93	4,926.92
B	650	456.7	1.343	1525.4	0.414	0.38	2.3	1.3	0.8	8.42	5.02
C	750	98.45	1.270	321.0	0.549	0.40	0.26	3.7	1.9	5.14	1.01
D	825	16.68	0.8566	44.68	11.9	0.60	0.11	21.2	26.0	4.94	0.12
E	875	13.40	0.8051	34.12	7.88	0.63	0.11	25.2	41.9	4.71	0.10
F	950	53.07	1.198	164.8	7.80	0.43	0.25	8.4	57.7	6.20	0.43
G	1000	23.27	1.458	67.00	3.07	0.35	0.25	15.4	64.0	5.00	0.21
H	1050	16.15	1.263	42.61	3.50	0.40	0.17	22.6	71.0	5.10	0.14
I	1100	14.91	1.064	38.96	2.54	0.48	0.16	23.3	76.2	4.84	0.13
J	1200	20.46	1.775	59.30	2.33	0.29	0.38	15.0	60.9	4.29	0.18
K	1300	38.62	6.409	119.3	7.71	0.080	0.78	10.0	96.5	5.41	0.29
L	1650	43.48	10.09	136.9	1.71	0.051	0.50	8.8	100.0	5.35	0.46
Total gas age plateau		n=12	none	N/A	49.4	0.42	N/A	N/A	5.26	0.72	N/A
Isochron age		n=12	none	N/A	MSWD=2.28	40/36=299.1±1.2	N/A	N/A	4.63	0.09	
RA-082, groundmass concentrate (55.16 mg), J=0.00077303±0.26%, Lab#=6993 (NM-54)											
A	550	628.6	0.0000	2082.9	0.027	-	-7.387	2.1	0.1	18.26	32.16
B	650	13.40	1.720	39.61	0.405	0.30	0.66	13.6	2.0	2.54	0.33
C	750	4.517	2.045	11.93	0.820	0.25	0.17	25.5	5.7	1.60	0.12
D	825	2.673	2.235	4.674	6.61	0.23	0.10	54.8	35.9	2.04	0.03
E	875	2.486	2.026	3.712	4.29	0.25	0.017	62.1	55.5	2.16	0.03
F	950	2.674	2.387	4.613	4.00	0.21	0.16	55.9	73.8	2.09	0.03
G	1000	3.797	3.531	9.214	1.20	0.14	0.32	35.4	79.3	1.88	0.09
H	1050	5.799	3.689	15.66	0.857	0.14	0.31	25.1	83.2	2.03	0.14
I	1100	8.658	3.505	27.45	0.423	0.15	0.17	9.4	85.1	1.14	0.23
J	1200	11.11	9.318	35.55	0.629	0.055	0.41	11.9	88.0	1.86	0.24
K	1300	7.282	19.23	24.55	2.12	0.027	0.81	20.6	97.7	2.12	0.09
L	1650	16.15	16.62	42.36	0.503	0.031	0.033	30.4	100.0	6.91	0.40
Total gas age plateau		n=12	steps D-F	21.9	0.19	N/A	N/A	2.17	0.12	N/A	
Isochron age		n=3	MSWD=27.69	14.9	0.23	N/A	N/A	68.1	2.10	0.04	0.02
Sedimented Isochron age		n=12	MSWD=287.4±3.3	N/A	N/A	N/A	N/A	40/36=302.0±1.9	2.05	0.02	0.02

D	Temp	$^{40}\text{Ar}/^{39}\text{Ar}$	$^{37}\text{Ar}/^{39}\text{Ar}$	$^{39}\text{Ar}/^{39}\text{Ar}$ ($\times 10^{-3}$)	$^{39}\text{Ar}_{\text{K}}$ ($\times 10^{-15}$ mol)	K/Ca	C/K ($\times 10^{-3}$)	$^{40}\text{Ar}^*$ (%)	^{39}Ar (%)	Age (Ma)	$\pm 1\sigma$ (Ma)
RA-083, groundmass concentrate (59.18 mg), J=0.0007728902±0.26%, Lab#=6994 (NM-54)											
Ute Mountain - pyroxene dacite											
A	550	87.09	0.0000	287.9	0.075	-	-1.926	2.3	0.8	2.82	2.34
B	650	7.710	0.6797	26.55	0.695	0.75	0.17	-1.1	7.9	-0.12	0.19
C	750	6.501	1.523	22.70	1.00	0.34	0.71	-1.4	18.1	-0.12	0.13
D	825	6.962	3.766	23.89	4.20	0.14	0.27	2.7	61.0	0.27	0.09
E	875	7.978	7.651	29.12	1.46	0.067	0.40	-0.5	75.9	-0.05	0.14
F	950	9.197	11.88	33.13	1.10	0.043	0.87	3.5	87.2	0.45	0.17
G	1000	14.63	14.51	55.07	0.398	0.035	0.77	-3.6	91.2	-0.75	0.36
H	1050	24.13	14.55	85.82	0.302	0.035	0.37	-0.5	94.3	-0.16	0.50
I	1100	45.82	13.10	156.6	0.173	0.039	1.5	1.2	96.1	0.77	1.00
J	1200	69.61	52.33	244.9	0.122	0.010	2.4	1.8	97.3	1.81	1.50
K	1300	21.20	212.8	128.3	0.107	0.002	-0.469	-1.8	98.4	-0.61	1.29
L	1650	32.86	124.3	135.5	0.156	0.004	1.1	7.3	100.0	3.64	1.25
total gas age	n=12				9.80	0.17			0.21	0.25	
plateau	n=5			steps B-F	8.47	0.19		86.4	0.11	0.12	
isochron age	n=12			MSWD=5.00			40/36=299.4±2.2		-0.04	0.01	
RA-084, groundmass concentrate (55.59 mg), J=0.000772843±0.26%, Lab#=6995 (NM-54)											
Ute Mountain - pyroxene dacite											
A	550	1313.6	0.0000	4366.3	0.031	-	-4.328	1.8	0.1	59.46	32.22
B	650	26.52	0.0000	81.91	0.474	-	-0.294	8.7	1.3	0.41	3.22
C	750	4.775	0.6290	9.672	1.28	0.81	0.54	41.2	4.7	0.08	2.74
D	825	2.498	0.5965	2.059	12.9	0.86	0.19	77.5	38.9	0.01	2.70
E	875	2.269	0.6090	1.312	7.73	0.84	0.16	85.0	59.4	0.01	2.69
F	950	2.458	0.8633	1.969	5.98	0.59	0.28	79.0	75.2	0.02	2.71
G	1000	2.633	1.386	2.669	1.83	0.37	0.36	74.1	80.1	0.05	2.72
H	1050	2.718	1.628	2.752	1.84	0.31	0.29	74.7	85.0	0.05	2.83
I	1100	2.560	1.901	2.682	1.42	0.27	0.49	74.7	88.8	0.06	2.67
J	1200	3.704	5.380	8.178	1.12	0.095	0.45	45.9	91.7	0.08	2.38
K	1300	6.228	22.10	20.85	1.80	0.023	0.73	28.3	96.5	0.10	2.50
L	1650	9.868	14.89	30.69	1.32	0.034	0.38	19.2	100.0	0.15	2.65
total gas age	n=12			steps B-G	37.7	0.64			0.11	0.12	
plateau	n=6			MSWD=5.99	30.2	0.77			0.01	0.01	
isochron age	n=12			MSWD=7.19			40/36=291.7±1.7		0.01	0.01	
edited isochron age	n=9			MSWD=296.4±2.8			40/36=291.7±1.7		0.01	0.01	

D	Temp (°C)	⁴⁰ Ar/ ³⁹ Ar	³⁷ Ar/ ³⁹ Ar	³⁶ Ar/ ³⁹ Ar (x 10 ⁻³)	³⁹ Ar/K (x 10 ¹⁵ mol)	K/Ca	C/K (x 10 ⁻³)	⁴⁰ Ar*	³⁹ Ar (%)	Age (Ma)	±1σ (Ma)
RA-085, groundmass concentrate (70.7 mg), J=0.0008363386±0.24%, Lab#=6136 (NM-44)											
Guadalupe Mountain - pyroxene dacite											
A	675	81.95	0.4810	250.8	5.70	1.1	0.76	9.6	4.2	11.85	0.81
B	725	15.93	0.4462	38.80	8.02	1.1	0.25	28.3	10.1	6.78	0.16
C	775	11.76	0.4368	25.37	3.39	1.2	0.39	36.5	12.6	6.48	0.13
D	825	6.642	0.5527	9.990	27.0	0.92	0.051	56.2	32.5	5.62	0.04
E	875	6.392	0.6687	9.742	19.9	0.76	0.13	55.8	47.2	5.37	0.04
F	950	7.788	0.8172	14.57	19.6	0.62	0.13	45.5	61.6	5.34	0.06
G	1050	13.22	0.7638	33.55	13.3	0.67	0.28	25.5	71.4	5.08	0.12
H	1200	16.01	0.3515	42.65	16.0	1.5	0.27	21.4	83.2	5.17	0.14
I	1650	31.72	0.7944	94.09	22.7	0.64	0.28	12.5	100.0	5.99	0.42
total gas age		n=9			135.6	0.87				5.85	0.17
plateau		n=5		steps E-I	91.6	0.81			67.5	5.34	0.06
isochron age		n=9			MSWD=26.50		40/36=305.8±1.4		5.30	0.04	
edited isochron age		n=6			MSWD=10.04		40/36=290.0±1.8		5.53	0.04	
RA-086, groundmass concentrate (58.54 mg), J=0.0008296439±0.24%, Lab#=6118 (NM-44)											
Guadalupe Mountain - pyroxene dacite											
A	675	1138.0	0.5246	3725.2	0.955	0.97	3.1	3.3	0.9	54.97	
B	725	56.09	0.5733	172.3	8.20	0.89	0.52	9.3	8.7	7.81	0.42
C	775	31.82	0.5380	92.32	3.47	0.95	0.30	14.4	11.9	6.84	0.26
D	825	15.88	0.5823	41.38	14.4	0.88	0.13	23.3	25.5	5.52	0.10
E	875	11.96	0.5048	29.24	12.9	1.0	0.23	28.1	37.8	5.02	0.09
F	950	12.66	0.6098	31.37	12.1	0.84	0.30	27.2	49.2	5.14	0.08
G	1050	22.69	0.6399	65.47	7.07	0.80	0.28	15.0	55.9	5.07	0.17
H	1200	71.91	0.6634	230.6	19.1	0.77	0.20	5.3	73.9	5.69	0.47
I	1650	47.40	1.612	147.4	27.6	0.32	0.56	8.4	100.0	5.92	0.51
total gas age		n=9		steps E-I	105.8	0.72				6.19	0.40
plateau		n=5			78.7	0.66				5.11	0.08
isochron age		n=9		MSWD=7.42			40/36=303.1±1.0		4.81	0.07	
edited isochron age		n=6		MSWD=3.96			40/36=298.1±1.3		5.05	0.09	

D	Temp (°C)	$^{40}\text{Ar}/^{39}\text{Ar}$	$^{37}\text{Ar}/^{39}\text{Ar}$	$^{36}\text{Ar}/^{39}\text{Ar}$ ($\times 10^{-3}$)	$^{39}\text{Ar}_{\text{K}}$ ($\times 10^{-15}$ mol)	K/Ca	C/K ($\times 10^{-3}$)	$^{40}\text{Ar}^*$ (%)	^{39}Ar (%)	Age (Ma)	$\pm 1\sigma$ (Ma)
RA-087, groundmass concentrate (37.7 mg), J=0.0008386132±0.24%, Lab#=6090 (NM-44)											
Guadalupe Mountain - pyroxene dacite											
A	725	123.0	0.3042	382.0	14.0	1.7	0.81	8.3	28.7	15.31	1.20
B	775	35.11	0.4766	102.2	12.2	1.1	0.44	14.1	53.8	7.49	0.34
C	825	23.38	0.8435	62.54	7.85	0.60	0.23	21.2	69.9	7.49	0.22
D	875	18.84	1.426	43.90	5.02	0.36	0.48	31.7	80.2	9.03	0.18
E	950	19.47	2.281	39.18	2.91	0.22	0.37	41.4	86.2	12.18	0.19
F	1000	24.01	2.210	46.90	1.11	0.23	-0.131	43.0	88.5	15.58	0.30
G	1100	26.03	1.166	42.03	1.23	0.44	0.44	52.6	91.0	20.63	0.25
H	1250	25.76	1.910	40.36	1.34	0.27	0.70	54.3	93.8	21.05	0.23
I	1650	24.39	3.498	48.38	3.02	0.15	0.62	42.5	100.0	15.65	0.24
total gas age		n=9			48.6	0.93				11.57	0.53
plateau		none			N/A	N/A				N/A	N/A
isochron age		n=9			MSWD=577.47	40/36=315.1±2.3				12.10	0.12
edited isochron age		n=4			MSWD=31.49	40/36=301.9±2.2				7.79	0.23
RA-088, groundmass concentrate (54.39 mg), J=0.0008348995±0.24%, Lab#=6117 (NM-44)											
Cerro Negro roadcut - pyroxene dacite											
A	675	83.28	0.5487	261.1	5.07	0.93	1.0	7.4	4.5	9.29	0.61
B	725	12.66	0.5083	30.89	10.6	1.0	0.19	28.2	13.9	5.37	0.08
C	775	7.464	0.5266	13.95	7.41	0.97	0.22	45.3	20.4	5.09	0.06
D	825	5.960	0.6201	9.324	19.5	0.82	0.12	54.6	37.7	4.89	0.03
E	875	5.264	0.6515	7.344	14.8	0.78	0.12	59.7	50.8	4.73	0.03
F	950	5.556	0.6907	8.340	16.2	0.74	0.045	56.6	65.2	4.73	0.04
G	1050	6.792	0.5418	12.53	14.1	0.94	0.33	46.1	77.7	4.71	0.05
H	1200	9.947	0.4790	23.47	8.21	1.1	0.26	30.6	84.9	4.59	0.08
I	1650	13.63	1.317	34.99	17.0	0.39	0.38	24.9	100.0	5.10	0.10
total gas age		n=9			steps E-H	112.9	0.80			5.09	0.08
preferred age		n=4			MSWD=10.41	0.86				4.72	0.03
isochron age		n=9			MSWD=13.64	40/36=306.5±1.2				4.64	0.03
edited isochron age		n=6				40/36=297.1±3.0				4.77	0.05

D	Temp (°C)	$^{40}\text{Ar}/^{39}\text{Ar}$	$^{37}\text{Ar}/^{39}\text{Ar}$	$^{36}\text{Ar}/^{39}\text{Ar}$ ($\times 10^{-3}$)	$^{39}\text{Ar}/\text{Ar}_K$ ($\times 10^{-15}$ mol)	K/Ca	C/K ($\times 10^{-3}$)	$^{40}\text{Ar}^*$ (%)	^{39}Ar (%)	Age (Ma)	$\pm 1\sigma$ (Ma)
RA-089, groundmass concentrate (34.39 mg), J=0.0008313692±0.24%, Lab#=6152 (NM-44)											
<i>Cerro Chileno - quartz latite</i>											
A	675	33.26	0.1375	93.69	10.8	3.7	0.42	16.8	12.3	8.37	0.27
B	725	6.457	0.1566	9.225	17.4	3.3	0.12	58.0	32.0	5.61	0.04
C	775	5.327	0.1930	5.982	15.5	2.6	0.095	67.1	49.6	5.35	0.03
D	825	5.398	0.2498	6.588	15.6	2.0	0.16	64.3	67.3	5.20	0.03
E	875	6.641	0.3051	10.80	9.65	1.7	0.18	52.3	78.3	5.20	0.05
F	950	10.57	0.3467	24.47	5.98	1.5	0.19	31.8	85.1	5.03	0.09
G	1050	18.38	0.3179	51.47	5.57	1.6	0.19	17.4	91.4	4.78	0.17
H	1200	24.05	1.147	67.92	3.37	0.44	0.68	16.9	95.2	0.23	0.23
I	1650	27.23	1.226	73.08	4.20	0.42	0.45	21.1	100.0	8.59	0.24
Total gas age		n=9			88.0	2.3				5.85	0.09
Preferred age		n=6		steps B-G	69.6	2.3				5.32	0.08
Isochron age		n=9		MSWD=41.30			40/36=309.3±1.2			5.15	0.02
Edatid isochron age		n=7		MSWD=26.07			40/36=295.5±1.5			5.33	0.03
RA-090, groundmass concentrate (51.0 mg), J=0.000827095±0.24%, Lab#=6128 (NM-44)											
<i>Cerro de la Olla - olivine andesite</i>											
A	675	783.5	0.3860	2474.9	1.05	1.3	3.7	6.7	1.7	76.30	8.37
B	725	40.08	0.4436	117.0	6.54	1.2	0.43	13.8	12.6	8.24	0.39
C	775	21.46	0.5157	58.25	2.59	0.99	-0.015	20.0	16.8	6.38	0.24
D	825	10.68	0.8915	24.92	13.7	0.57	0.25	31.7	39.5	5.04	0.09
E	875	7.883	1.207	15.64	9.48	0.42	0.27	42.5	55.2	5.00	0.07
F	950	8.289	1.653	17.23	9.14	0.31	0.10	40.1	70.3	4.96	0.07
G	1050	11.20	2.084	27.67	4.91	0.24	0.26	28.4	78.5	4.75	0.11
H	1200	19.90	2.006	56.31	6.43	0.25	0.51	17.2	89.1	5.10	0.19
I	1650	28.72	9.159	84.91	6.59	0.056	0.69	15.1	100.0	6.50	0.28
Total gas age plateau		n=9		steps D-H	43.7	0.40	40/36=312.3±1.4			72.2	4.97
Isochron age		n=9		MSWD=6.26			40/36=295.8±1.4			0.06	0.09
Edatid isochron age		n=5		MSWD=1.93			40/36=309.5±1.5			4.46	4.96

D	Temp (°C)	$^{40}\text{Ar}/^{39}\text{Ar}$	$^{37}\text{Ar}/^{39}\text{Ar}$	$^{36}\text{Ar}/^{39}\text{Ar}$ ($\times 10^{-3}$)	$^{39}\text{Ar}_{\text{K}}$ ($\times 10^{15}$ mol)	K/Ca	C/K ($\times 10^{-3}$)	$^{40}\text{Ar}^*$ (%)	^{39}Ar (%)	Age (Ma)	$\pm 1\sigma$
RA-091, groundmass concentrate (74.78 mg), J=0.0008348975±0.24%, Lab#=6112 (NM-44)											
Cerro Montoso - olivine andesite											
A	675	364.9	0.2601	1143.2	0.985	2.0	2.6	7.4	1.6	40.35	3.85
B	725	57.35	0.5454	174.0	8.25	0.94	0.51	10.4	14.7	9.00	0.55
C	775	37.29	0.6625	110.0	3.23	0.77	0.63	12.9	19.9	7.25	0.40
D	825	21.72	1.222	59.86	14.5	0.42	0.48	19.0	42.9	6.21	0.20
E	875	18.97	1.381	51.86	9.98	0.37	0.42	19.8	58.8	5.65	0.18
F	950	24.14	1.559	69.31	9.01	0.33	0.30	15.7	73.2	5.70	0.22
G	1050	52.74	1.941	164.3	4.08	0.26	0.52	8.2	79.7	6.52	0.55
H	1200	108.8	1.677	355.2	6.25	0.30	0.96	3.6	89.6	5.97	1.17
I	1650	79.42	9.862	249.1	6.51	0.052	1.0	8.3	100.0	9.91	0.79
total gas age		n=9			62.8	0.45				7.38	0.49
plateau		n=5			steps D-H	0.36				5.88	0.18
isochron age		n=9			MSWD=6.89		40/36=308.4±1.3			4.70	0.18
edited isochron age		n=6			MSWD=3.55		40/36=299.4±2.0			5.57	0.23
RA-092, groundmass concentrate (58.02 mg), J=0.0008348979±0.24%, Lab#=6113 (NM-44)											
Cerro Montoso area - pyroxene dacite											
A	675	183.7	0.9037	565.4	6.00	0.56	1.7	9.1	21.9	24.94	1.82
B	725	57.47	1.541	174.9	4.67	0.33	1.0	10.3	39.0	8.88	0.57
C	775	35.93	2.195	103.7	3.05	0.23	0.83	15.1	50.1	8.19	0.37
D	825	23.93	2.627	68.32	4.51	0.19	0.33	16.5	66.6	5.94	0.25
E	875	24.84	3.103	72.30	2.71	0.16	0.47	14.9	76.5	5.59	0.28
F	950	34.08	5.085	104.6	1.98	0.10	0.40	10.4	83.7	5.37	0.45
G	1050	63.63	6.686	203.8	1.05	0.076	0.98	6.1	87.6	5.91	0.77
H	1200	107.8	6.386	344.3	0.853	0.080	1.8	6.1	90.7	9.94	1.33
I	1650	41.08	13.12	114.8	2.55	0.039	1.1	19.9	100.0	12.37	0.44
total gas age		n=9			27.4	0.27				11.50	0.75
plateau		none			N/A					N/A	N/A
isochron age		n=9			MSWD=28.04		40/36=316.4±1.7			4.04	0.20
edited isochron age		n=4			MSWD=0.87		40/36=294.9±3.7			5.82	0.46

D	Temp (°C)	$^{40}\text{Ar}/^{39}\text{Ar}$	$^{39}\text{Ar}/^{39}\text{Ar}$ ($\times 10^{-3}$)	$^{36}\text{Ar}/^{39}\text{Ar}$ ($\times 10^{-3}$)	$^{39}\text{Ar}_{\text{K}}$ ($\times 10^{-15}$ mol)	K/Ca	Ci/K ($\times 10^{-3}$)	$^{40}\text{Ar}^*$ (%)	^{39}Ar (%)	Age (Ma)	$\pm 1\sigma$ (Ma)
RA-093, groundmass concentrate (50.76 mg), J=0.00083827788±0.24%, Lab#=6109 (NM-44)											
A	675	233.3	0.8950	740.2	3.55	0.57	1.1	6.3	24.6	22.03	2.55
B	725	83.92	1.562	261.3	2.76	0.33	0.86	8.1	43.8	10.28	0.87
C	775	65.34	2.380	204.3	1.72	0.21	0.69	7.9	55.7	7.77	0.72
D	825	54.92	3.638	170.6	2.03	0.14	1.0	8.7	69.8	7.27	0.63
E	875	52.10	4.615	159.9	1.23	0.11	0.92	10.0	78.4	7.90	0.71
F	950	44.50	6.200	139.1	1.11	0.082	0.74	8.7	86.1	5.88	0.56
G	1050	39.54	7.483	121.6	0.698	0.068	0.98	10.6	90.9	6.36	0.65
H	1200	29.45	11.42	94.85	0.419	0.045	3.2	7.8	93.8	3.50	0.71
I	1650	48.29	22.13	148.2	0.888	0.023	2.6	12.8	100.0	9.50	0.94
total gas age		n=9		14.4	0.27				11.47	1.19	
plateau		n=4	steps B-E	7.7	0.22			53.7	8.07	0.70	
Isochron age		n=9				MSWD=2.67	40/36=315.1±2.4	9.70	2.33	0.40	
edited Isochron age		n=5				MSWD=1.02	40/36=311.1±7.2	3.24	1.23		
RA-102, groundmass concentrate (51.24 mg), J=0.000770638±0.26%, Lab#=6998 (NM-54)											
Cerro de la Olla area - pyroxene dacite											
A	550	13035.8	0.1693	43602.4	0.018	3.0	24.1	1.2	0.1	198.97	1,081.68
B	650	57.54	0.8187	188.5	0.926	0.62	0.64	3.3	7.4	2.62	0.57
C	750	9.120	1.667	25.40	1.18	0.31	0.69	19.1	16.6	2.42	0.14
D	825	5.160	3.898	8.774	4.95	0.13	0.27	55.6	55.2	3.99	0.04
E	875	4.393	4.776	5.043	1.97	0.11	0.50	74.4	70.6	4.56	0.05
F	950	4.238	5.620	5.005	1.36	0.091	0.086	75.3	81.1	4.45	0.07
G	1000	4.478	5.498	6.260	0.518	0.093	0.080	68.1	85.2	4.25	0.16
H	1050	4.925	3.492	6.453	0.322	0.15	0.41	66.7	45.7	0.26	
I	1100	5.202	4.099	8.889	0.395	0.12	0.42	55.6	90.8	4.02	0.23
J	1200	6.941	14.39	17.71	0.318	0.035	0.80	40.5	93.3	3.95	0.27
K	1300	11.24	49.20	40.43	0.460	0.010	1.5	27.3	96.9	4.41	0.29
L	1650	54.69	50.94	184.0	0.404	0.010	0.46	7.8	100.0	6.11	0.80
total gas age		n=12		12.8	0.17				4.26	1.68	
plateau		none	N/A			N/A			N/A	N/A	
Isochron age		n=12				MSWD=36.30	40/36=286.5±1.5	4.37	0.04		
edited Isochron age		n=8				MSWD=4.30	40/36=283.0±2.3	4.47	0.03		

D	Temp (°C)	$^{40}\text{Ar}/^{39}\text{Ar}$	$^{37}\text{Ar}/^{39}\text{Ar}$	$^{36}\text{Ar}/^{39}\text{Ar}$ ($\times 10^{-3}$)	$^{39}\text{Ar}_\text{K}$ ($\times 10^{-15}$ mol)	K/Ca	Cl/K ($\times 10^{-3}$)	$^{40}\text{Ar}^*$ (%)	^{39}Ar (%)	Age (Ma)	$\pm 1\sigma$ (Ma)
RA-103, groundmass concentrate (64.6 mg), J=0.0008242041±0.24%, Lab#=6134 (NM-44)											
Cerro Chillo - quartz latite											
A	675	122.5	0.2493	371.0	4.93	2.0	1.2	10.5	3.2	19.04	1.21
B	725	5.628	0.1494	5.433	18.9	3.4	0.084	71.7	15.7	5.99	0.03
C	775	4.313	0.1556	1.631	21.7	3.3	-0.062	89.1	29.9	5.71	0.02
D	825	3.872	0.1640	0.8182	41.0	3.1	0.011	94.1	56.8	5.41	0.02
E	875	3.842	0.2027	1.027	26.2	2.5	0.16	92.5	74.1	5.28	0.02
F	950	4.211	0.2819	2.477	15.3	1.8	0.15	83.1	84.1	5.20	0.02
G	1050	6.193	0.4138	9.334	8.40	1.2	0.37	56.0	89.7	5.15	0.06
H	1200	23.28	0.7455	69.37	9.31	0.68	0.55	12.2	95.8	4.22	0.23
I	1650	18.64	1.453	33.36	6.42	0.35	0.37	47.7	100.0	13.19	0.17
total gas age		n=9			152.2	2.5				6.16	0.08
preferred age		n=4		steps D-G	90.9	2.5				5.31	0.05
isochron age		n=9		MSWD=328.68			40/36=343.3±1.5			5.32	0.01
edited isochron age		n=7		MSWD=181.54			40/36=302.5±1.9			5.42	0.02
RA-104, groundmass concentrate (50.7 mg), J=0.0008241839±0.24%, Lab#=6132 (NM-44)											
Cerro Chillo - quartz latite											
A	675	246.1	0.1947	750.9	4.35	2.6	1.3	9.8	3.4	35.65	2.47
B	725	7.574	0.1350	10.58	12.5	3.8	-0.044	58.9	13.1	6.62	0.05
C	775	4.929	0.1319	2.426	29.2	3.9	-0.038	85.7	35.9	6.27	0.02
D	825	4.914	0.1333	1.221	31.0	3.8	-0.069	92.9	60.0	6.77	0.02
E	875	4.329	0.1578	1.112	21.8	3.2	0.013	92.7	76.9	5.96	0.02
F	950	4.853	0.2315	1.854	12.7	2.2	0.11	89.1	86.8	6.42	0.02
G	1050	6.626	0.4758	5.866	6.47	1.1	0.22	74.4	91.9	7.32	0.04
H	1200	14.40	1.222	33.90	3.99	0.42	0.44	31.1	95.0	6.64	0.16
I	1650	29.17	1.037	2.853	6.45	0.49	2.8	97.4	100.0	41.77	3.50
total gas age		n=9		128.5	3.1					9.23	0.29
plateau		none		N/A	N/A					N/A	N/A
isochron age		n=9		MSWD=210.47		40/36=327.5±1.7				6.31	0.02
edited isochron age		n=7		MSWD=269.14		40/36=330.6±2.5				6.30	0.02

D	Temp (°C)	$^{40}\text{Ar}/^{39}\text{Ar}$	$^{37}\text{Ar}/^{39}\text{Ar}$	$^{36}\text{Ar}/^{39}\text{Ar}$ ($\times 10^{-3}$)	$^{39}\text{Ar}_K$ ($\times 10^{-15}$ mol)	K/Ca	C/K ($\times 10^{-3}$)	$^{40}\text{Ar}^*$ (%)	^{39}Ar (%)	Age (Ma)	$\pm 1\sigma$ (Ma)
RA-107, groundmass concentrate (51.36 mg), J=0.000771222±0.26%, Lab#=6999 (NM-54)											
No Agua Peaks area - olivine andesite											
A	550	11266.2	0.2263	37902.5	0.019	2.3	61.8	0.8	0.0	115.88	910.34
B	650	57.77	0.2559	188.7	1.62	2.0	0.81	3.5	2.4	2.83	0.55
C	750	15.76	0.2964	45.19	2.45	1.7	0.28	15.4	5.9	3.37	0.14
D	825	10.88	0.4072	27.56	17.7	1.3	0.19	25.4	31.5	3.84	0.07
E	875	13.42	0.5088	36.21	9.30	1.0	0.18	20.5	44.9	3.83	0.10
F	950	18.65	0.6352	54.10	9.30	0.80	0.28	14.6	58.3	3.78	0.14
G	1000	31.24	0.6175	95.37	4.48	0.83	0.34	9.9	64.8	4.31	0.26
H	1050	35.36	0.4714	109.7	2.77	1.1	0.24	8.4	68.8	4.15	0.29
I	1100	35.32	0.3861	108.9	3.91	1.3	0.10	9.0	74.4	4.40	0.30
J	1200	55.83	0.6876	175.6	7.35	0.74	0.43	7.2	85.0	5.56	0.45
K	1300	48.32	1.564	150.6	7.52	0.33	0.41	8.1	95.9	5.46	0.37
L	1650	43.72	2.853	133.3	2.85	0.18	0.52	10.4	100.0	6.33	0.37
total gas age		n=12		69.3	0.96					4.36	0.46
plateau		n=6		47.5	1.07					3.87	0.08
isochron age		n=12		MSWD=5.97						3.46	0.08
edited isochron age		n=10		MSWD=4.86						3.37	0.08
RA-95-109, groundmass concentrate (58.4 mg), J=0.0008363312±0.24%, Lab#=6137 (NM-44)											
Red Hill - basaltic andesite											
A	675	147.4	0.9349	459.1	0.923	0.55	2.1	8.0	1.0	17.71	1.52
B	725	10.71	0.9195	27.51	6.36	0.55	0.27	24.7	7.8	3.99	0.13
C	775	4.980	0.8450	9.582	4.23	0.60	-0.060	44.4	12.4	3.34	0.07
D	825	3.018	0.8234	3.586	18.3	0.62	0.16	67.0	32.0	3.05	0.02
E	875	2.629	0.7556	2.417	17.6	0.68	0.19	75.0	50.9	2.98	0.02
F	950	3.127	0.8182	4.154	21.8	0.62	0.12	62.8	74.4	2.96	0.02
G	1050	5.207	1.015	10.90	13.7	0.50	0.23	39.6	89.1	3.11	0.05
H	1200	16.96	1.813	50.57	5.62	0.28	0.45	12.7	95.2	3.26	0.21
I	1650	39.20	10.11	123.0	4.48	0.050	0.96	9.3	100.0	5.51	0.45
total gas age		n=9		93.0	0.56					3.38	0.08
plateau		n=3		steps D-F	57.6					62.0	2.99
isochron age		n=9		MSWD=8.01	0.64					2.91	0.03
edited isochron age		n=7		MSWD=9.91						2.93	0.02

D	Temp (°C)	$^{40}\text{Ar}/^{39}\text{Ar}$	$^{37}\text{Ar}/^{39}\text{Ar}$	$^{36}\text{Ar}/^{39}\text{Ar}$	$^{39}\text{Ar}_{\text{K}}$ ($\times 10^{-3}$)	K/Ca	C/K ($\times 10^{-3}$)	$^{40}\text{Ar}^*$ (%)	^{39}Ar (%)	Age (Ma)	$\pm 1\sigma$ (Ma)
RA-112, groundmass concentrate (52.69 mg), J=0.000759491±0.26%, Lab#=6966 (NM-54)											
Servilleta Plaza Quad vent - pyroxene dacite											
A	550	1716.0	0.2057	5772.6	0.043	2.5	-6.810	0.6	0.1	13.98	44.07
B	650	30.50	0.4584	93.65	1.33	1.1	0.86	9.4	2.6	3.92	0.30
C	750	8.086	0.5168	16.58	4.37	0.99	0.13	39.9	10.9	4.42	0.06
D	825	6.667	0.6720	10.89	14.5	0.76	0.11	52.5	38.4	4.79	0.04
E	875	6.789	0.7088	11.48	8.30	0.72	0.18	50.8	54.1	4.72	0.04
F	950	7.382	0.8820	13.73	8.04	0.58	0.36	46.0	69.3	4.65	0.05
G	1000	11.13	0.9440	26.23	3.13	0.54	0.12	31.0	75.3	4.73	0.09
H	1050	16.48	0.6955	44.97	3.69	0.73	0.077	19.7	82.3	4.44	0.13
I	1100	21.88	0.6003	63.91	3.36	0.85	0.19	13.9	88.6	4.17	0.19
J	1200	26.46	1.070	77.88	2.89	0.48	0.45	13.3	94.1	4.82	0.22
K	1300	25.96	7.040	77.53	2.37	0.072	0.66	13.8	98.6	4.93	0.21
L	1650	30.72	5.312	90.99	0.753	0.096	0.21	13.8	100.0	5.83	0.41
total gas age		n=12		52.8	0.69					4.67	0.13
plateau		n=6		steps B-G	39.7	0.73				4.69	0.06
isochron age		n=12		MSWD=5.69			4/36=293.7±1.1			4.73	0.03
RA-113, groundmass concentrate (53.01 mg), J=0.000758885±0.26%, Lab#=6967 (NM-54)											
Servilleta Plaza Quad vent - pyroxene dacite											
A	550	136.6	0.3006	458.2	0.436	1.7	1.1	0.9	1.2	1.65	1.45
B	650	21.98	0.5444	68.94	2.65	0.94	0.73	7.5	8.5	2.26	0.19
C	750	17.30	0.8041	48.53	4.65	0.63	0.31	17.5	21.3	4.13	0.14
D	825	15.58	1.051	41.19	11.6	0.49	0.26	22.4	53.3	4.78	0.11
E	875	21.81	1.182	61.79	6.13	0.43	0.22	16.7	70.1	4.99	0.17
F	950	37.24	1.675	114.0	3.77	0.30	0.61	9.9	80.5	5.04	0.32
G	1000	108.9	1.938	355.9	1.01	0.26	1.2	3.5	83.2	5.28	1.01
H	1050	183.9	1.659	607.9	0.783	0.31	0.36	2.4	85.4	6.05	1.69
I	1100	203.4	1.855	666.5	0.625	0.28	-0.004	3.2	87.1	8.96	1.84
J	1200	119.2	5.737	382.3	1.17	0.089	0.96	5.6	90.3	9.20	1.04
K	1300	47.90	6.020	147.9	2.21	0.085	0.93	9.7	96.4	6.37	0.38
L	1650	35.92	4.211	105.4	1.30	0.12	0.72	14.2	100.0	6.99	0.36
total gas age		n=12		steps B-G	36.4	0.46				4.97	0.31
plateau		n=6		MSWD=24.19	0.51		4/36=300.8±0.9			4.35	0.39
isochron age		n=12		MSWD=7.64			4/36=302.3±1.0			4.08	0.10
edited isochron age		n=10								4.27	0.11

D	Temp (°C)	$^{40}\text{Ar}/^{39}\text{Ar}$	$^{37}\text{Ar}/^{39}\text{Ar}$ ($\times 10^{-3}$)	$^{36}\text{Ar}/^{39}\text{Ar}$ ($\times 10^{-3}$)	$^{39}\text{Ar}_{\text{K}}$ ($\times 10^{-15}$ mol)	K/Ca	C/K ($\times 10^{-3}$)	$^{40}\text{Ar}^*$ (%)	^{39}Ar (%)	Age (Ma)	$\pm 1\sigma$ (Ma)
RA-114, groundmass concentrate (54.90 mg), J=0.000758274±0.26%, Lab#=6968 (NM-54)											
Meltia vent - basaltic andesite											
A	550	72.69	0.2772	254.5	0.115	1.8	3.3	-3.4	0.2	-3.42	1.79
B	650	3.331	0.5361	9.740	1.10	0.95	0.45	14.8	1.9	0.68	0.10
C	750	2.216	0.6097	5.470	2.65	0.84	0.23	29.2	5.9	0.88	0.04
D	825	1.589	0.5472	2.930	18.9	0.93	0.14	48.2	34.7	1.05	0.01
E	875	1.454	0.5069	2.509	15.1	1.0	0.20	51.7	57.7	1.03	0.01
F	950	1.447	0.5798	2.543	17.1	0.88	0.22	51.1	83.8	1.01	0.01
G	1000	2.210	0.7772	5.197	5.15	0.66	0.27	33.2	91.6	1.00	0.03
H	1050	4.900	0.9612	14.72	1.95	0.53	0.53	12.7	94.6	0.85	0.07
I	1100	8.865	1.552	28.02	0.955	0.33	0.79	7.9	96.1	0.96	0.15
J	1200	6.353	4.451	20.87	1.32	0.11	1.6	8.3	98.1	0.73	0.12
K	1300	20.14	16.62	71.49	0.460	0.031	1.4	1.5	98.8	0.41	0.34
L	1650	18.62	12.81	61.05	0.795	0.040	0.60	8.4	100.0	2.15	0.29
total gas age		n=12			65.7	0.86				1.01	0.03
plateau		n=4		steps D-G	56.3	0.91				1.03	0.01
isochron age		n=12		MSWD=6.78	40/36=291.5±1.5					1.03	0.01
edited isochron age		n=10		MSWD=6.81	40/36=293.1±1.3					1.03	0.01
RA-115, groundmass concentrate (53.93 mg), J=0.000758669±0.26%, Lab#=6969 (NM-54)											
UCEM - pyroxene dacite											
A	550	92.51	0.1610	317.1	0.056	3.2	4.8	-1.3	0.1	-1.62	2.59
B	650	20.06	1.389	60.24	0.464	0.37	0.42	11.8	1.0	3.24	0.35
C	750	19.92	0.8181	59.49	1.02	0.62	-0.010	12.1	3.1	3.29	0.19
D	825	22.36	0.9592	66.66	4.41	0.53	0.34	12.2	11.9	3.75	0.18
E	875	24.51	1.056	73.35	4.09	0.48	0.34	11.9	20.0	3.98	0.19
F	950	25.64	1.010	77.25	6.36	0.51	0.24	11.3	32.7	3.96	0.20
G	1000	25.92	1.045	77.52	5.81	0.49	0.32	11.9	44.3	4.23	0.20
H	1050	26.61	1.001	79.34	6.72	0.51	0.20	12.2	57.7	4.43	0.21
I	1100	27.03	1.053	81.11	5.51	0.48	0.45	11.6	68.7	4.31	0.22
J	1200	32.58	2.021	99.89	5.23	0.25	0.61	9.9	79.1	4.40	0.25
K	1300	33.40	2.427	99.50	6.96	0.21	0.54	12.5	93.0	5.73	0.24
L	1650	35.24	2.771	104.2	3.48	0.18	0.63	13.3	100.0	6.40	0.28
total gas age		n=12		steps D-J	50.1	0.42				4.51	0.22
plateau		n=7		MSWD=5.97	40/36=327.4±3.6					4.11	0.13
isochron age		n=12		MSWD=0.77	40/36=312.0±6.7					0.84	0.10
edited isochron age		n=7								2.36	0.60

D	Temp (°C)	$^{40}\text{Ar}/^{39}\text{Ar}$	$^{37}\text{Ar}/^{39}\text{Ar}$	$^{39}\text{Ar}/^{38}\text{Ar}$ ($\times 10^{-3}$)	$^{39}\text{Ar}_{\text{K}}$ ($\times 10^{-15}$ mol)	K/Ca	C/U ($\times 10^{-3}$)	$^{40}\text{Ar}^*$ (%)	^{39}Ar (%)	Age (Ma)	$\pm 1\sigma$ (Ma)
RA-116, groundmass concentrate (57.17 mg), J=0.0000759475±0.26%, Lab#=6970 (NM-54)											
NE of San Antonio Mountain - Servilleta Basalt											
A	550	93.05	1.833	306.2	0.231	0.28	1.5	2.9	1.1	3.70	1.39
B	650	16.01	0.8351	52.41	1.07	0.61	0.34	8.2	6.2	1.90	0.20
C	750	15.29	1.040	44.70	2.45	0.49	0.68	14.1	17.8	2.96	0.15
D	825	17.24	1.734	49.74	6.54	0.29	0.43	15.5	49.0	3.66	0.13
E	875	21.47	2.918	63.23	3.49	0.17	0.26	14.0	65.5	4.13	0.18
F	950	26.27	4.025	79.43	2.98	0.13	0.39	11.8	79.7	4.27	0.20
G	1000	44.82	5.145	141.5	1.18	0.099	0.41	7.6	85.4	4.65	0.41
H	1050	64.09	5.784	206.0	0.871	0.088	0.74	5.7	89.5	5.04	0.67
I	1100	92.51	5.922	298.9	0.485	0.086	2.3	5.0	91.8	6.39	0.92
J	1200	108.0	12.69	355.0	0.846	0.040	2.4	3.8	95.9	5.64	1.05
K	1300	65.82	51.31	215.4	0.585	0.010	2.3	9.3	98.6	8.65	0.70
L	1650	107.3	20.25	331.2	0.285	0.025	2.2	10.2	100.0	15.21	1.50
total gas age		n=12		21.0		0.24				4.21	0.30
plateau		n=5		steps D-H	15.1	0.21				3.97	0.19
isochron age		n=12		MSWD=13.08			40/36=309.3±1.2			2.38	0.11
edited isochron age		n=7		MSWD=0.90			40/36=302.1±1.5			3.38	0.19
RA-117, groundmass concentrate (56.79 mg), J=0.0000759886±0.26%, Lab#=6971 (NM-54)											
Dunn Bridge - Servilleta Basalt											
A	550	1389.2	2.071	4535.5	0.003	0.25	15.9	3.5	0.0	66.19	450.26
B	650	21.09	1.535	66.82	0.320	0.33	-0.156	6.9	0.7	2.00	0.45
C	750	4.099	1.237	3.486	1.66	0.41	0.18	77.2	4.3	4.34	0.05
D	825	3.449	1.215	1.155	9.90	0.42	0.19	92.8	25.8	4.39	0.02
E	875	3.321	1.005	0.7898	8.86	0.51	0.22	95.3	45.0	4.34	0.01
F	950	3.509	0.8320	1.409	11.7	0.61	0.24	90.0	70.3	4.32	0.01
G	1000	5.007	0.8755	6.371	5.46	0.58	0.26	63.7	82.2	4.37	0.04
H	1050	3.462	1.022	1.437	3.64	0.50	0.18	90.0	90.1	4.27	0.02
I	1100	3.842	1.295	2.612	1.50	0.39	0.47	82.5	93.3	4.34	0.05
J	1200	6.344	4.121	10.77	1.15	0.12	0.60	54.8	95.8	4.78	0.10
K	1300	11.56	23.09	25.14	1.20	0.022	0.79	51.1	98.4	8.21	0.14
L	1650	36.68	2.266	31.17	0.732	0.23	0.79	76.6	100.0	40.25	3.25
total gas age		n=12		steps C-I	46.1	0.49				5.01	0.11
plateau		n=7		MSWD=96.45		0.52				92.6	4.34
isochron age		n=12		MSWD=13.09			40/36=379.9±2.8			4.23	0.01
edited isochron age		n=9		MSWD=13.09			40/36=295.9±2.9			4.34	0.01

D	Temp (°C)	$^{40}\text{Ar}/^{39}\text{Ar}$	$^{37}\text{Ar}/^{39}\text{Ar}$	$^{36}\text{Ar}/^{39}\text{Ar}$ ($\times 10^{-3}$)	$^{39}\text{Ar}_{\text{K}}$ ($\times 10^{-15}$ mol)	K/Ca	Ci/K ($\times 10^{-3}$)	$^{40}\text{Ar}^*$ (%)	^{39}Ar (%)	Age (Ma)	$\pm 1\sigma$ (Ma)
RA-118, groundmass concentrate (54.27 mg), J=0.000761452±0.26%, Lab#=6972 (NM-54)											
Cerro del Aire area - Servilleta Basalt											
A	550	-153.7158	9.170	-628.6338	-0.041	0.056	-7.313	-2.1	-0.1	4.42	6.65
B	650	42.83	0.1116	138.5	0.468	4.6	0.74	4.5	0.9	2.62	0.59
C	750	10.06	0.7606	24.81	1.78	0.67	0.29	27.7	4.6	3.82	0.10
D	825	6.292	0.7407	12.44	10.9	0.69	0.25	42.5	27.5	3.67	0.04
E	875	5.703	0.6994	10.60	8.54	0.73	0.21	46.0	45.4	3.60	0.04
F	950	5.110	0.7027	8.546	10.5	0.73	0.21	51.6	67.3	3.62	0.03
G	1000	6.158	0.7637	12.21	4.37	0.67	0.14	42.3	76.5	3.58	0.05
H	1050	8.174	0.8571	19.01	3.81	0.60	0.18	32.1	84.5	3.60	0.07
I	1100	10.46	1.063	26.82	2.24	0.48	0.29	25.0	89.2	3.59	0.10
J	1200	12.62	2.196	35.25	2.44	0.23	0.28	18.8	94.3	3.26	0.11
K	1300	16.86	16.51	53.69	1.59	0.031	0.63	13.4	97.6	3.15	0.17
L	1650	10.80	3.874	23.64	1.13	0.13	1.5	38.1	100.0	5.65	3.00
total gas age		n=12			47.7	0.66				3.63	0.13
plateau		n=8		steps C-J	44.5	0.66				3.62	0.03
isochron age		n=12		MSWD=2.07			40/36=290.2±1.5			3.70	0.03
edited isochron age		n=8		MSWD=0.83			40/36=292.3±2.1			3.67	0.04
RA-119, groundmass concentrate (51.96 mg), J=0.000761114±0.26%, Lab#=6973 (NM-54)											
Cerro del Aire area - Servilleta Basalt											
A	550	-1193.6830	6.263	-3982.4550	-0.009	0.081	2.7	1.8	0.0	-29.74	118.04
B	650	18.57	0.8077	55.16	0.587	0.63	0.15	12.6	1.3	3.21	0.32
C	750	4.547	0.9869	6.873	2.08	0.52	0.17	57.0	5.8	3.56	0.05
D	825	3.571	0.8772	3.464	11.9	0.58	0.14	73.2	31.6	3.59	0.02
E	875	3.399	0.7822	2.909	7.95	0.65	0.18	76.5	48.8	3.57	0.02
F	950	3.566	0.6847	3.631	8.26	0.75	0.26	71.4	66.7	3.49	0.02
G	1000	4.012	0.5210	4.979	3.81	0.98	0.19	64.3	74.9	3.54	0.04
H	1050	4.197	0.4119	5.508	4.08	1.2	0.26	62.0	83.7	3.57	0.04
I	1100	4.036	0.6460	5.351	2.42	0.79	0.52	62.0	89.0	3.44	0.05
J	1200	4.088	3.442	6.799	1.45	0.15	0.56	57.3	92.1	3.22	0.06
K	1300	5.557	11.89	13.69	1.94	0.043	0.46	43.6	96.3	3.35	0.08
L	1650	6.464	11.59	16.85	1.71	0.044	0.69	36.8	100.0	3.29	0.13
total gas age		n=12	steps C-I	46.2	0.67	0.74				3.52	0.02
plateau		n=7	MSWD=7.09	40.5	0.74					3.55	0.02
isochron age		n=12	MSWD=3.79				40/36=282.4±2.6			3.60	0.02
edited isochron age		n=7					40/36=289.6±6.4			3.58	0.03

D	Temp (°C)	$^{40}\text{Ar}/^{39}\text{Ar}$	$^{37}\text{Ar}/^{39}\text{Ar}$	$^{36}\text{Ar}/^{39}\text{Ar}$ ($\times 10^{-3}$)	$^{39}\text{Ar}_{\text{K}}$ ($\times 10^{15}$ mol)	K/Ca	Cl/K ($\times 10^{-3}$)	$^{40}\text{Ar}^*$ (%)	^{39}Ar (%)	Age (Ma)	$\pm 1\sigma$ (Ma)
RA-120, groundmass concentrate (50.16 mg), J=0.000762108±0.26%, Lab#=6975 (NM-54)											
Cerro del Aire area - Servilleta Basalt											
A	550	74.44	0.0000	245.5	0.052	-	4.9	2.5	0.1	2.60	2.64
B	650	4.815	0.6401	9.596	0.708	0.80	0.37	42.1	1.7	2.79	0.12
C	750	3.400	0.6966	2.796	2.22	0.73	0.30	77.3	6.7	3.61	0.04
D	825	2.954	0.7654	1.370	14.9	0.67	0.20	88.3	40.2	3.58	0.01
E	875	2.853	0.7099	1.113	9.02	0.72	0.17	90.4	60.5	3.54	0.01
F	950	2.916	0.6446	1.409	8.56	0.79	0.21	87.4	79.8	3.50	0.02
G	1000	3.123	0.6018	2.227	3.00	0.85	0.21	80.4	86.5	3.45	0.03
H	1050	3.387	0.6561	3.128	2.39	0.78	0.58	74.2	91.9	3.45	0.04
I	1100	3.518	1.166	4.386	1.16	0.44	0.58	65.7	94.5	3.18	0.07
J	1200	4.768	12.30	12.12	0.896	0.041	1.1	44.7	96.5	2.95	0.11
K	1300	6.357	38.64	24.50	0.783	0.013	0.47	32.8	98.3	2.95	0.16
L	1650	6.597	11.77	15.73	0.753	0.043	0.71	43.3	100.0	3.95	0.20
total gas age		n=12			44.4	0.68				3.50	0.04
plateau		n=6			steps C-H	40.0	0.73	40/36=267.5±2.1		3.54	0.02
isochron age		n=12			MSWD=18.26			40/36=293.0±6.5		3.58	0.01
edited isochron age		n=6			MSWD=10.66					3.55	0.01
RA-121, groundmass concentrate (51.34 mg), J=0.000761469±0.26%, Lab#=6974 (NM-54)											
Cerro de los Taos - olivine andesite											
A	550	333.0	0.0000	1110.9	0.027	-	7.6	1.4	0.1	6.46	30.14
B	650	8.166	0.0474	21.68	1.26	10.8	0.66	21.6	2.8	2.42	0.13
C	750	6.438	0.5854	12.65	3.32	0.87	0.33	42.6	10.1	3.77	0.07
D	825	6.381	1.035	10.81	14.5	0.49	0.24	51.2	41.8	4.49	0.03
E	875	6.684	1.087	10.91	8.53	0.47	0.21	53.0	60.4	4.86	0.04
F	950	7.182	1.089	12.61	7.52	0.47	0.12	49.3	76.9	4.86	0.05
G	1000	9.981	1.057	21.70	2.38	0.48	0.36	36.6	82.1	5.01	0.09
H	1050	14.45	0.7916	37.72	2.37	0.64	0.51	23.3	87.3	4.61	0.14
I	1100	19.64	0.8364	54.74	1.75	0.61	0.55	17.9	91.1	4.84	0.20
J	1200	22.94	2.063	66.92	1.53	0.25	0.38	14.5	94.5	4.57	0.21
K	1300	23.56	11.10	71.26	1.32	0.046	0.49	14.3	97.3	4.64	0.25
L	1650	20.67	10.31	60.12	1.21	0.050	0.49	17.9	100.0	5.11	0.24
total gas age		n=12			45.7	0.77				4.58	0.09
plateau		n=8			steps E-L	26.6	0.44			58.2	4.86
isochron age		n=12			MSWD=56.35		40/36=299.0±1.4			4.52	0.03
edited isochron age		n=8			MSWD=1.49		40/36=293.9±1.5			4.90	0.04

D	Temp (°C)	$^{40}\text{Ar}/^{39}\text{Ar}$	$^{37}\text{Ar}/^{39}\text{Ar}$	$^{36}\text{Ar}/^{39}\text{Ar}$ ($\times 10^{-3}$)	$^{39}\text{Ar}_\text{K}$ ($\times 10^{15}$ mol)	K/Ca	C/K ($\times 10^{-3}$)	$^{40}\text{Ar}_\star$ (%)	^{39}Ar (%)	Age (Ma)	$\pm 1\sigma$ (Ma)
RA-122, groundmass concentrate (55.41 mg), J=0.00076242±0.26%, Lab#=6976 (NM-54)											
<i>Cerro de los Taos - olivine andesite</i>											
A	550	186.8	0.0000	603.7	0.076	-	-1.484	4.5	0.1	11.46	3.23
B	650	23.71	0.0345	71.62	0.696	14.8	-0.225	10.8	1.4	3.50	0.28
C	750	13.40	0.7194	33.70	2.17	0.71	0.37	26.1	5.2	4.80	0.12
D	825	10.12	0.9745	22.55	12.4	0.52	0.22	34.9	27.3	4.85	0.06
E	875	9.269	0.7237	19.61	9.29	0.71	0.28	38.1	43.8	4.85	0.06
F	950	7.987	0.6342	15.37	11.1	0.80	0.18	43.7	63.6	4.80	0.05
G	1000	8.859	0.6812	18.30	4.78	0.75	0.15	39.6	72.1	4.82	0.06
H	1050	10.11	0.5473	22.94	5.86	0.93	0.23	33.4	82.5	4.64	0.08
I	1100	11.12	0.5336	26.08	4.13	0.96	0.30	31.1	89.9	4.75	0.09
J	1200	17.77	1.389	48.56	2.35	0.37	0.51	19.9	94.1	4.86	0.17
K	1300	25.20	15.94	74.31	0.418	0.032	0.63	17.7	94.8	6.20	0.47
L	1650	14.22	8.719	37.81	2.91	0.059	0.55	26.2	100.0	5.14	0.18
total gas age		n=12			56.2	0.85				4.82	0.09
plateau		n=8		steps C-J	52.1	0.72				4.80	0.03
isochron age		n=12		MSWD=4.91			40/36=296.5±1.9			4.77	0.06
RA-123, groundmass concentrate (50.96 mg), J=0.000762091±0.26%, Lab#=6977 (NM-54)											
<i>Cerro de los Taos - olivine andesite</i>											
A	675	-2.8749	0.2048	-21.1290	0.004	2.5	56.6	%-117.7	4.8	4.65	11.50
B	725	-11.8072	1.126	-243.0629	-0.002	0.45	-26.242	%-509.0	2.3	80.86	35.37
C	775	-23.4740	4.152	-185.8713	0.002	0.12	-21.044	%-135.3	4.4	43.28	36.97
D	825	-8.5913	8.923	-65.6298	0.005	0.057	-37.848	%-133.7	10.1	15.82	12.80
E	875	43.71	20.51	67.14	-0.001	0.025	66.7	58.2	8.7	35.15	53.92
F	950	-10734.7500	38.52	-37754.5100	0.000	0.013	14361.9	-4.0	8.7	518.01	643.716.10
G	1050	-40.8071	16.42	202.4	0.002	0.031	90.9	243.4	10.7	-143.75	37.19
H	1200	5.075	26.14	18.81	0.003	0.020	-1.786	30.0	13.8	2.13	19.78
I	1650	87.66	18.29	294.9	0.081	0.028	4.5	2.2	100.0	2.68	2.10
total gas age		n=9			0.094	0.14				-0.99	53.40
plateau		none		N/A	MSWD=3.62					N/A	N/A
isochron age		n=9					40/36=295.6±1.1			2.81	0.59

D	Temp (°C)	$^{40}\text{Ar}/^{39}\text{Ar}$	$^{37}\text{Ar}/^{39}\text{Ar}$	$^{36}\text{Ar}/^{39}\text{Ar}$ ($\times 10^{-3}$)	$^{39}\text{Ar}_\text{K}$ ($\times 10^{15}$ mol)	K/Ca	C/K ($\times 10^{-3}$)	$^{40}\text{Ar}^*$ (%)	^{39}Ar (%)	Age (Ma)	$\pm 1\sigma$ (Ma)
---	--------------	---------------------------------	---------------------------------	---	--	------	-----------------------------	---------------------------	-------------------------	-------------	-----------------------

RA-128, groundmass concentrate (55.82 mg), J=0.000764655±0.26%, Lab#=6980 (NM-54)

San Cristobal Ranch - pyroxene dacite											
A	675	24.17	0.3203	73.74	0.863	1.6	0.85	10.0	1.1	3.32	0.27
B	725	16.00	0.3717	46.55	1.65	1.4	0.60	14.2	3.3	3.13	0.18
C	775	10.08	0.4260	24.77	1.81	1.2	0.23	27.7	5.7	3.85	0.13
D	825	11.22	0.5605	27.76	5.66	0.91	0.34	27.2	13.2	4.21	0.09
E	875	10.65	0.6013	25.39	6.93	0.85	0.36	30.0	22.3	4.40	0.08
F	950	10.31	0.6537	24.18	11.8	0.78	0.37	31.2	37.9	4.43	0.07
G	1050	10.44	0.6155	24.27	12.4	0.83	0.19	31.7	54.3	4.57	0.07
H	1200	28.00	0.7951	83.11	15.7	0.64	0.33	12.5	75.0	4.82	0.23
I	1650	92.94	1.238	295.9	18.9	0.41	0.77	6.0	100.0	7.71	0.87
total gas age		n=9			75.8	0.72				5.28	0.31
plateau		n=4		steps E-H	46.9	0.76				4.48	0.07
isochron age		n=9			MSWD=3.62		J=0/36=297.0±1.6			4.28	0.07
edited isochron age		n=6			MSWD=3.37		40/36=302.4±1.8			4.19	0.07

RA-129, groundmass concentrate (54.71 mg), J=0.000765176±0.26%, Lab#=6981 (NM-54)

Gorge Bridge section - Servilleta Basalt											
A	675	48.93	1.031	153.8	0.057	0.49	-0.138	7.3	0.3	4.90	2.59
B	725	8.697	2.903	20.38	1.62	0.18	0.52	33.3	9.1	4.00	0.14
C	775	6.016	3.916	10.64	0.994	0.13	0.25	52.7	14.6	4.39	0.13
D	825	4.280	4.122	4.226	3.15	0.12	0.32	78.2	31.8	4.63	0.03
E	875	3.771	3.222	2.156	3.30	0.16	0.073	89.7	49.8	4.67	0.03
F	950	3.779	2.642	1.879	3.22	0.19	0.30	90.7	67.4	4.73	0.03
G	1050	4.127	2.466	4.018	1.72	0.21	0.35	75.8	76.7	4.32	0.05
H	1200	6.377	9.233	14.39	1.52	0.055	0.72	44.4	85.0	3.93	0.08
I	1650	25.92	22.80	81.10	2.75	0.022	0.76	14.3	100.0	5.20	0.26
total gas age		n=9		steps C-F	18.3	0.14				4.59	0.11
plateau		n=4			10.7	0.16				58.2	4.68
isochron age		n=9			MSWD=37.02		J=40/36=286.5±1.7			4.66	0.02
edited isochron age		n=3			MSWD=45.69		40/36=300.4±2.2			4.18	0.04

D	Temp (°C)	$^{40}\text{Ar}/^{39}\text{Ar}$	$^{37}\text{Ar}/^{39}\text{Ar}$	$^{36}\text{Ar}/^{39}\text{Ar}$ ($\times 10^{-3}$)	$^{39}\text{Ar}_{\text{K}}$ ($\times 10^{15}$ mol)	K/Ca	C/K ($\times 10^{-3}$)	$^{40}\text{Ar}^*$ (%)	^{39}Ar (%)	Age (Ma)	$\pm 1\sigma$ (Ma)
RA-131, groundmass concentrate (48.15 mg), J=0.000765391±0.26%, Lab#=6982 (NM-54)											
Gorge Bridge section - Servilleta Basalt											
A	675	102.0	2.350	322.8	0.220	0.83	6.6	0.8	9.35	1.58	
B	725	7.314	2.235	14.73	0.463	0.23	0.49	42.8	2.8	4.33	0.17
C	775	5.308	2.148	5.235	0.499	0.24	-0.076	74.0	4.8	5.42	0.16
D	825	4.225	2.546	2.806	3.45	0.20	0.074	85.0	19.2	4.96	0.03
E	875	3.986	2.601	2.293	2.79	0.20	0.28	88.0	30.8	4.85	0.03
F	950	4.147	1.965	2.703	4.06	0.26	0.21	84.4	47.7	4.83	0.03
G	1050	4.796	1.456	5.008	4.33	0.35	0.32	71.5	65.7	4.73	0.04
H	1200	8.439	1.239	17.08	4.69	0.41	0.36	41.3	85.2	4.81	0.07
I	1650	14.36	13.59	40.40	3.55	0.038	0.53	24.1	100.0	4.82	0.15
total gas age		n=9			24.0	0.26				4.87	0.08
plateau		n=5			steps E-I	19.4	0.27		80.8	4.81	0.03
isochron age		n=9			MSWD=12.09			40/36=295.6±1.7	4.86	0.02	
edited isochron age		n=6			MSWD=10.77			40/36=292.9±1.9	4.87	0.02	
RA-132, groundmass concentrate (52.28 mg), J=0.000765085±0.26%, Lab#=6983 (NM-54)											
Gorge Bridge section - Servilleta Basalt											
A	675	105.1	3.919	343.9	0.265	0.13	2.1	3.6	1.9	5.23	1.40
B	725	9.977	3.963	25.84	0.382	0.13	0.48	26.5	4.6	3.66	0.23
C	775	4.553	3.919	5.872	0.378	0.13	0.89	68.5	7.3	4.31	0.19
D	825	3.625	4.713	3.734	2.58	0.11	0.30	79.5	25.6	3.99	0.04
E	875	3.393	3.884	2.727	2.54	0.13	0.23	85.0	43.7	3.99	0.04
F	950	3.486	2.545	2.532	3.03	0.20	0.091	84.1	65.2	4.05	0.03
G	1050	3.612	2.266	2.852	2.42	0.23	0.26	81.5	82.4	4.06	0.04
H	1200	6.494	2.590	12.76	1.49	0.20	-0.063	45.0	93.0	4.04	0.09
I	1650	57.49	46.83	194.8	0.983	0.011	0.27	6.1	100.0	5.00	0.59
total gas age		n=9			steps A-I	14.1	0.16			4.11	0.13
plateau		n=9			MSWD=2.95	14.1	0.16		100.0	4.03	0.03
isochron age		n=9			MSWD=2.90			40/36=298.2±1.6	4.01	0.01	
edited isochron age		n=6						40/36=299.1±1.9	4.01	0.01	

D	Temp (°C)	$^{40}\text{Ar}/^{39}\text{Ar}$	$^{39}\text{Ar}/^{39}\text{Ar}$ ($\times 10^{-3}$)	$^{39}\text{Ar}_\text{K}$ ($\times 10^{-15}$ mol)	K/Ca	C/K ($\times 10^{-3}$)	$^{40}\text{Ar}^*$ (%)	^{39}Ar (%)	Age (Ma)	$\pm 1\sigma$ (Ma)
RA-133, groundmass concentrate (52.00 mg), J=0.000767899±0.26%, Lab#=6984 (NM-54)										
Gorge Bridge section - Servilleta Basalt										
A	675	23.92	0.9897	75.95	1.24	0.52	0.22	6.5	12.3	2.15
B	725	9.818	1.538	28.62	1.51	0.33	0.39	15.1	27.4	2.05
C	775	10.60	2.149	29.62	0.830	0.24	-0.001	19.0	35.6	2.79
D	825	10.93	4.259	30.21	2.18	0.12	0.62	21.3	57.3	3.23
E	875	11.91	7.230	34.78	1.20	0.071	0.041	18.4	69.2	3.05
F	950	11.76	10.91	34.02	1.08	0.047	0.36	21.6	80.0	3.55
G	1050	13.11	14.17	40.45	0.749	0.036	0.26	17.1	87.5	3.14
H	1200	33.91	18.75	112.0	0.604	0.027	1.6	6.6	93.5	3.14
I	1650	38.85	63.55	142.0	0.659	0.008	2.0	4.5	100.0	0.45
total gas age		n=9			10.1	0.18			2.56	0.48
plateau		n=6		steps D-I	6.5	0.07			2.84	0.23
isochron age		n=9		MSWD=13.09					3.23	0.12
edited isochron age		n=7		MSWD=3.08					2.95	0.10
					40/36=294.2±2.0				3.28	0.12
RA-135, groundmass concentrate (49.83 mg), J=0.000764349±0.26%, Lab#=6979 (NM-54)										
Gorge Bridge section - Servilleta Basalt										
A	675	364.0	6.272	1218.1	0.121	0.081	1.8	1.2	2.0	6.29
B	725	25.56	6.946	82.32	0.257	0.073	-0.418	6.9	6.3	2.45
C	775	9.386	7.405	25.06	0.306	0.069	0.95	27.2	11.3	3.53
D	825	4.707	9.046	9.713	1.52	0.056	0.32	53.8	36.6	0.29
E	875	4.484	9.268	8.505	1.11	0.055	0.42	59.8	55.0	3.51
F	950	6.024	9.575	14.21	1.22	0.053	0.26	42.5	75.2	0.07
G	1050	10.10	11.88	27.14	0.715	0.043	0.68	29.7	87.1	4.16
H	1200	23.23	18.60	75.85	0.366	0.027	0.75	9.7	93.2	0.20
I	1650	101.3	98.68	343.2	0.411	0.005	3.6	7.4	100.0	0.42
total gas age		n=9			0.411	0.051			11.10	1.32
plateau		n=4		steps C-F	4.16	0.056			4.14	0.43
isochron age		n=9		MSWD=8.48					3.58	0.08
edited isochron age		n=7		MSWD=6.29					3.52	0.03
					40/36=302.6±1.7				3.60	0.04
					40/36=295.5±2.8					

D	Temp (°C)	⁴⁰ Ar/ ³⁹ Ar	³⁹ Ar/ ³⁸ Ar ($\times 10^{-3}$)	³⁸ Ar/ ³⁹ Ar ($\times 10^{-3}$)	³⁹ Ar _K ($\times 10^{-5}$ mol)	K/Ca	Ci/K ($\times 10^{-2}$)	⁴⁰ Ar*	³⁹ Ar (%)	Age (Ma)	$\pm 1\sigma$ (Ma)
RA-136, groundmass concentrate (54.95 mg), J=0.000766837±0.26%, Lab#=6985 (NM-54)											
Gorge Bridge section - Servilleta Basalt											
A	675	17.55	0.8031	56.77	0.748	0.64	0.46	4.8	8.9	1.16	0.28
B	725	9.845	1.257	29.55	1.20	0.41	0.50	12.3	23.3	1.67	0.15
C	775	11.41	1.850	33.26	0.701	0.28	1.1	15.1	31.7	2.38	0.20
D	825	10.77	5.513	30.51	2.17	0.093	0.55	20.2	57.7	3.03	0.11
E	875	9.913	10.95	28.92	1.07	0.047	0.19	22.3	70.4	3.08	0.17
F	950	9.325	14.95	27.16	1.07	0.034	0.31	26.2	83.2	3.42	0.14
G	1050	13.67	18.75	43.96	0.684	0.027	0.49	15.5	91.4	2.98	0.29
H	1200	67.75	24.70	225.7	0.332	0.021	1.5	4.4	95.4	4.17	0.91
I	1650	70.09	97.07	246.3	0.386	0.005	2.4	5.9	100.0	6.17	1.04
total gas age		n=9									
plateau		n=4									
isochron age		n=9									
edited isochron age		n=5									
			steps C-F	5.01	MSWD=22.32	4.0/36=299.6±2.1	59.9	3.00	0.20		
					MSWD=3.44	4.0/36=297.1±3.1		2.69	0.09		
								3.12	0.13		

APPENDIX B*EXPLANATION OF PROBABILITY DISTRIBUTION PLOTS*

The following section contains the probability distribution plots for the 4 feldspar concentrates analyzed by the $^{40}\text{Ar}/^{39}\text{Ar}$ laser fusion method in this study. Each plot displays the individual ages of the samples with accompanying errors at the 1σ level. The plots are accompanied by plots of the radiogenic yield and K/Ca ratios for the analyses as discussed in the Field and Analytical Methods section of this study. The two plots on each page represent the total available data points (upper) and the final edited data point set (lower) that was used to calculate the final ages for the samples that are given in Table B1. The curve at the bottom of each plot represents the relative probability of a sample of a given age being present. A high, peak shaped curve is indicative of a closely grouped set of analyses and one that is more likely to a better estimate of the eruption age of the sample.

TABLE B1. Summary of mean ages for comparison of samples analyzed with the CO₂ laser as single crystals. The age cited is the mean age with the error calculated by the Taylor (1982) method.

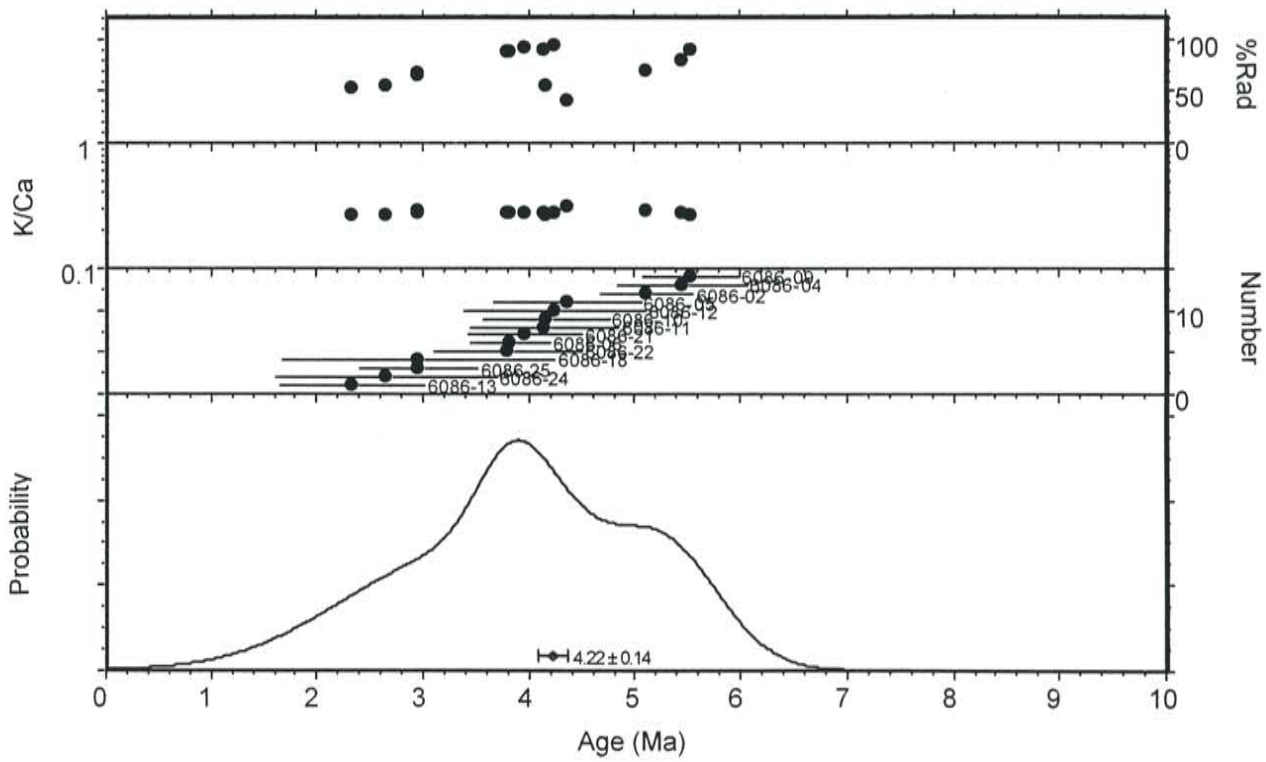
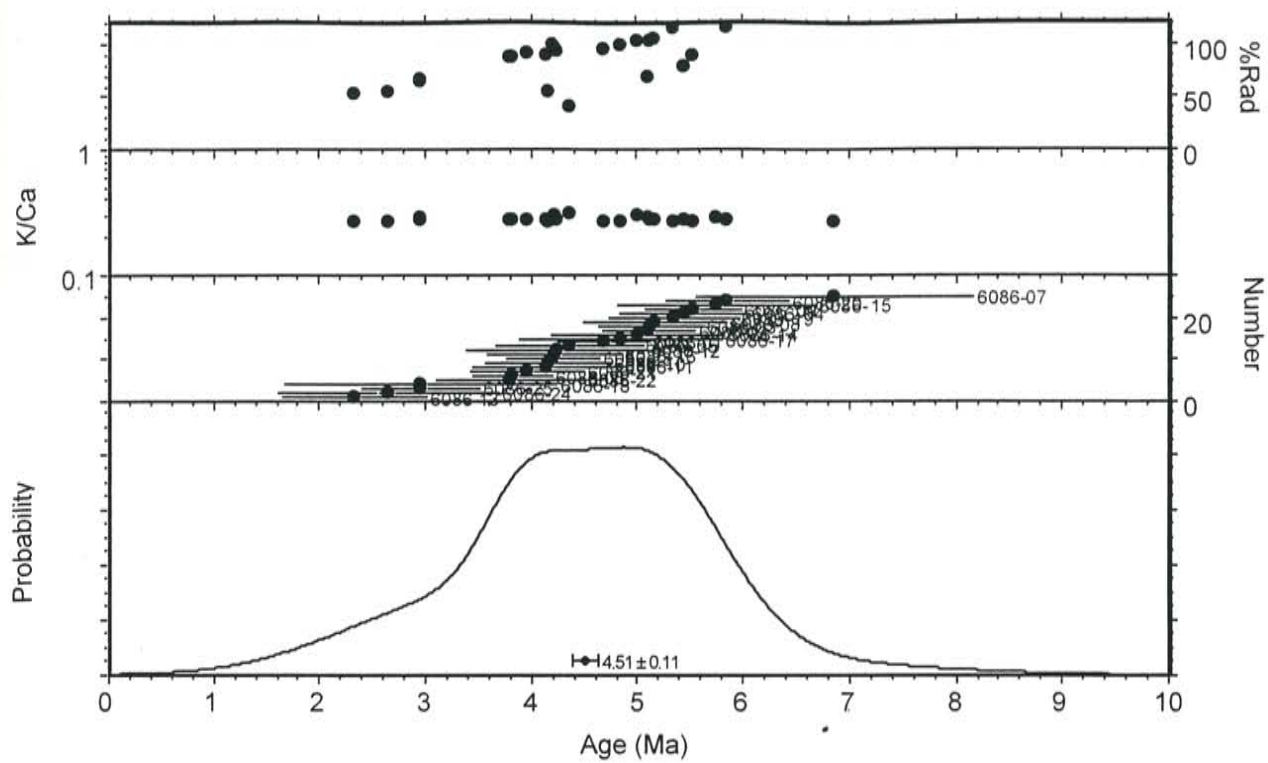
Sample	Mean Age (Ma)	No. of analyses	No. used
RA-001	4.22±0.14	25	14
RA-003	3.51±0.12	25	14
RA-004	4.01±0.09	25	14
RA-005	4.06±0.05	25	19

Number of analyses refers to the total number of single crystals analyzed.

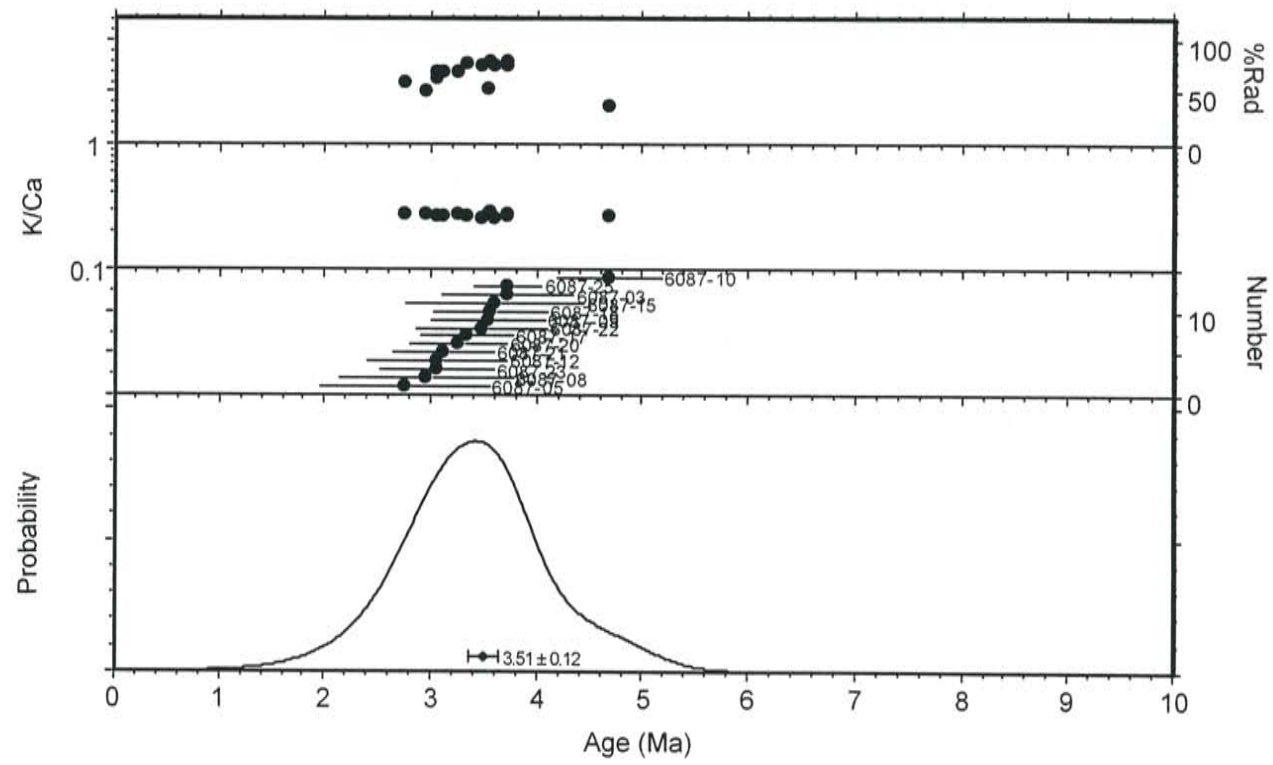
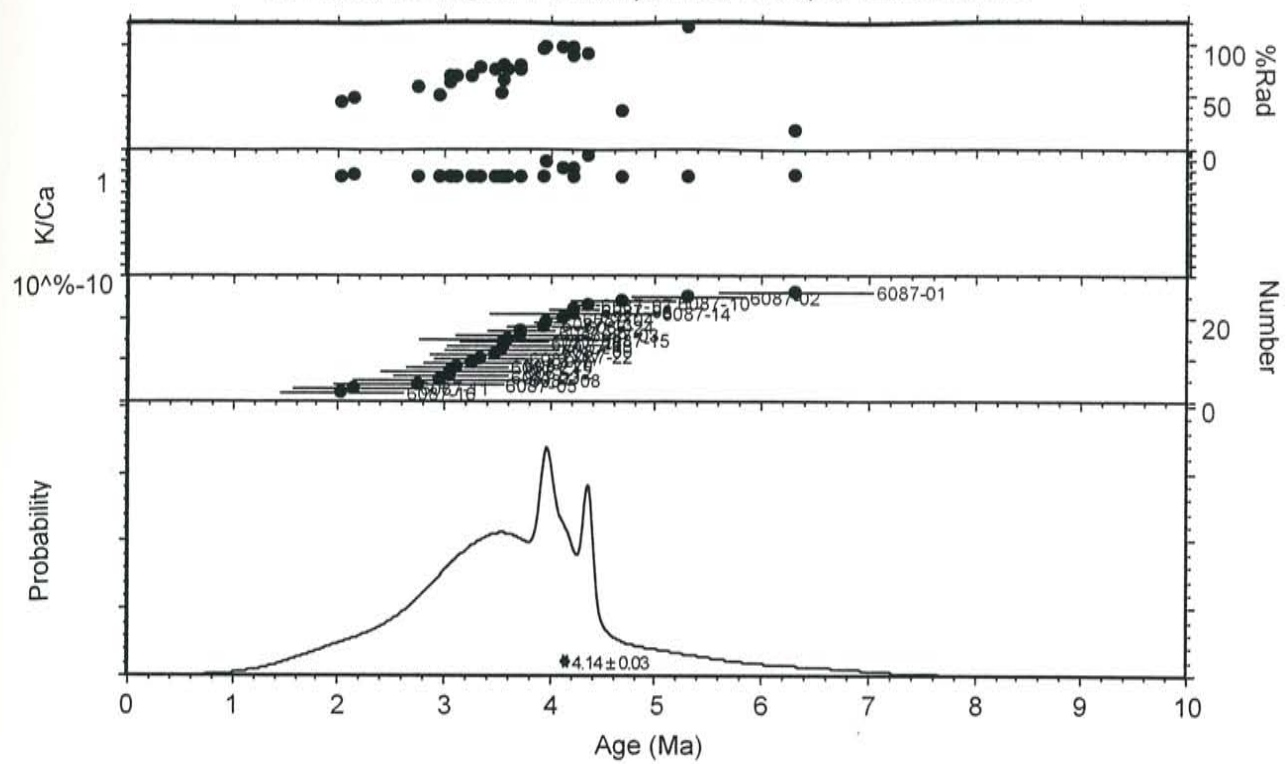
Number used refers to the number of analyzed crystals used to calculate the mean age.

Errors for quoted ages given at the 1σ level.

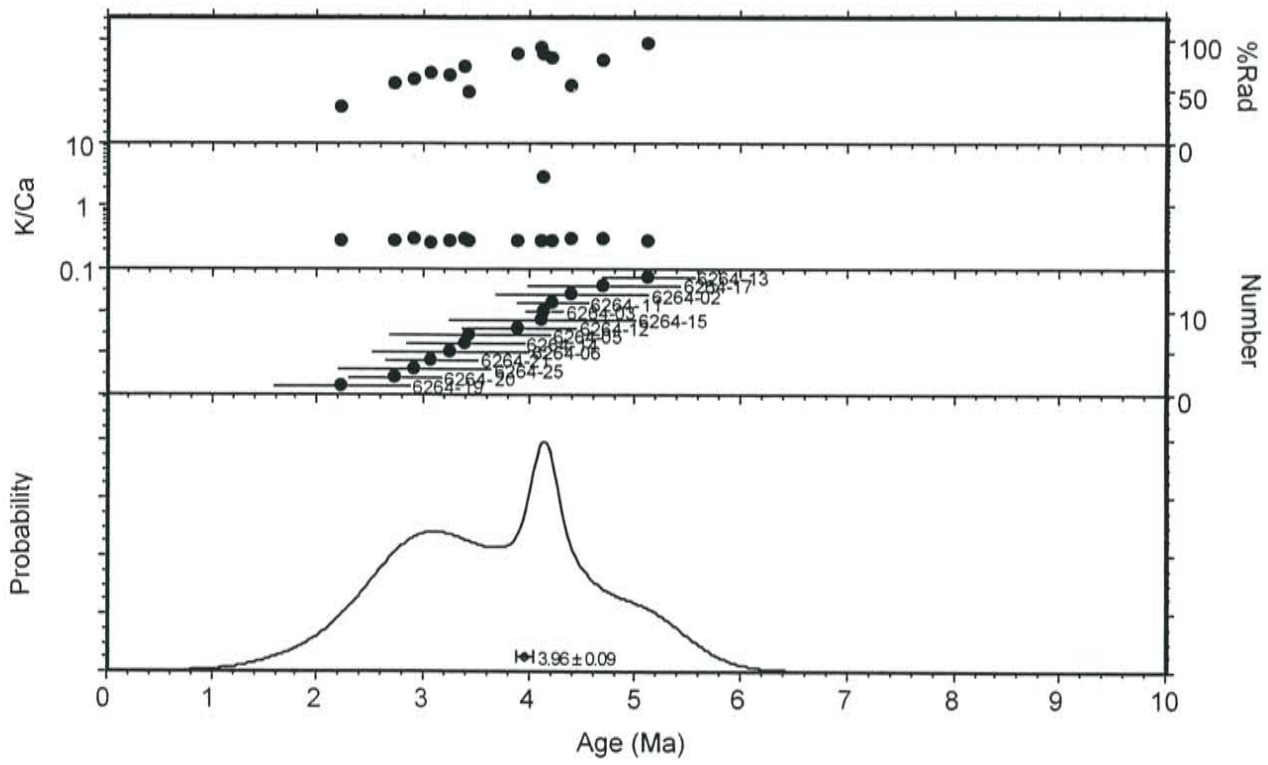
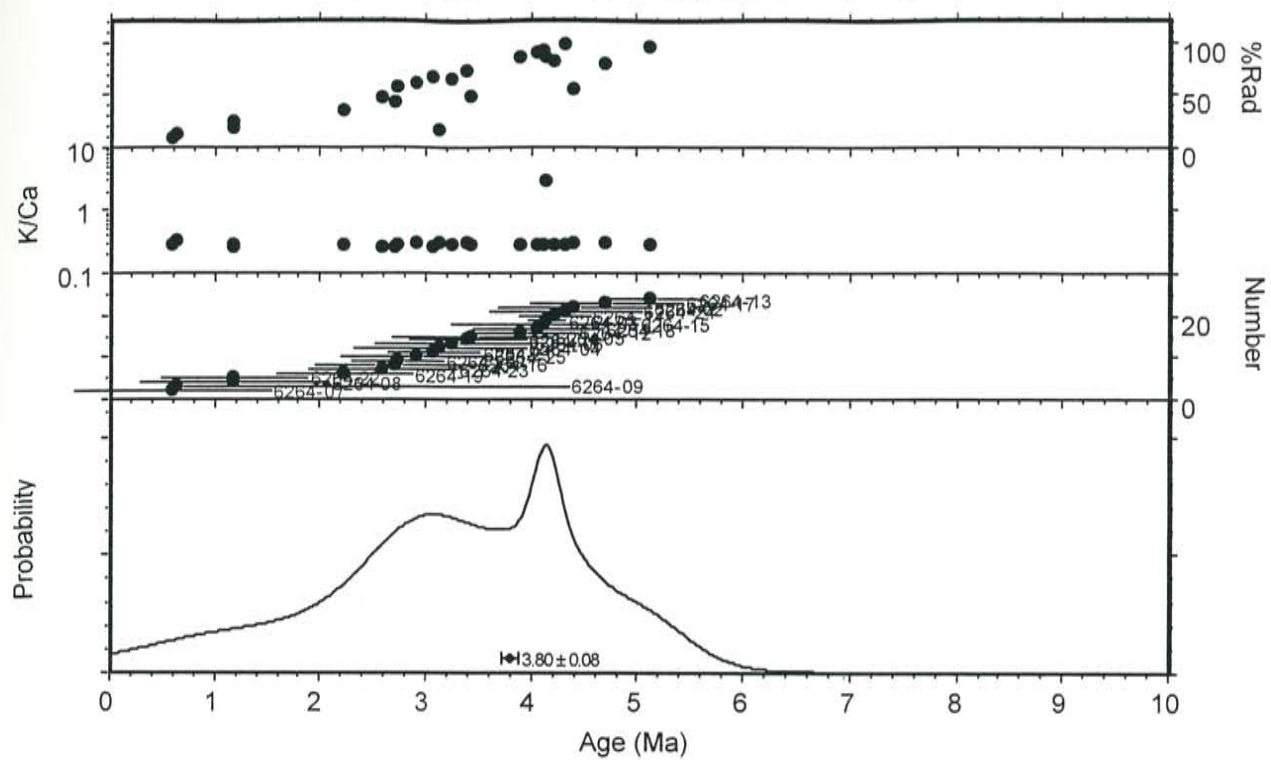
RA-001, No Agua Peaks, perlite, feldspar concentrate



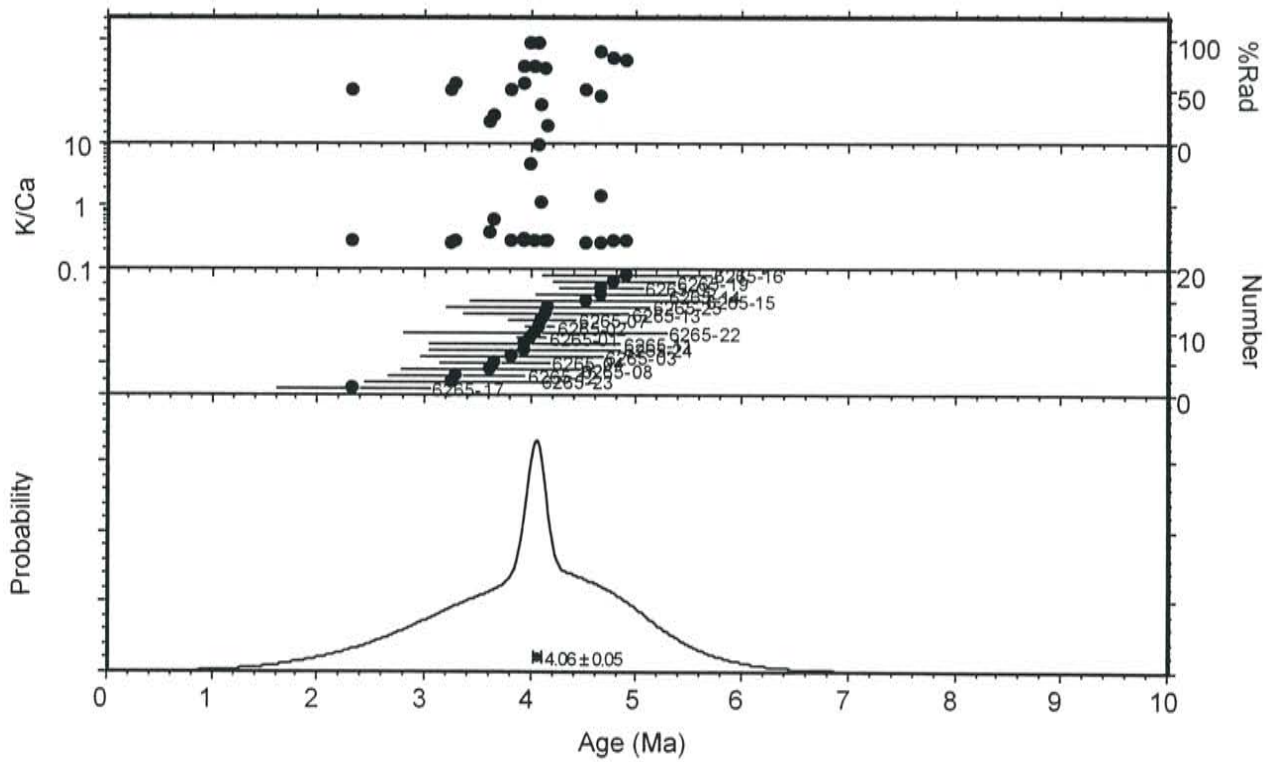
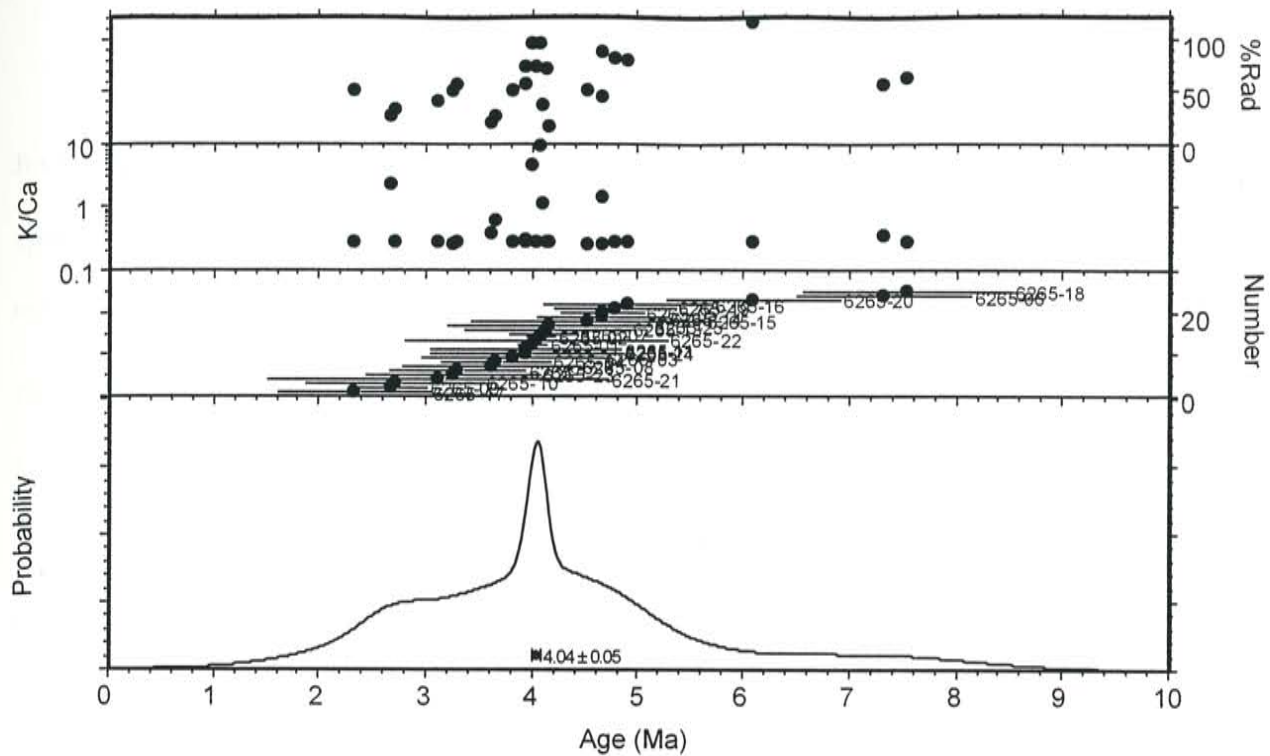
RA-003, No Agua Peaks, perlite, feldspar concentrate



RA-004, No Agua Peaks, perlite, feldspar concentrate



RA-005, No Agua Peaks, perlite, feldspar concentrate



EXPLANATION OF SPECTRA AND ISOCHRON PLOTS

The following section contains two types of plots that graphically display the data for the resistance-furnace step-heated groundmass concentrates. The upper plot is a spectra and consists of the age of the individual heating steps plotted against the total $\%^{39}\text{Ar}$ in the sample. The gray step represent the steps that were used in the calculation of either plateau or preferred (shown in italics) ages as described in the Field and Analytical Methods section of this study. Each plot also is accompanied by plots of the radiogenic yield and K/Ca for the individual heating steps. The lower plot is a reverse isotope correlation diagram as also discussed in the Field and Analytical Methods section. The dark line represents the best fit line for the entire data set for each sample, while the gray/dashed line represents the best fit line for the final edited data set. The final accepted age for each sample is denoted by the boxed age. The information from these plots is summarized in Table B2 for ease of reference.

TABLE B2. Compilation of the plateau, isochron, and reverse isochron ages calculated for step-heated samples from Appendix B.

Sample	Plateau Age (Ma)	Isochron Age (Ma)	$^{40}\text{Ar}/^{39}\text{Ar}$	MSWD	Edited Iso. Age (Ma)	$^{40}\text{Ar}/^{39}\text{Ar}$	MSWD	Confidence Level
RA-007*	3.00±0.03 (5)	2.81±0.47 (12)	307.8±1.3	3.51	2.97±0.08 (6)	299.3±3.7	4.94	high
RA-008*	3.18±0.08 (5)	3.17±0.02 (9)	302.5±1.2	43.25	3.07±0.02 (5)	292.9±1.5	13.32	high
RA-009*	3.05±0.05 (7)	2.99±0.01 (12)	313.3±1.5	84.48	3.07±0.01 (11)	286.9±11.0	50.10	high
RA-010	none	2.66±0.08 (11)	313.2±1.1	6.04	2.75±0.09 (8)	314.6±1.2	0.58	moderate
RA-011	4.34±0.18 (5)	2.61±0.17 (9)	315.8±1.5	1.60	3.52±0.47 (5)	305.2±5.8	2.33	low
RA-012	2.89±0.02 (7)	2.85±0.03 (12)	300.8±1.5	5.56	2.89±0.03 (10)	295.7±2.0	4.91	high
RA-013	3.65±0.16 (3)	3.47±0.13 (11)	301.9±1.8	3.86	3.58±0.17 (9)	299.9±2.8	4.74	high
RA-014	3.74±0.12 (4)	3.43±0.09 (12)	300.1±1.4	2.21	3.43±0.09 (10)	299.9±1.5	2.39	high
RA-015*	3.61±0.12 (5)	2.75±0.16 (12)	305.8±1.9	3.09	3.61±0.45 (7)	294.7±7.2	2.10	low
RA-016	none	3.00±0.10 (12)	303.2±1.7	14.04	4.15±0.16 (9)	272.1±3.6	6.49	low
RA-017*	3.94±0.05 (9)	3.89±0.05 (12)	300.4±1.3	5.66	3.91±0.05 (11)	299.4±1.5	6.06	high
RA-018	3.96±0.13 (7)	3.48±0.16 (10)	302.8±1.6	1.16	3.97±0.26 (6)	295.8±3.6	0.63	low
RA-019	3.19±0.08 (7)	3.11±0.05 (11)	299.0±1.2	5.80	3.00±0.06 (8)	303.0±1.8	4.74	high
RA-020	2.92±0.05 (6)	2.78±0.04 (12)	301.6±1.3	10.13	3.00±0.10 (4)	289.6±5.7	2.55	high
RA-021	3.69±0.03 (7)	3.65±0.04 (12)	299.0±0.9	1.80	3.59±0.05 (5)	303.9±3.0	2.99	high
RA-022*	2.13±0.03 (3)	2.07±0.03 (11)	302.0±1.6	8.99	2.13±0.04 (9)	297.3±1.9	9.24	high
RA-023	3.35±0.12 (6)	2.48±0.16 (12)	301.5±1.1	0.84	2.99±0.19 (9)	299.1±1.6	0.26	low
RA-024	3.66±0.16 (6)	3.60±0.14 (12)	307.5±1.2	4.11	3.66±0.27 (6)	295.5±2.7	2.18	low
RA-025	3.53±0.08 (7)	3.07±0.09 (12)	304.5±1.2	3.93	3.19±0.10 (8)	301.8±1.4	1.33	low
RA-026	17.45±0.05 (9)	17.48±0.03 (11)	292.6±1.4	1.84	17.47±0.03 (9)	293.1±1.4	1.37	high
RA-027	4.33±0.02 (8)	4.13±0.01 (11)	397.7±2.0	315.62	4.34±0.01 (9)	289.3±2.2	3.06	high
RA-028	3.92±0.05 (9)	4.00±0.01 (12)	289.7±1.2	16.54	3.95±0.01 (8)	300.9±2.2	13.81	high
RA-029	4.03±0.26 (3)	2.56±0.18 (12)	314.4±1.4	0.76	2.53±0.31 (8)	314.9±3.2	1.14	low
RA-030	2.62±0.17 (3)	2.84±0.10 (12)	297.6±1.4	4.61	2.93±0.14 (9)	296.0±2.2	3.65	moderate
RA-031	4.97±0.09 (5)	4.62±0.14 (10)	300.1±2.0	4.76	5.04±0.19 (8)	292.6±3.2	4.73	high
RA-032	4.84±0.02 (6)	4.82±0.01 (9)	298.5±1.4	4.25	4.84±0.02 (7)	294.7±2.0	3.80	high
RA-033	4.82±0.19 (8)	3.76±0.20 (12)	306.7±1.9	12.80	3.94±0.23 (7)	304.1±1.9	2.25	low
RA-034*	4.85±0.03 (5)	4.86±0.05 (12)	305.8±1.4	17.88	4.86±0.05 (7)	304.7±3.8	31.98	high
RA-035*	4.84±0.05 (8)	4.86±0.01 (11)	288.4±1.3	11.63	4.84±0.01 (8)	293.8±1.6	9.25	moderate
RA-038	2.72±0.06(8)	2.49±0.08 (12)	299.9±1.1	2.40	2.82±0.11 (8)	293.7±1.7	0.51	moderate
RA-039	2.86±0.07 (5)	2.68±0.06 (12)	299.7±1.0	7.62	2.91±0.07 (10)	293.7±1.3	2.47	moderate

Sample	Plateau Age (Ma)	Isochron Age (Ma)	$^{40}\text{Ar}/^{39}\text{Ar}$	MSWD	Edited Iso. Age (Ma)	$^{40}\text{Ar}/^{39}\text{Ar}$	MSWD	Confidence Level
RA-041*	2.64±0.13 (5)	1.87±0.09 (9)	312.5±1.3	8.37	2.47±0.13 (5)	299.2±2.6	4.73	low
RA-042*	2.38±0.11 (5)	1.21±0.13 (9)	309.1±1.8	4.24	1.99±0.27 (8)	299.6±3.4	2.03	low
RA-045	17.33±0.07 (3)	17.41±0.05 (9)	304.6±1.3	36.46	17.47±0.05 (8)	298.4±1.6	36.45	high
RA-046	2.58±0.08 (6)	2.14±0.07 (9)	312.8±1.6	1.14	2.34±0.10 (6)	304.8±3.7	0.55	moderate
RA-047	none	0.91±0.10 (11)	316.5±1.2	2.72	1.06±0.16 (7)	314.0±3.1	4.57	none
RA-048	6.43±0.16 (3)	4.22±0.21 (9)	318.3±1.5	0.67	4.70±0.32 (6)	313.9±2.7	0.17	low
RA-049	7.76±0.23 (5)	4.76±0.26 (11)	310.4±1.0	4.42	6.87±0.50 (5)	299.8±2.4	0.96	low
RA-050	4.83±0.03 (4)	4.79±0.26 (9)	304.0±1.4	6.15	4.81±0.50 (5)	300.8±3.6	6.80	low
RA-051	none	5.15±0.09 (9)	324.2±1.4	13.81	5.19±0.10 (7)	321.0±1.6	1.86	none
RA-052	4.75±0.01 (5)	4.74±0.01 (9)	301.0±1.6	7.08	4.74±0.01 (8)	298.7±1.9	7.54	high
RA-055	4.49±0.12 (4)	3.51±0.13 (9)	306.1±1.4	34.01	4.75±0.31 (5)	291.8±3.7	3.58	low
RA-056	4.64±0.13 (6)	-1.10±0.02 (9)	376.0±1.9	363.09	4.03±0.19 (7)	303.8±2.3	0.83	moderate
RA-058	4.33±0.10 (5)	4.09±0.08 (9)	308.2±1.5	181.68	3.34±0.13 (7)	308.4±1.6	1.36	low
RA-060	none	3.39±0.32 (9)	315.8±1.5	1.40	3.69±0.41 (7)	314.1±2.2	1.72	low
RA-061	none	2.81±0.13 (9)	318.9±1.9	2.82	2.51±0.26 (6)	324.5±5.4	2.65	moderate
RA-062	5.68±0.22 (4)	3.29±0.29 (9)	316.3±2.5	7.59	4.07±0.55 (6)	300.3±4.4	2.62	low
RA-064*	4.84±0.05 (7)	4.67±0.01 (9)	332.1±1.5	130.72	4.70±0.03 (5)	323.7±8.5	39.30	high
RA-065	5.24±0.12 (4)	4.25±0.08 (9)	314.6±1.7	30.40	5.03±0.14 (4)	299.8±2.5	1.47	low
RA-072	none	0.65±0.02 (12)	412.1±3.9	122.33	3.72±0.11 (8)	354.3±3.6	24.83	moderate
RA-076	none	2.98±0.65 (9)	317.0±1.6	4.92	3.95±0.29 (5)	301.9±4.3	4.48	moderate
RA-079*	4.32±0.03 (6)	4.33±0.02 (12)	293.7±1.2	17.67	4.32±0.02 (9)	297.7±1.5	6.69	high
RA-080	none	4.63±0.09 (12)	299.1±1.2	2.28	2.13±0.02 (8)	287.4±3.3	6.98	high
RA-082	2.10±0.04 (3)	2.05±0.02 (12)	302.0±1.9	27.69				
RA-083	0.11±0.12 (5)	-0.04±0.01 (12)	299.4±2.2	5.00				
RA-084	2.70±0.01 (6)	2.70±0.01 (12)	291.7±1.7	5.99	2.70±0.01 (9)	296.4±2.8	7.19	high
RA-085	5.34±0.06 (5)	5.30±0.04 (9)	305.8±1.4	26.50	5.53±0.04 (6)	290.0±1.8	10.04	high
RA-086	5.11±0.08 (5)	4.81±0.07 (9)	303.1±1.0	7.42	5.05±0.09 (6)	298.1±1.3	3.96	high
RA-087	none	12.10±0.12 (9)	315.1±2.3	577.47	7.79±0.23 (4)	301.9±2.2	31.49	none
RA-088*	4.72±0.03 (4)	4.64±0.03 (9)	306.5±1.2	10.41	4.77±0.05 (6)	297.1±3.0	13.64	high
RA-089*	5.32±0.08 (6)	5.15±0.02 (9)	309.9±1.2	41.30	5.33±0.03 (7)	295.5±1.5	26.07	high
RA-090	4.97±0.06 (5)	4.46±0.06 (9)	312.3±1.4	6.26	4.96±0.09 (5)	295.8±2.9	1.93	high
RA-091	5.88±0.18 (5)	4.70±0.18 (9)	308.4±1.3	6.89	5.57±0.23 (6)	299.4±2.0	3.55	low
RA-092	none	4.04±0.20 (9)	316.4±1.7	28.04	5.82±0.46 (4)	294.9±3.7	0.87	low

Sample	Plateau Age (Ma)	Isochron Age (Ma)	$^{40}\text{Ar}/^{39}\text{Ar}$	MSWD	Edited Iso. Age (Ma)	$^{40}\text{Ar}/^{39}\text{Ar}$	MSWD	Confidence Level
RA-093	8.07±0.70 (4)	2.33±0.40 (9)	315.1±2.4	2.67	3.24±1.23 (5)	311.1±7.2	1.02	none
RA-102	none	4.37±0.04 (12)	286.5±1.5	36.30	4.47±0.03 (8)	293.0±2.3	4.30	high
RA-103*	5.31±0.05 (4)	5.32±0.01 (9)	343.3±1.5	328.68	5.42±0.02 (7)	302.5±1.9	181.54	moderate
RA-104	none	6.31±0.02 (9)	327.5±1.7	210.47	6.30±0.02 (7)	330.6±2.5	269.14	none
RA-107	3.87±0.08 (6)	3.46±0.08 (12)	302.1±1.0	5.97	3.37±0.08 (10)	303.9±1.1	4.86	moderate
RA-109	2.99±0.03 (3)	2.91±0.01 (9)	312.1±1.3	8.01	2.93±0.02 (7)	310.0±2.0	9.91	high
RA-112	4.69±0.06 (6)	4.73±0.03 (12)	293.7±1.1	5.69				high
RA-113	4.35±0.39 (6)	4.08±0.10 (12)	300.8±0.9	24.19	4.27±0.11 (10)	302.3±1.0	7.64	moderate
RA-114	1.03±0.01 (4)	1.03±0.01 (12)	291.5±1.5	6.78	1.03±0.01 (10)	293.1±1.6	6.81	high
RA-115	4.11±0.13 (7)	0.84±0.10 (12)	327.4±3.6	5.97	2.36±0.60 (7)	312.0±6.7	0.77	moderate
RA-116	3.97±0.19 (5)	2.38±0.11 (12)	309.3±1.2	13.08	3.38±0.19 (7)	302.1±1.5	0.90	moderate
RA-117	4.34±0.02 (7)	4.23±0.01 (12)	379.9±2.8	96.45	4.34±0.01 (9)	295.9±2.9	13.09	high
RA-118	3.62±0.03 (8)	3.70±0.03 (12)	290.2±1.5	2.07	3.67±0.04 (8)	292.3±2.1	0.83	high
RA-119	3.55±0.02 (7)	3.60±0.02 (12)	282.4±2.6	7.09	3.58±0.03 (7)	289.6±6.4	3.79	high
RA-120	3.54±0.02 (6)	3.58±0.01 (12)	267.5±2.1	18.26	3.55±0.01 (6)	293.0±6.5	10.66	high
RA-121	4.86±0.04 (8)	4.52±0.03 (12)	299.0±1.4	56.35	4.90±0.04 (8)	293.9±1.5	1.49	high
RA-122	4.80±0.03 (8)	4.77±0.06 (12)	296.5±1.9	4.91				high
RA-123	none	2.81±0.59 (8)	295.6±15.1	3.62				none
RA-128	4.48±0.09 (4)	4.28±0.07 (9)	297.0±1.6	15.56	4.18±0.07	302.4±1.8	3.37	high
RA-129	4.68±0.04 (4)	4.66±0.02 (9)	286.5±1.7	37.02	4.18±0.04 (3)	300.4±2.2	45.69	high
RA-131	4.81±0.03 (5)	4.86±0.02 (9)	295.6±1.7	12.09	4.87±0.02 (6)	292.9±1.9	10.77	high
RA-132	4.03±0.03 (9)	4.01±0.01 (9)	298.2±1.6	2.95	4.01±0.01 (6)	299.1±1.9	2.90	high
RA-133	3.23±0.12 (6)	2.95±0.10 (9)	294.2±2.0	13.09	3.28±0.12 (7)	292.9±2.2	3.08	low
RA-135	3.58±0.08 (4)	3.52±0.03 (9)	302.6±1.7	8.48	3.60±0.04 (7)	295.5±2.8	6.29	high
RA-136	3.00±0.20 (5)	2.69±0.09 (9)	299.6±2.1	22.32	3.12±0.13 (5)	297.1±3.1	3.44	moderate

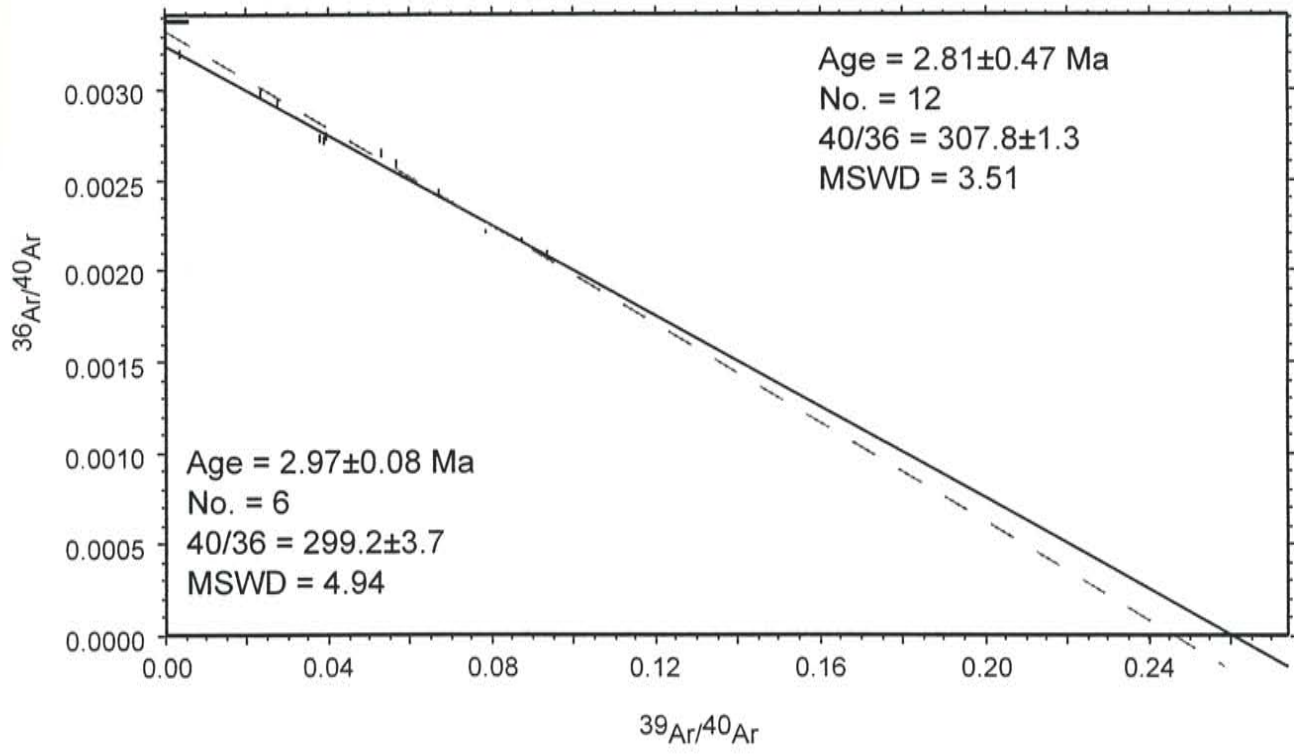
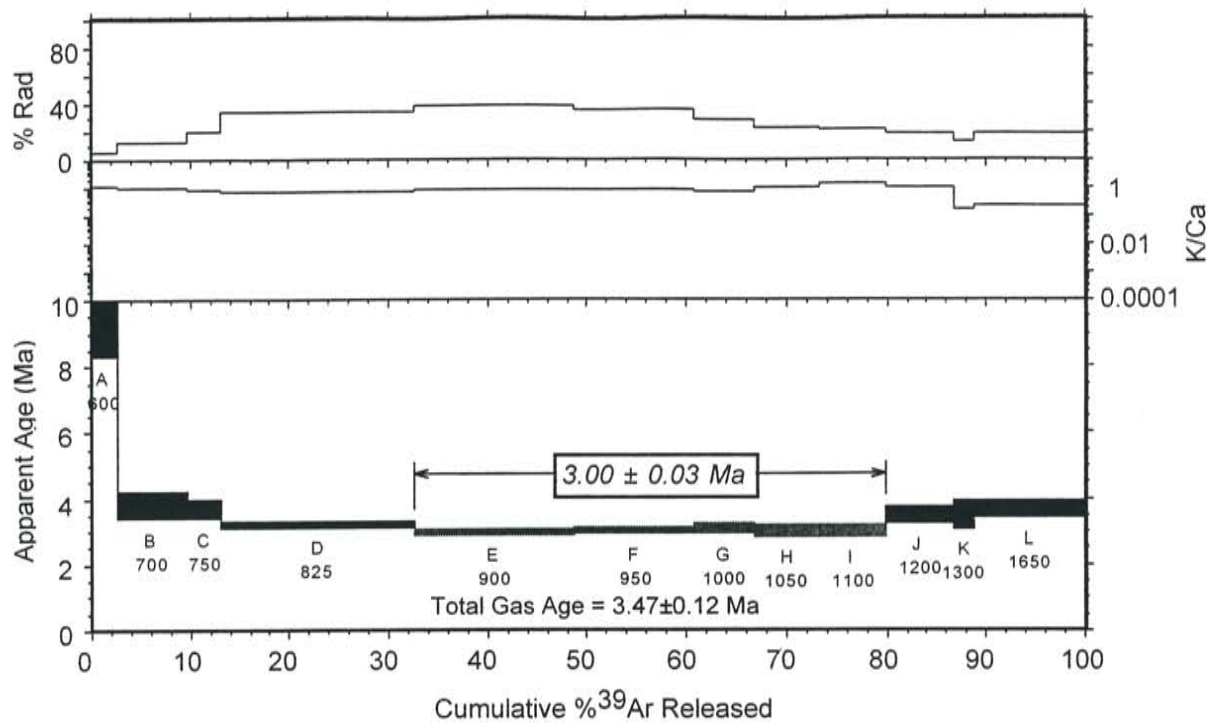
Number in () represents the number of steps used in the calculation of the given age.

* denotes samples whose plateau age was "forced"

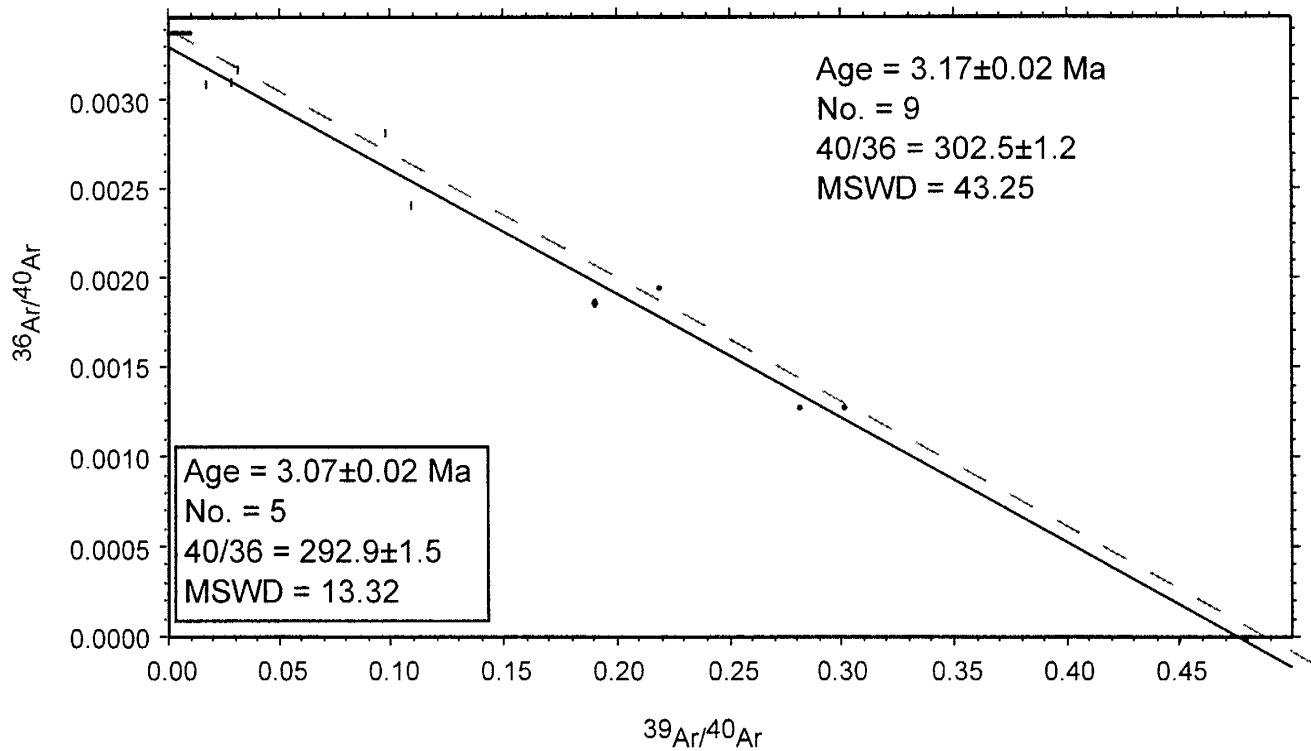
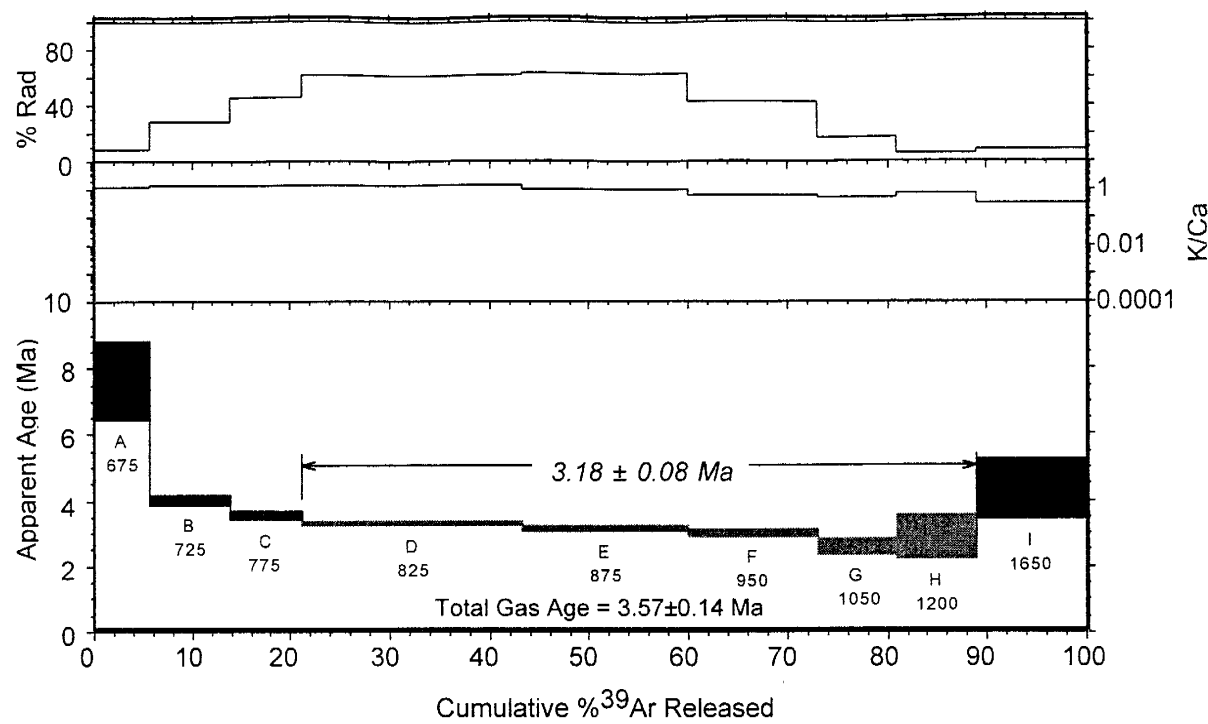
BOLDFACED ages are the accepted age for this sample.

Errors for ages given here quoted at the 1σ level.

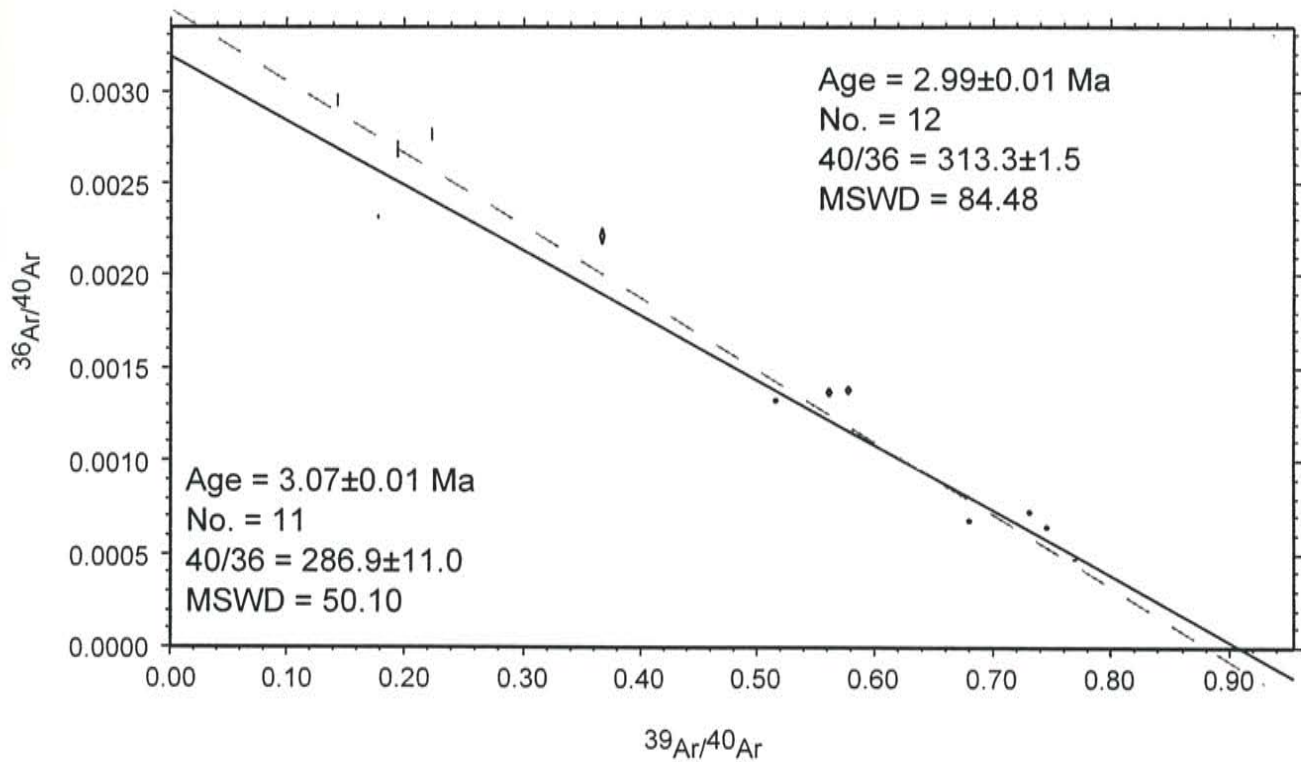
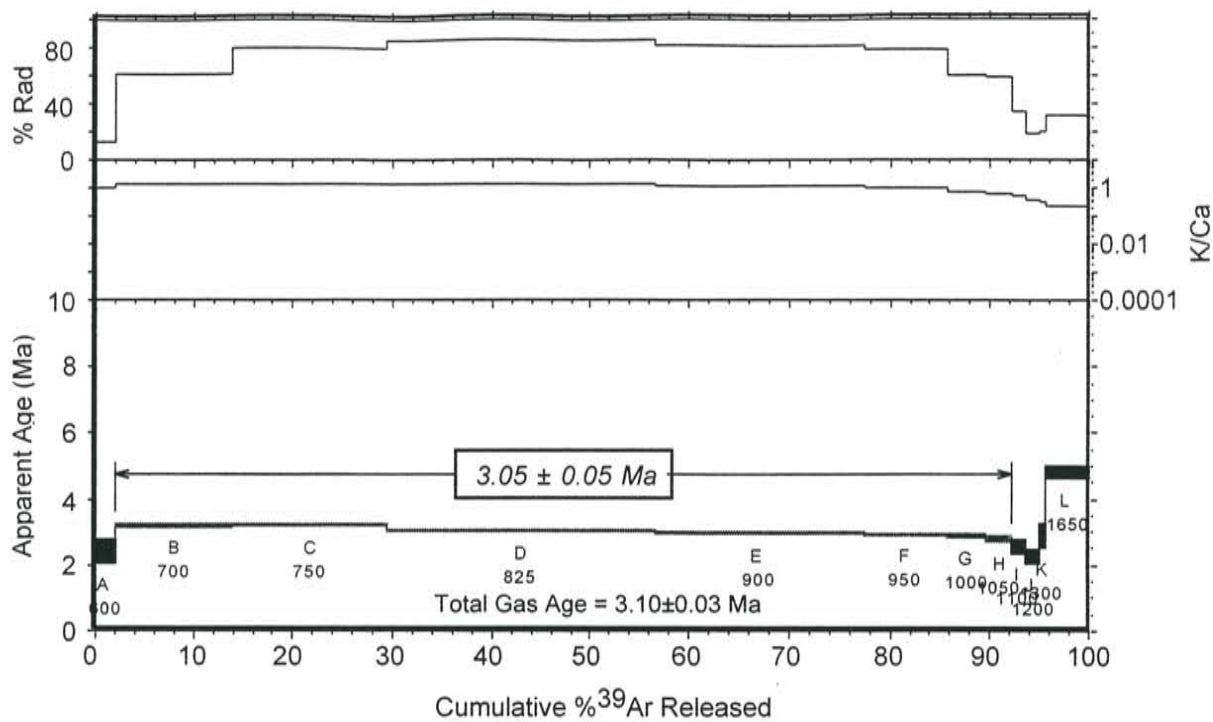
RA-007, pyroxene dacite, San Antonio Mt., groundmass concentrate



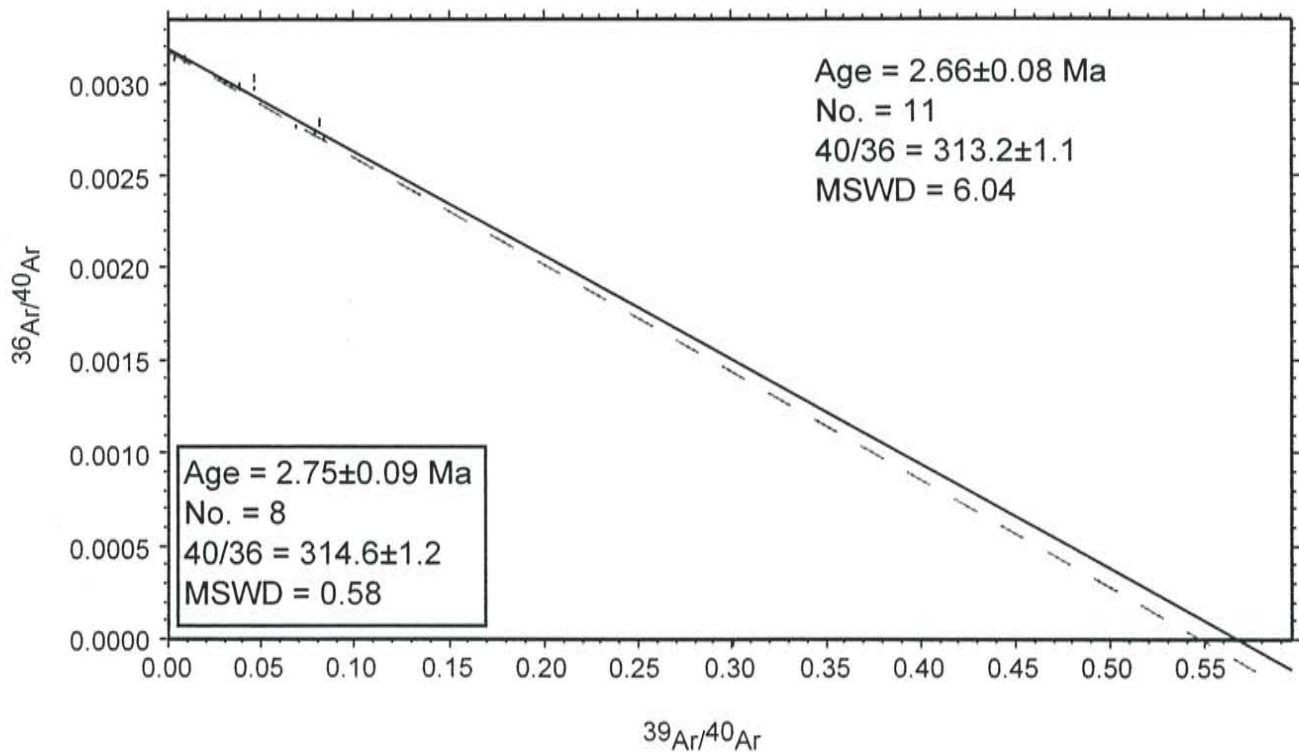
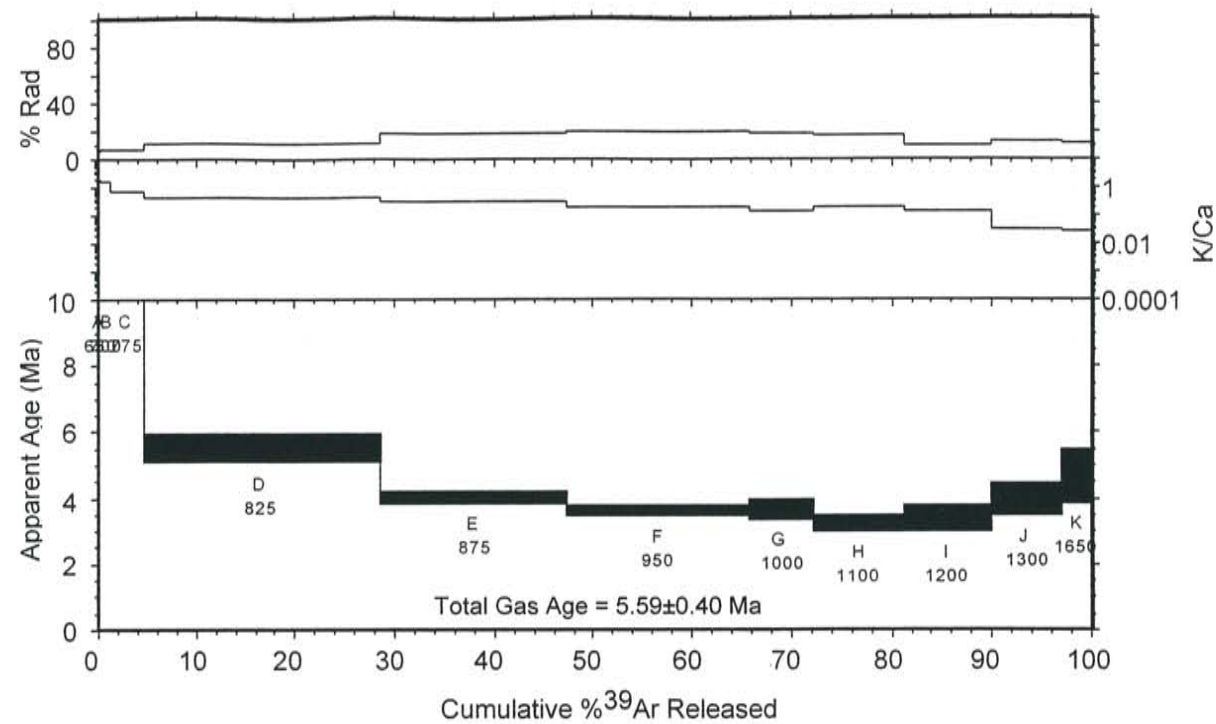
RA-008, pyroxene dacite, San Antonio Mt., groundmass concentrate



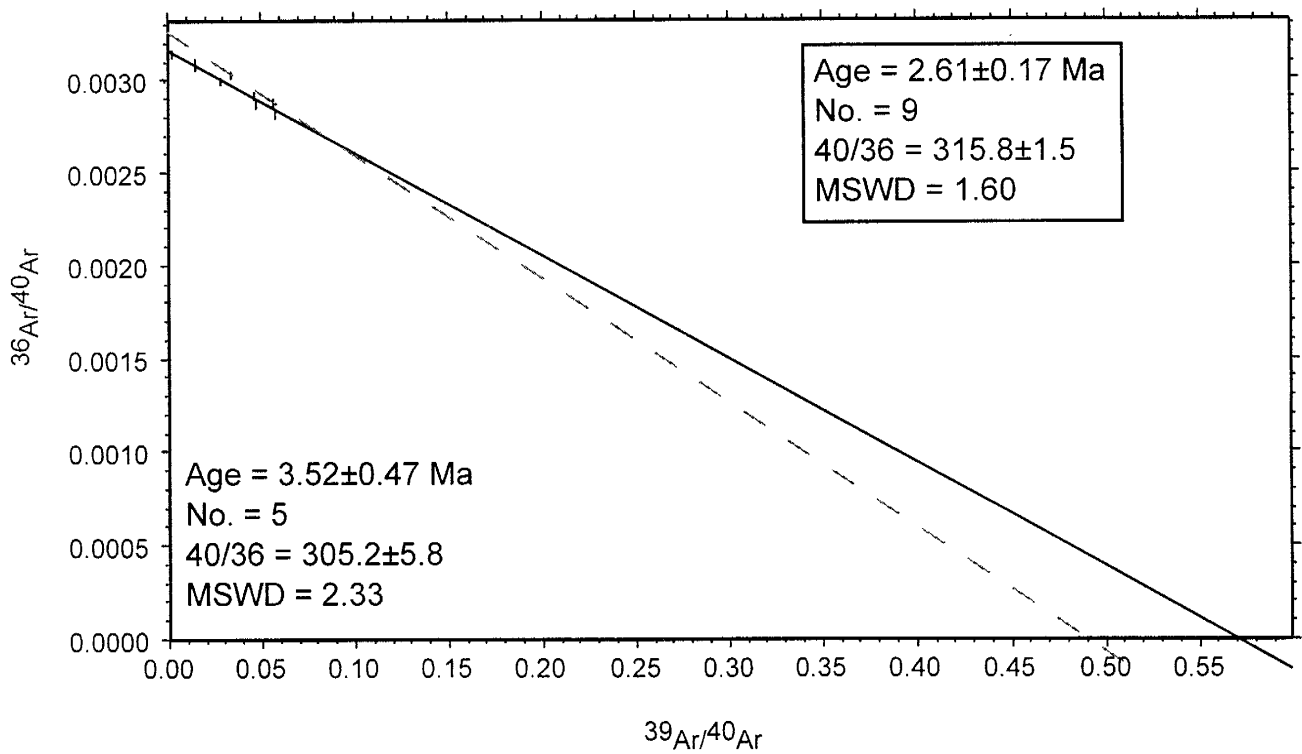
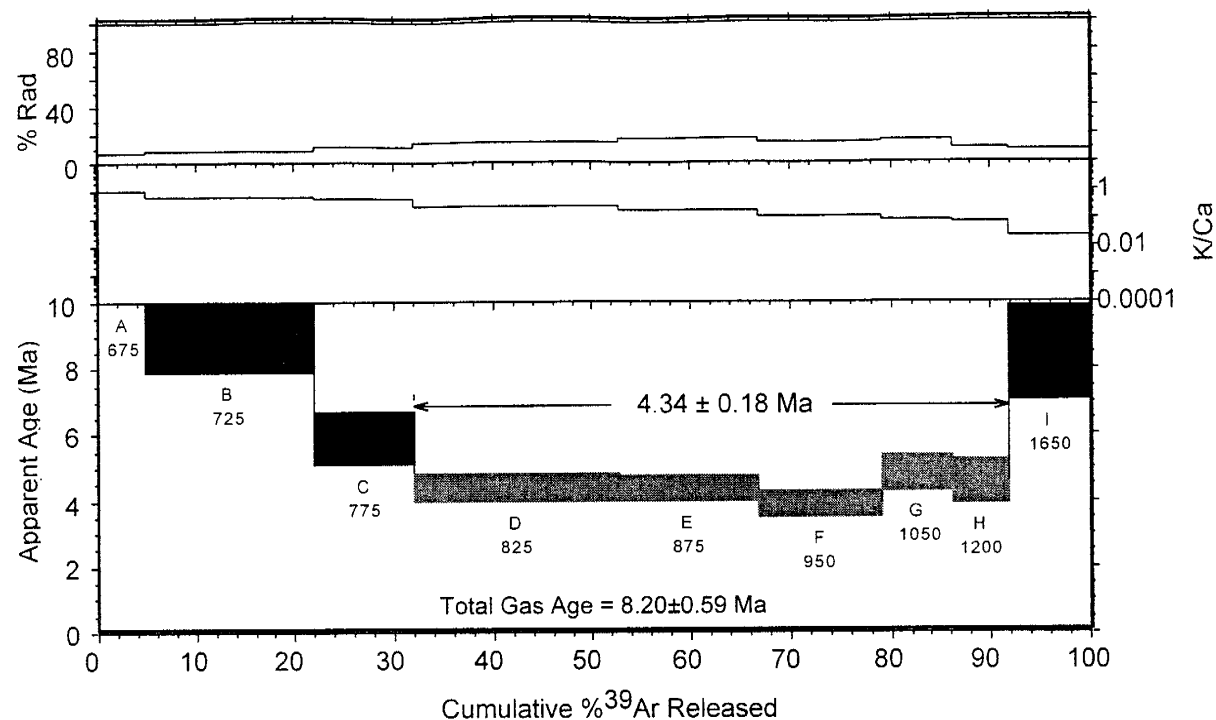
RA-009, pyroxene dacite, San Antonio Mt., groundmass concentrate



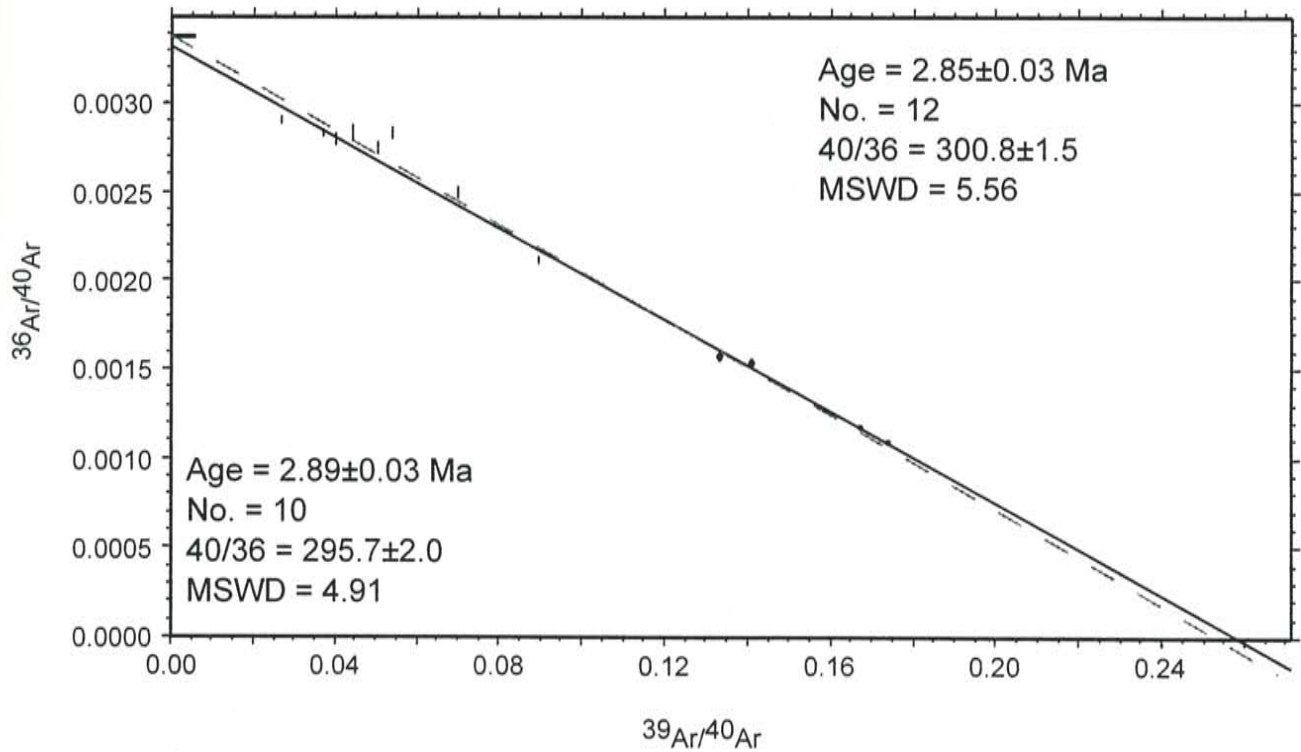
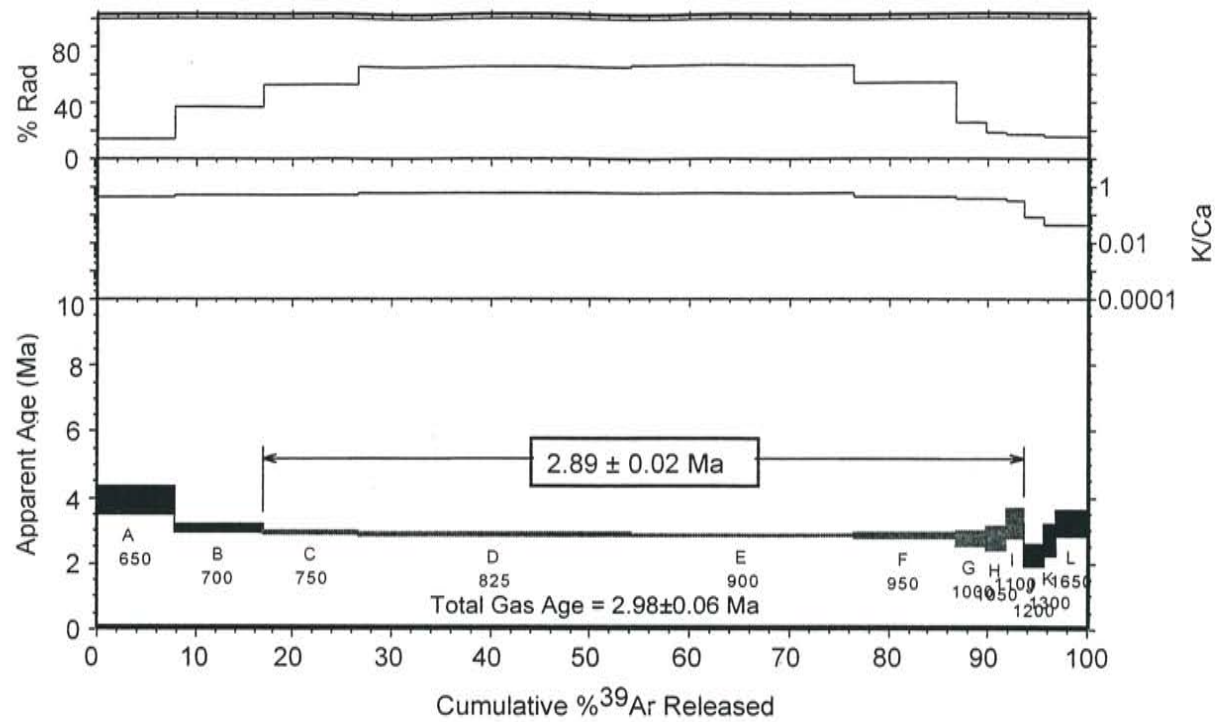
RA-010, Servilleta Basalt, San Antonio Mt. area, groundmass concentrate



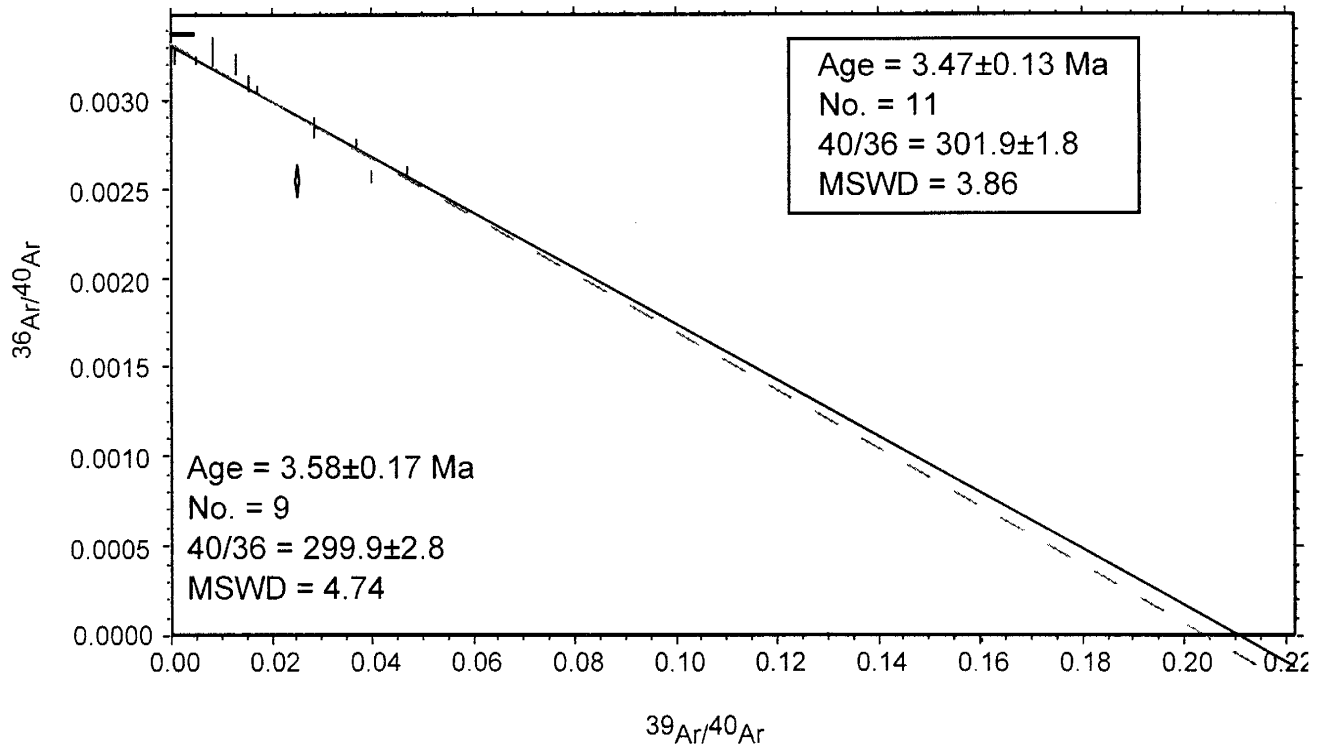
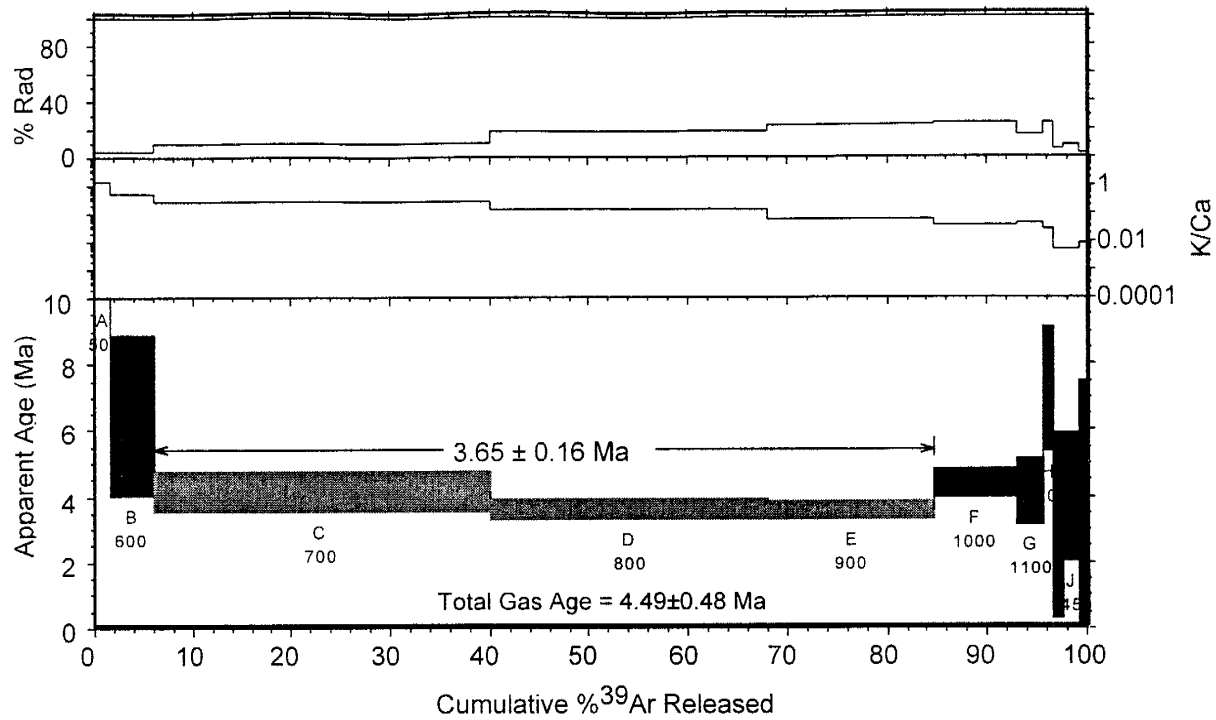
RA-011, Servilleta Basalt, San Antonio Mt. area, groundmass concentrate



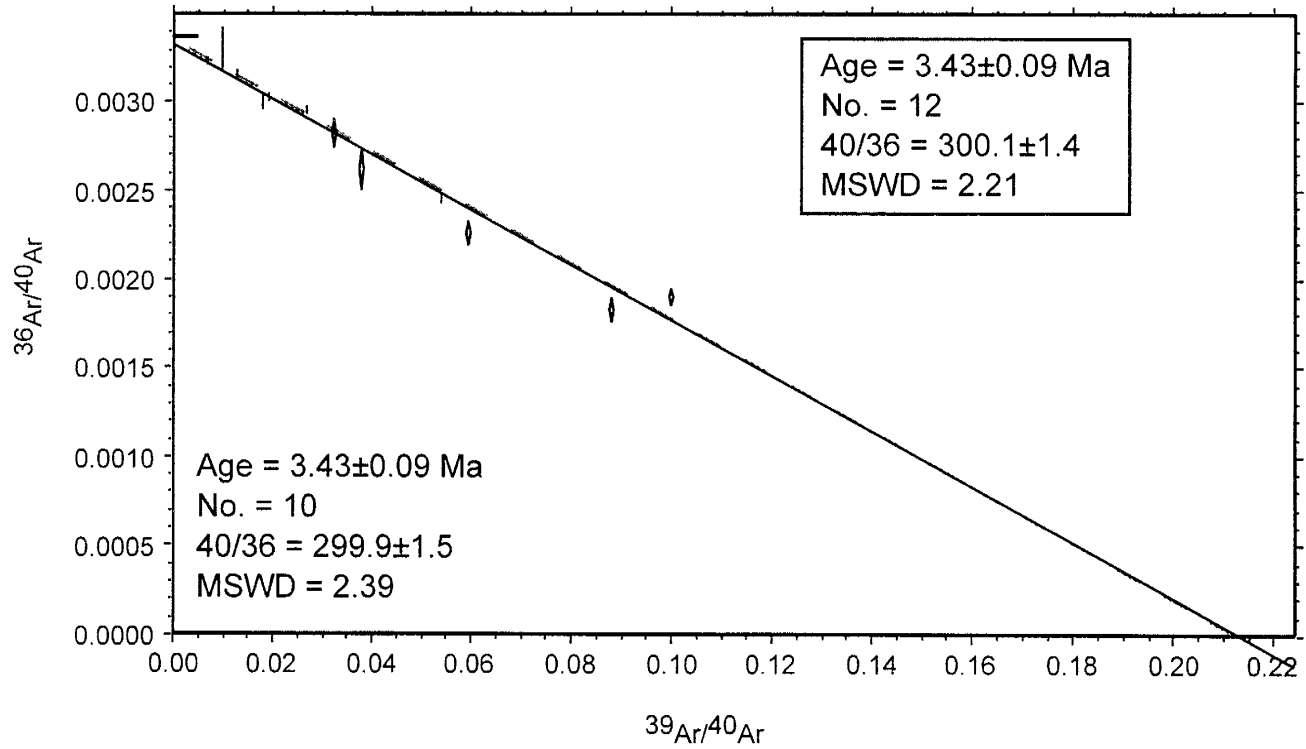
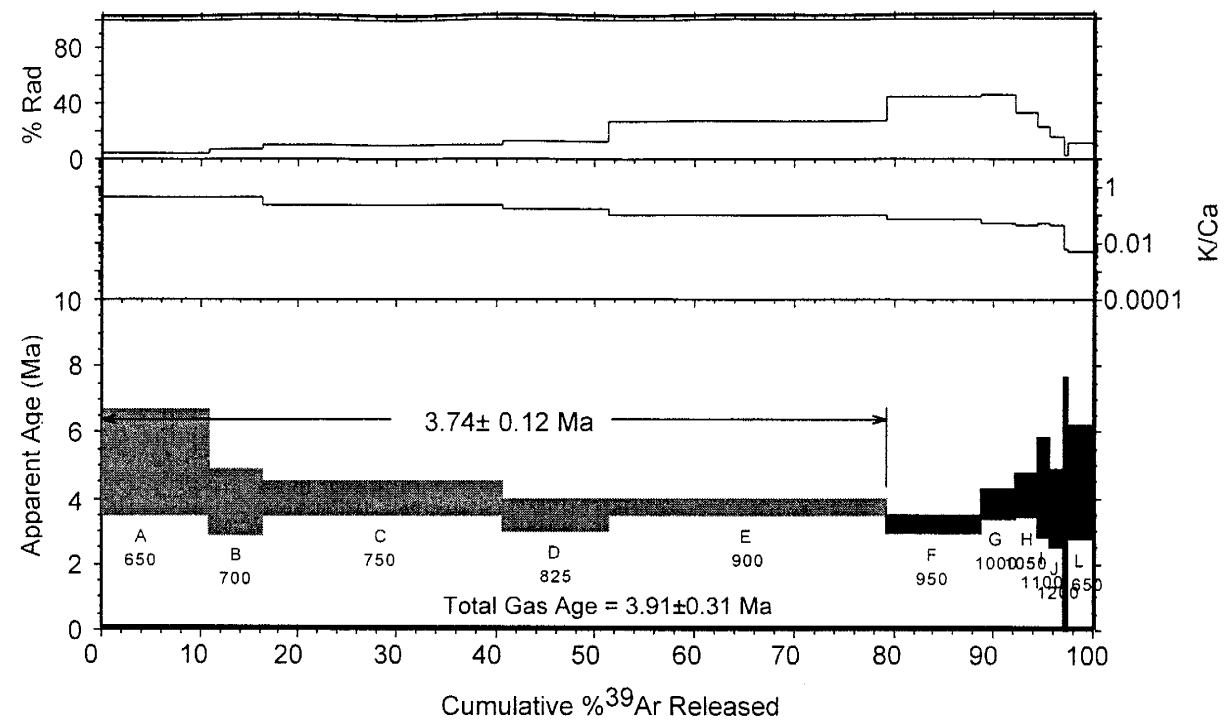
RA-012, basaltic andesite, No Agua roadcut, groundmass concentrate



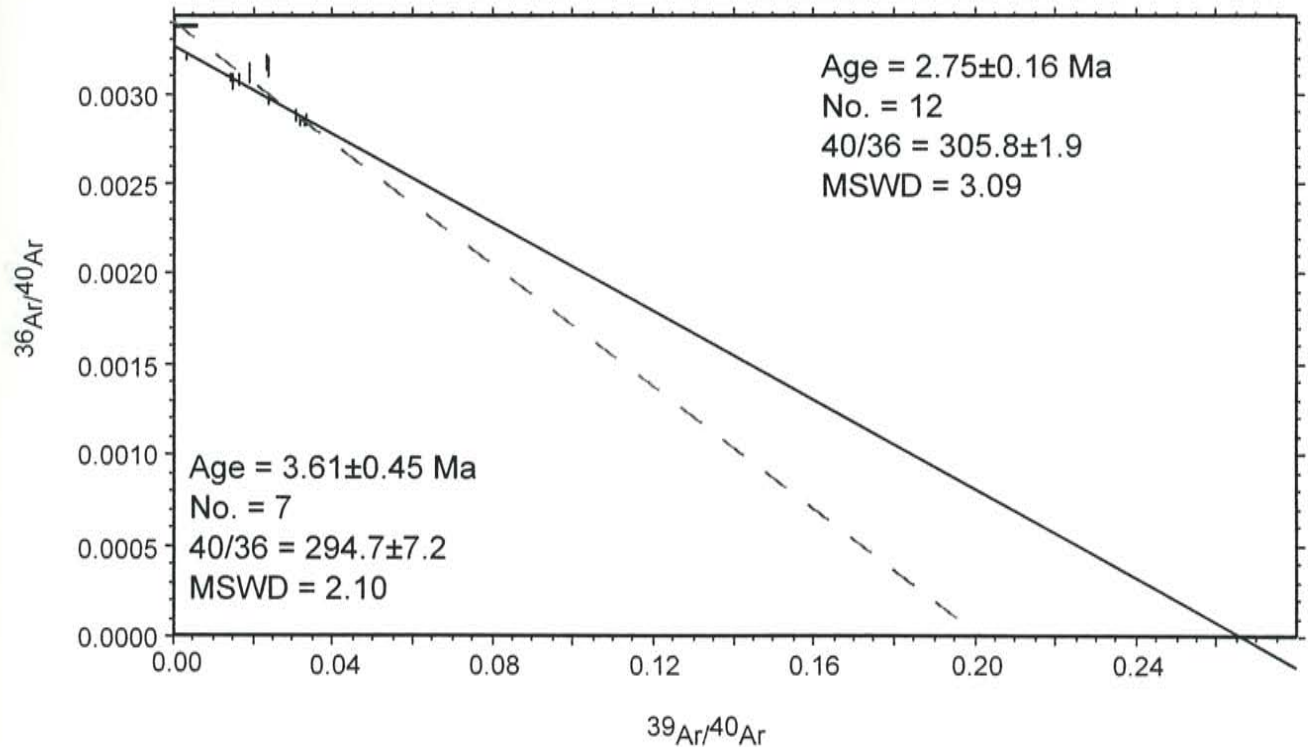
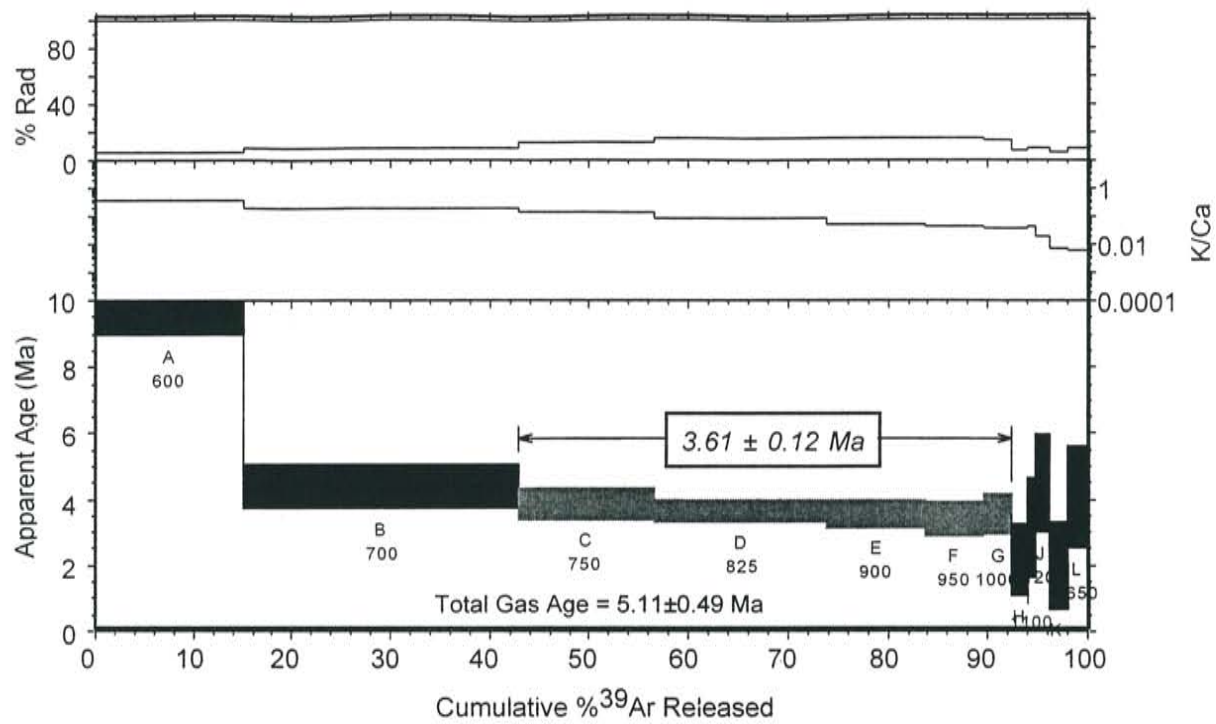
RA-013, Servilleta Basalt, US 285, groundmass concentrate



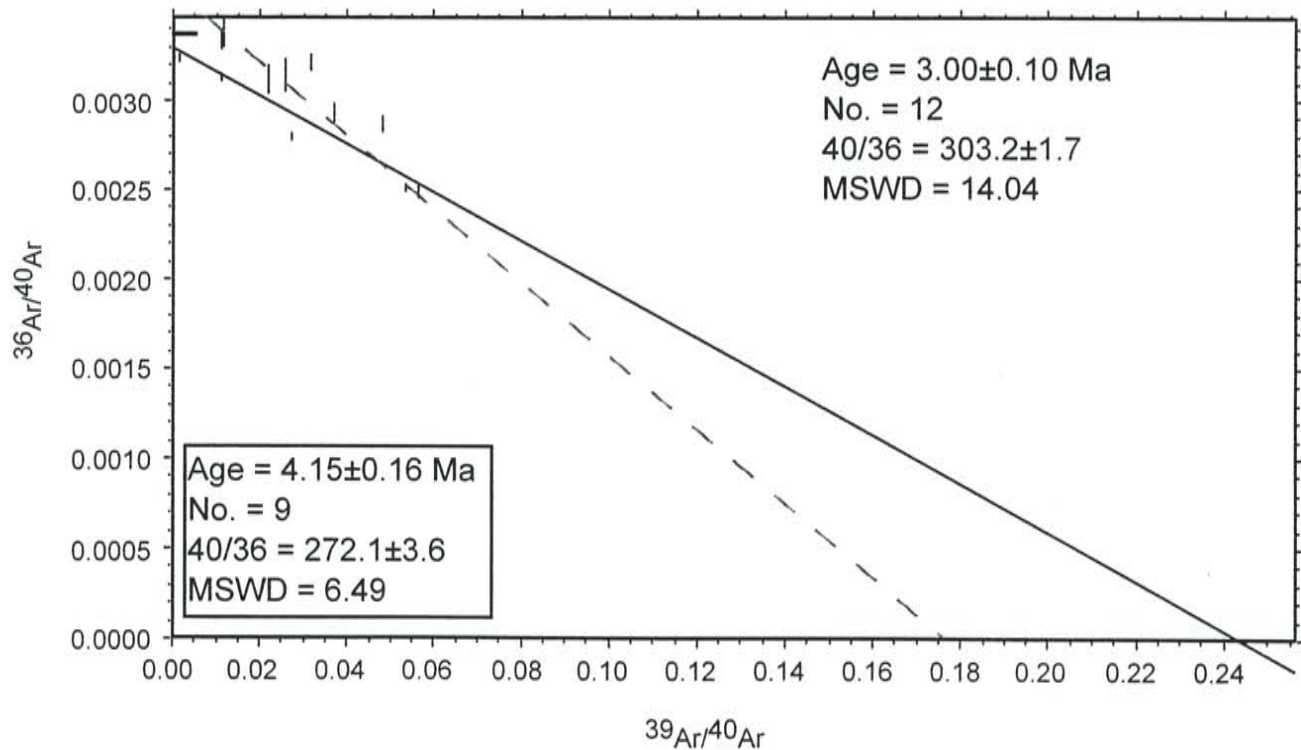
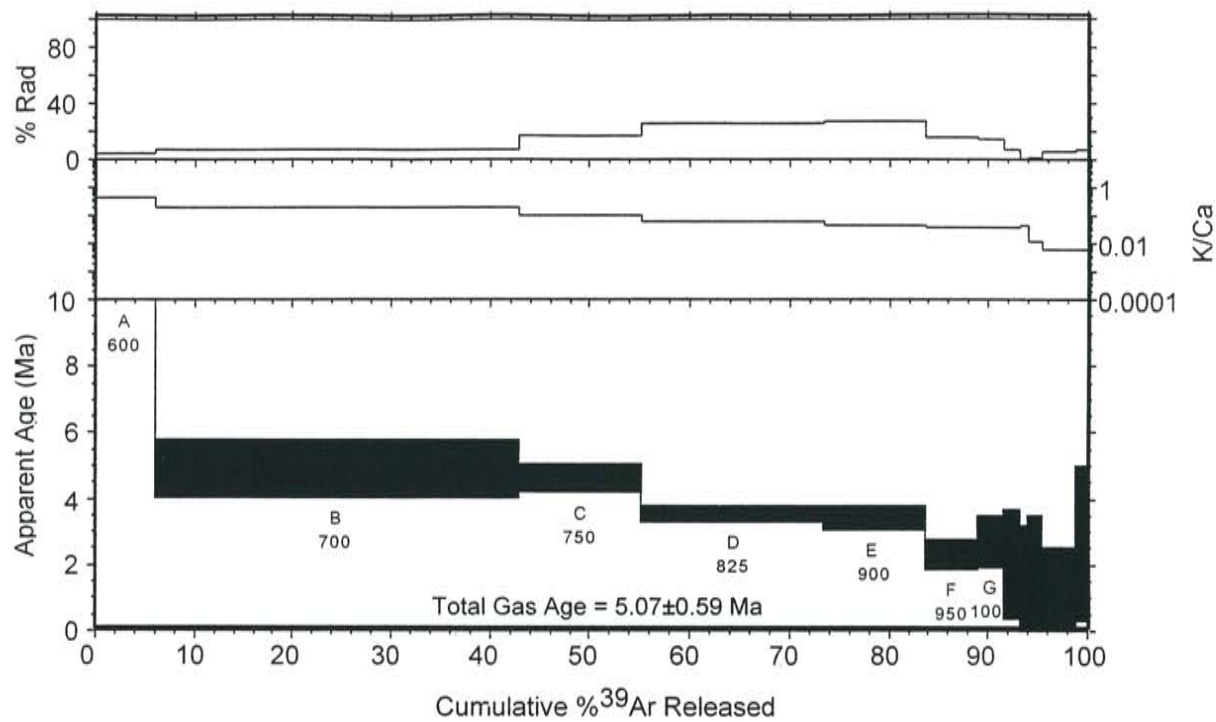
RA-014, Servilleta Basalt, US 285, groundmass concentrate



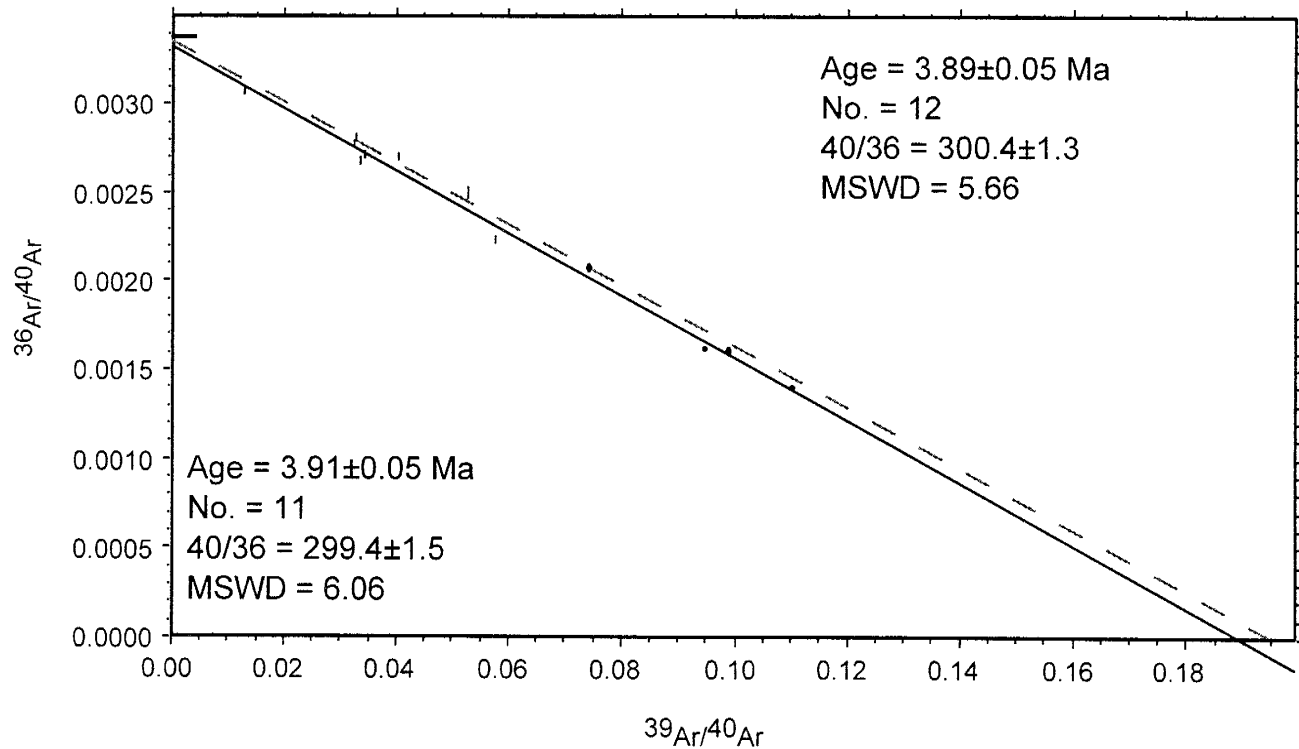
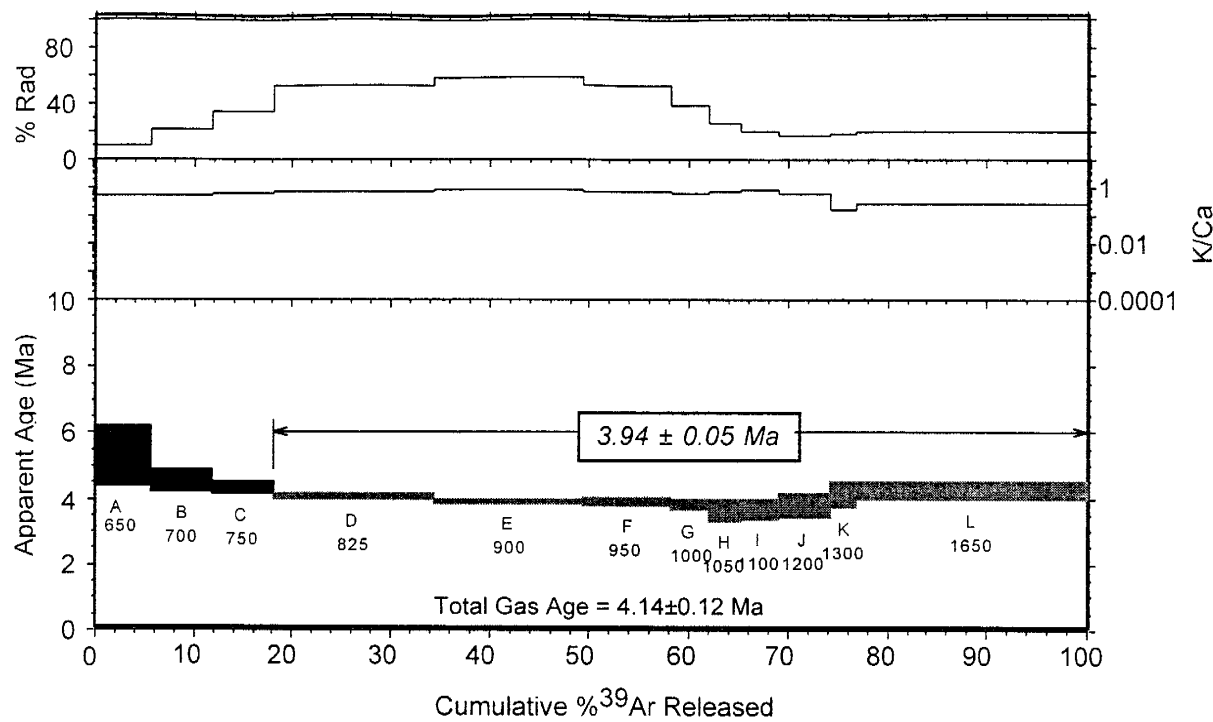
RA-015, Servilleta Basalt, US 285, groundmass concentrate



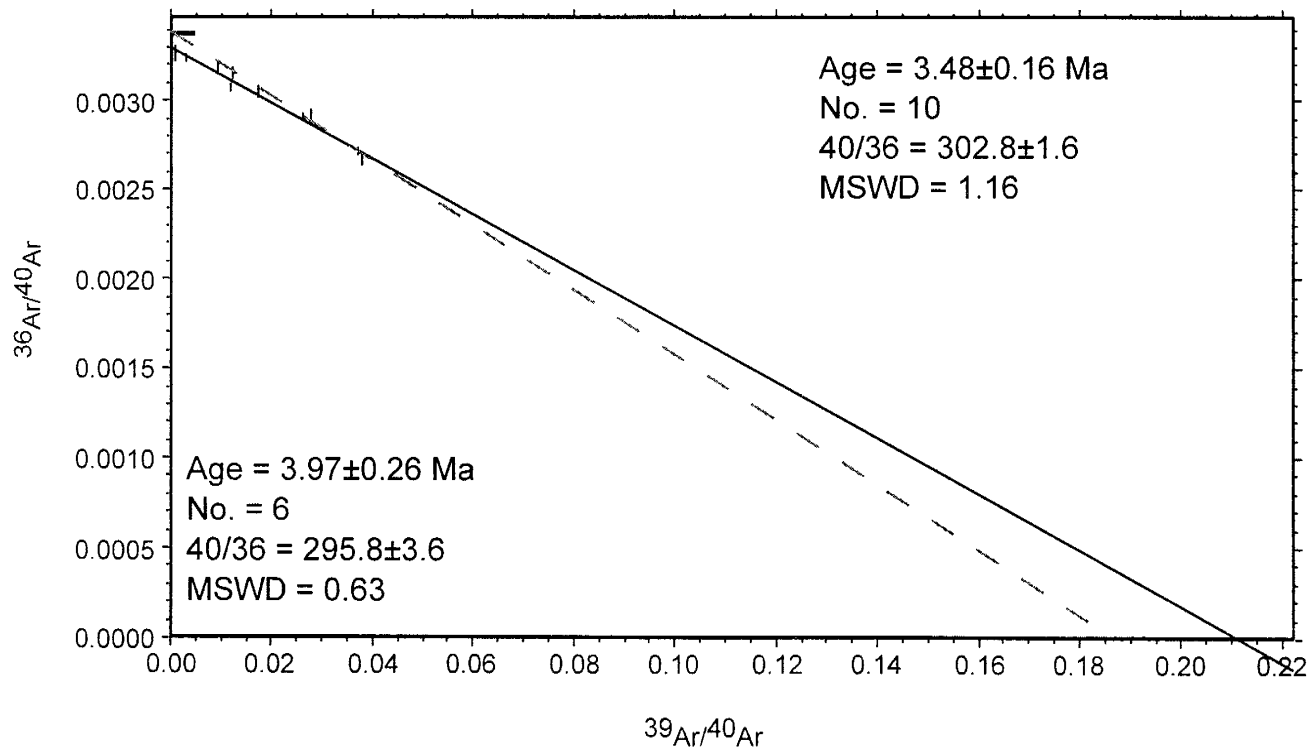
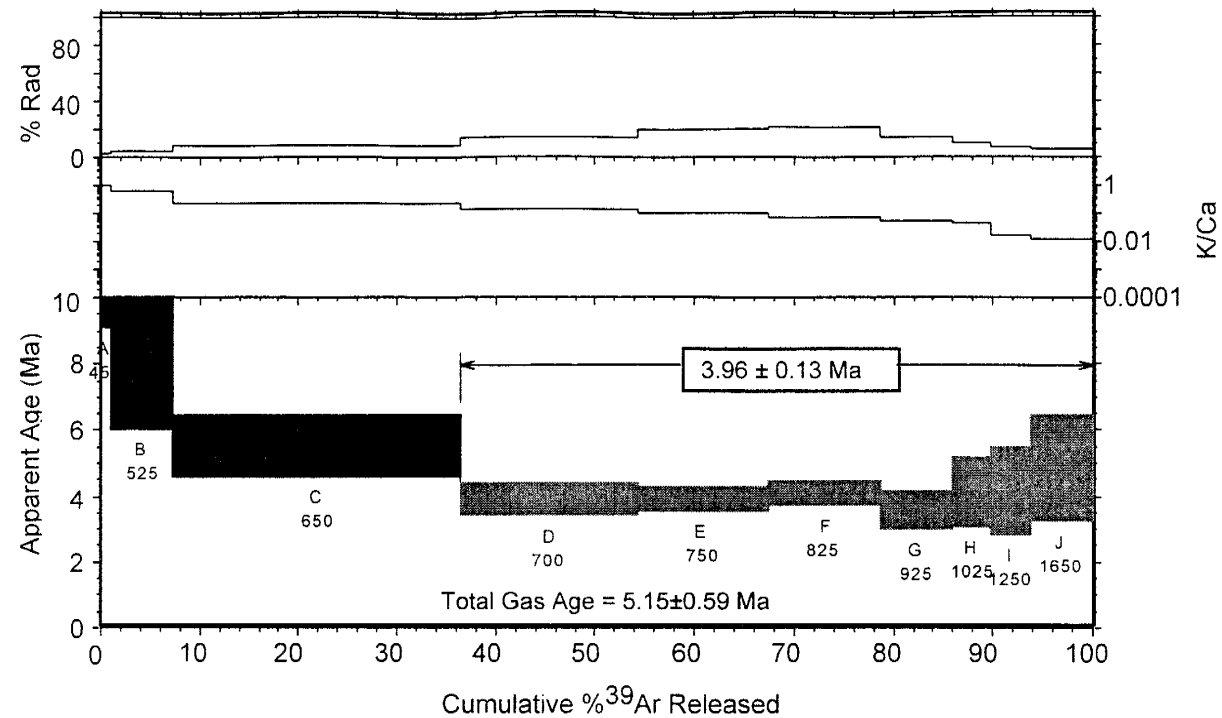
RA-016, Servilleta Basalt, US 285, groundmass concentrate



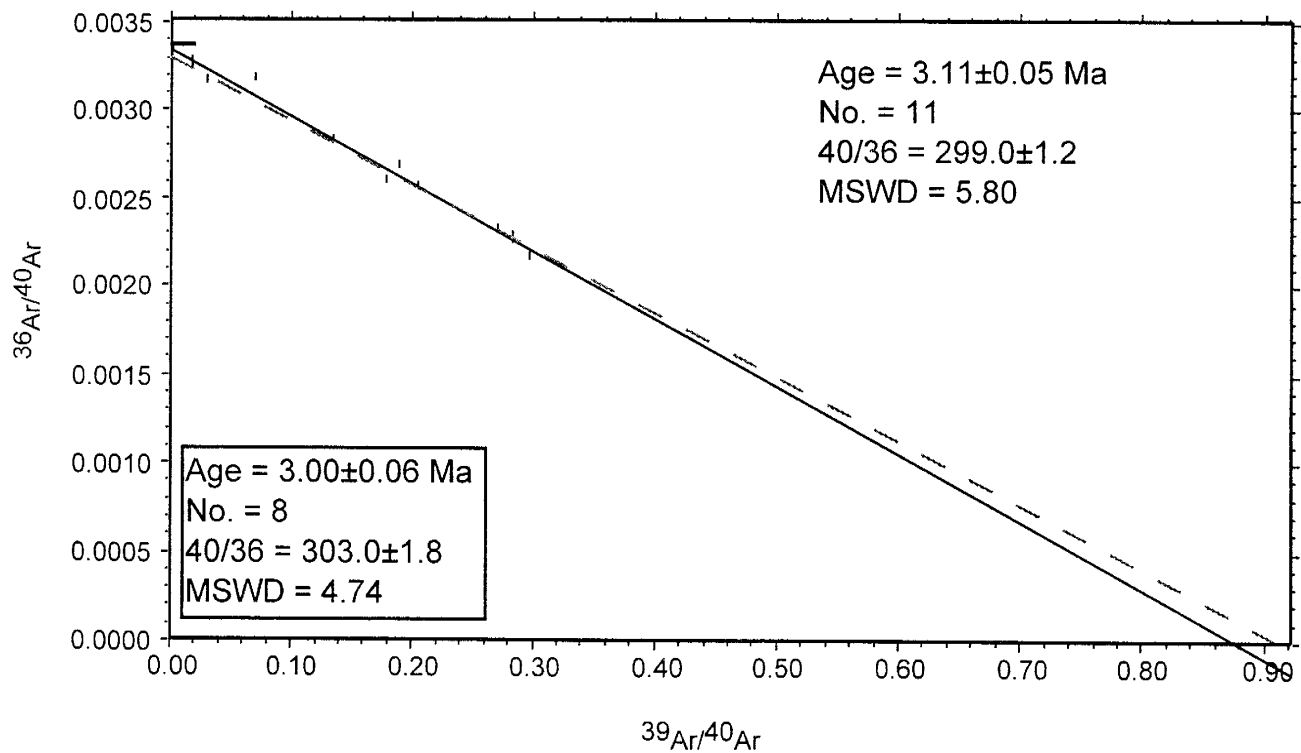
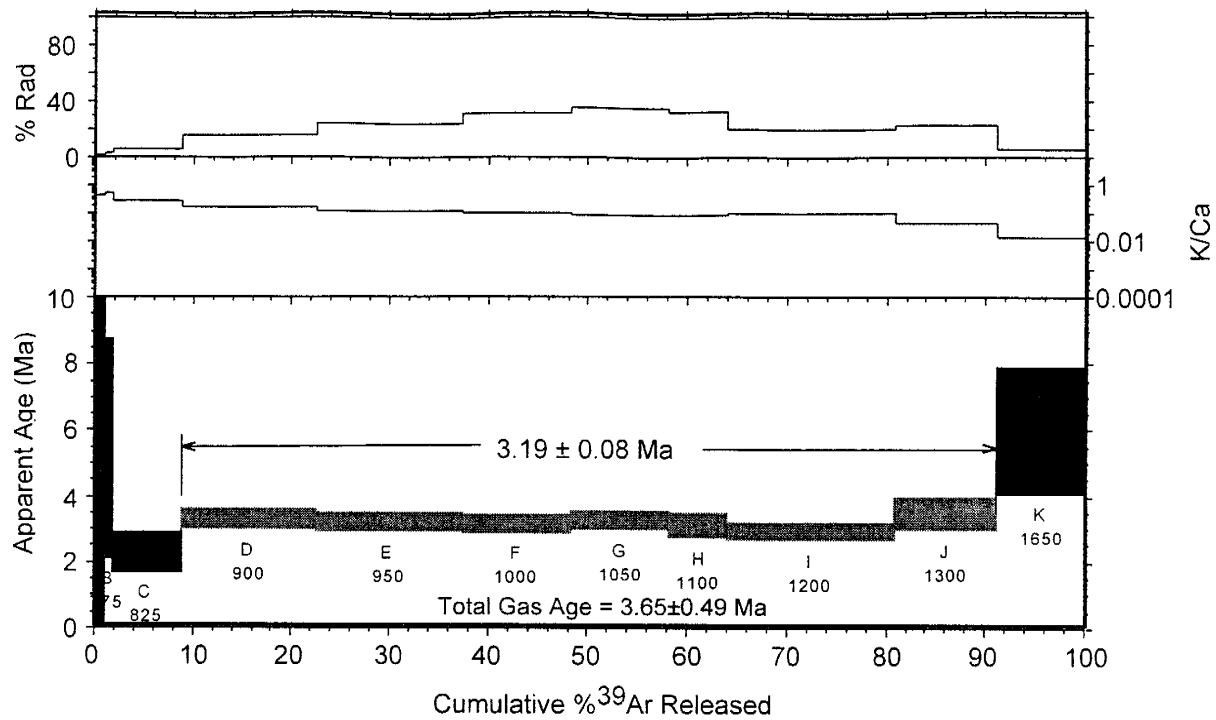
RA-017, basaltic andesite, Los Cerritos de la Cruz, groundmass concentrate



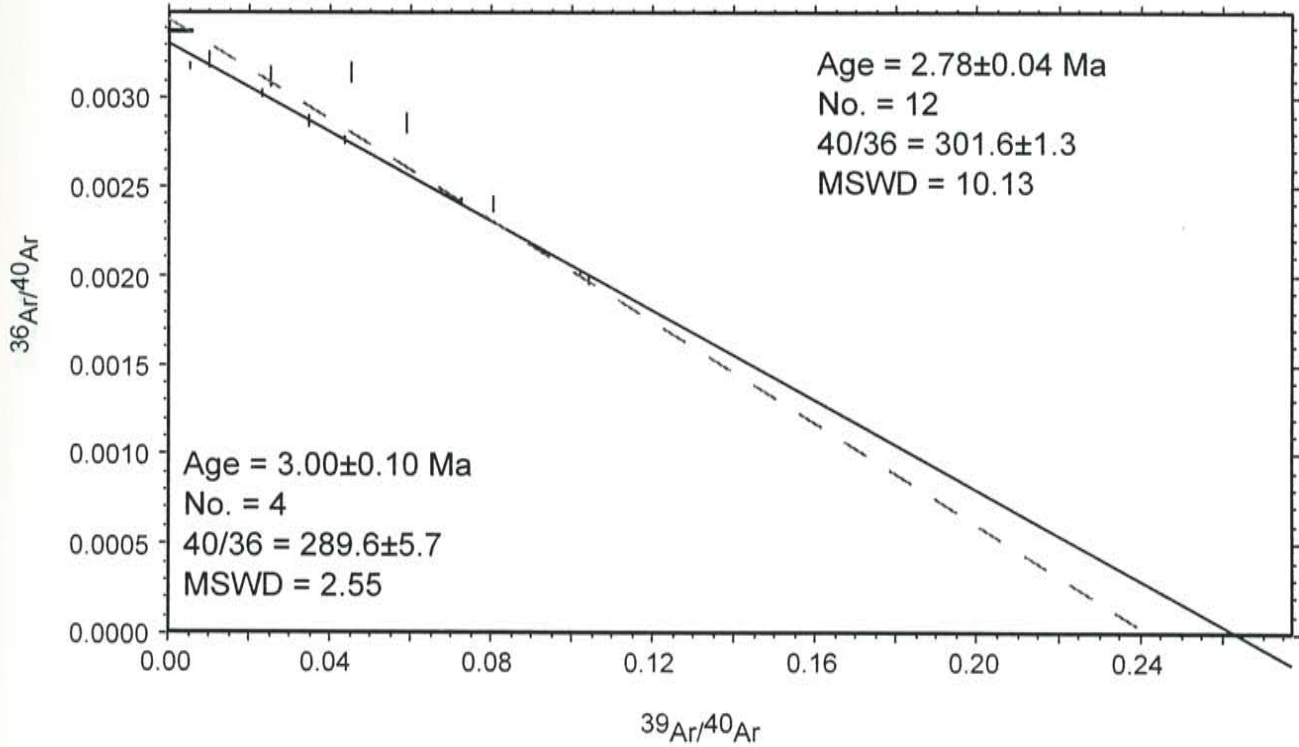
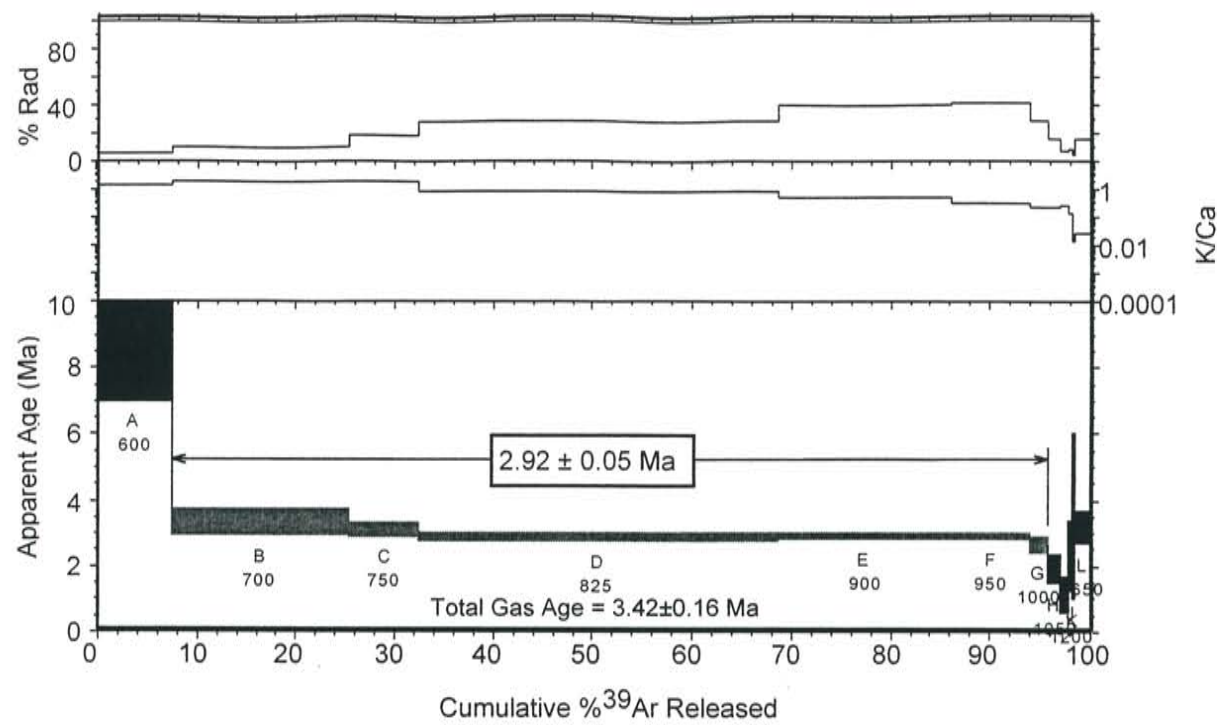
RA-018, basaltic andesite, Los Cerritos de la Cruz, groundmass concentrate



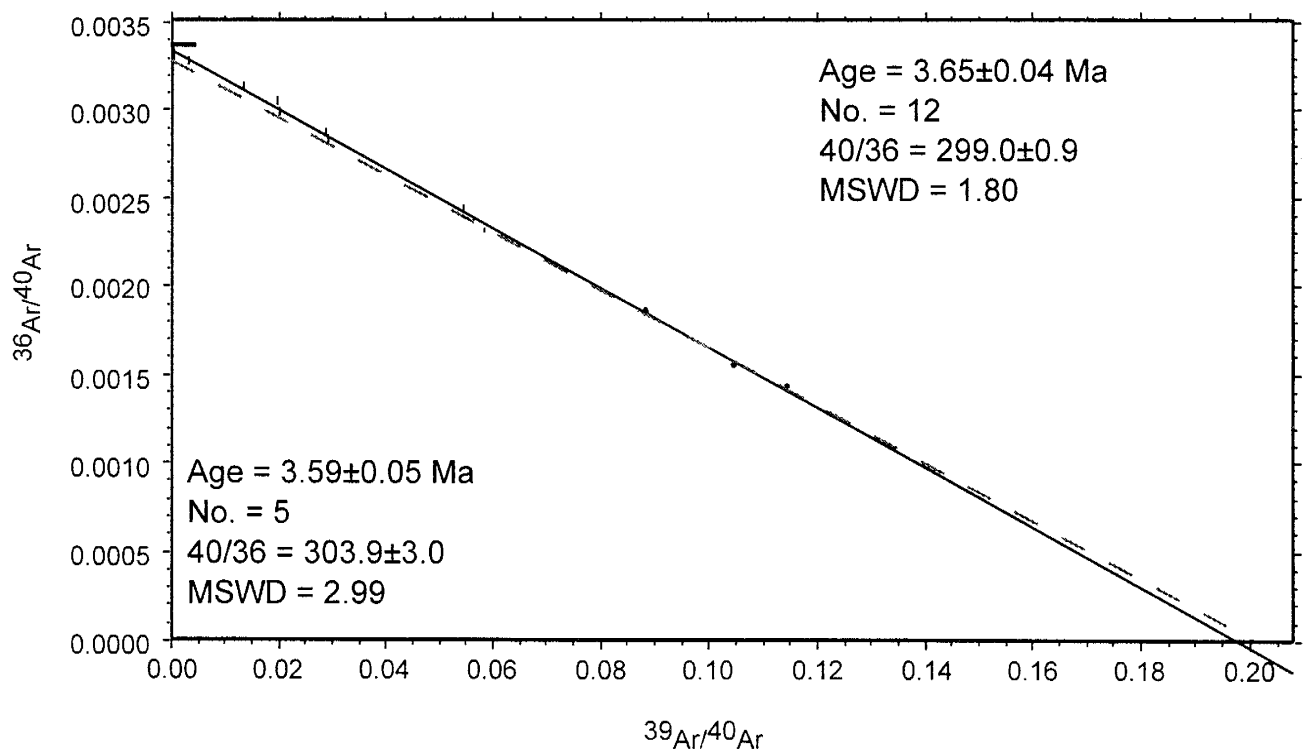
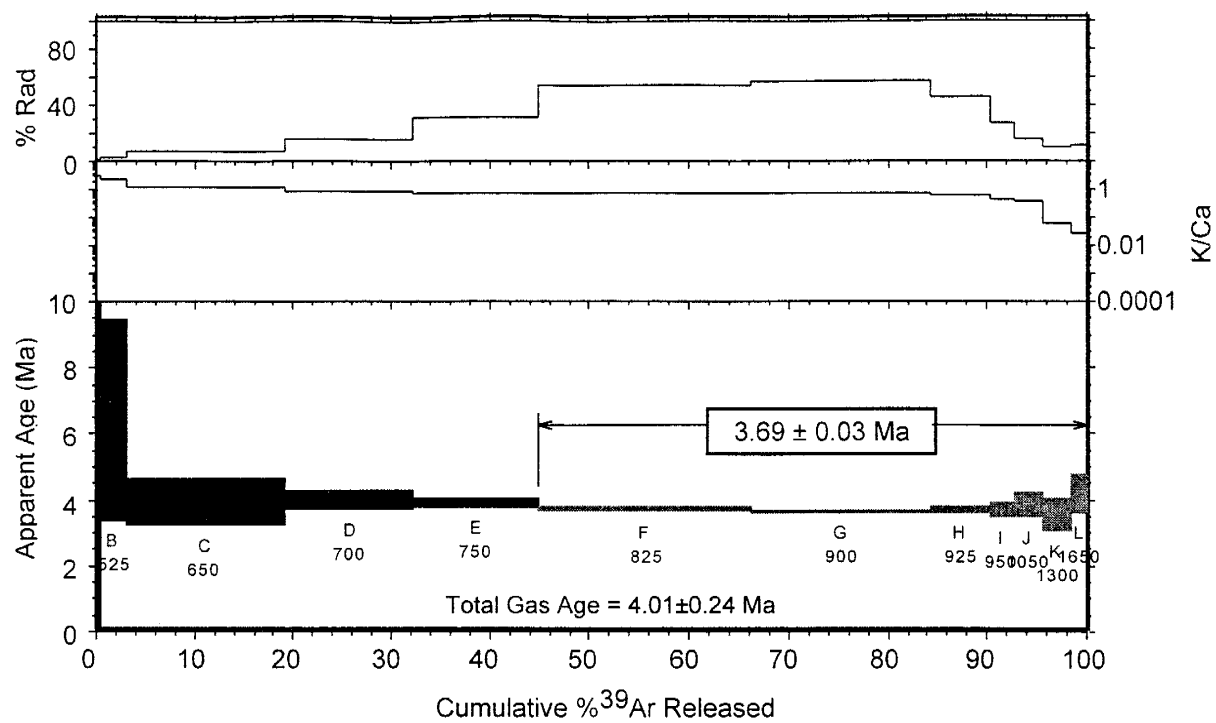
RA-019, Servilleta Basalt, Rio San Antonio, groundmass concentrate



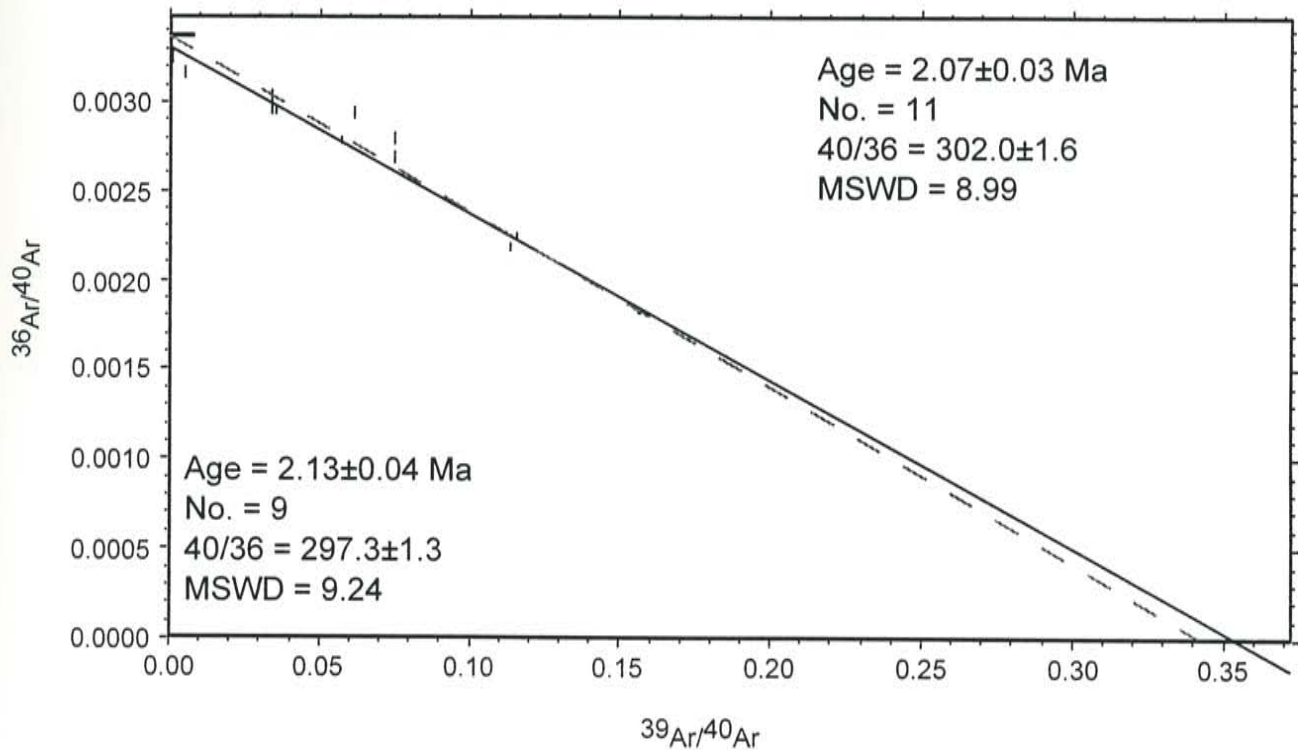
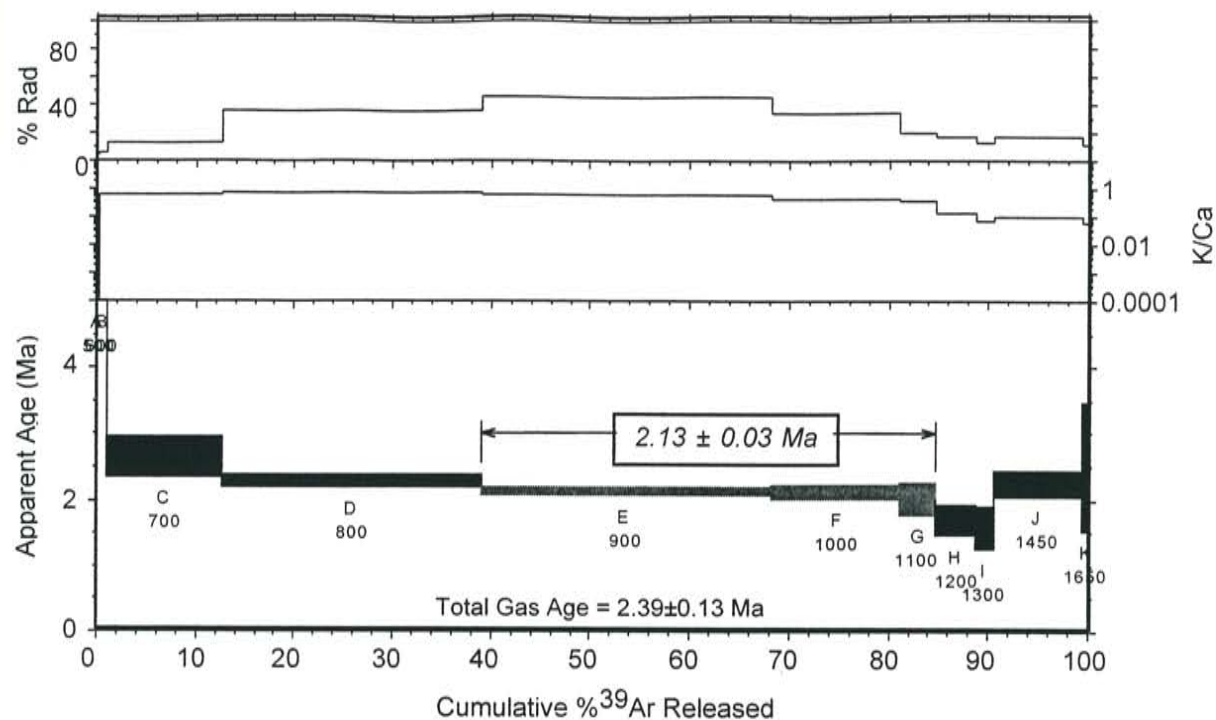
RA-020, andesite, San Antonio Mt., groundmass concentrate



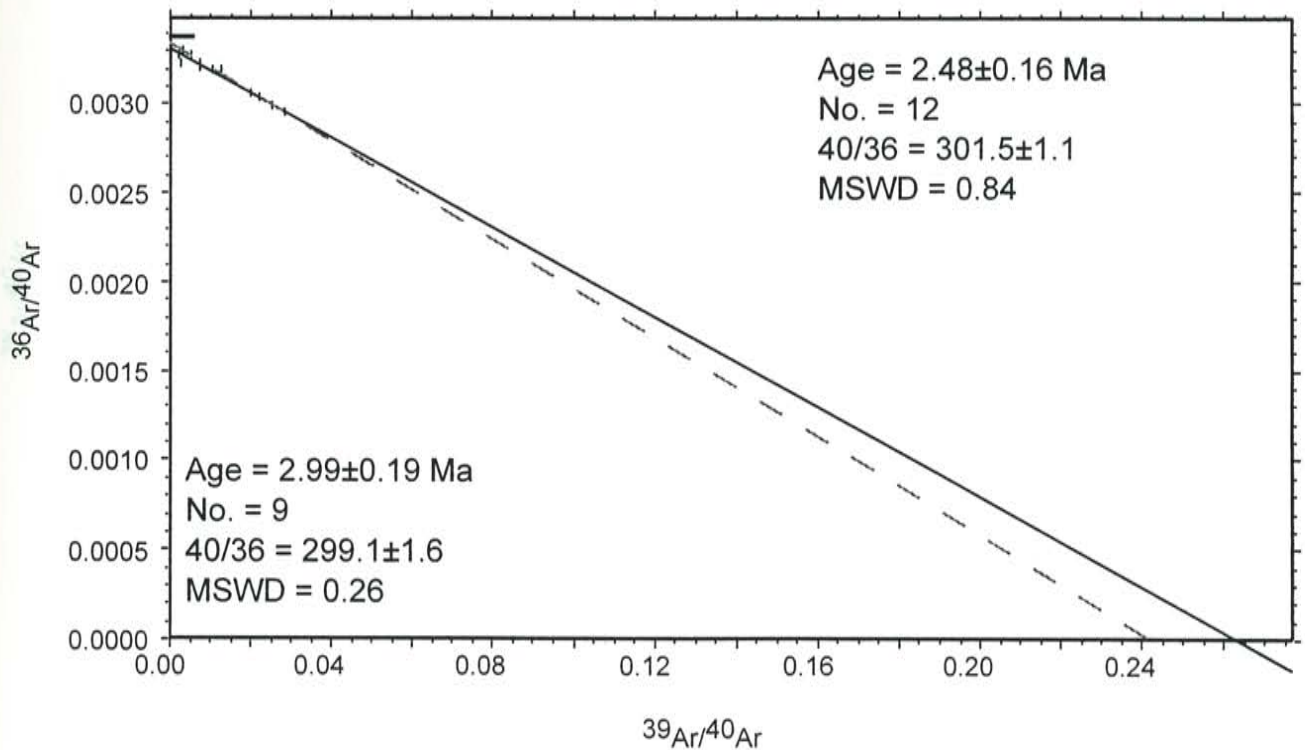
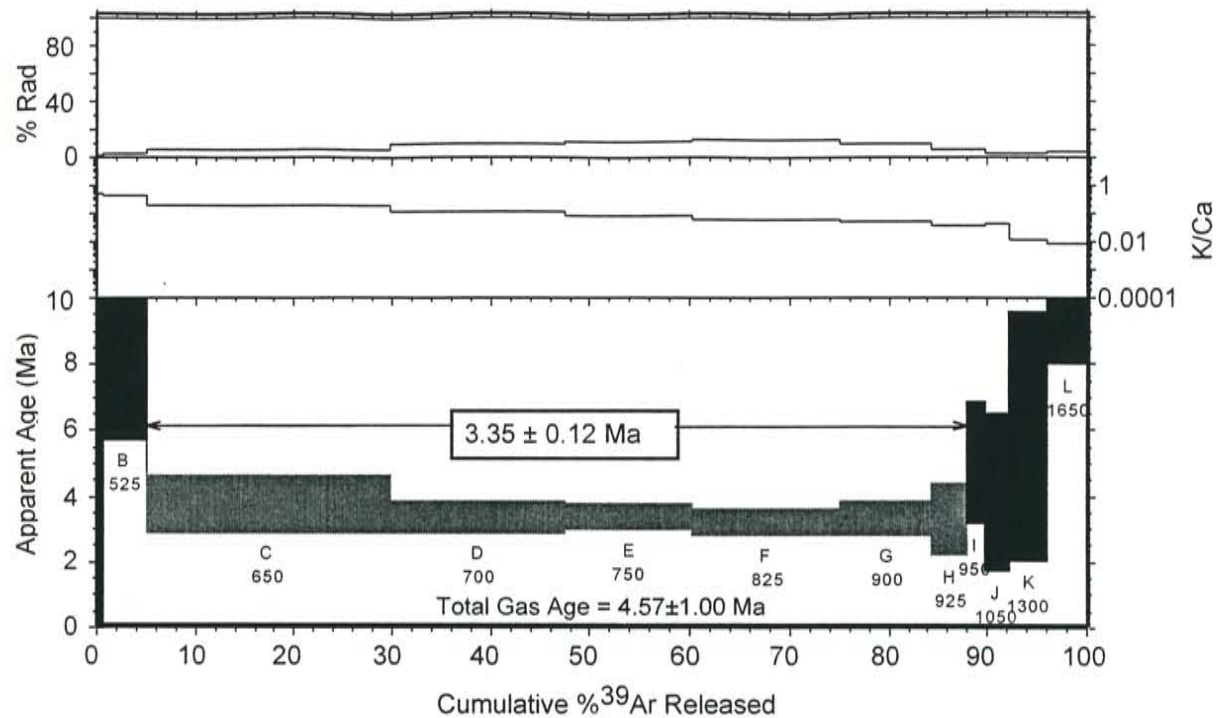
RA-021, olivine andesite, Cerro del Aire, groundmass concentrate



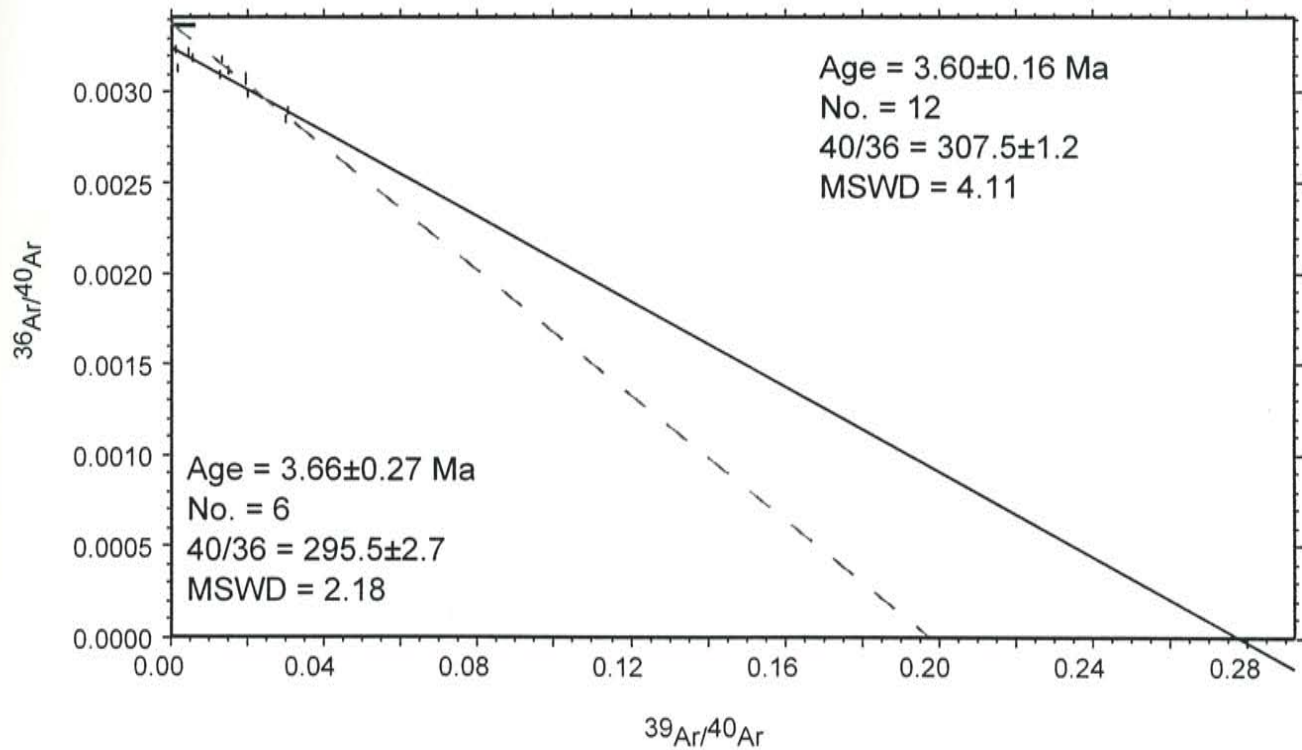
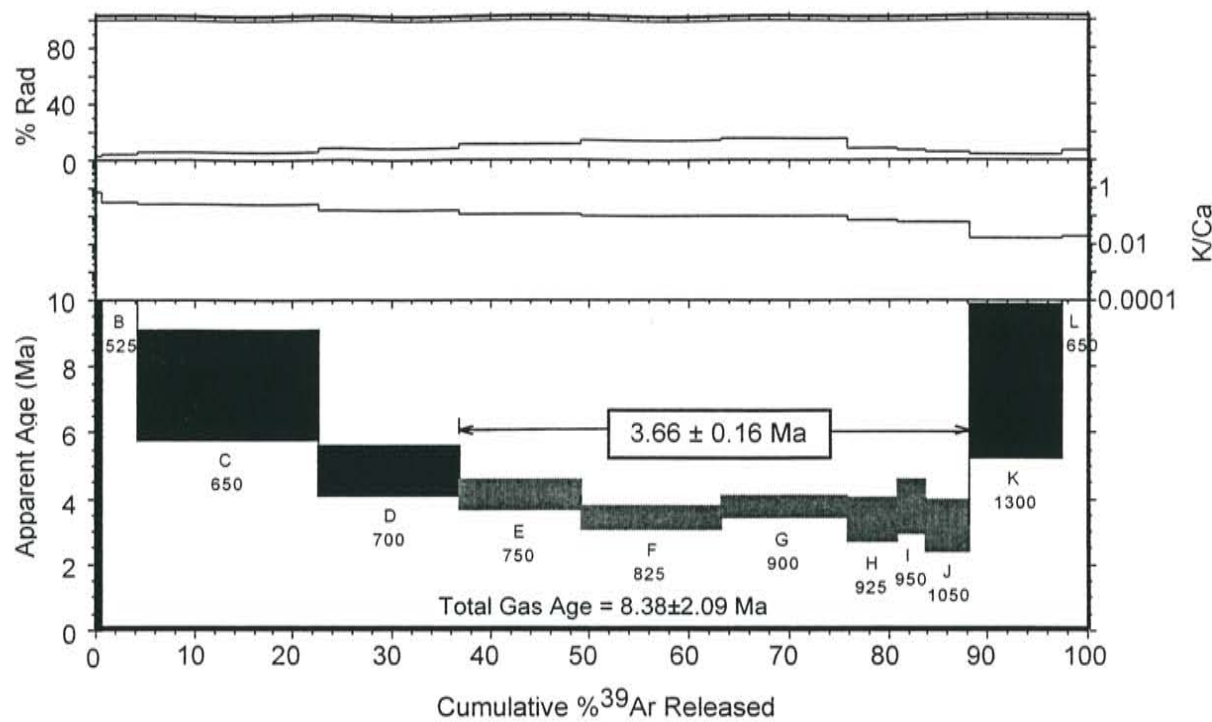
RA-022, basaltic andesite, La Segita Peaks, groundmass concentrate



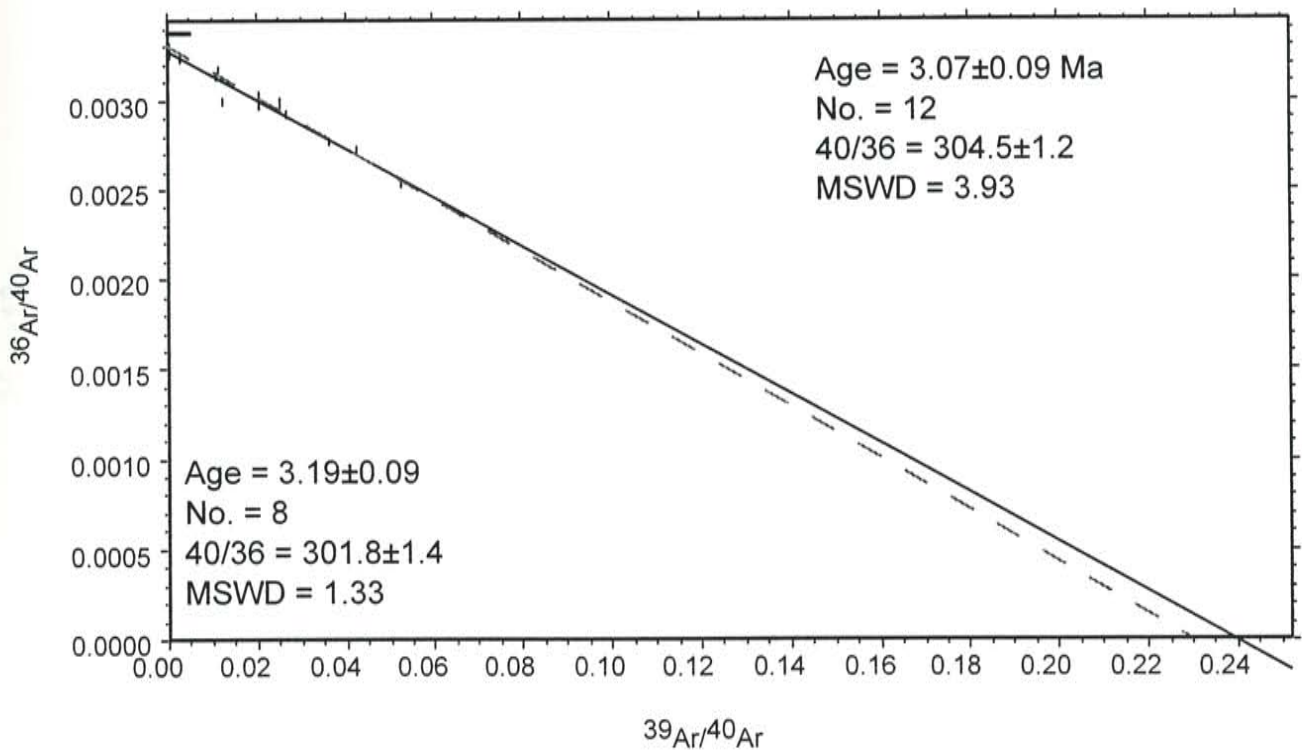
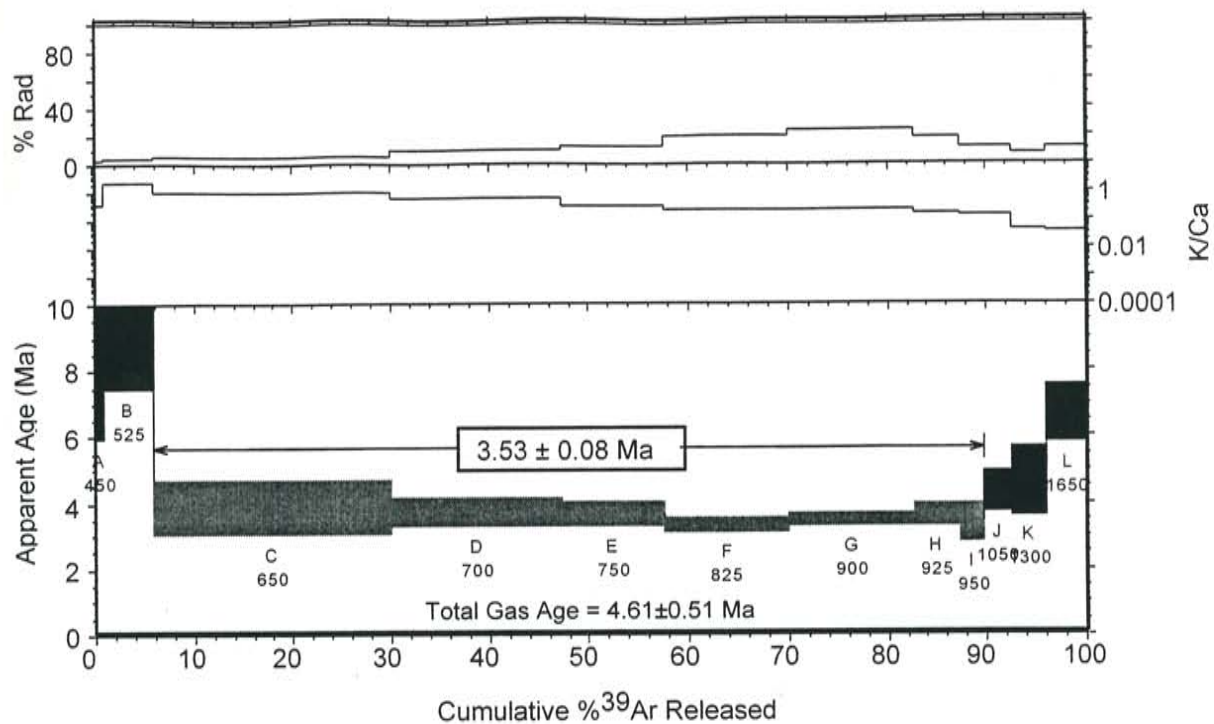
RA-023, Servilleta Basalt, La Segita Peaks, groundmass concentrate



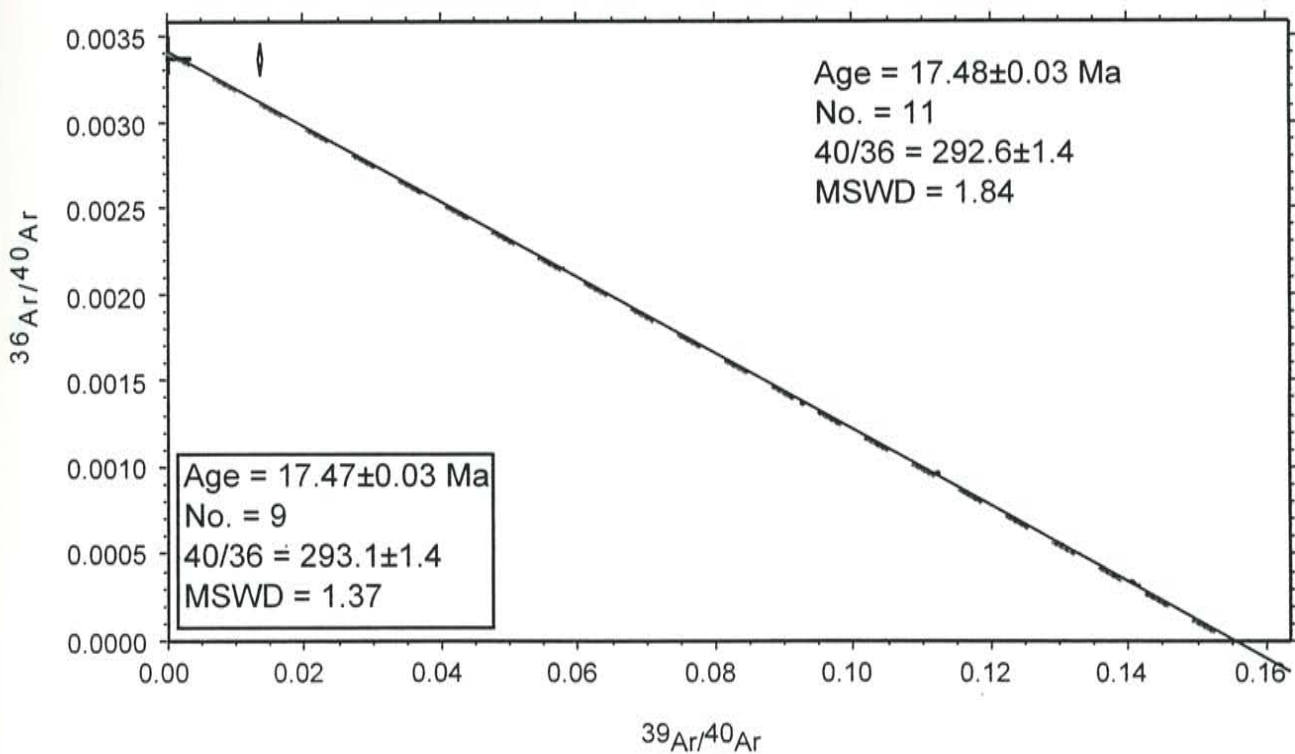
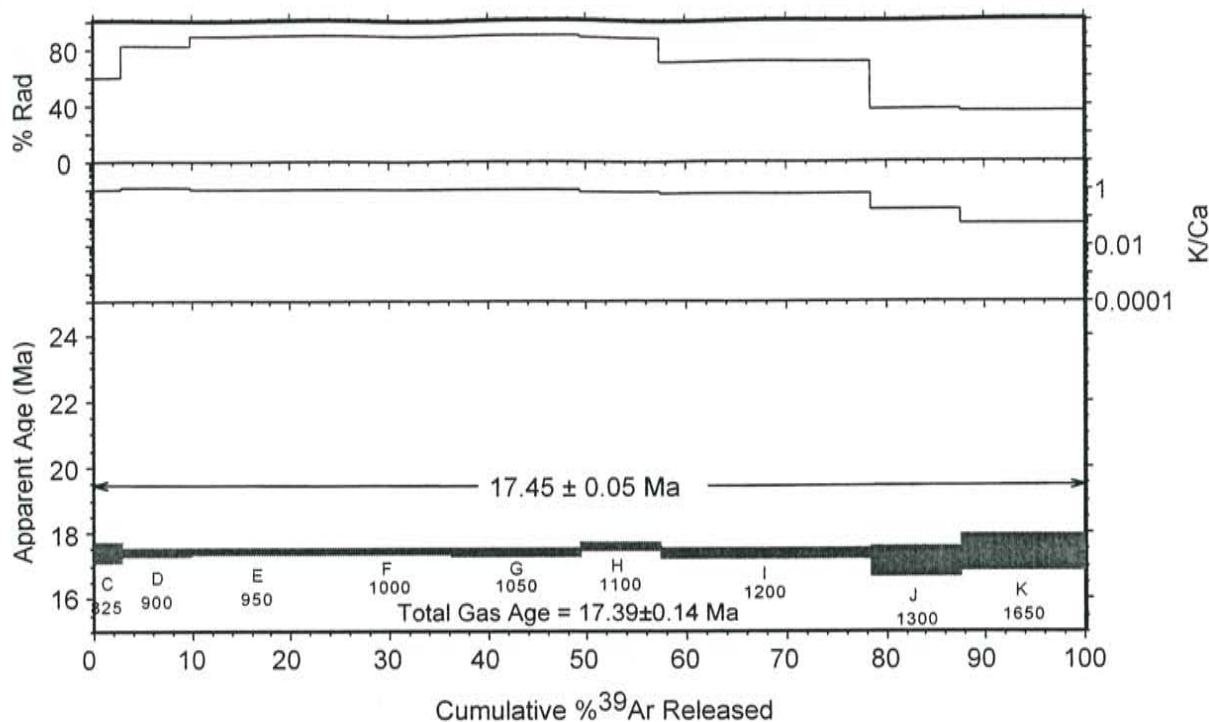
RA-024, Servilleta Basalt, La Segita Peaks, groundmass concentrate



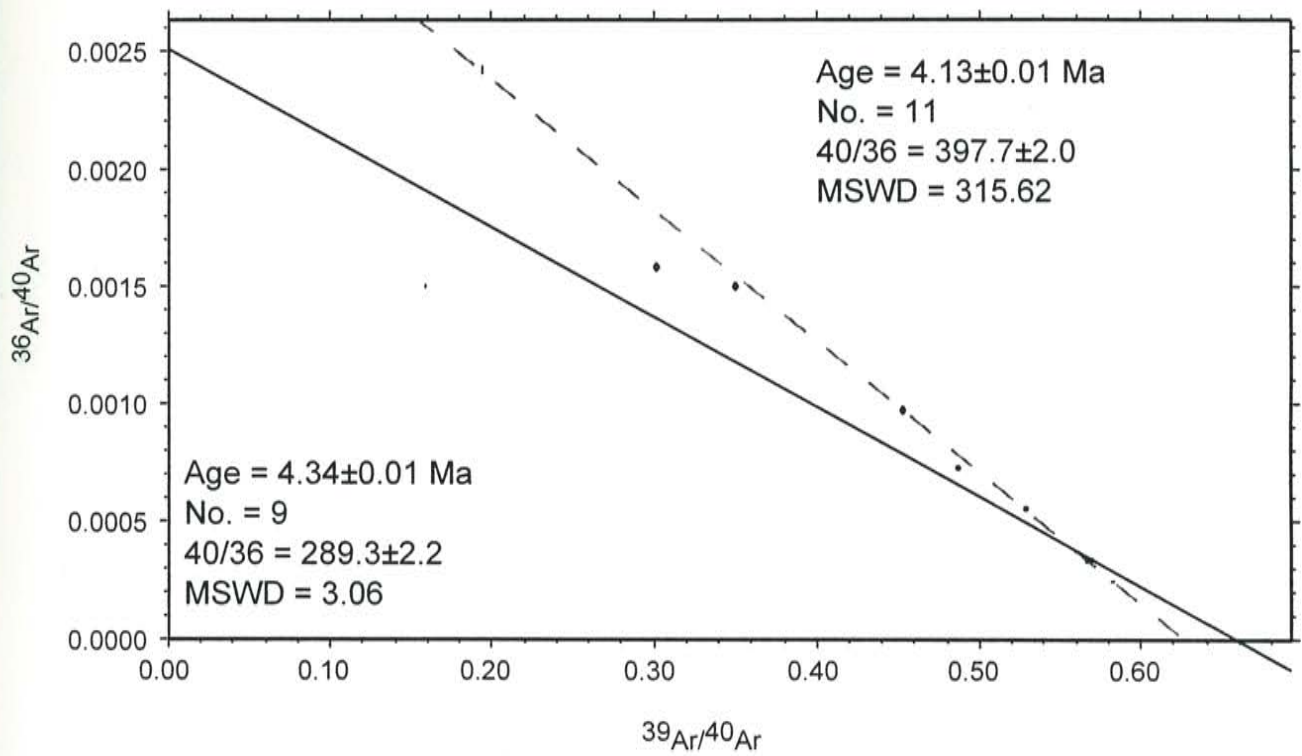
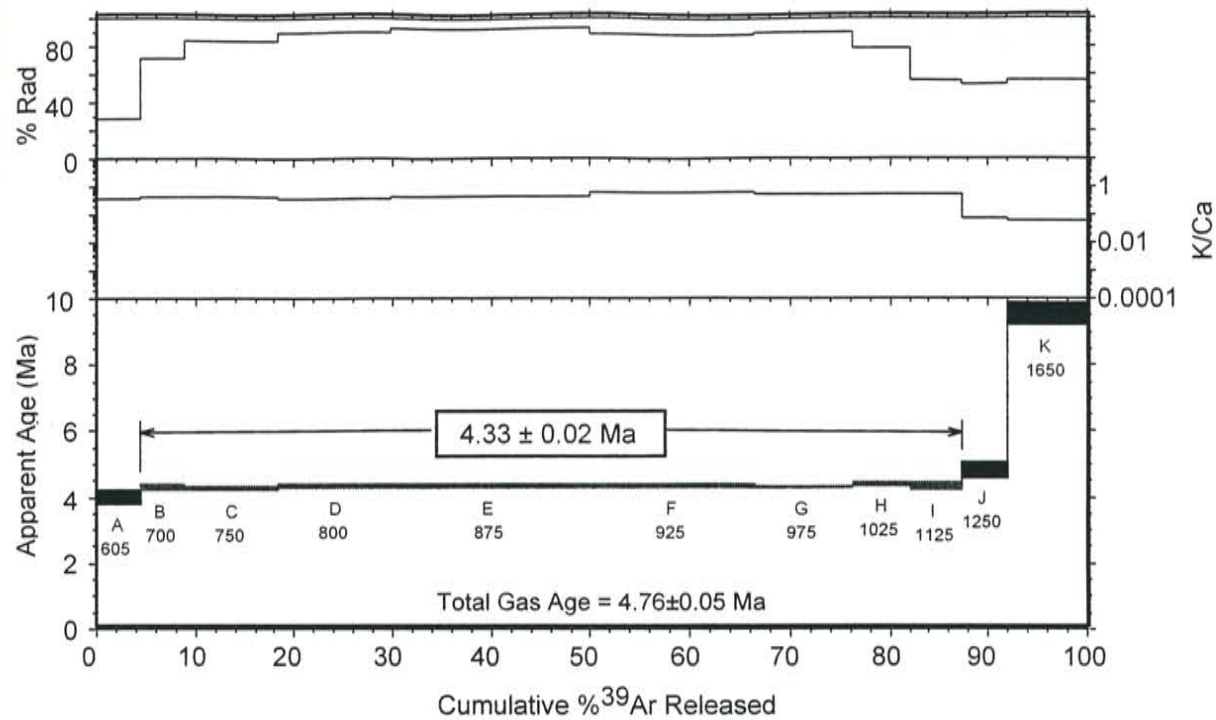
RA-025, Servilleta Basalt, La Segita Peaks, groundmass concentrate



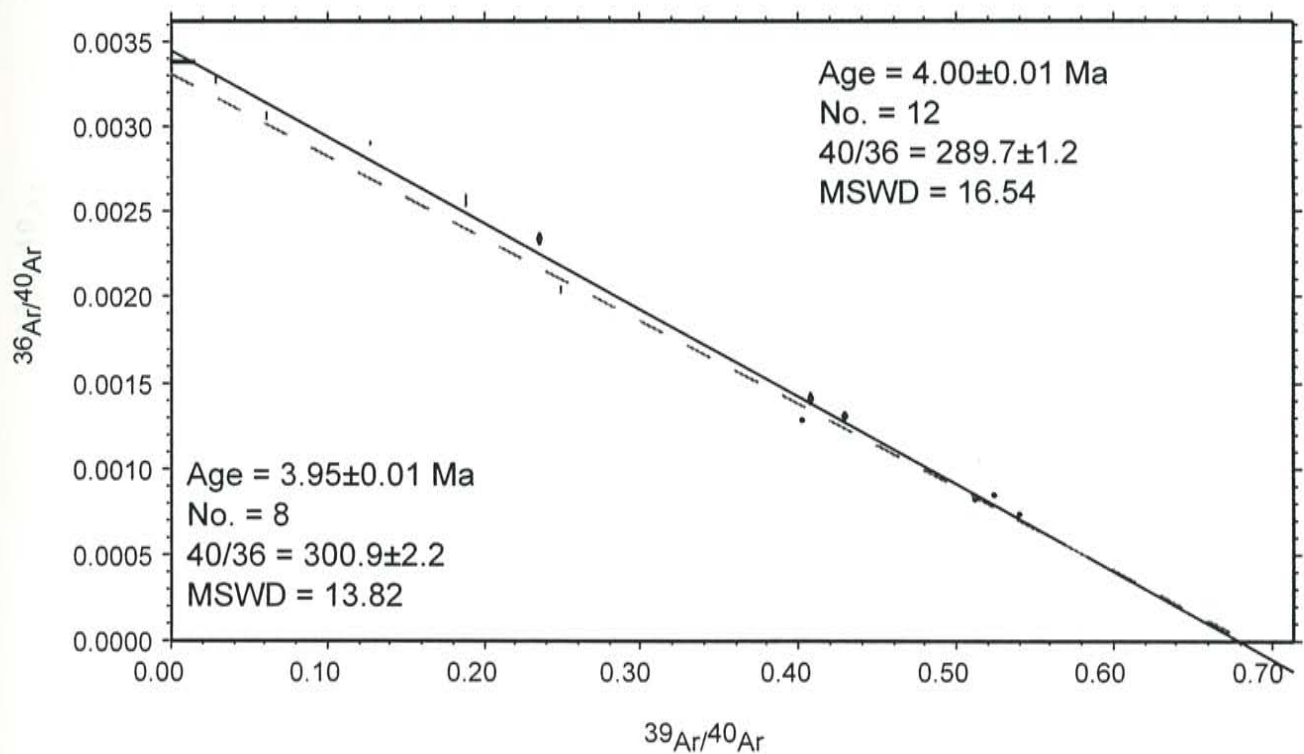
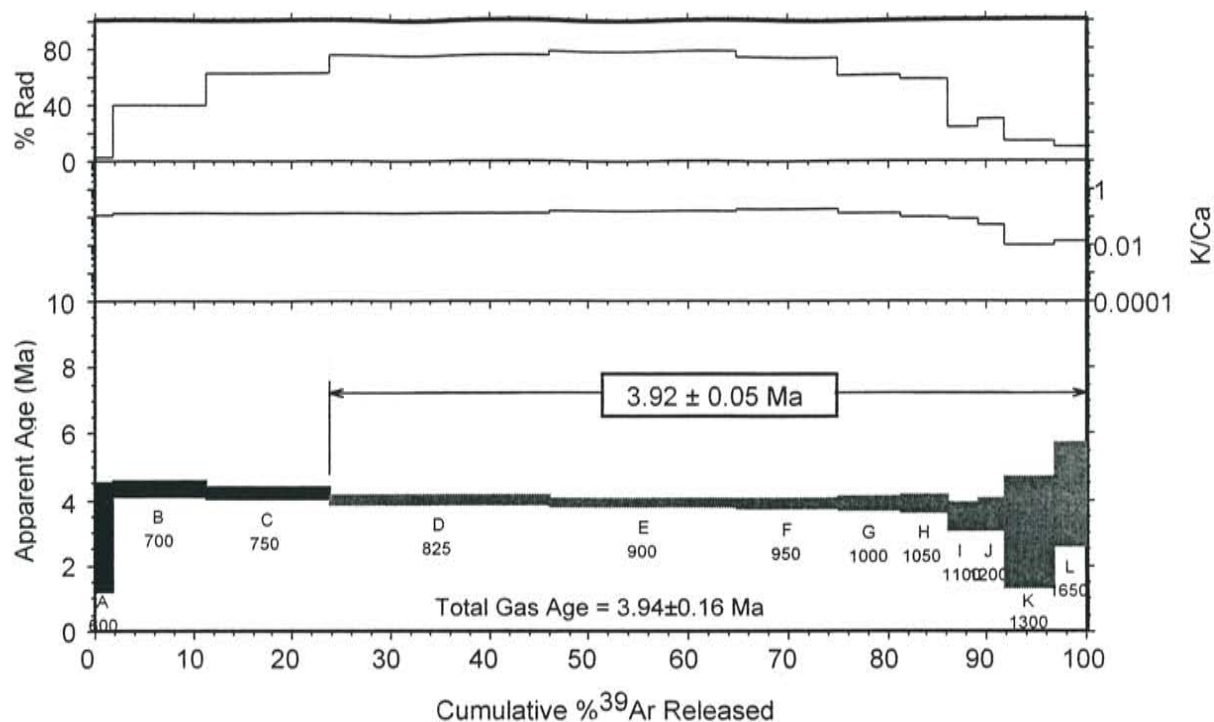
RA-026, basaltic andesite, Cerro de la Olla area, groundmass concentrate



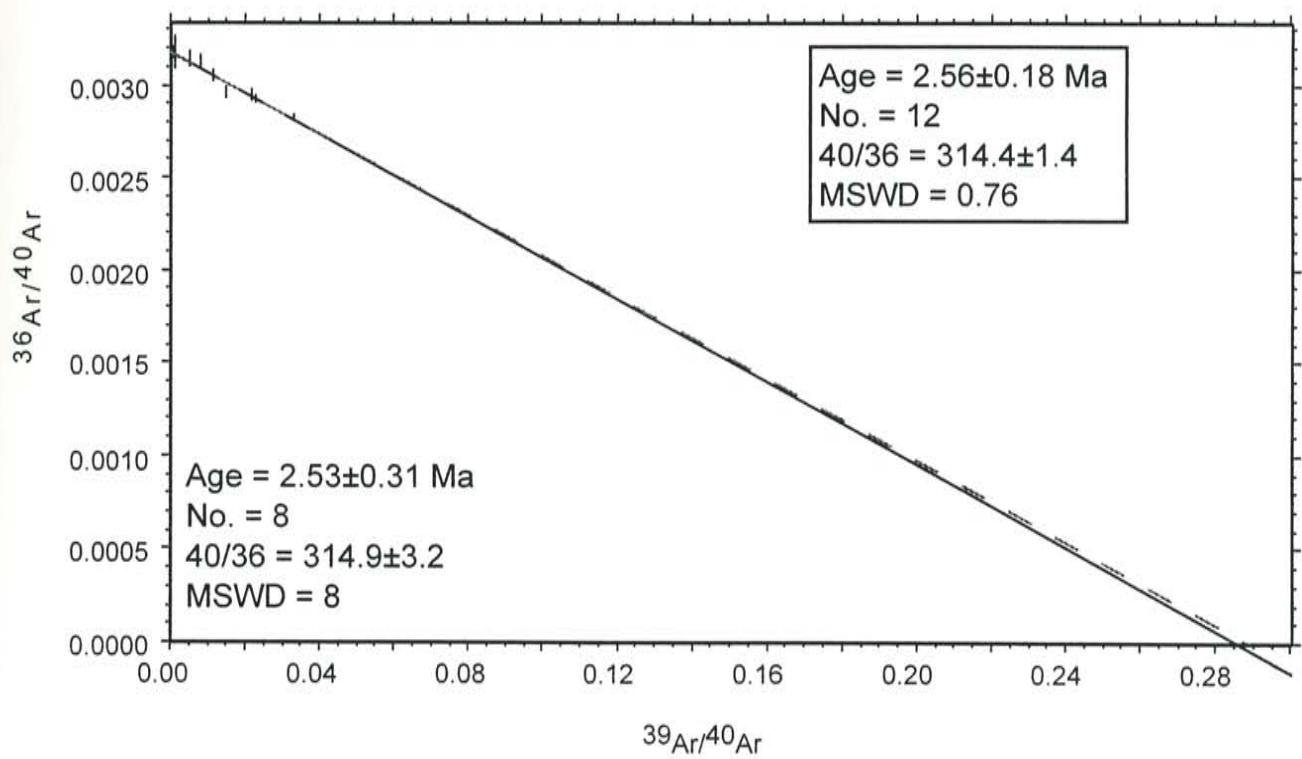
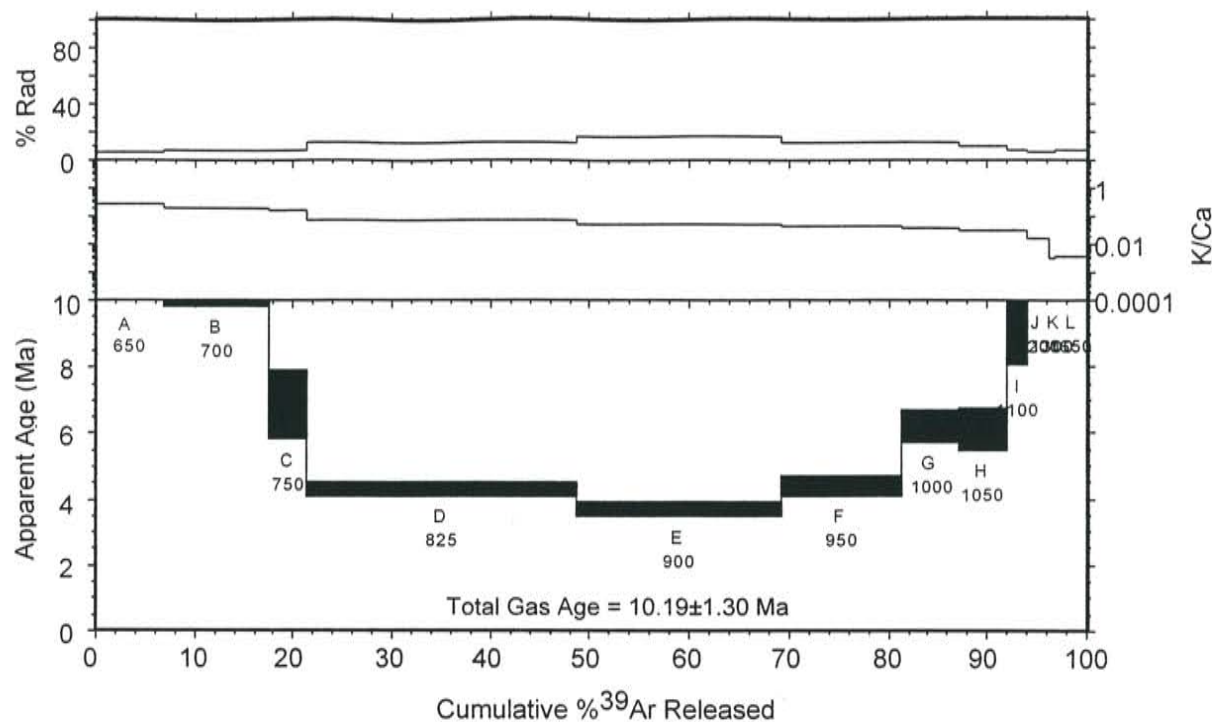
RA-027, Servilleta Basalt, Dunn Bridge, groundmass concentrate



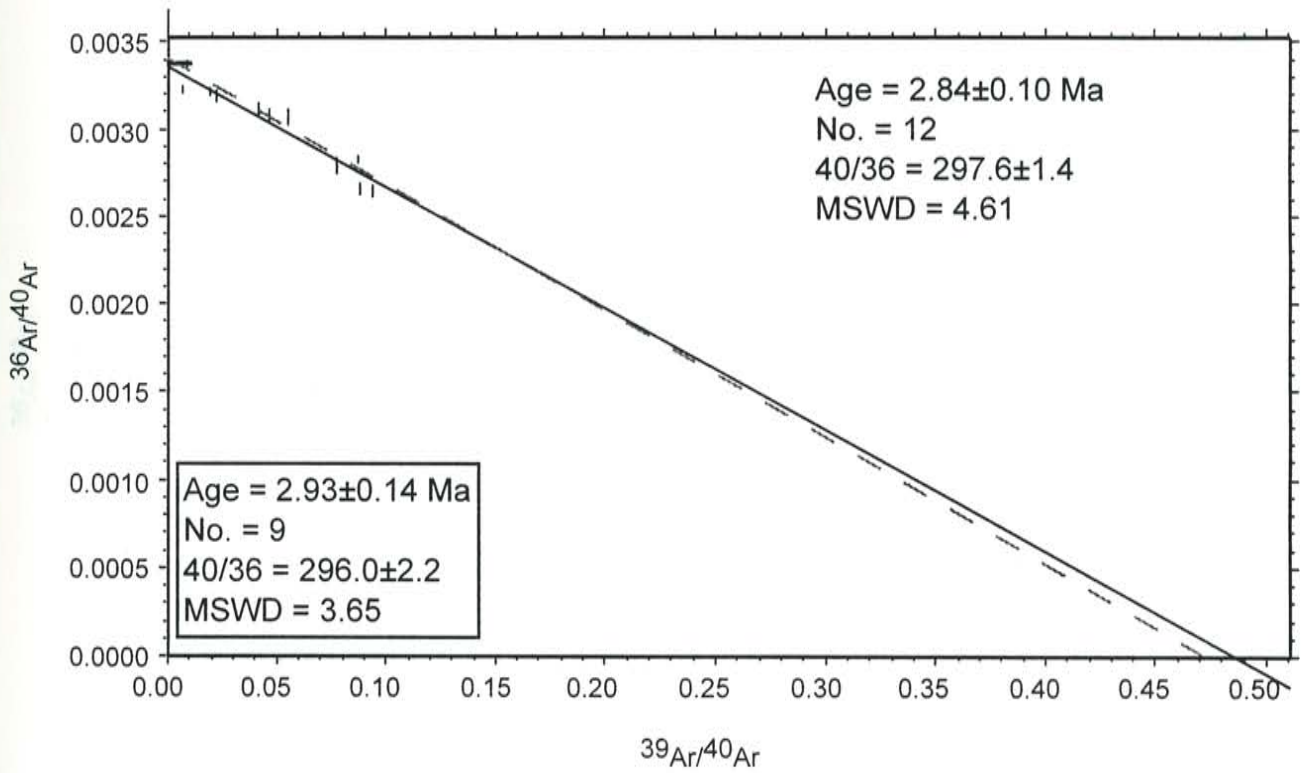
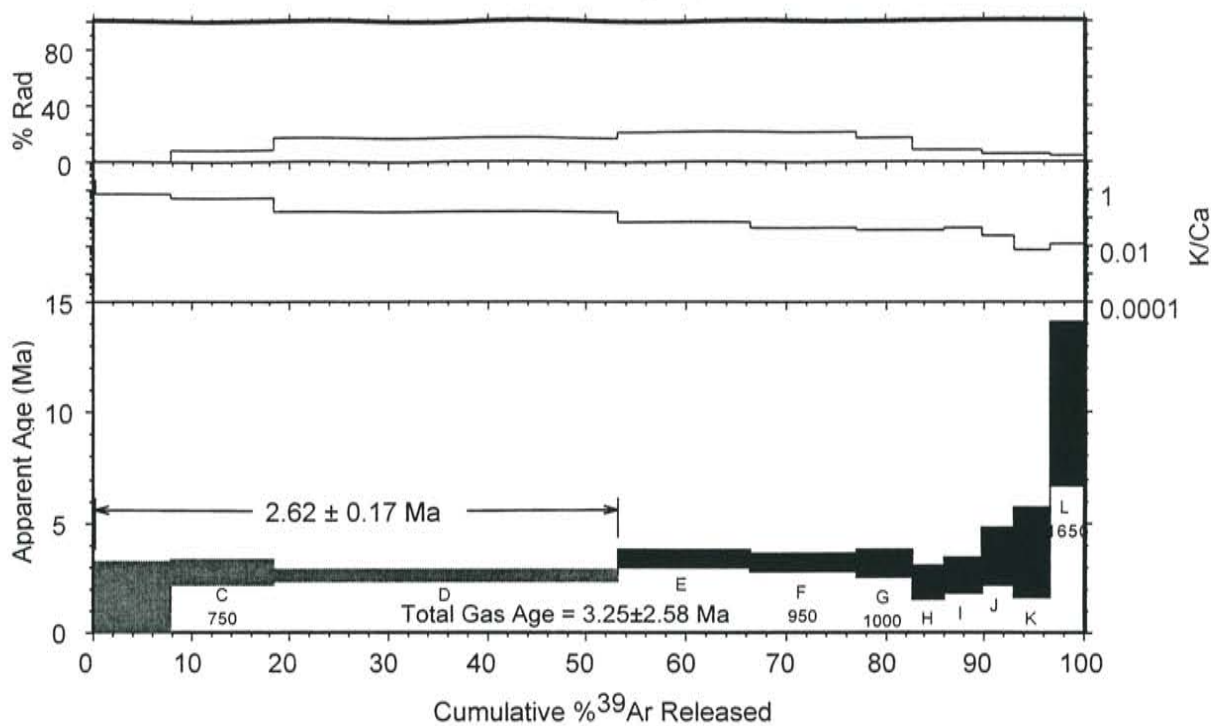
RA-028, Servilleta Basalt, Dunn Bridge, groundmass concentrate



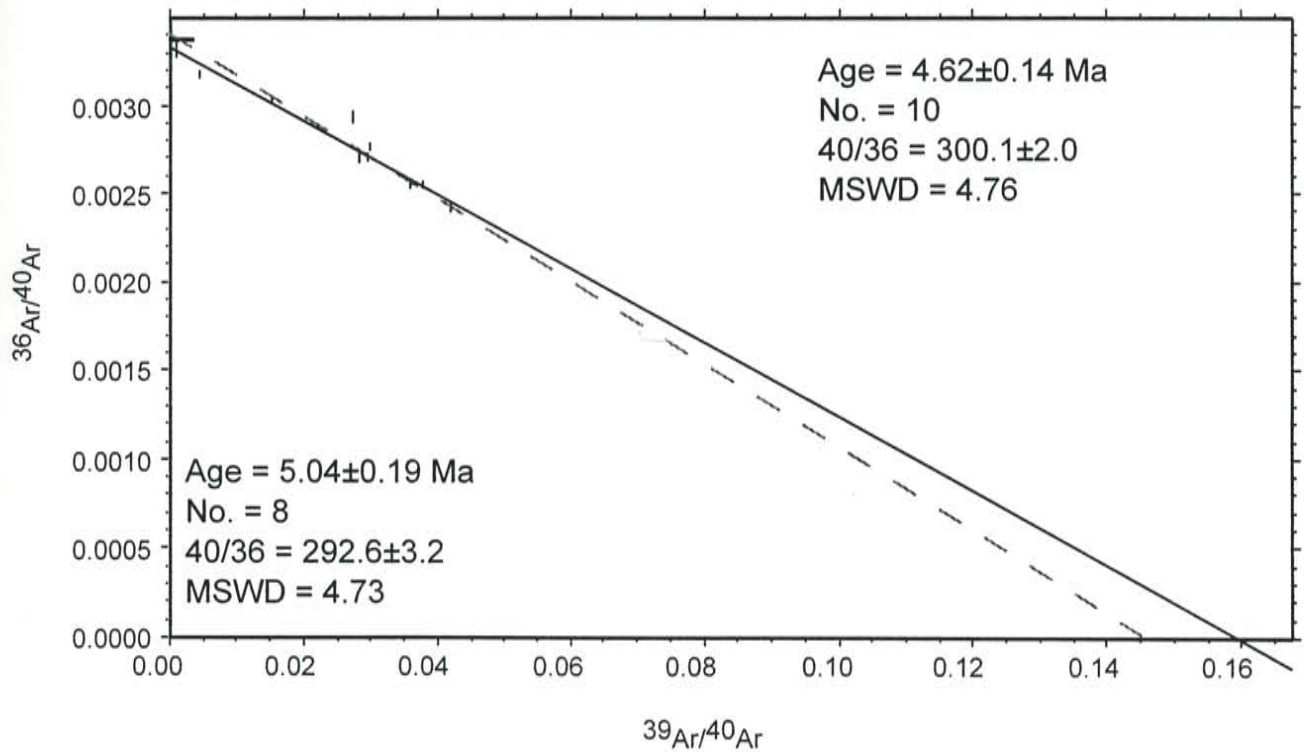
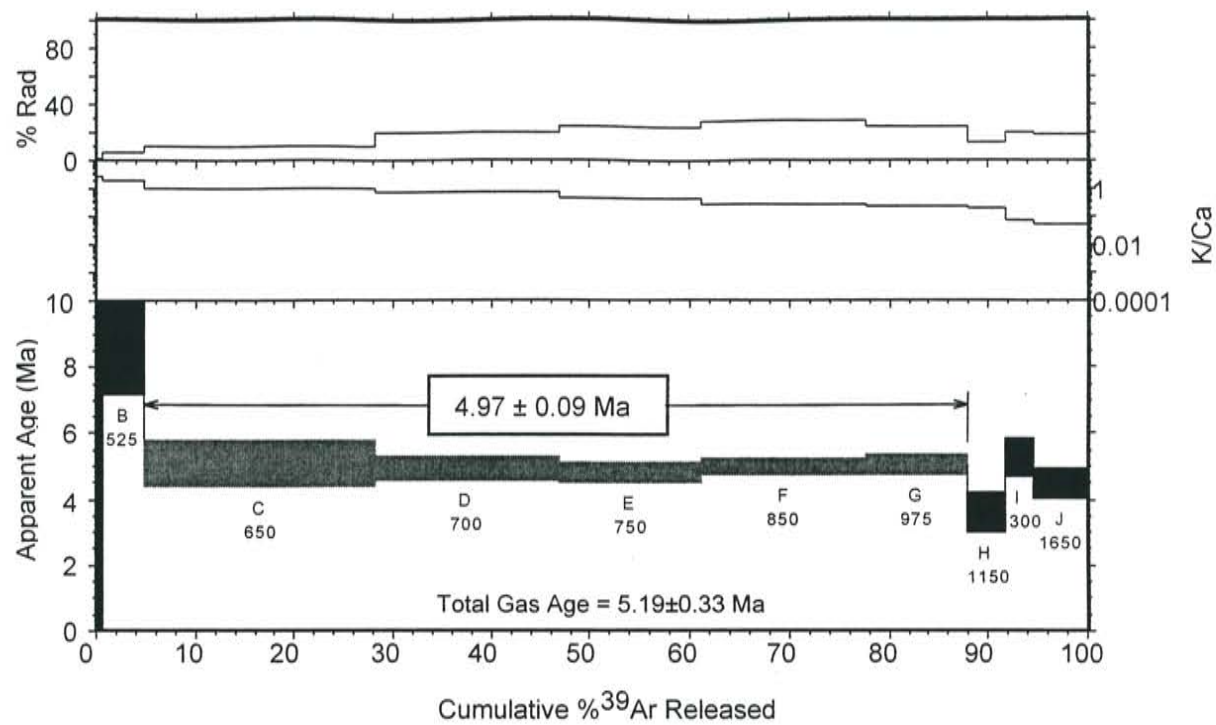
RA-029, Servilleta Basalt, Dunn Bridge, groundmass concentrate



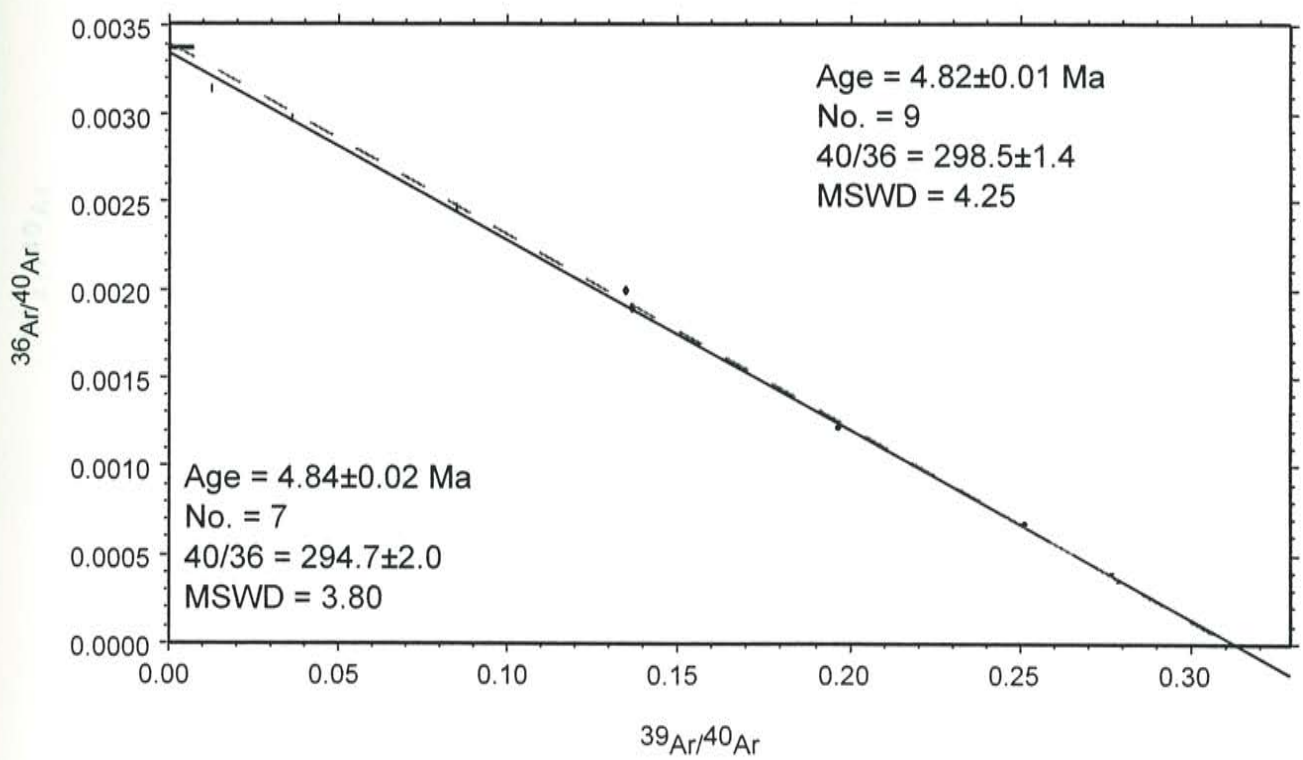
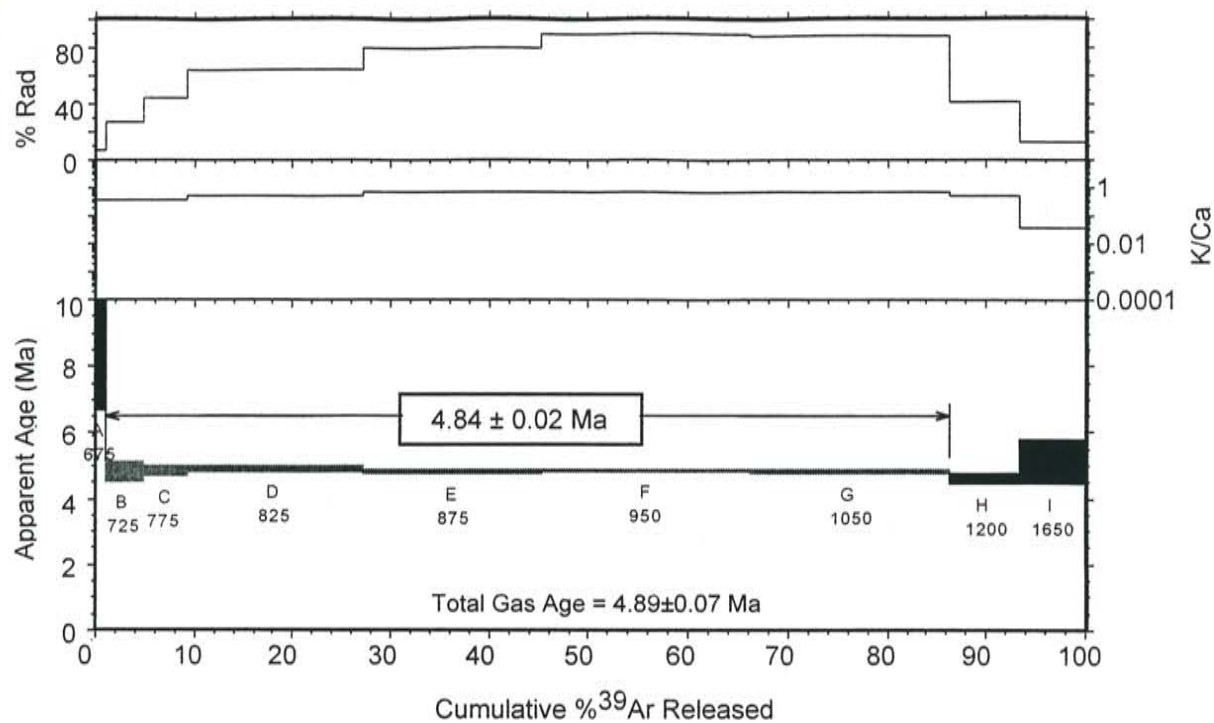
RA-030, Servilleta Basalt, Dunn Bridge, groundmass concentrate



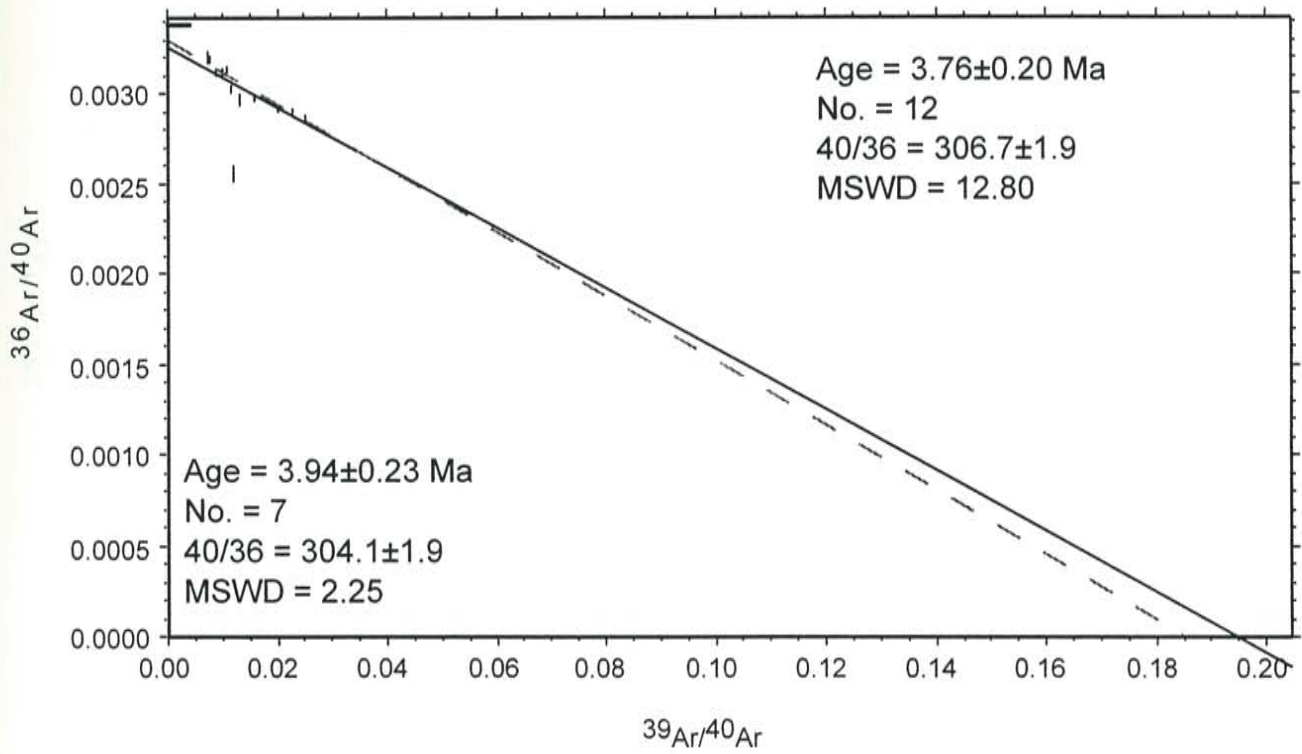
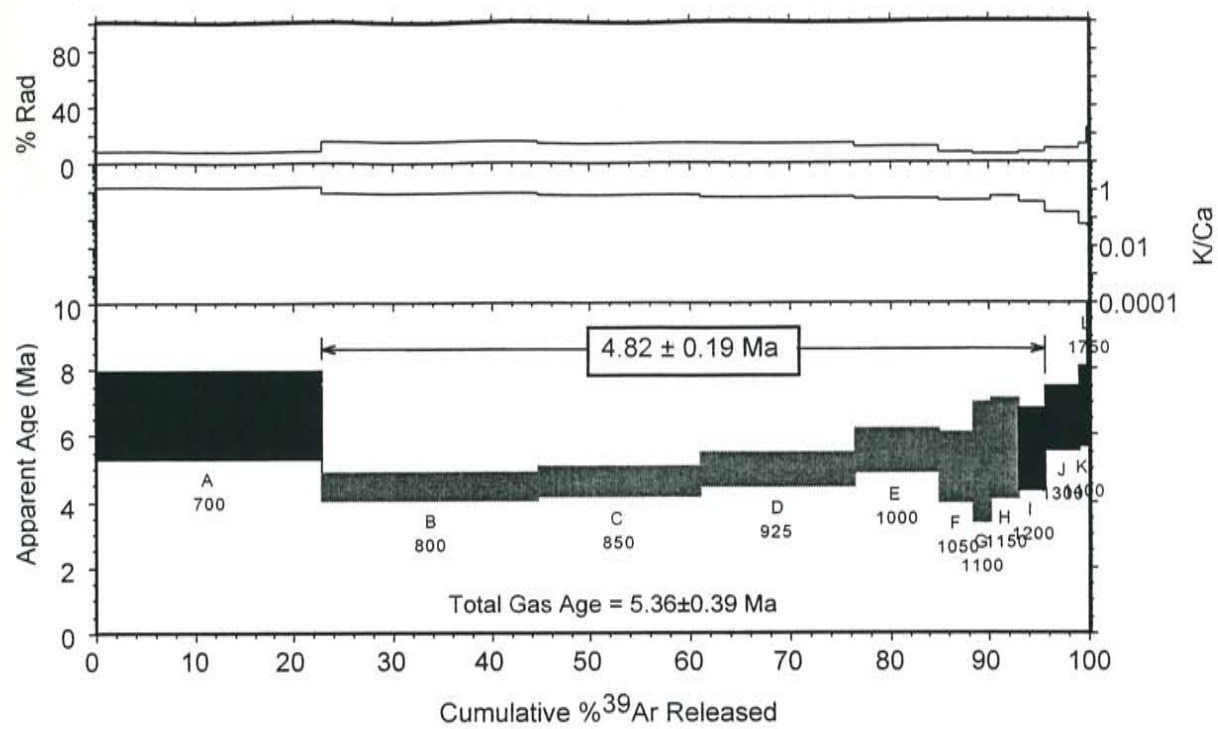
RA-031, olivine andesite, Cerros de los Taos, groundmass concentrate



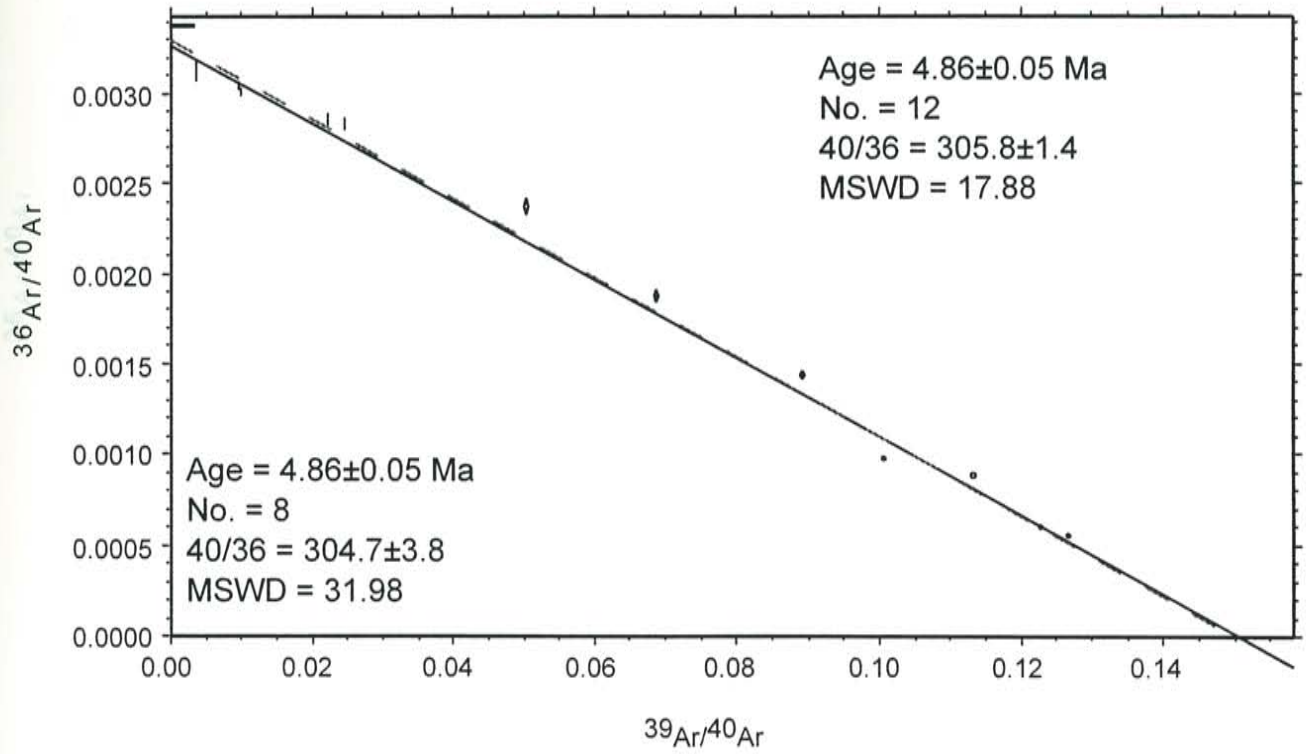
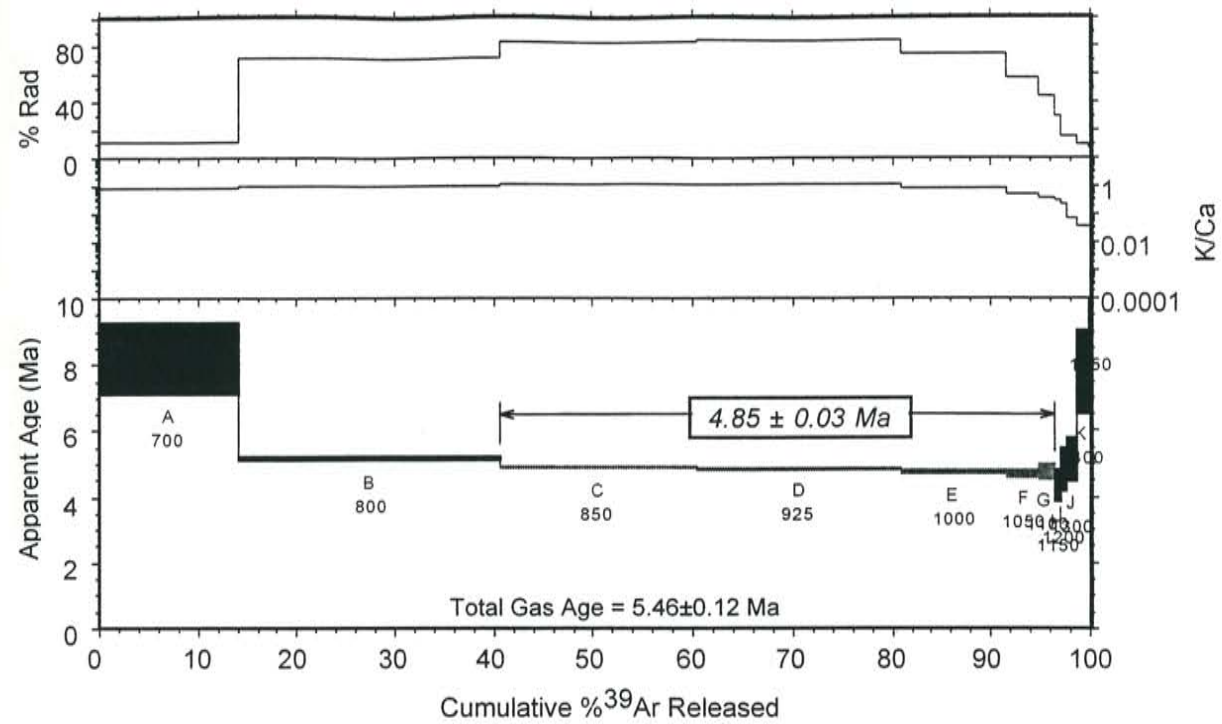
RA-032, pyroxene dacite, Tres Orejas, groundmass concentrate



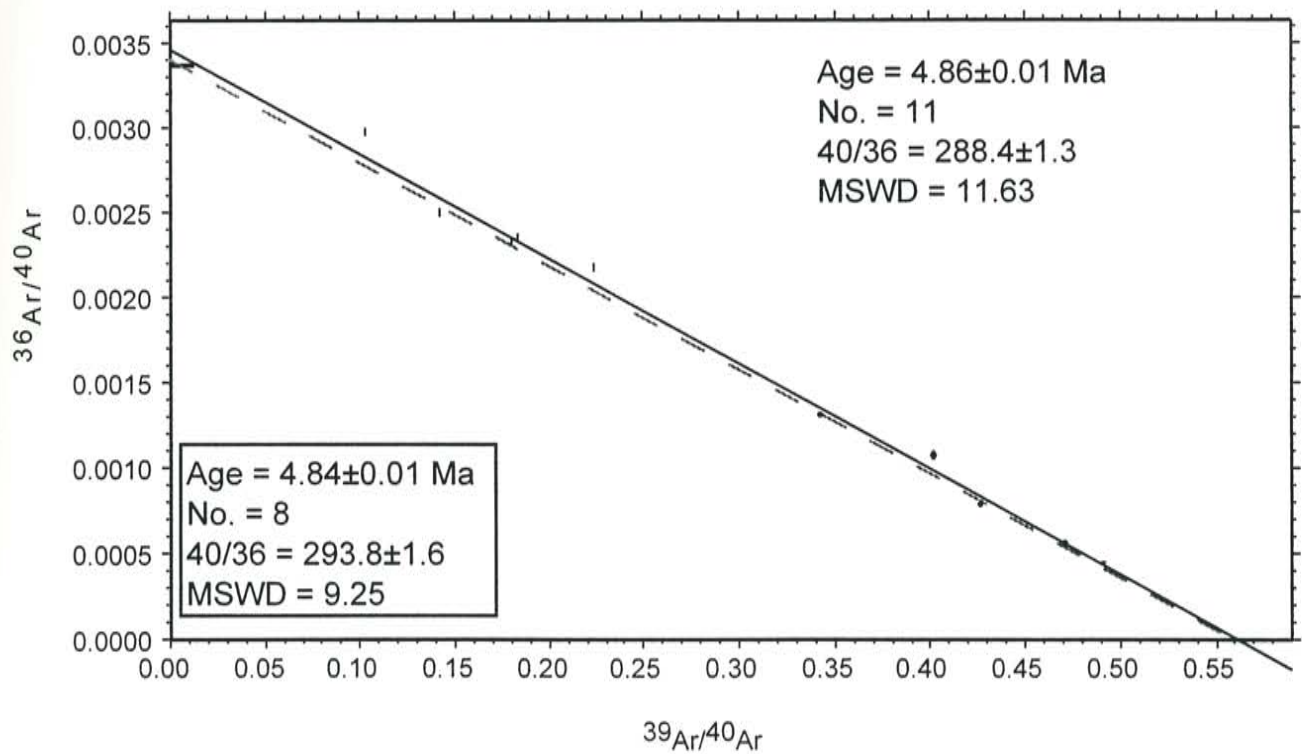
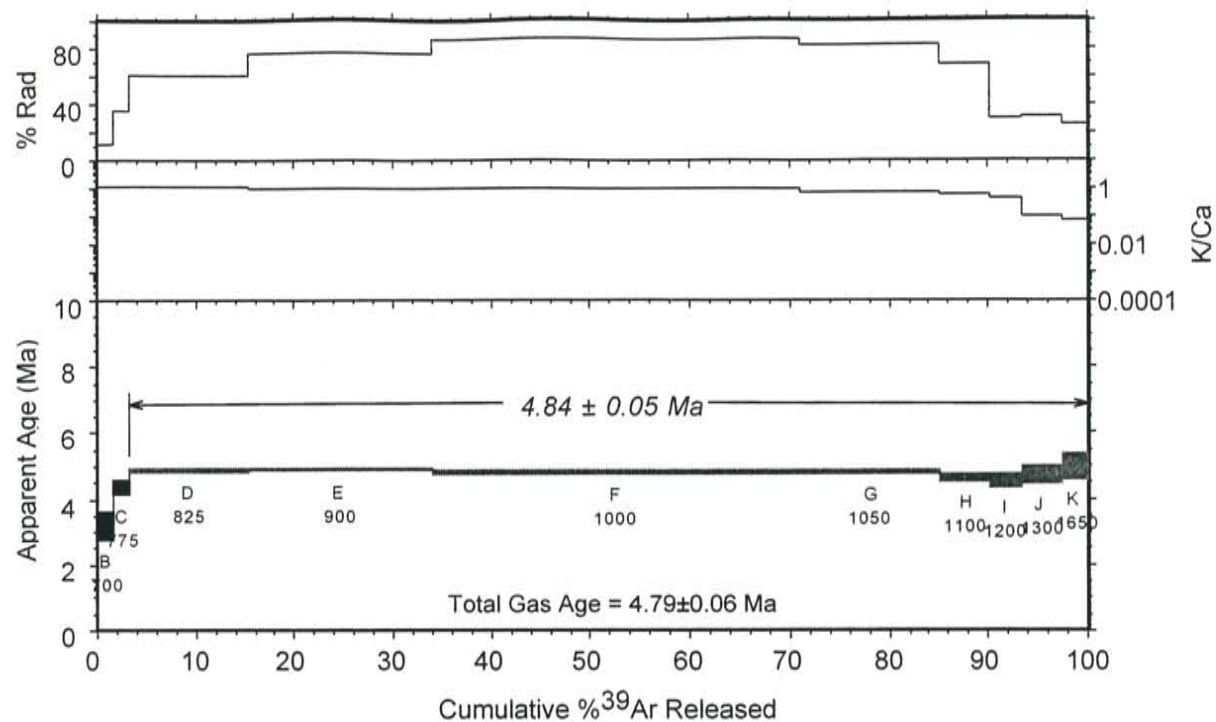
RA-033, pyroxene dacite, Tres Orejas, groundmass concentrate



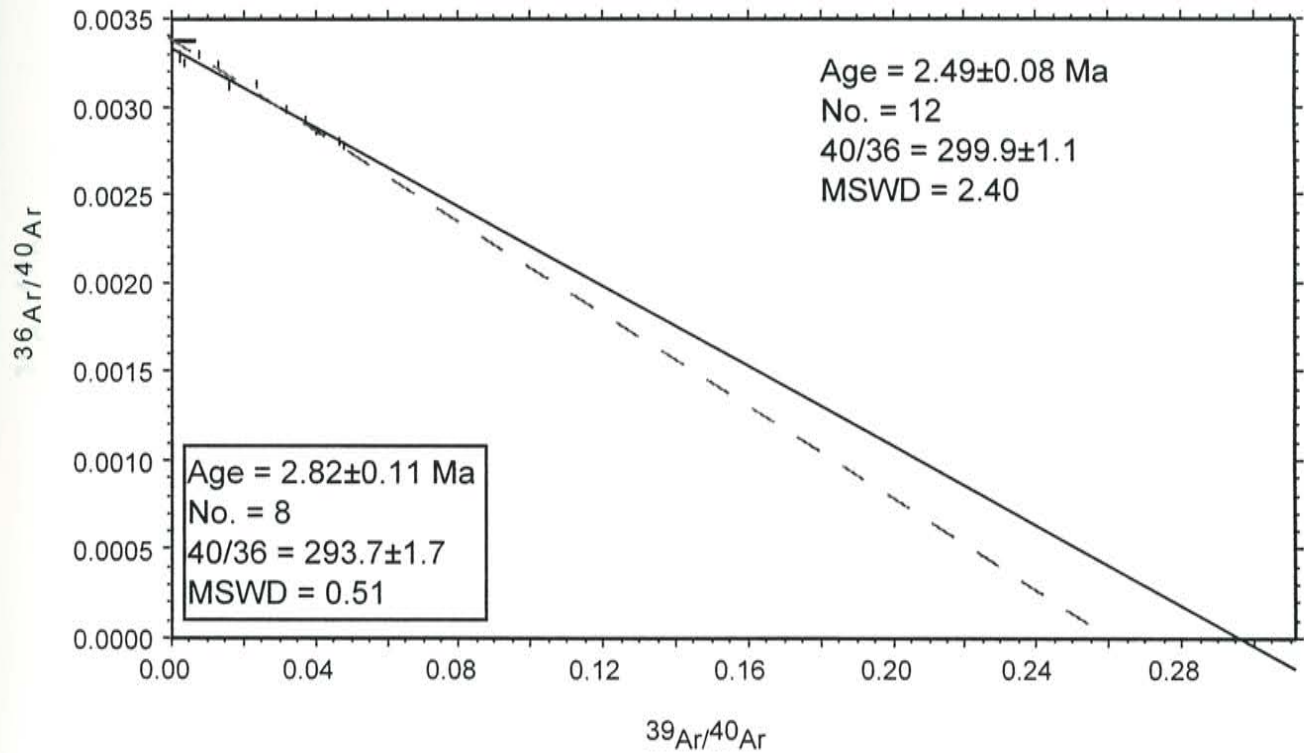
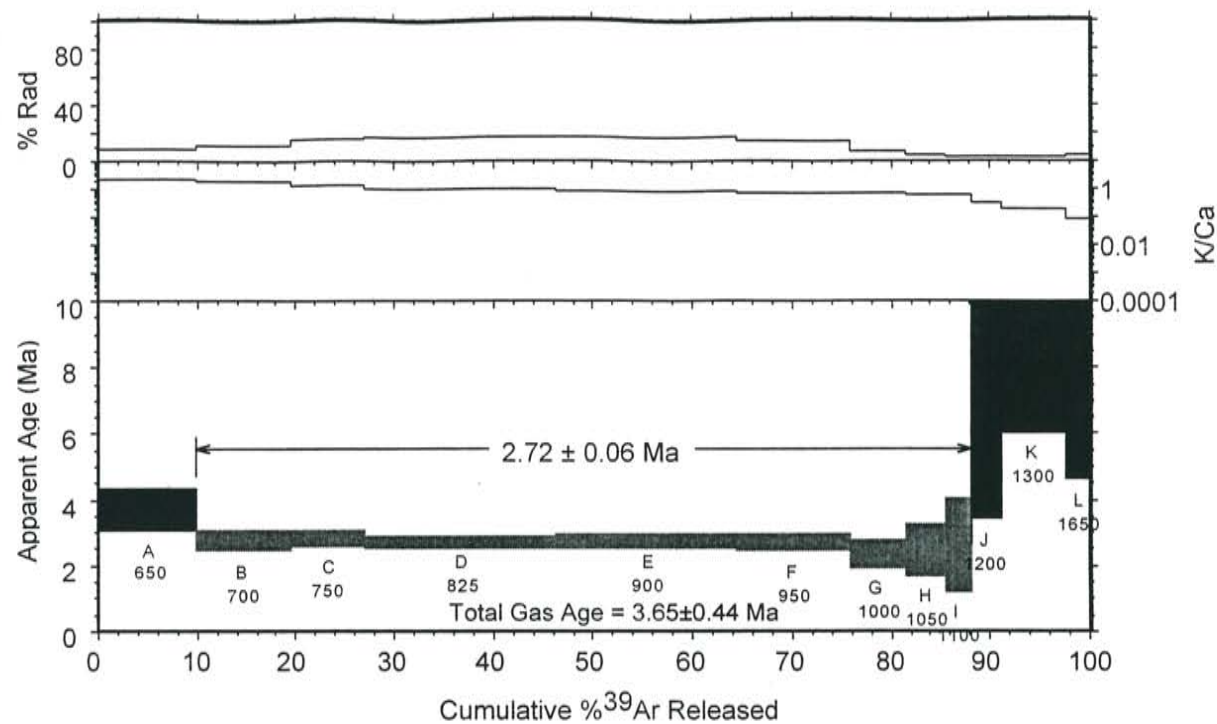
RA-034, pyroxene dacite, Tres Orejas, groundmass concentrate



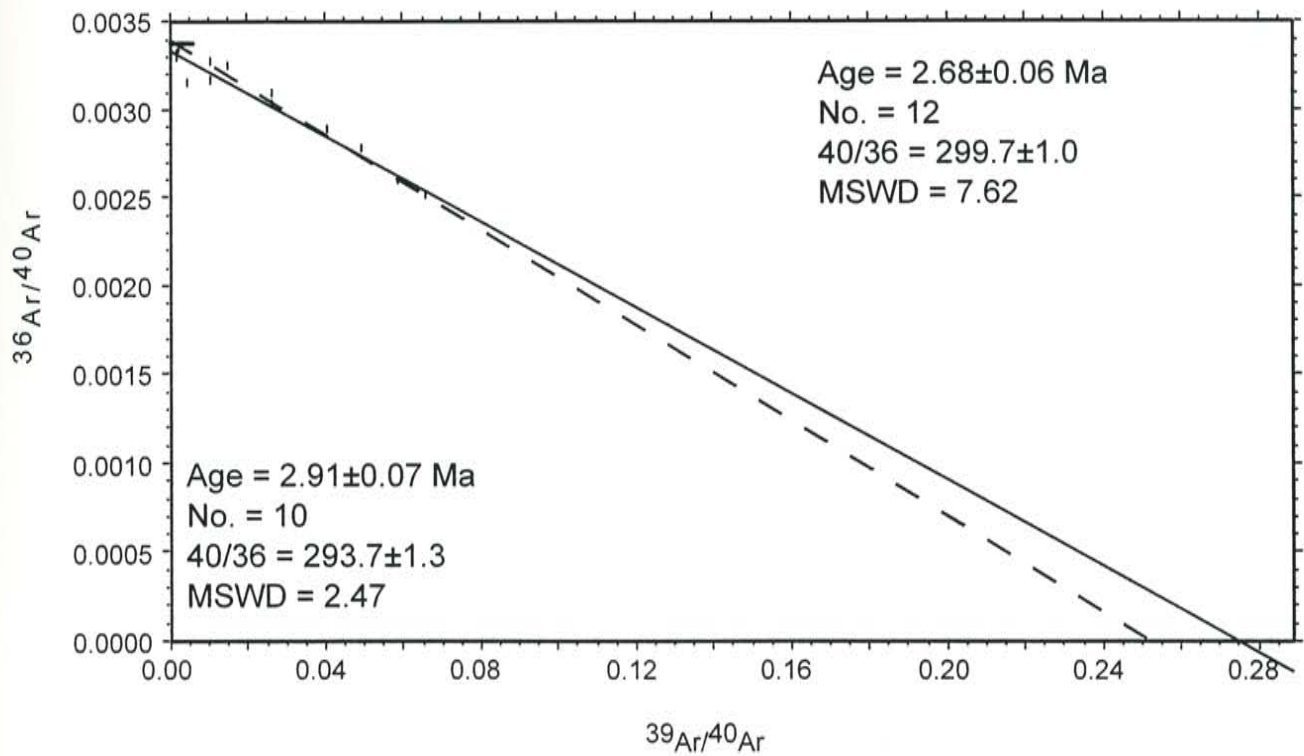
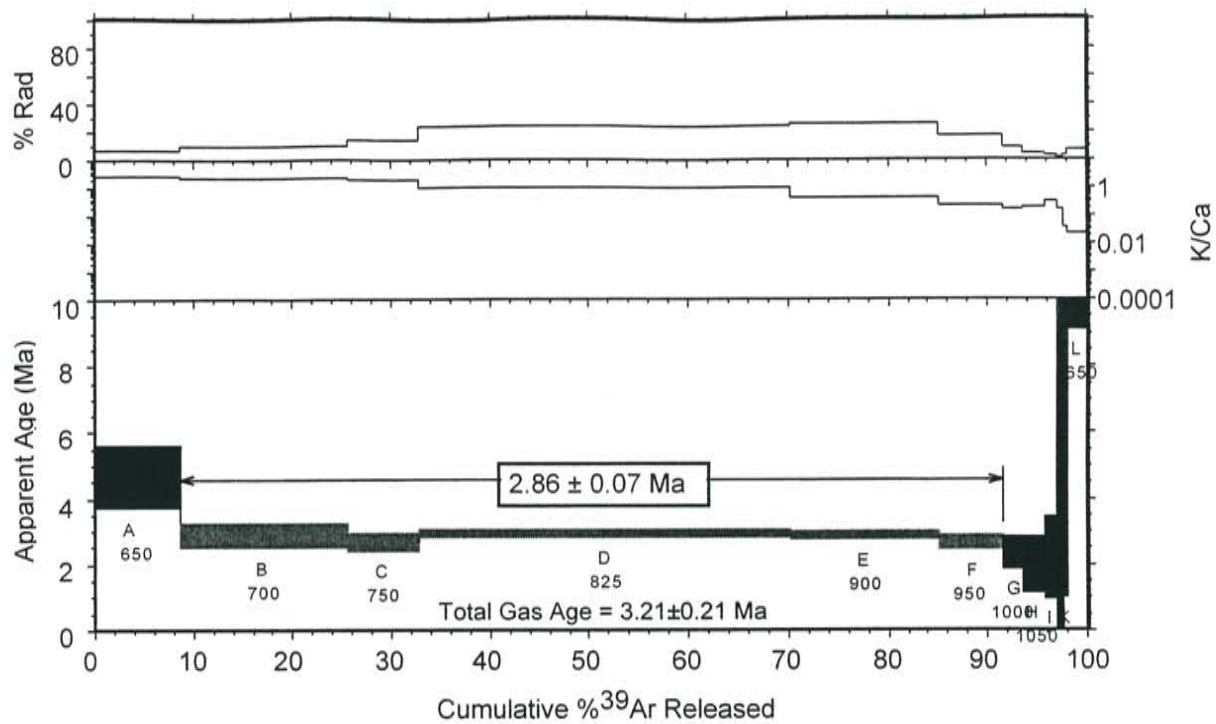
RA-035, pyroxene dacite, Tres Orejas, groundmass concentrate



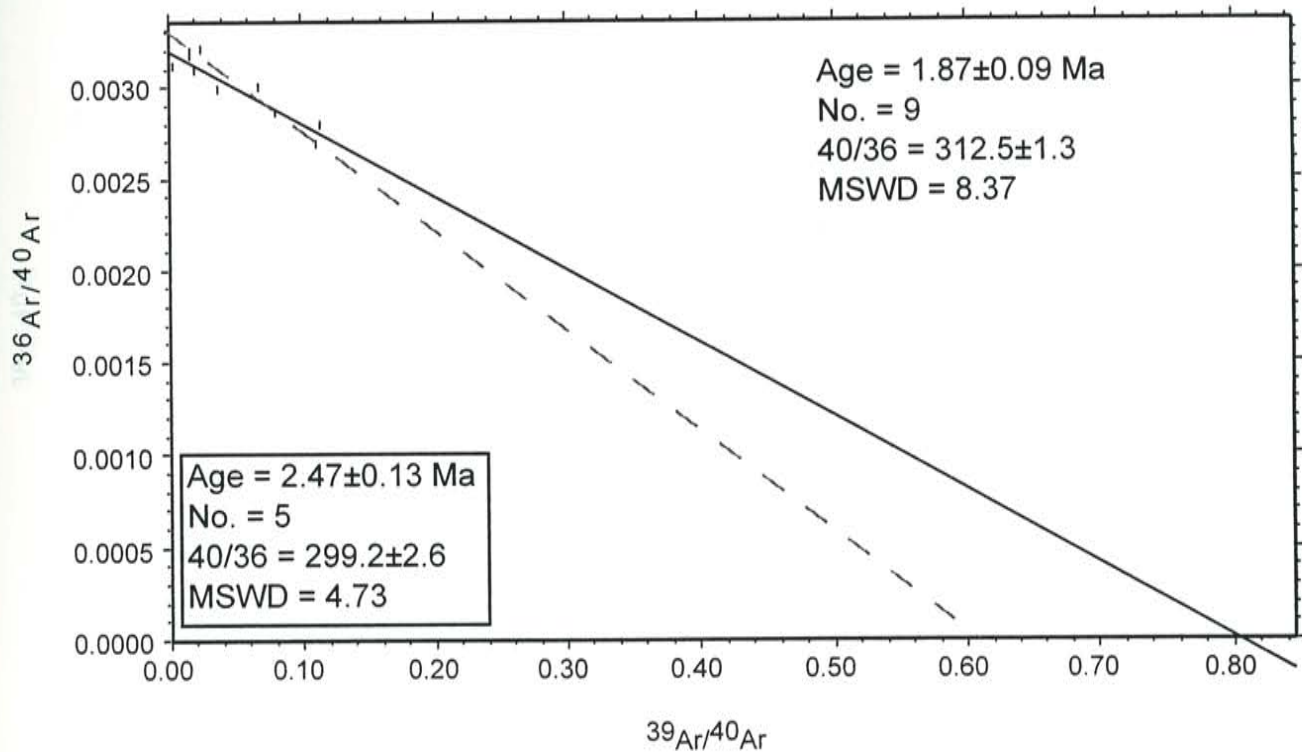
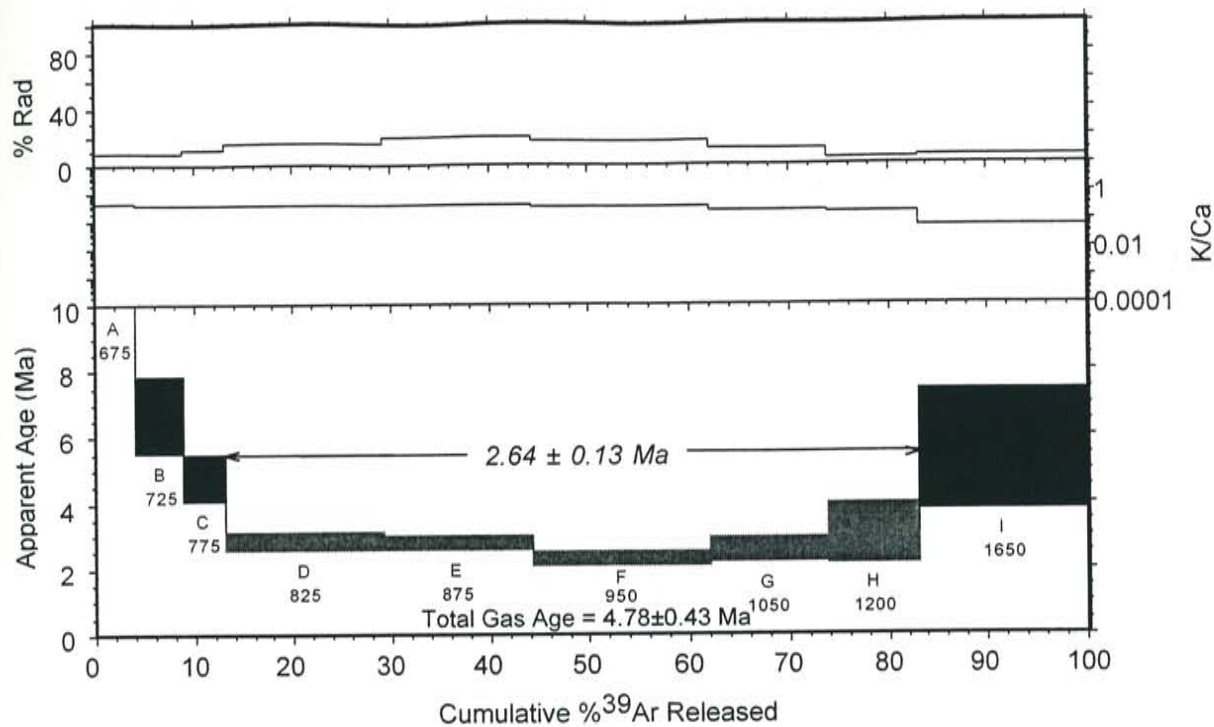
RA-038, basaltic andesite, San Antonio Mt., groundmass concentrate



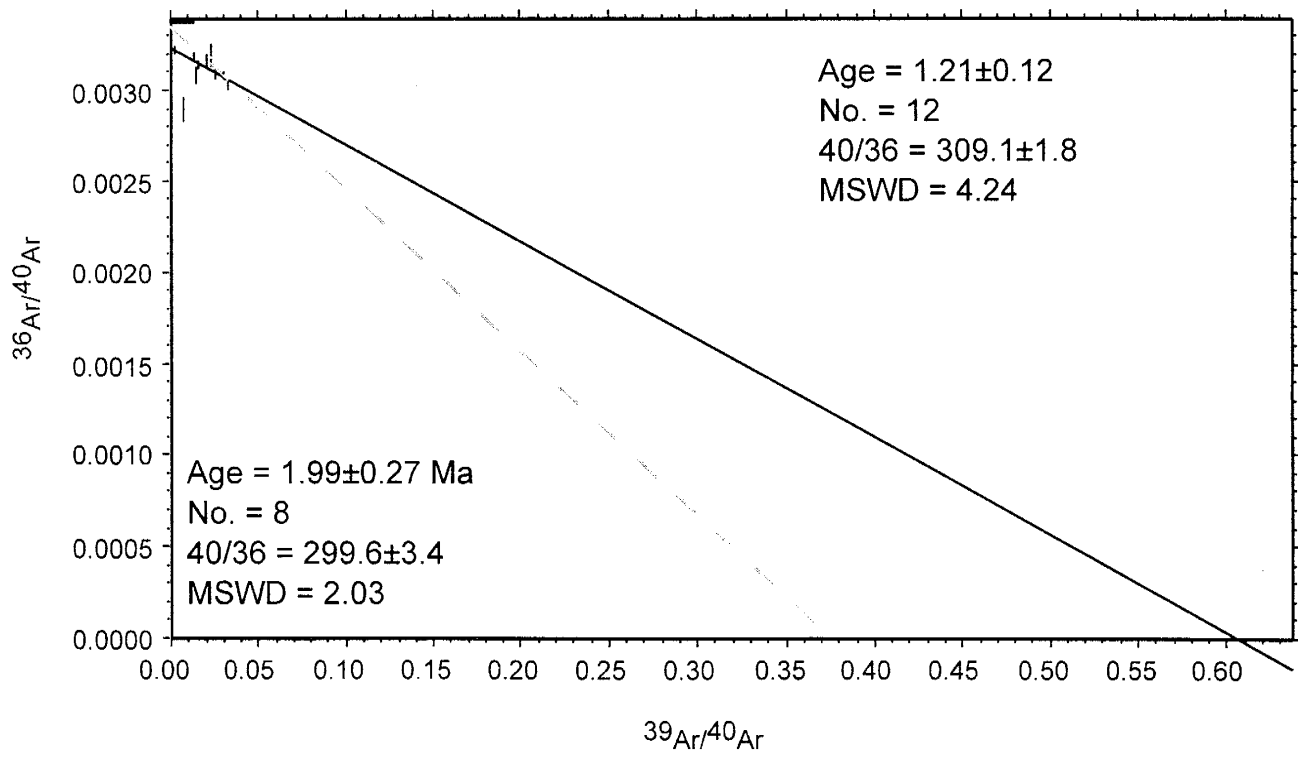
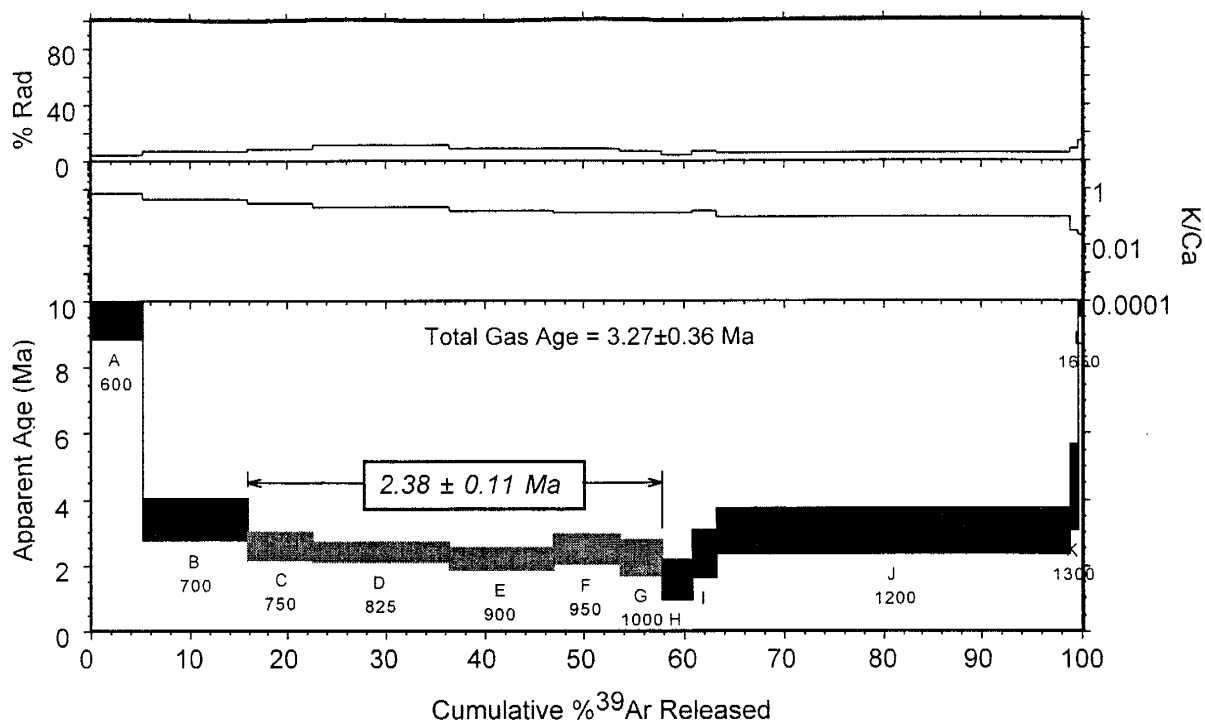
RA-039, basaltic andesite, San Antonio Mt., groundmass concentrate



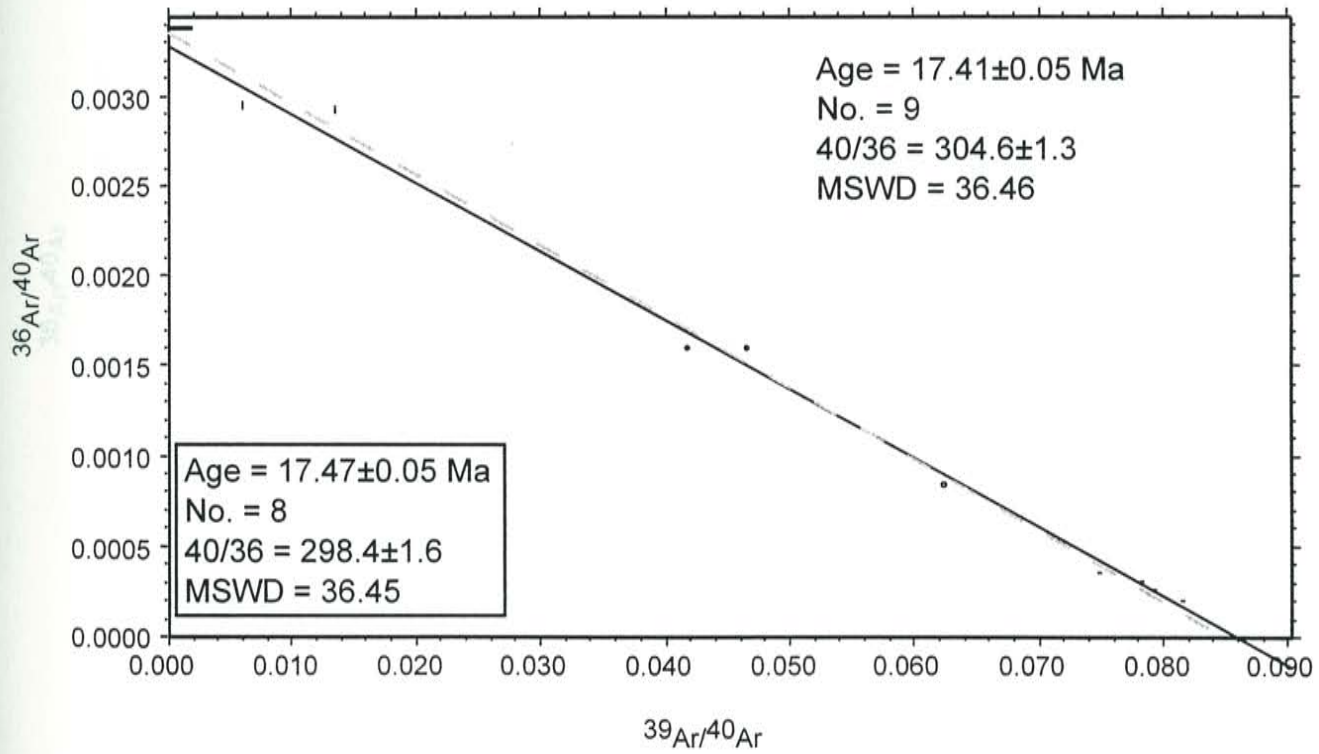
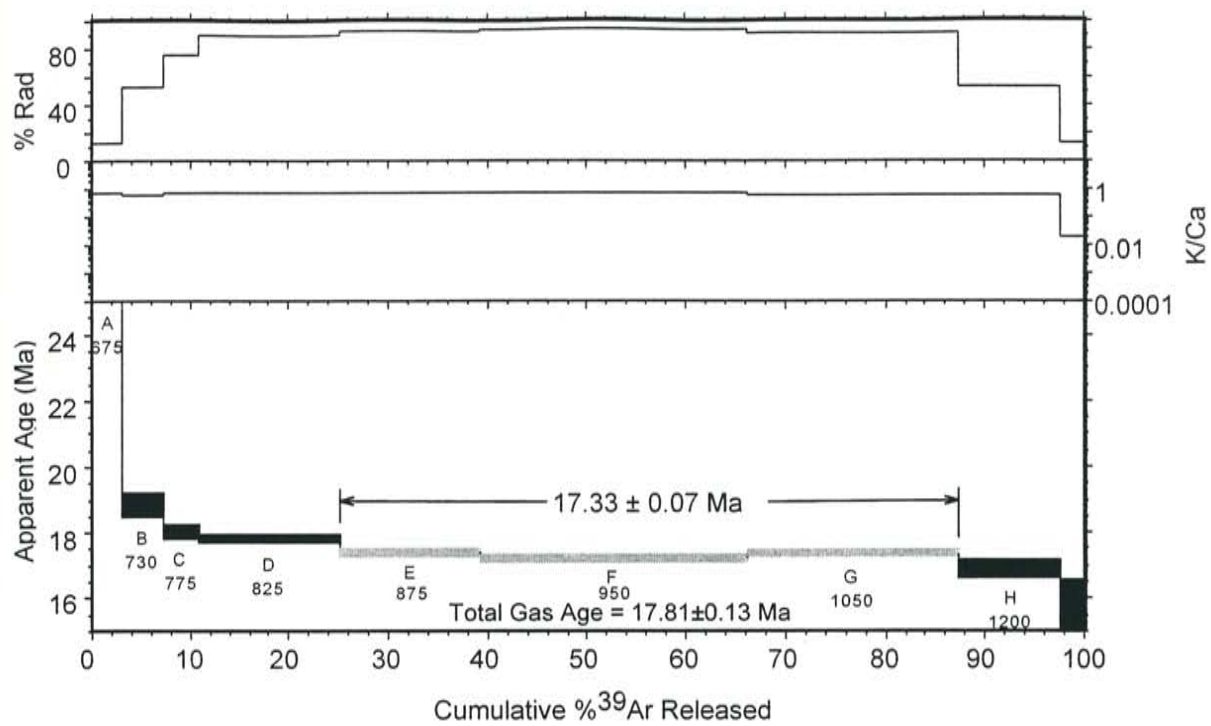
RA-041, basaltic andesite, Pinebetoso Peaks, groundmass concentrate



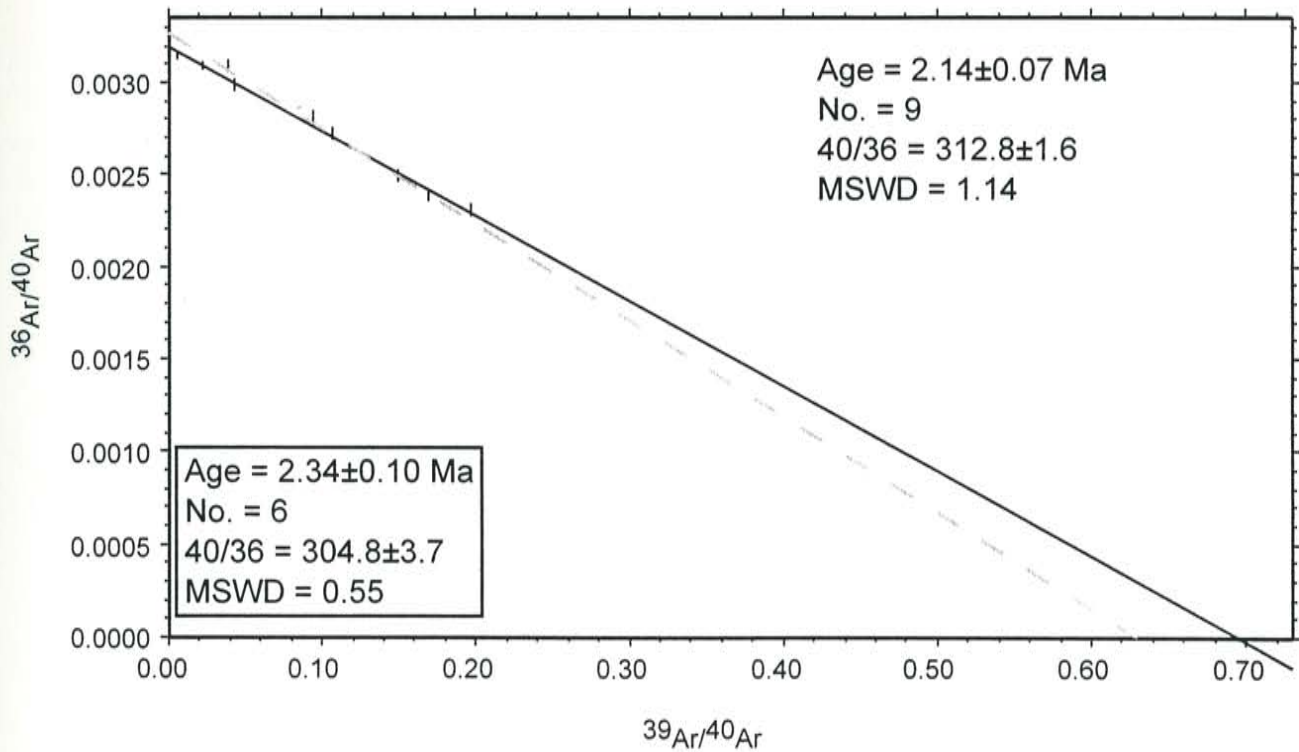
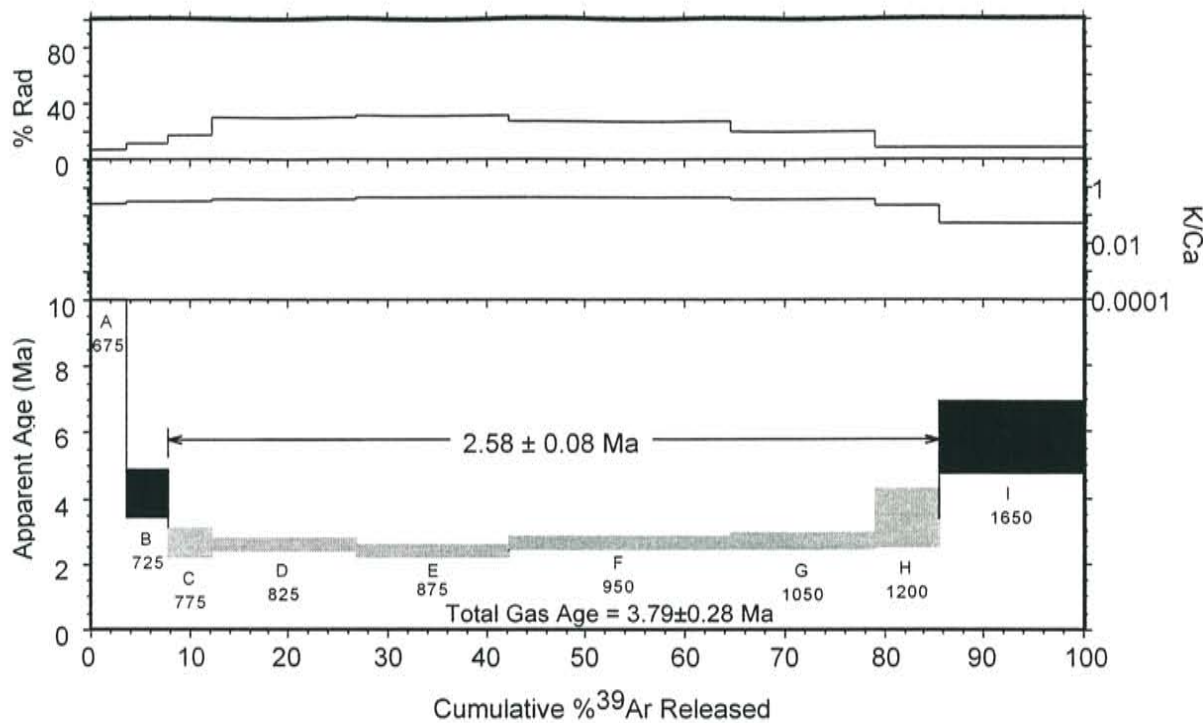
RA-042, basaltic andesite, Pinebetoso Peaks, groundmass concentrate



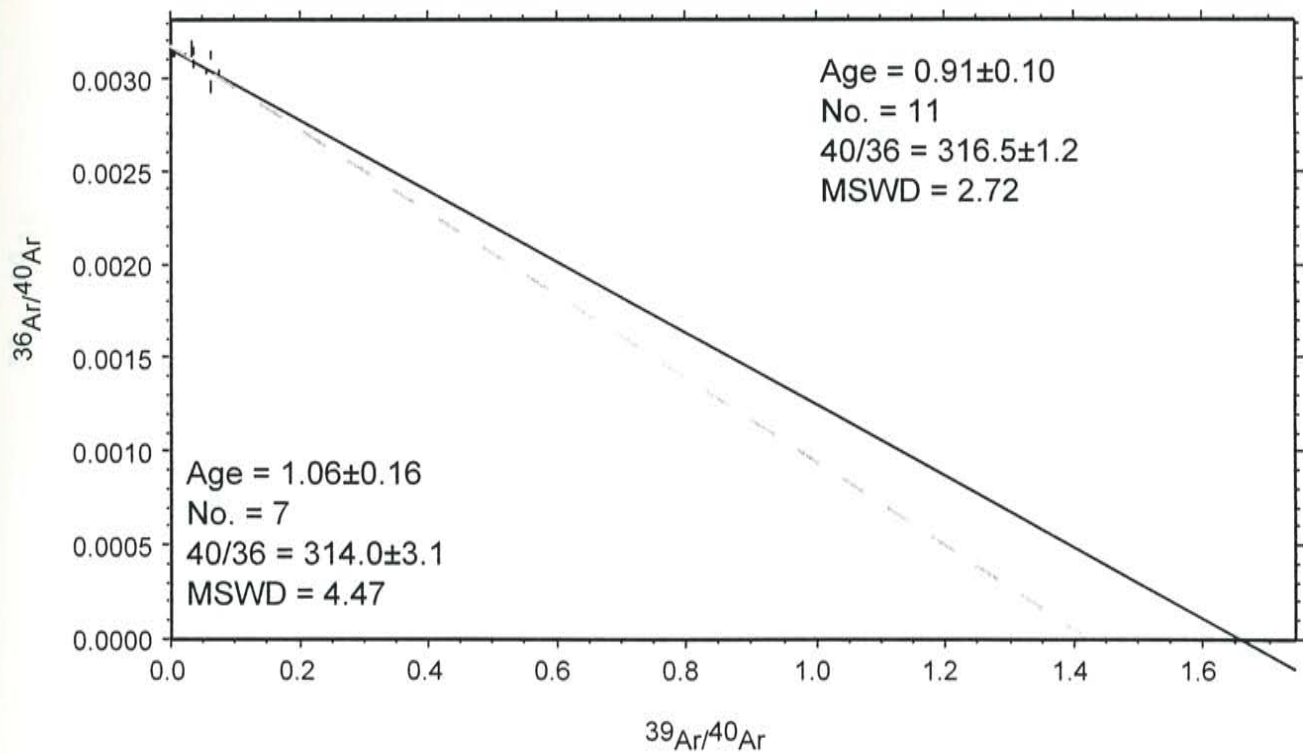
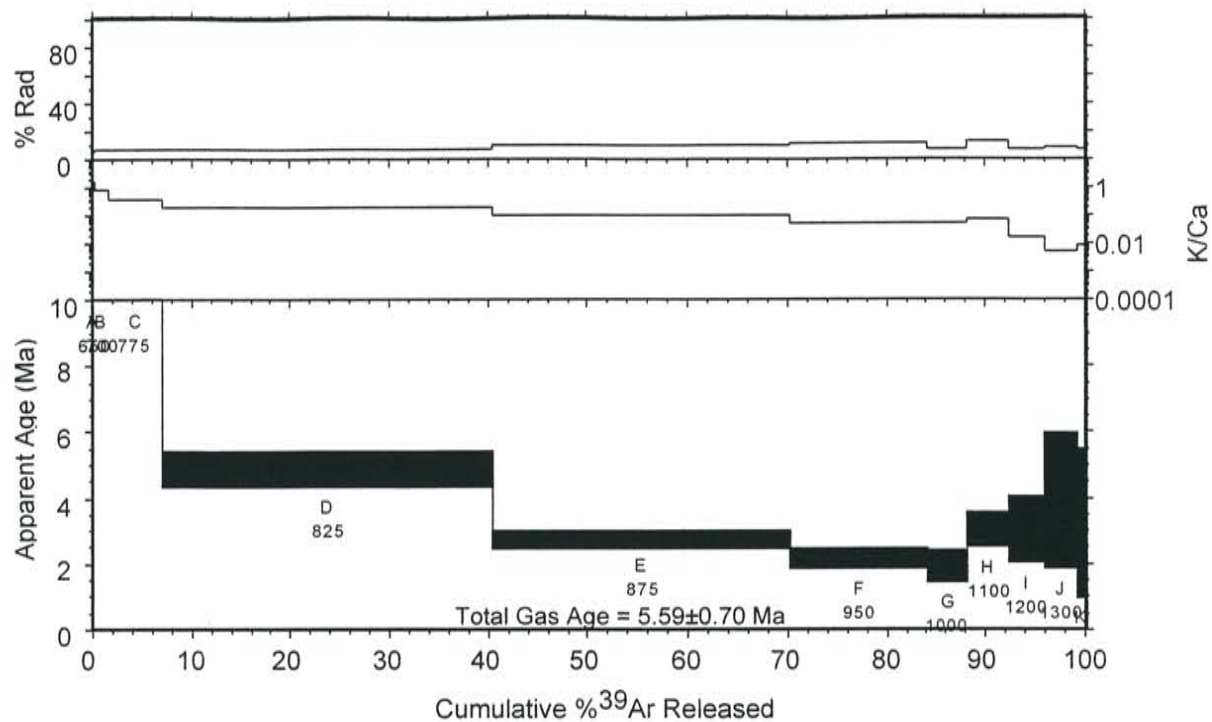
RA-045, basaltic andesite Cerro Montoso, groundmass concentrate



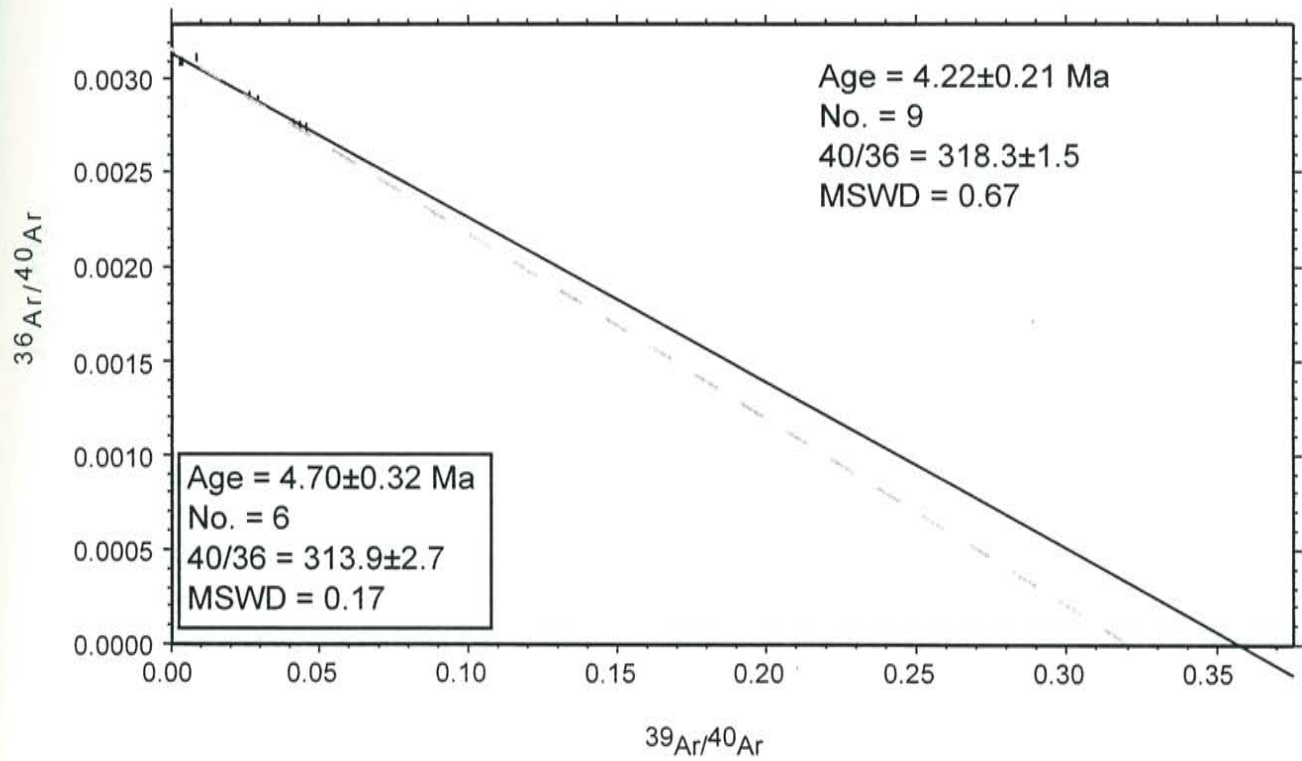
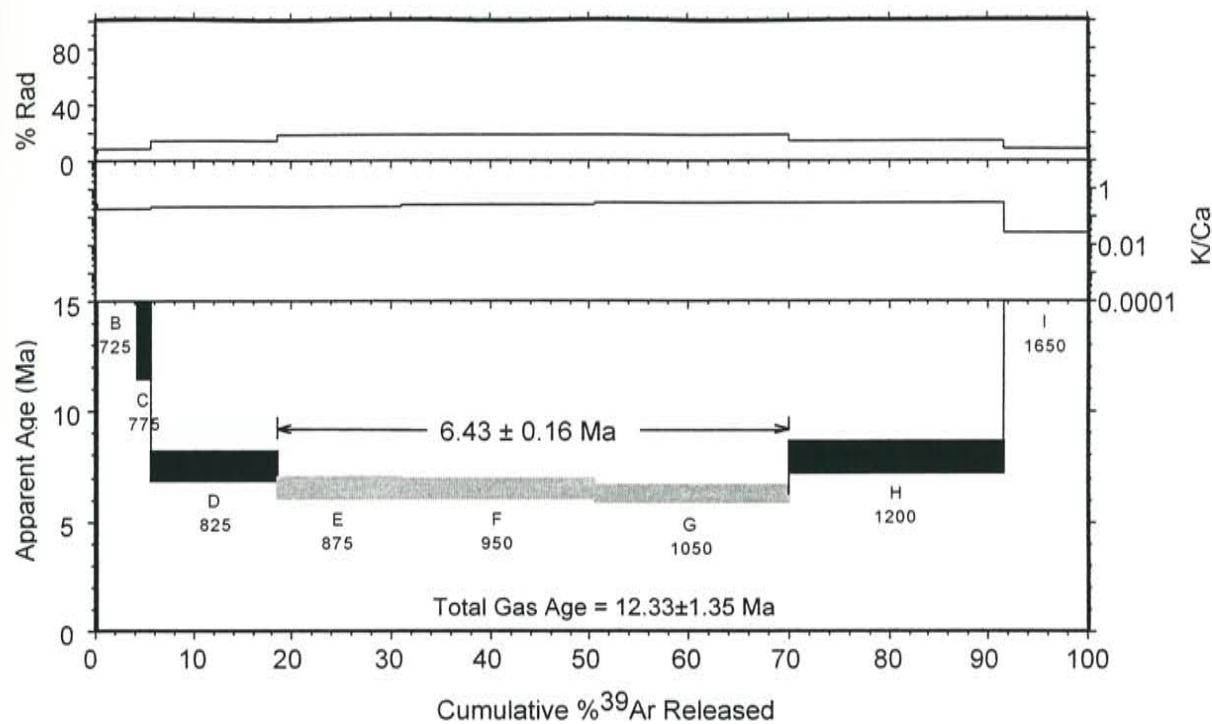
RA-046, basaltic andesite, Pinebetoso Peaks, groundmass concentrate



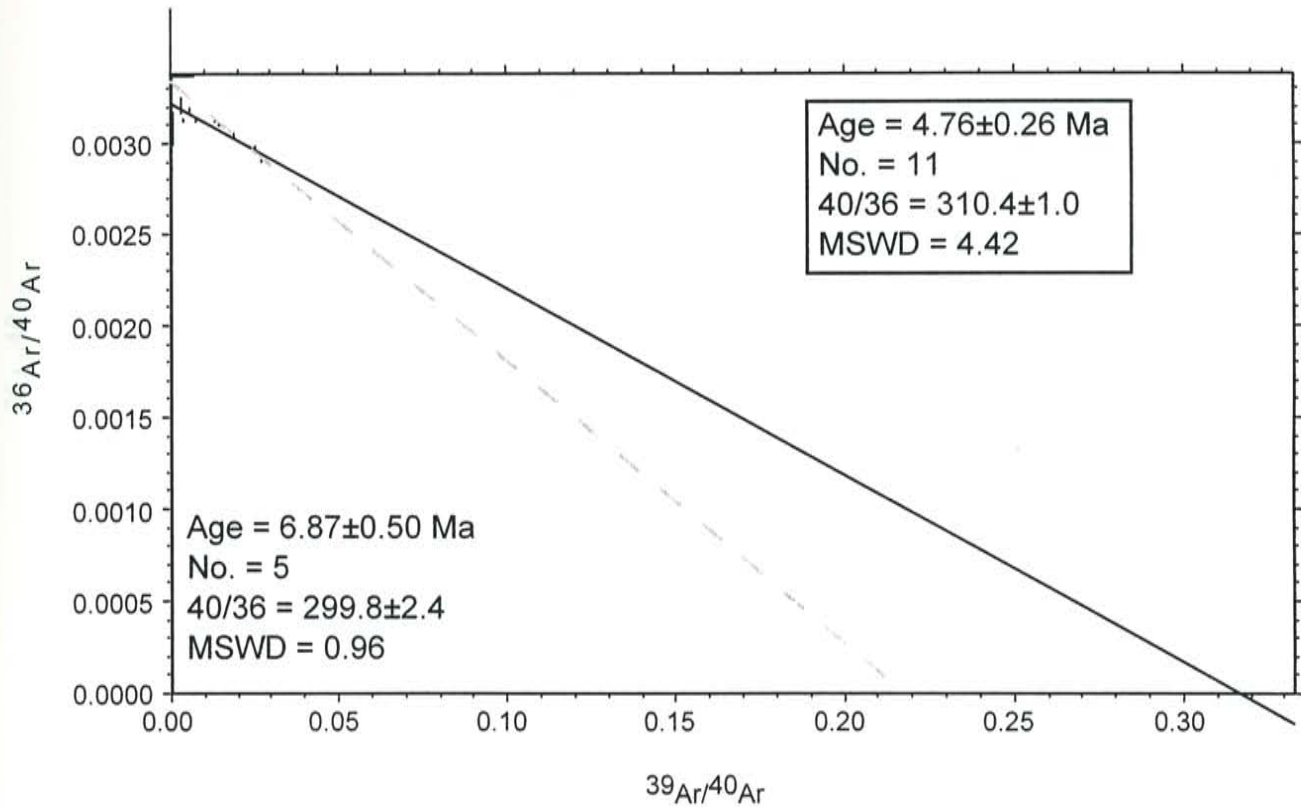
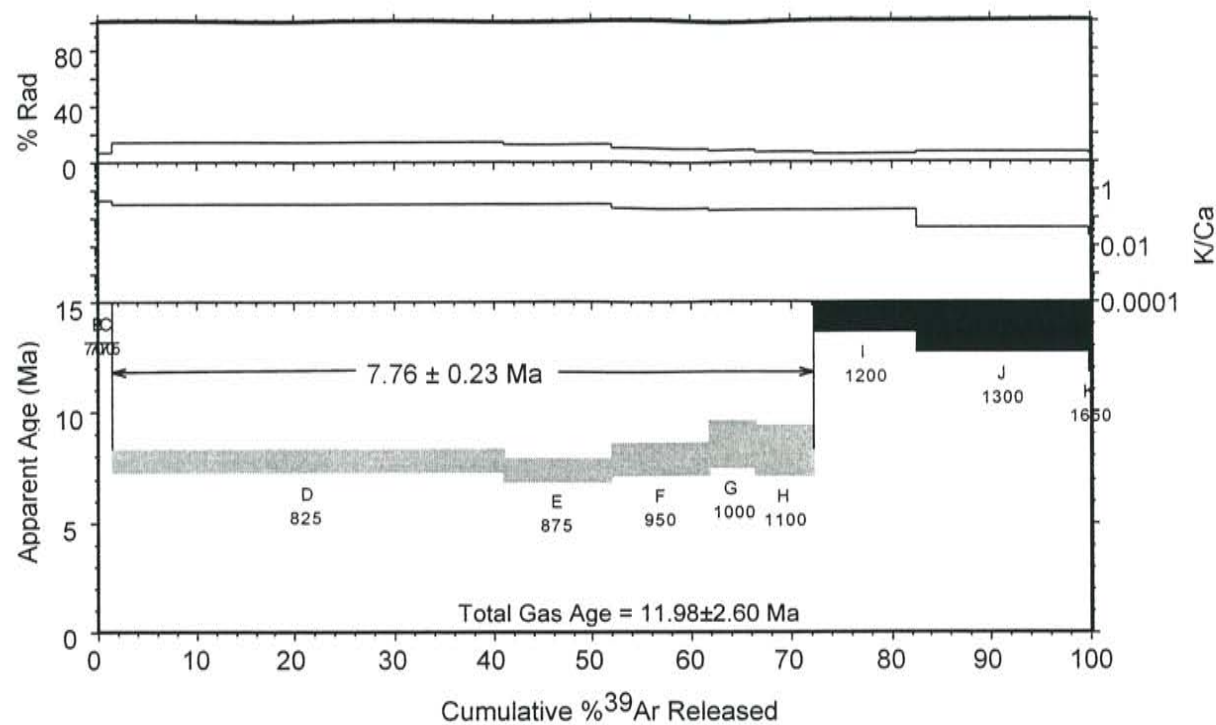
RA-047, tholeiitic basalt, Los Mogotes, groundmass concentrate



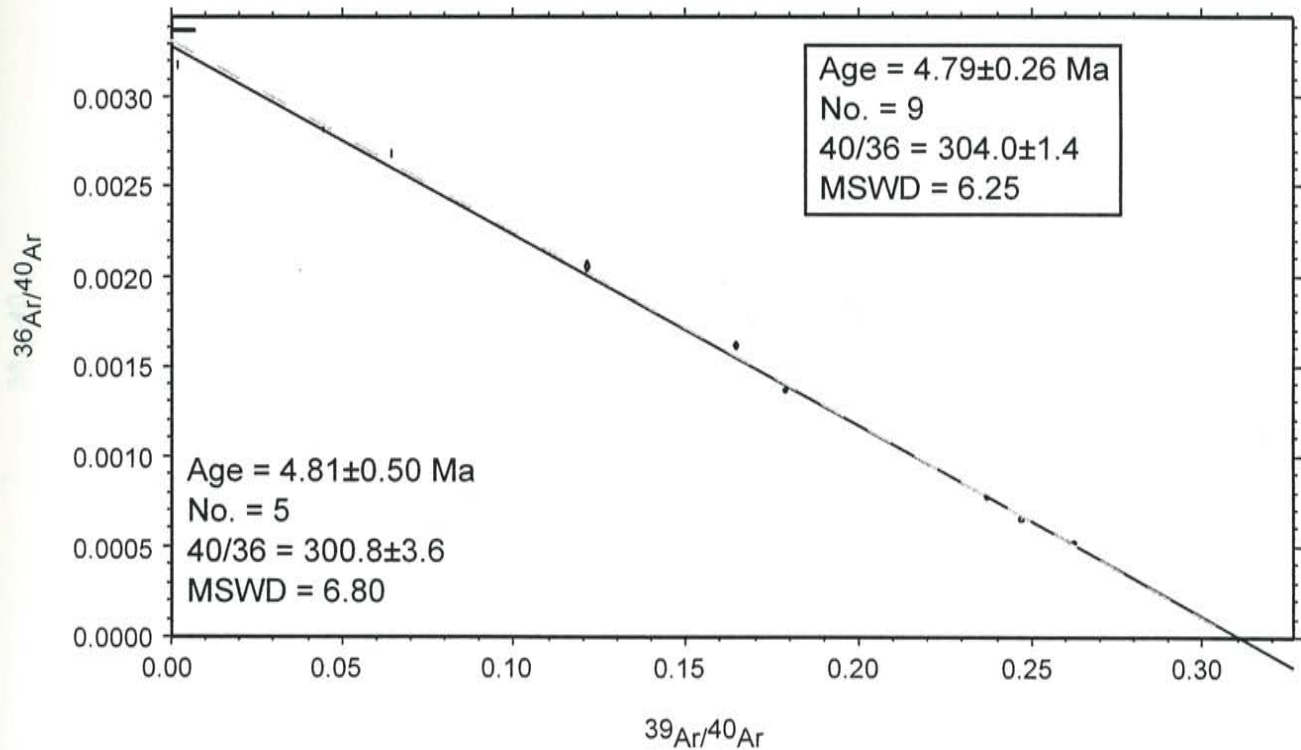
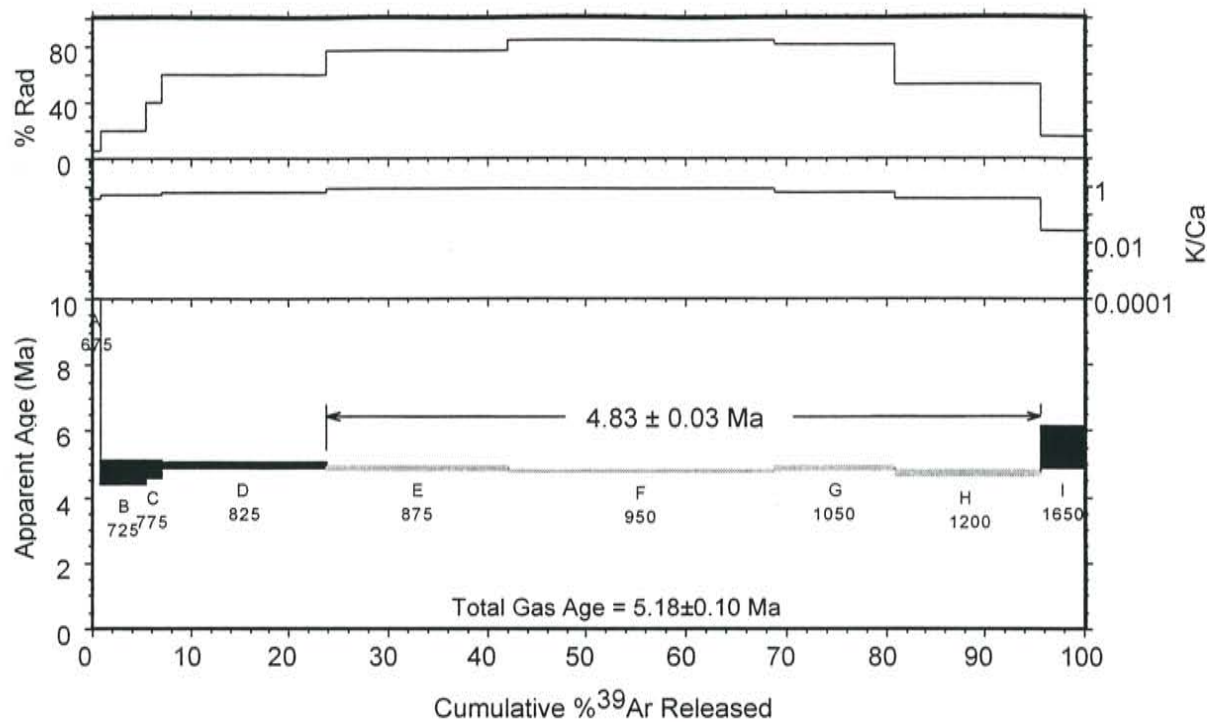
RA-048, tholeiitic basalt, Los Mogotes, groundmass concentrate



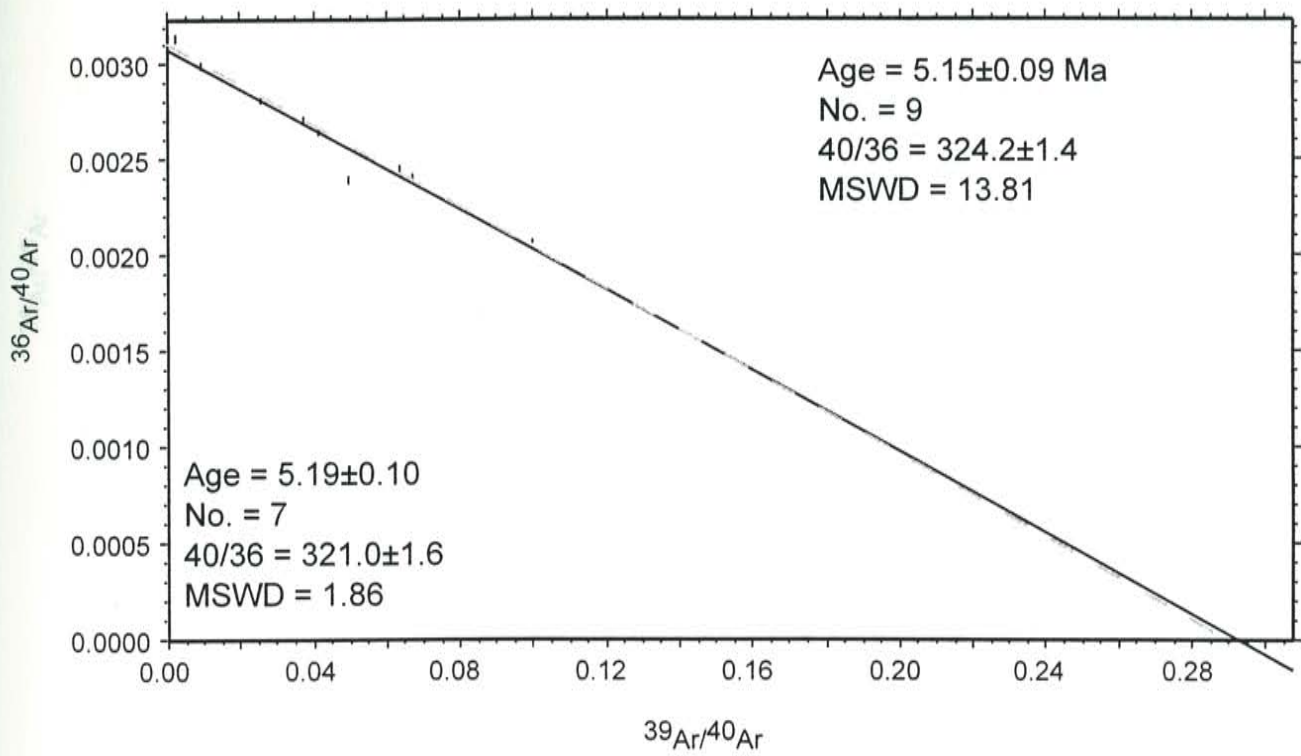
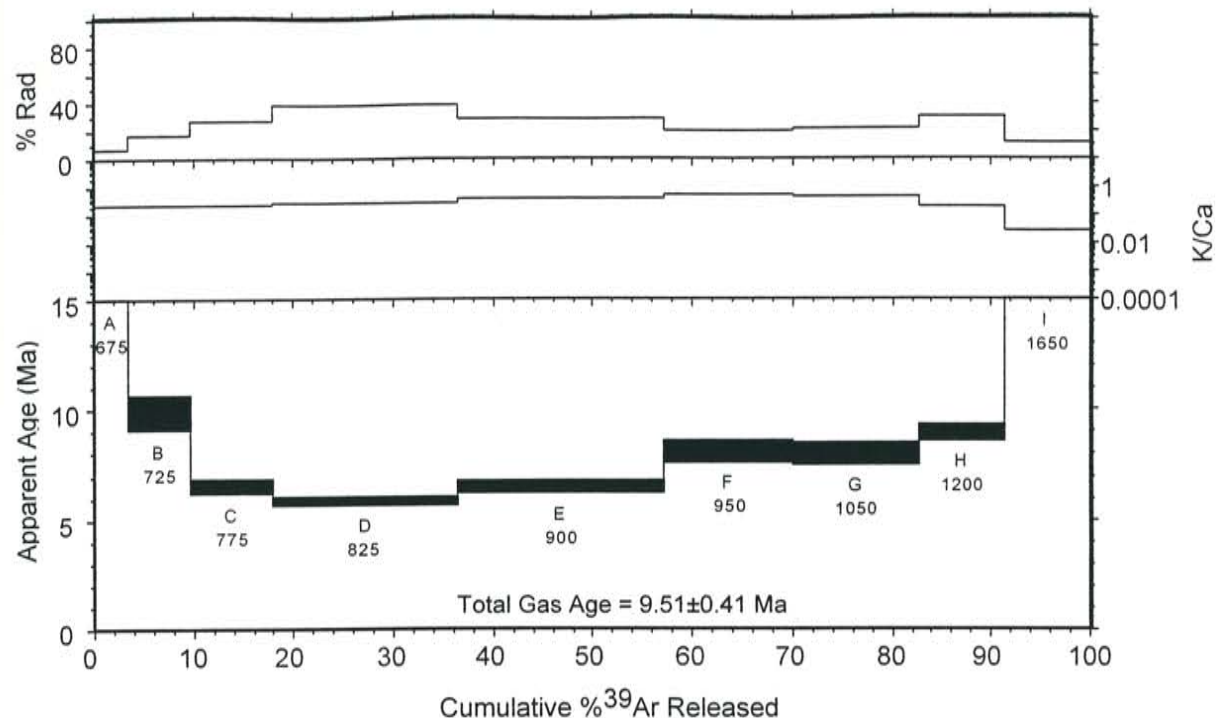
RA-049, tholeiitic basalt, Los Mogotes, groundmass concentrate



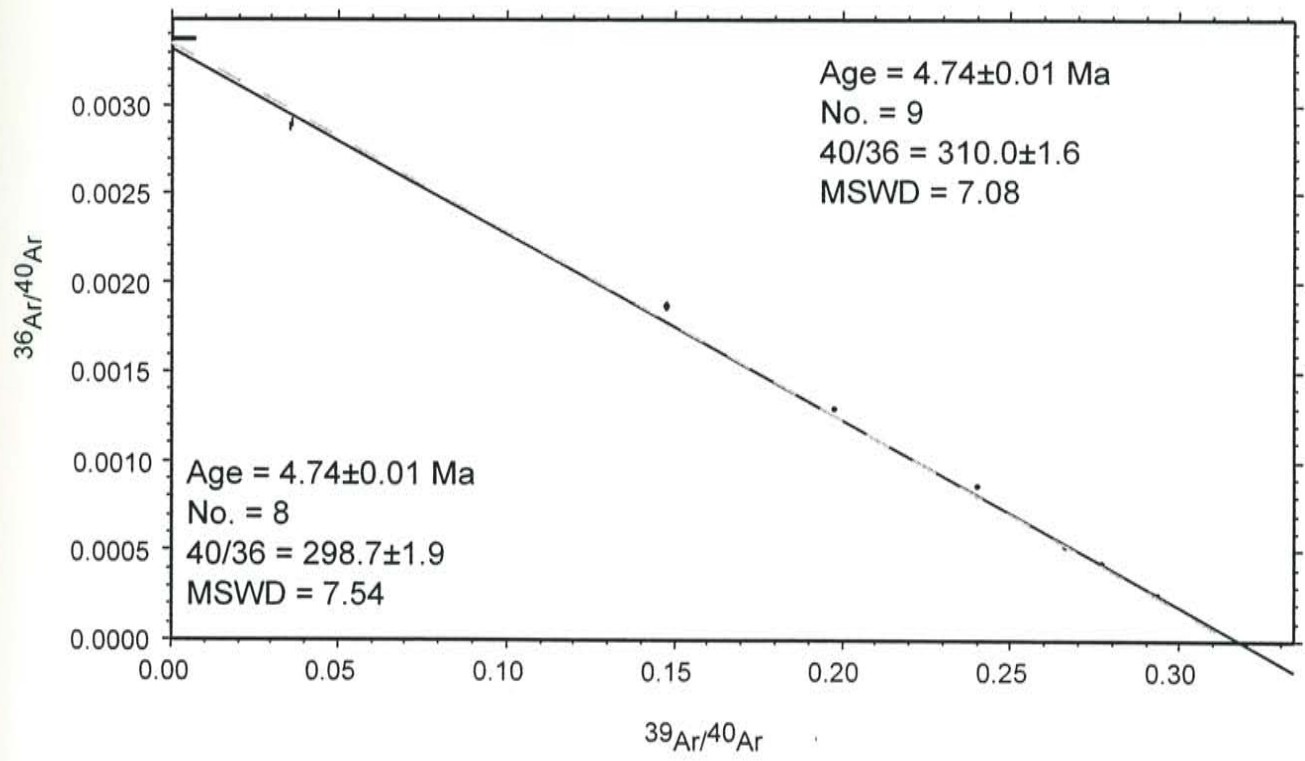
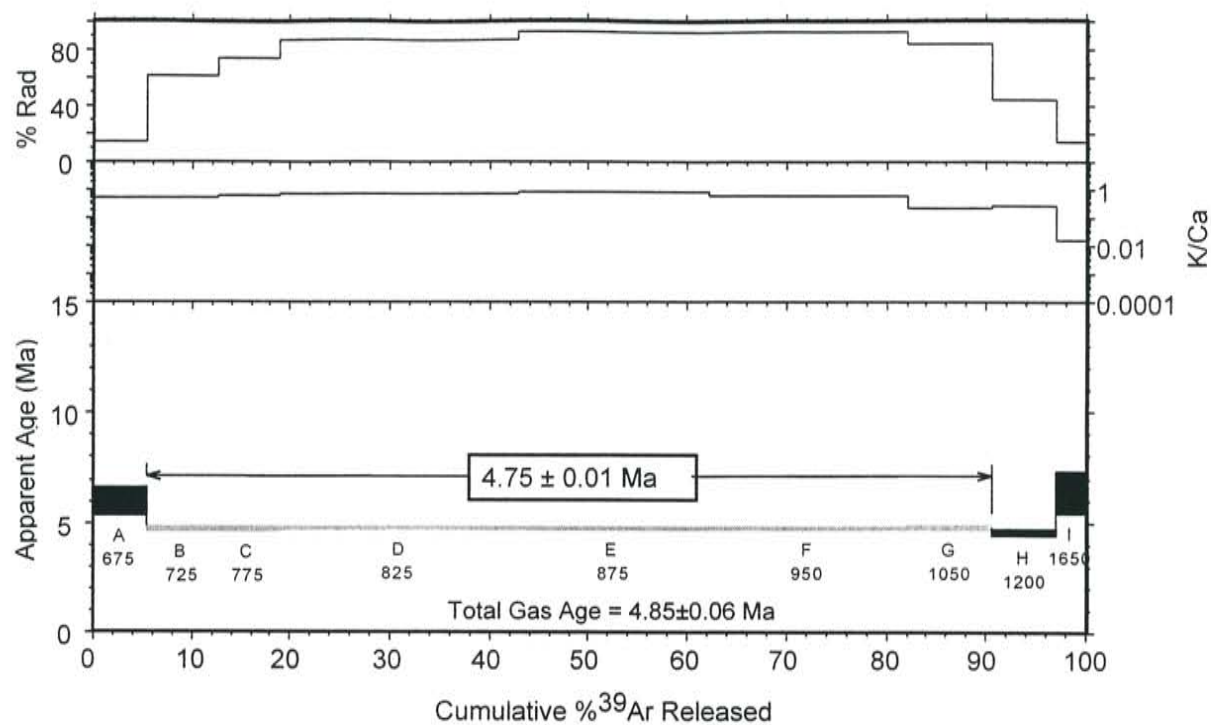
RA-050, tholeiitic basalt, Los Mogotos, groundmass concentrate



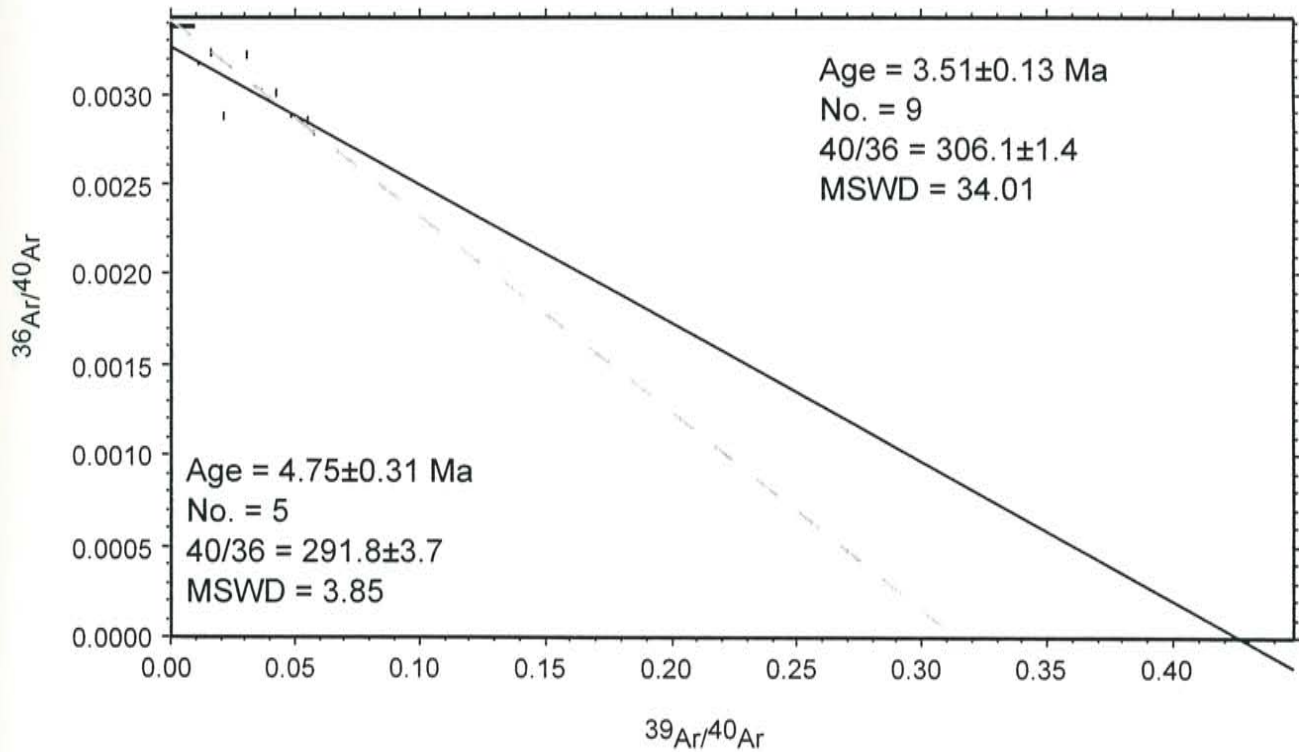
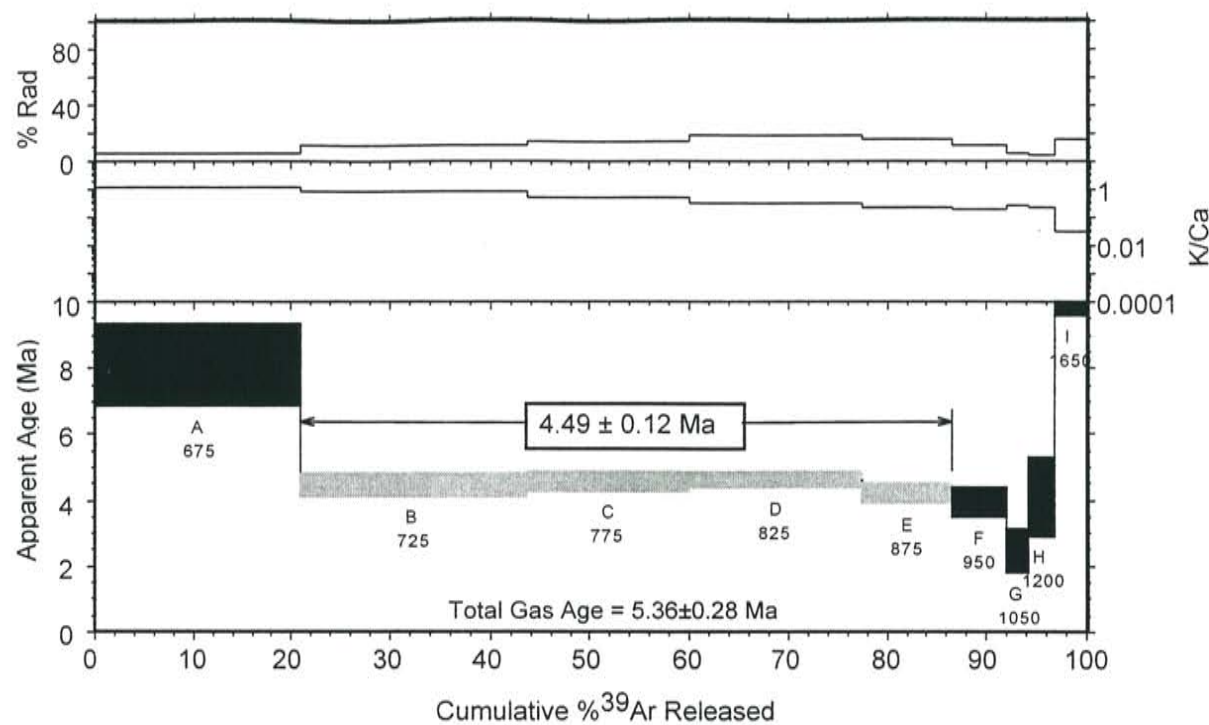
RA-051, tholeiitic basalt, Los Mogotes, groundmass concentrate



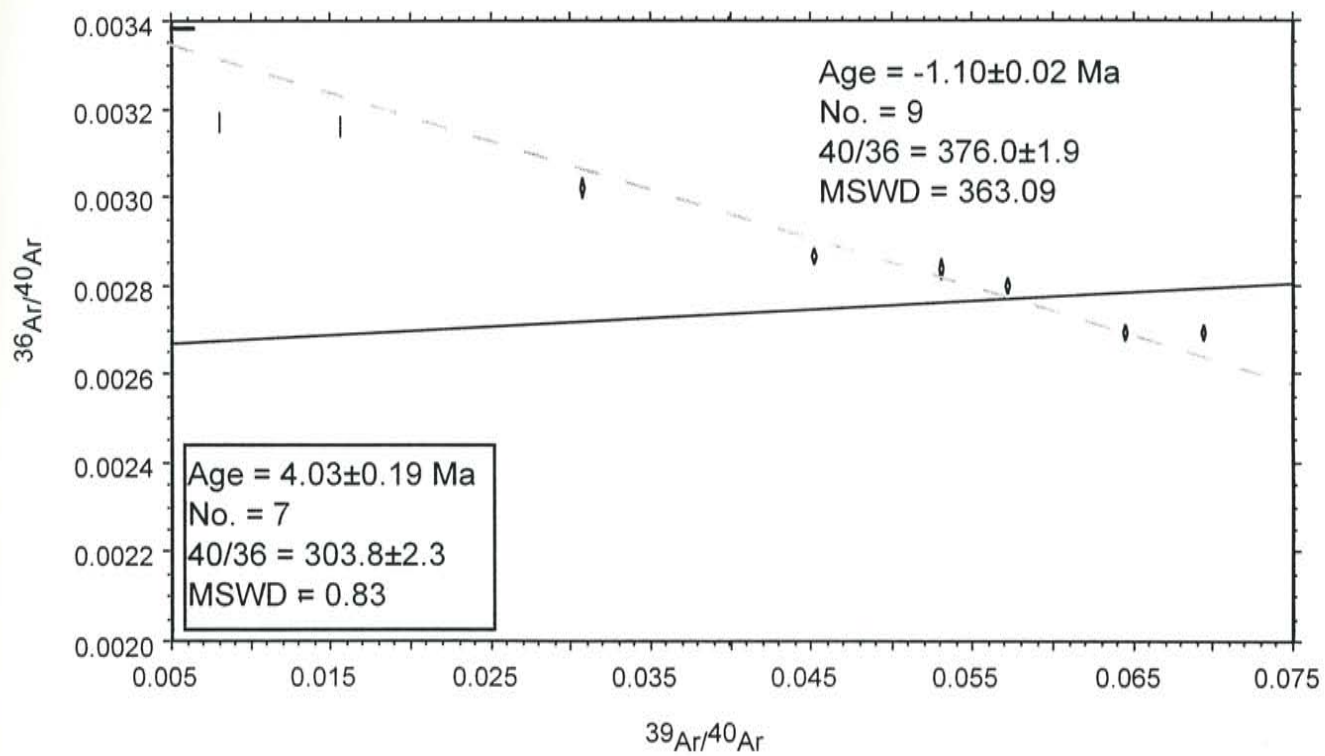
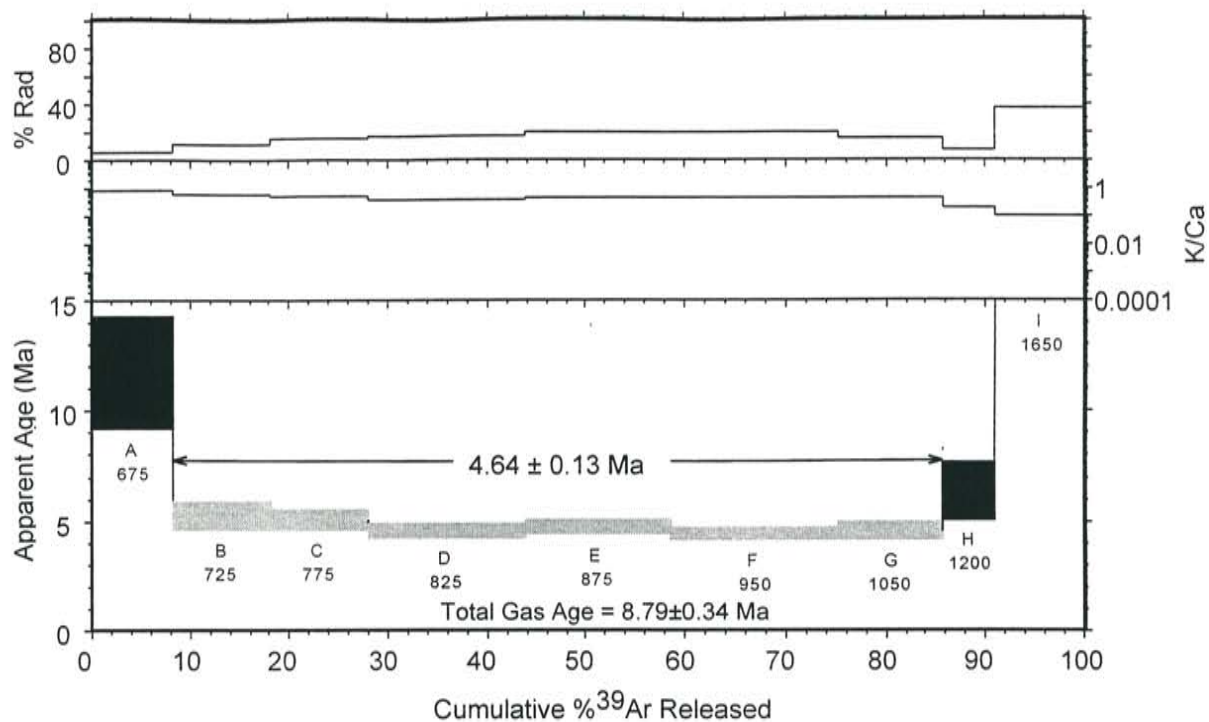
RA-052, tholeiitic basalt, Los Mogotos, groundmass concentrate



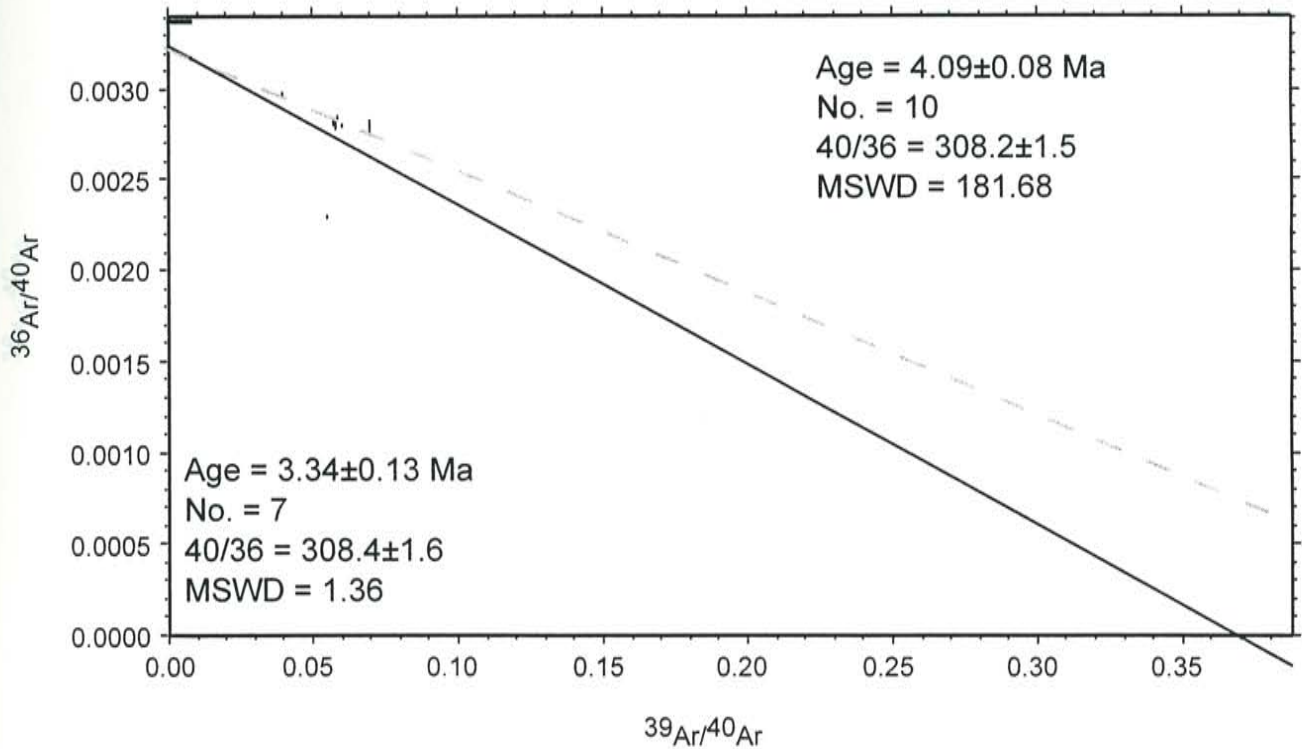
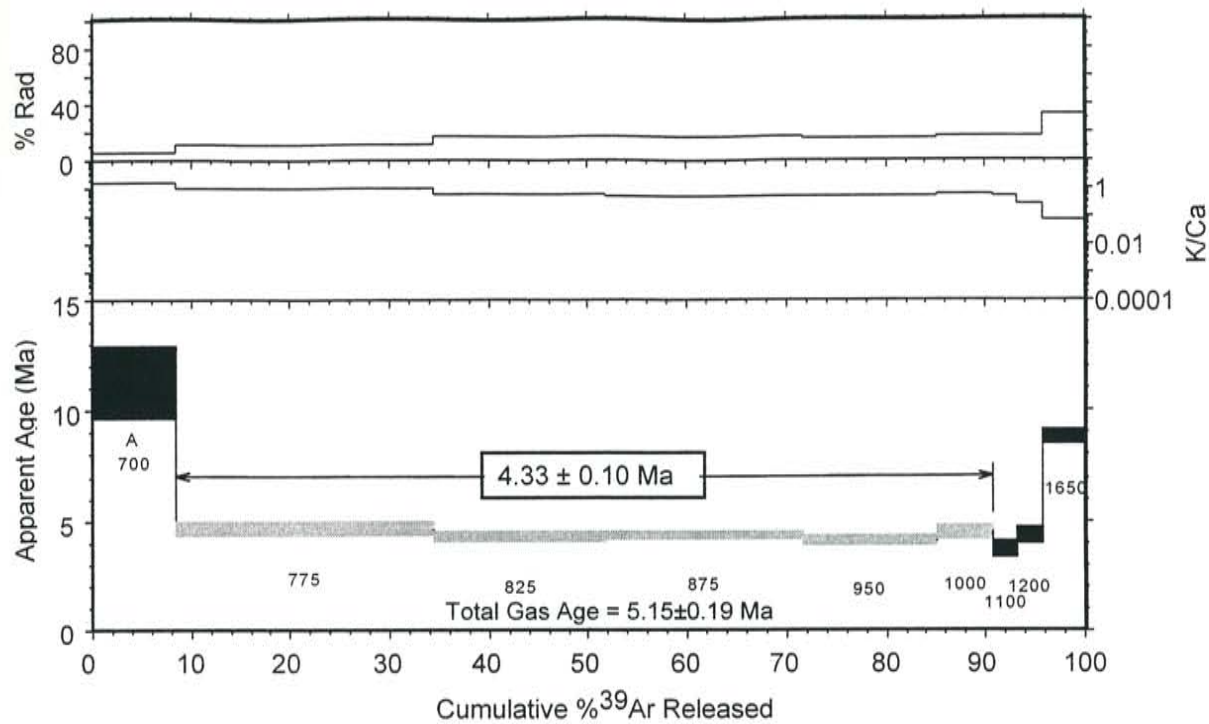
RA-055, basalt, Mesa Vibora, groundmass concentrate



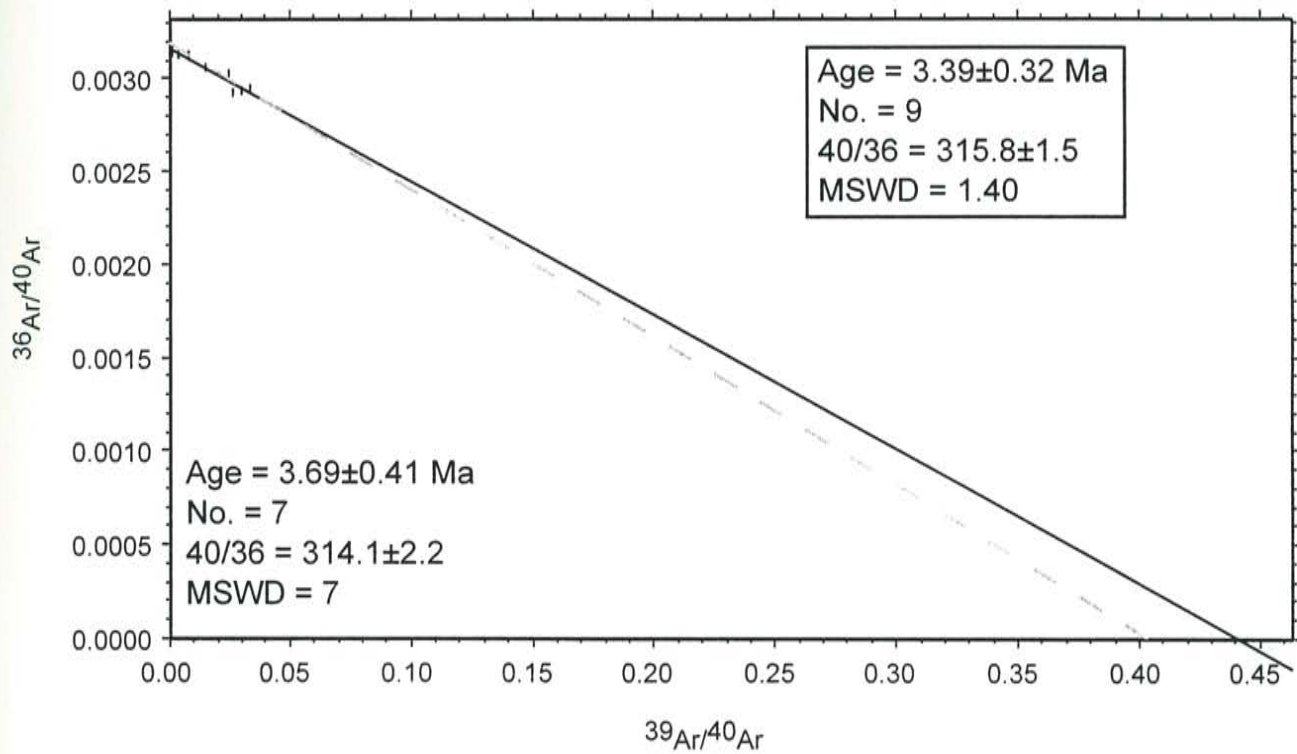
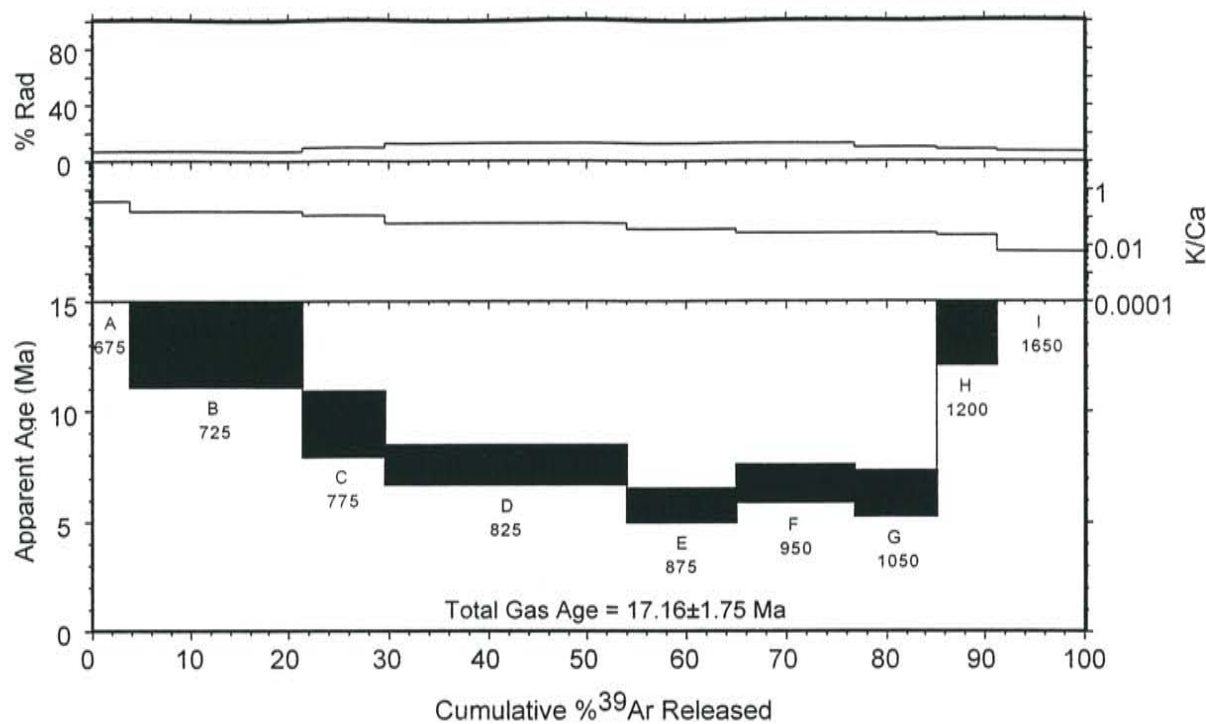
RA-056, basalt, Mesa Vibora, groundmass concentrate



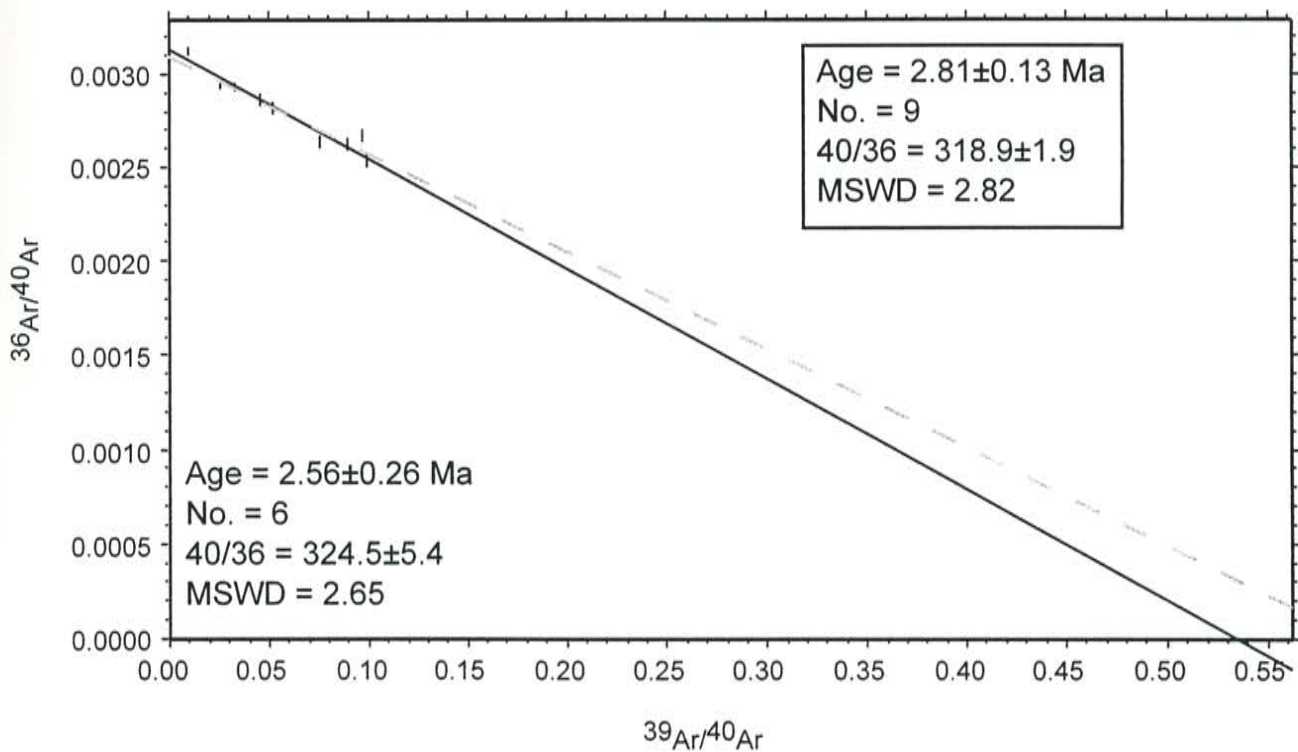
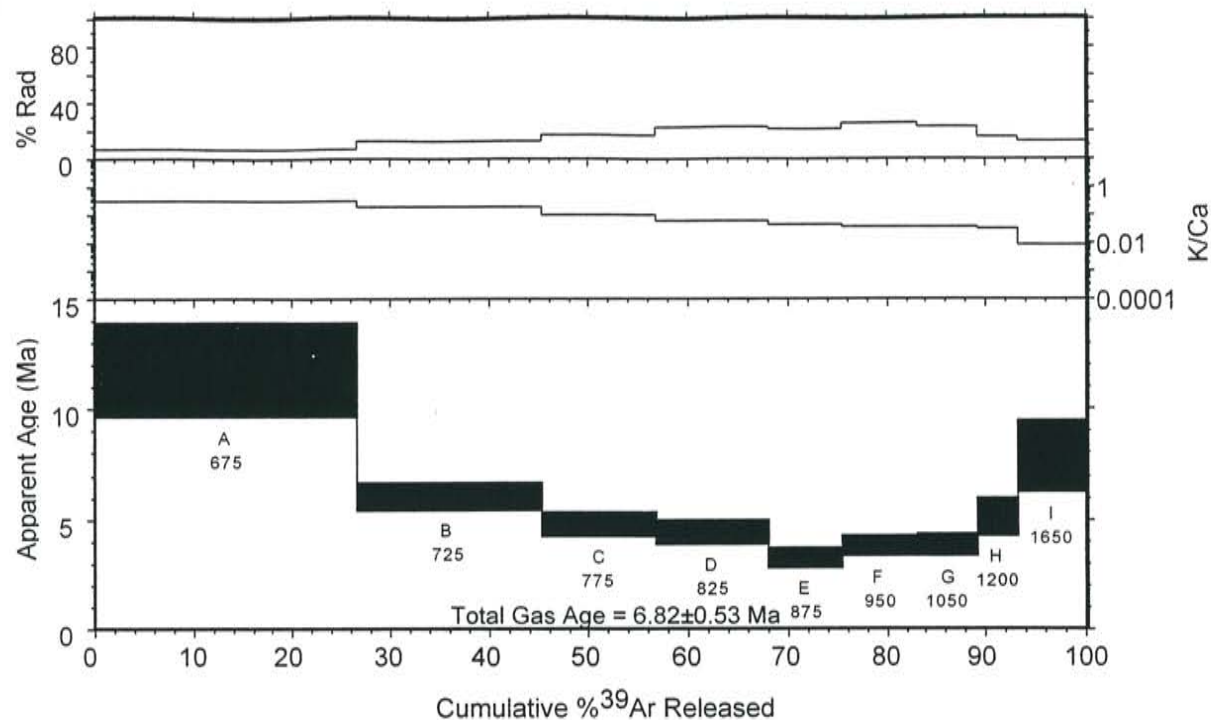
RA-058, basalt, Mesa Vibora area, groundmass concentrate



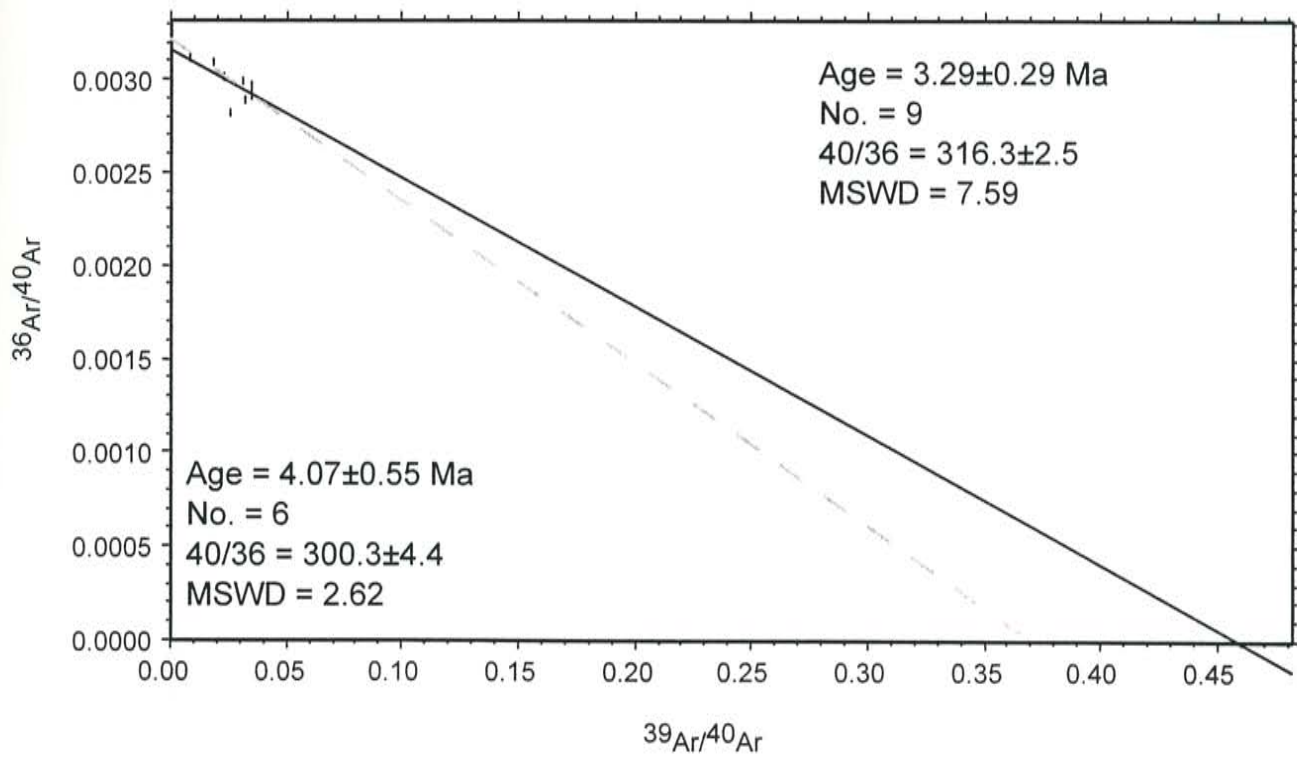
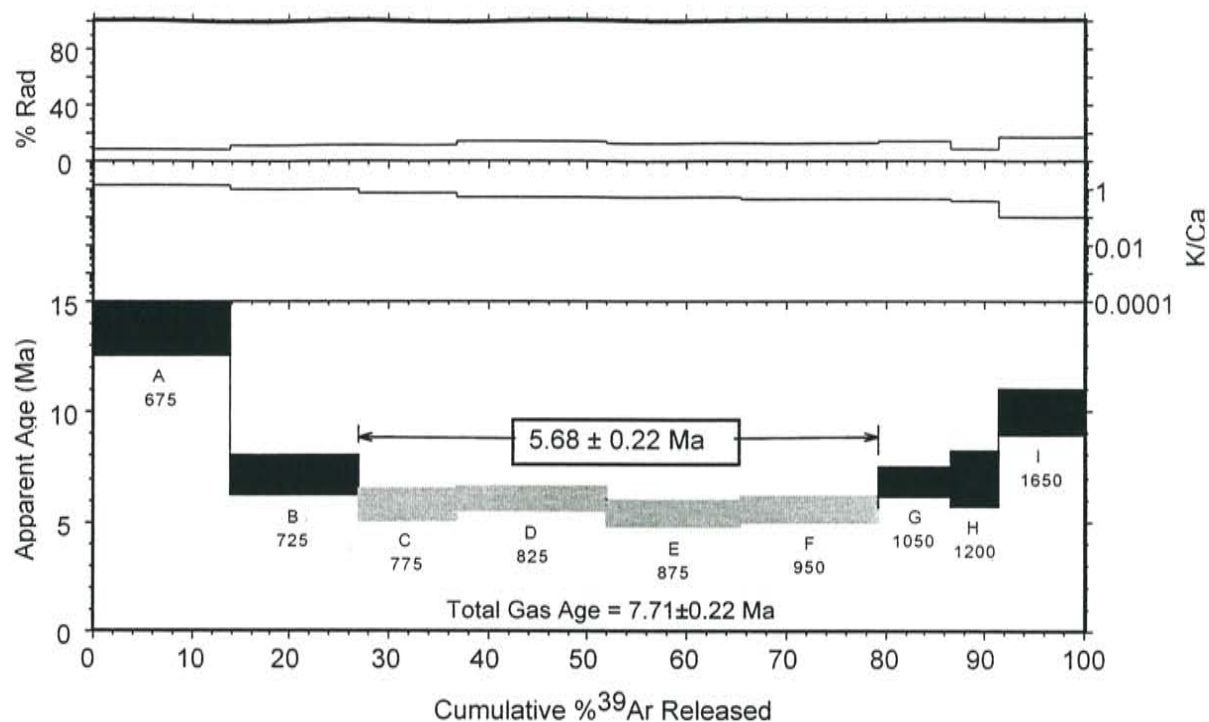
RA-060, Servilleta Basalt, Riconada Area, groundmass concentrate



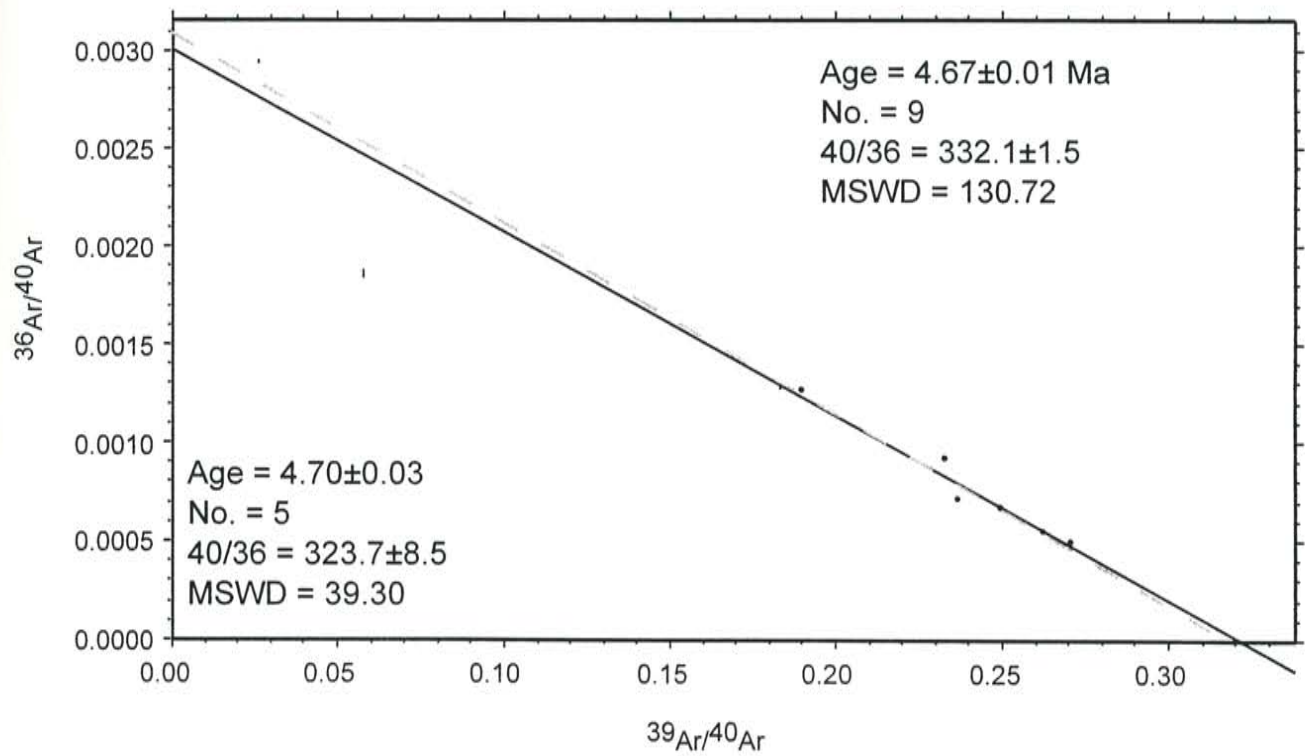
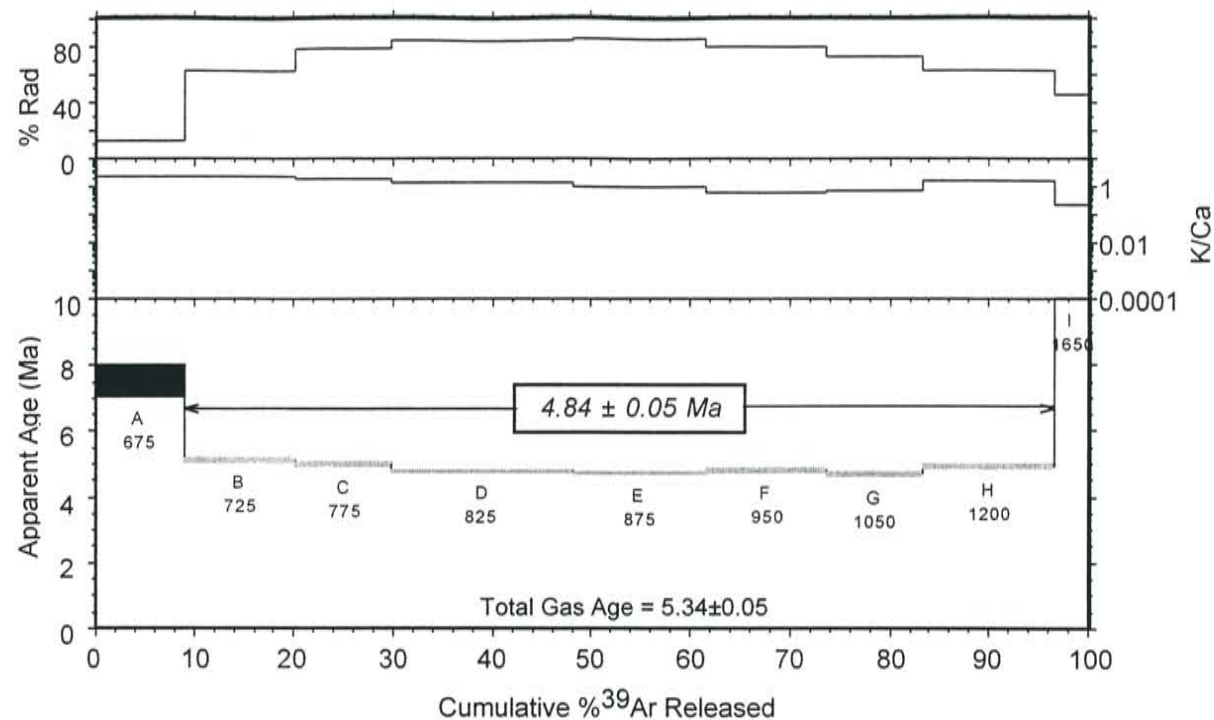
RA-061, pyroxene dacite, Cerro Negro, groundmass concentrate



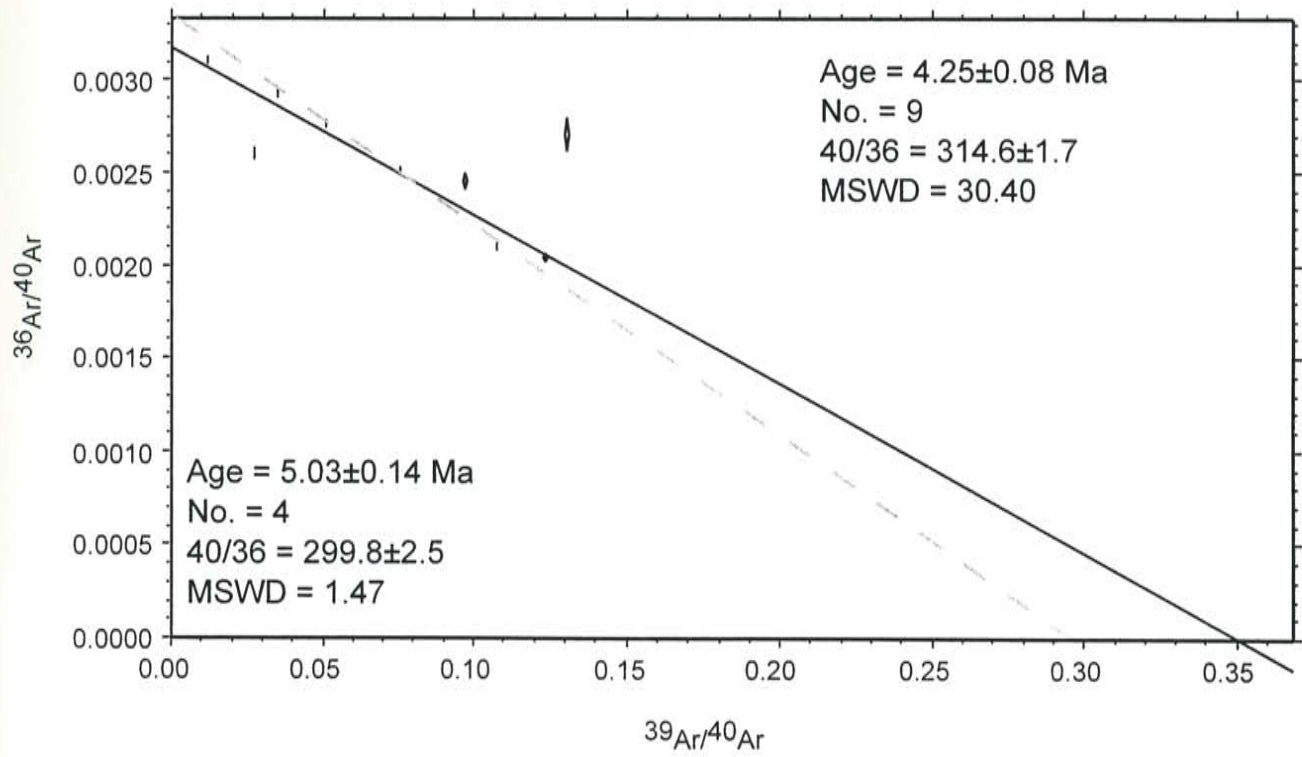
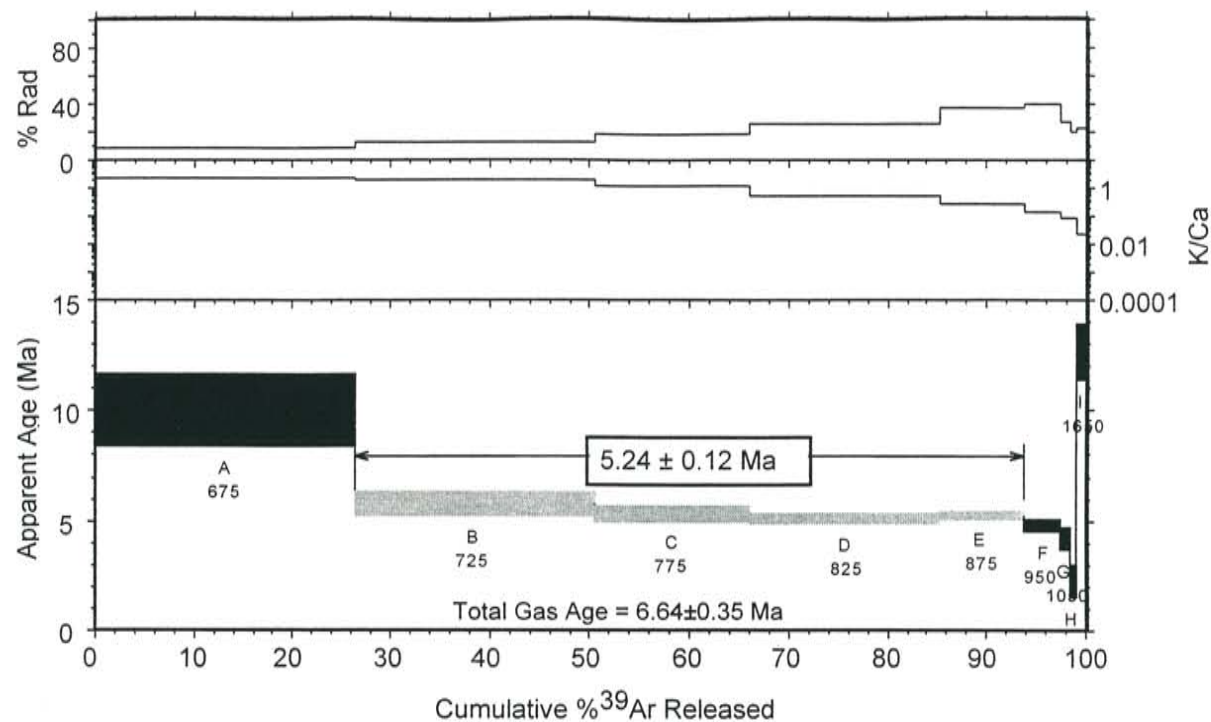
RA-062, pyroxene dacite, Cerro Negro, groundmass concentrate



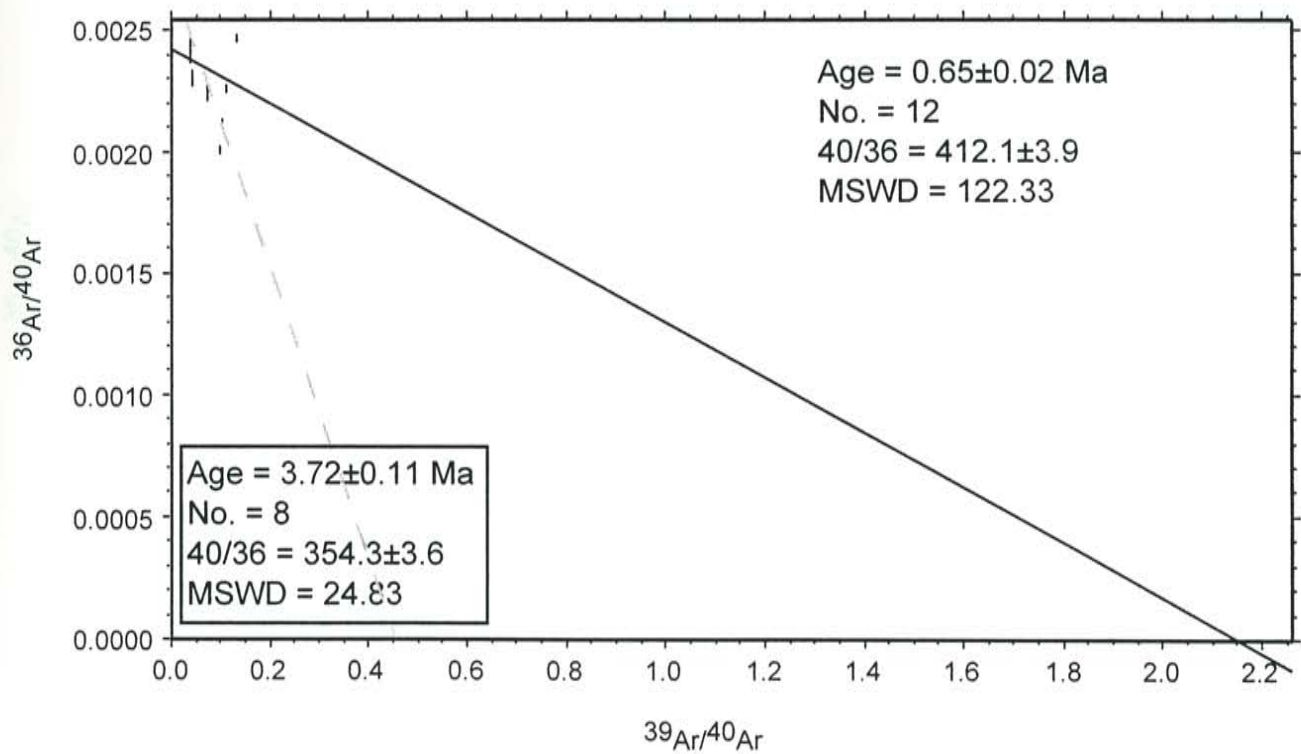
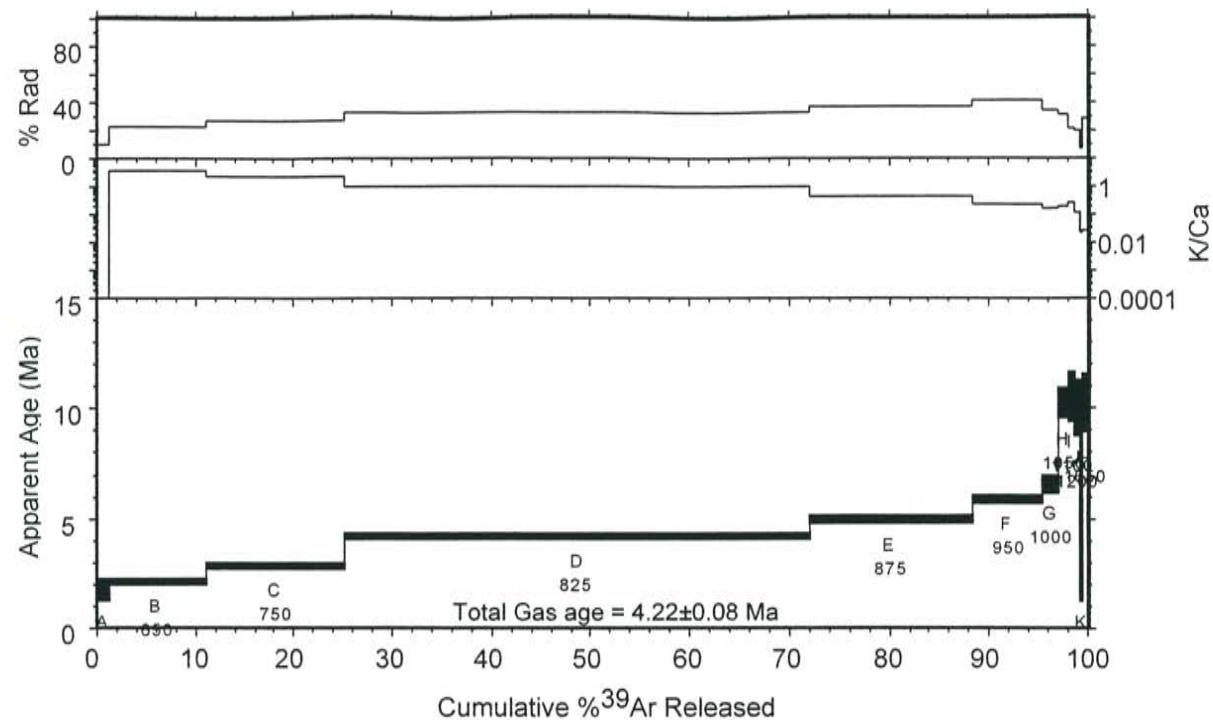
RA-064, pyroxene dacite, Hondo roadcut, groundmass concentrate



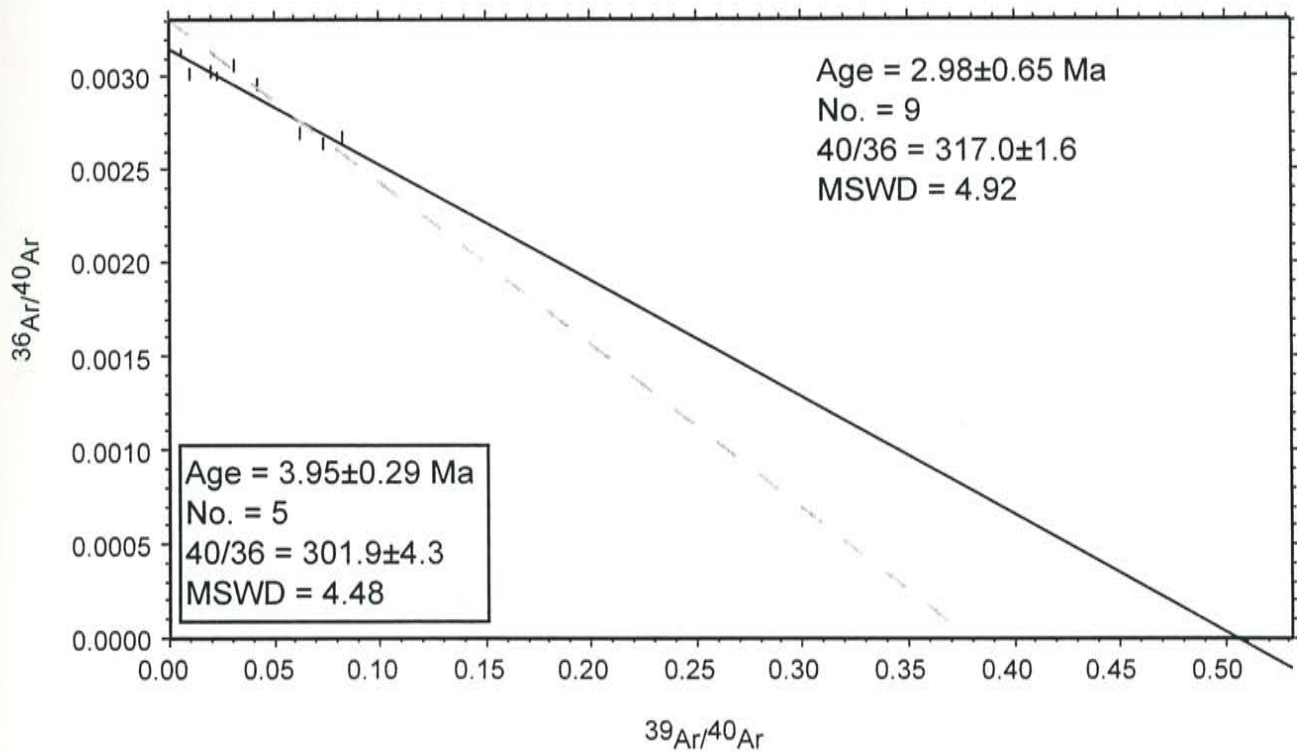
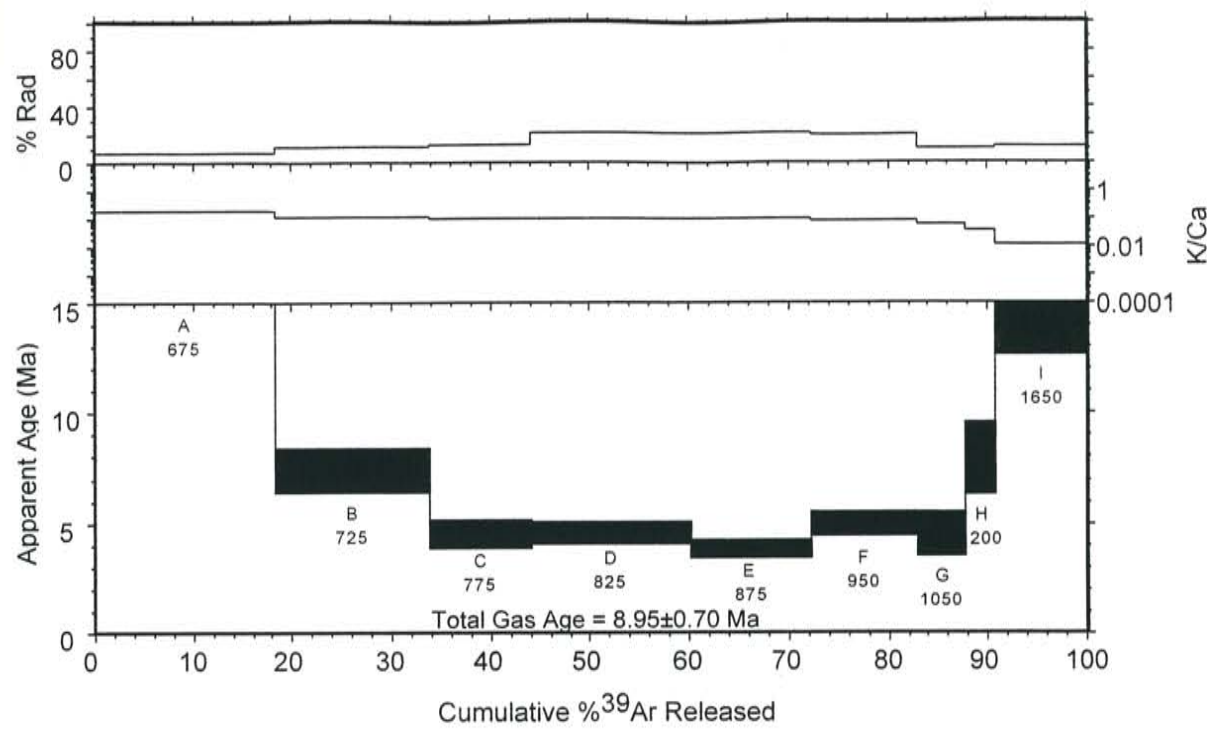
RA-065, pyroxene dacite, Hondo roadcut, groundmass concentrate



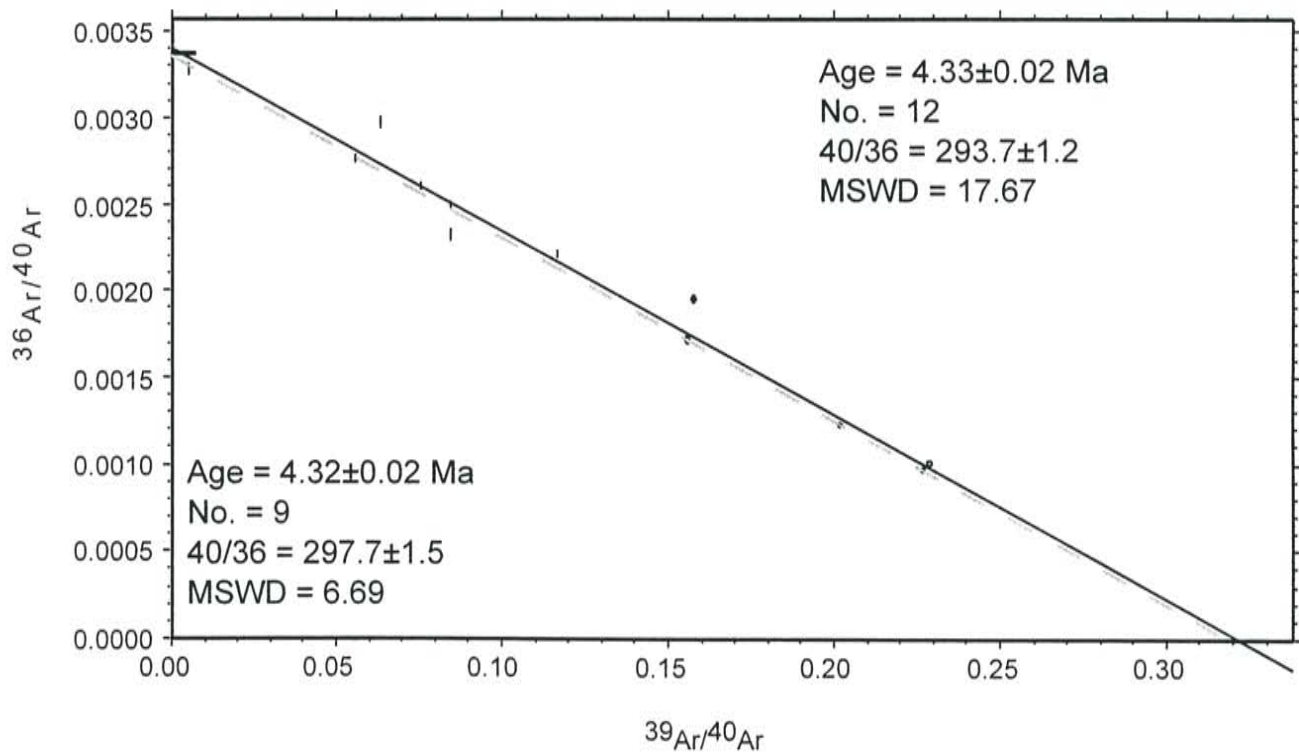
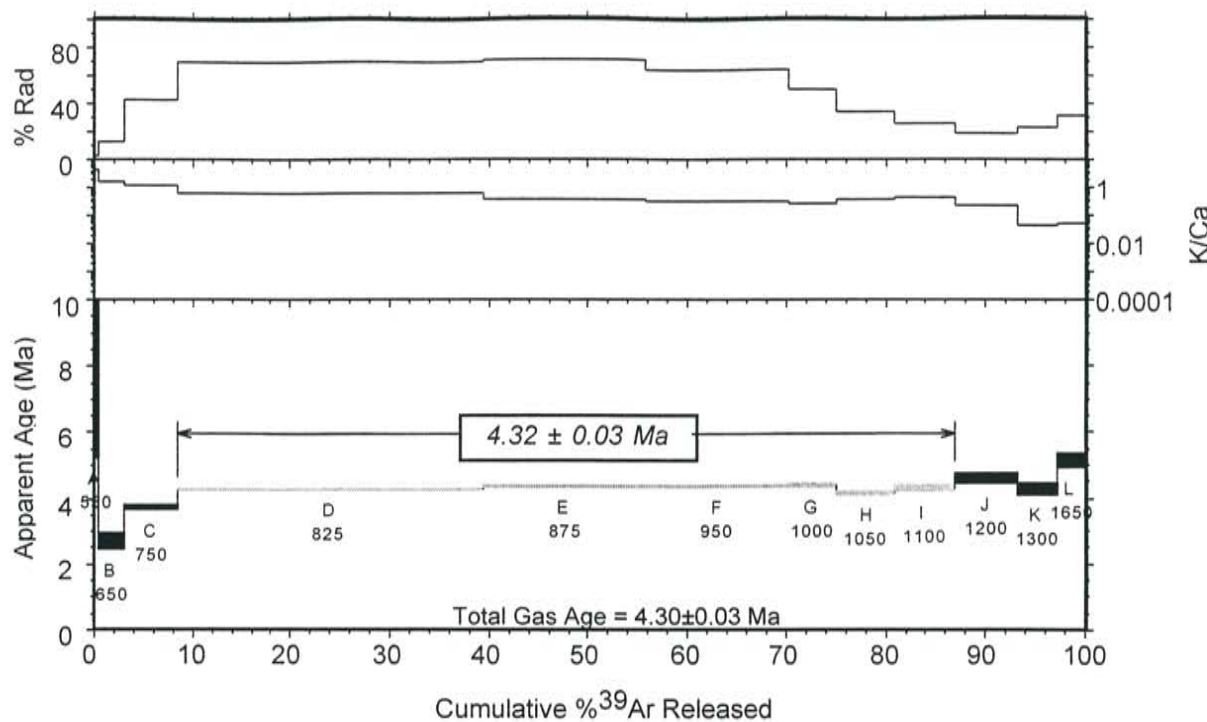
RA-072, Servilleta Basalt, northern Rio Grande gorge, groundmass concentrate



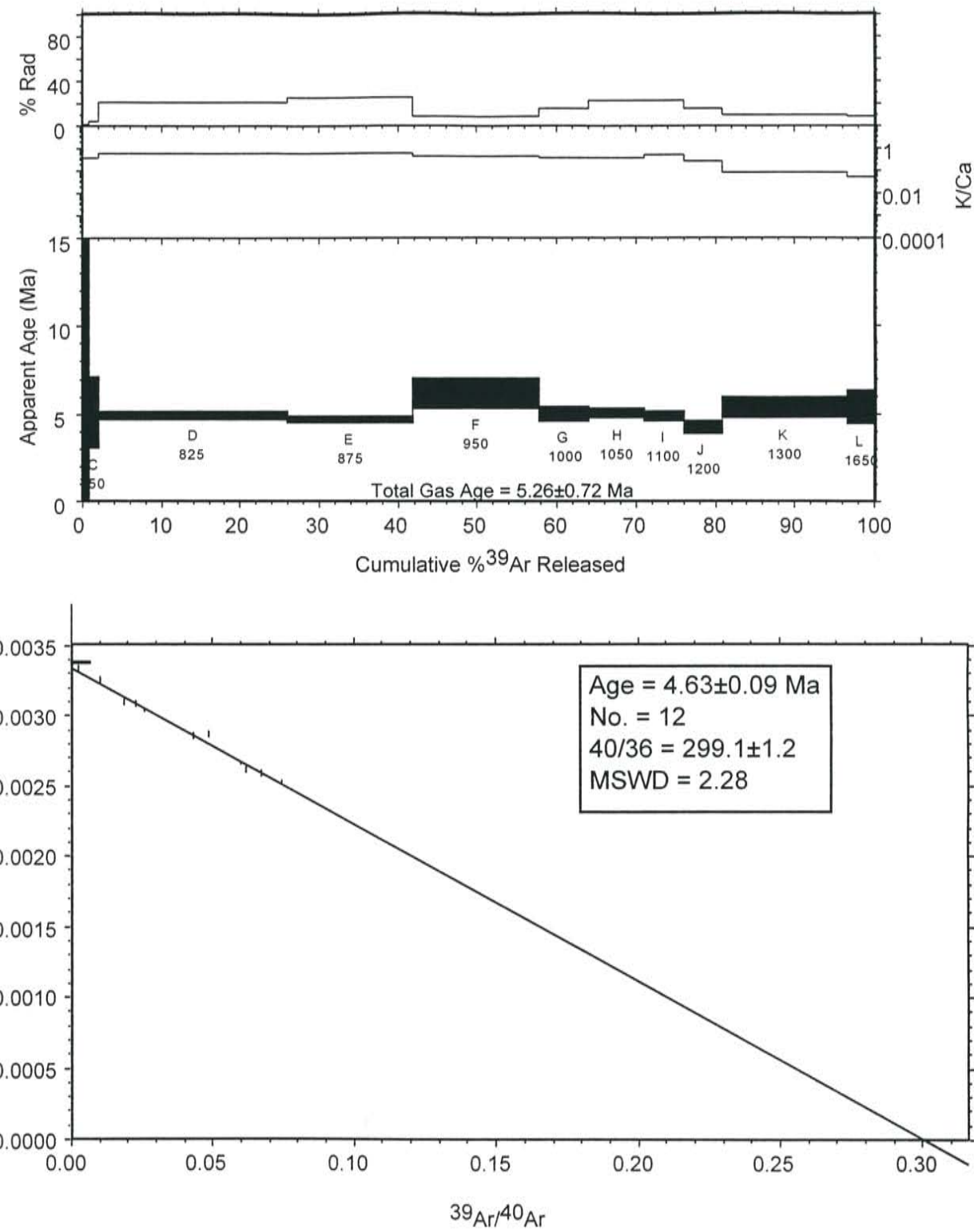
RA-076, tholeiitic basalt, Bighorn Peak area, groundmass concentrate



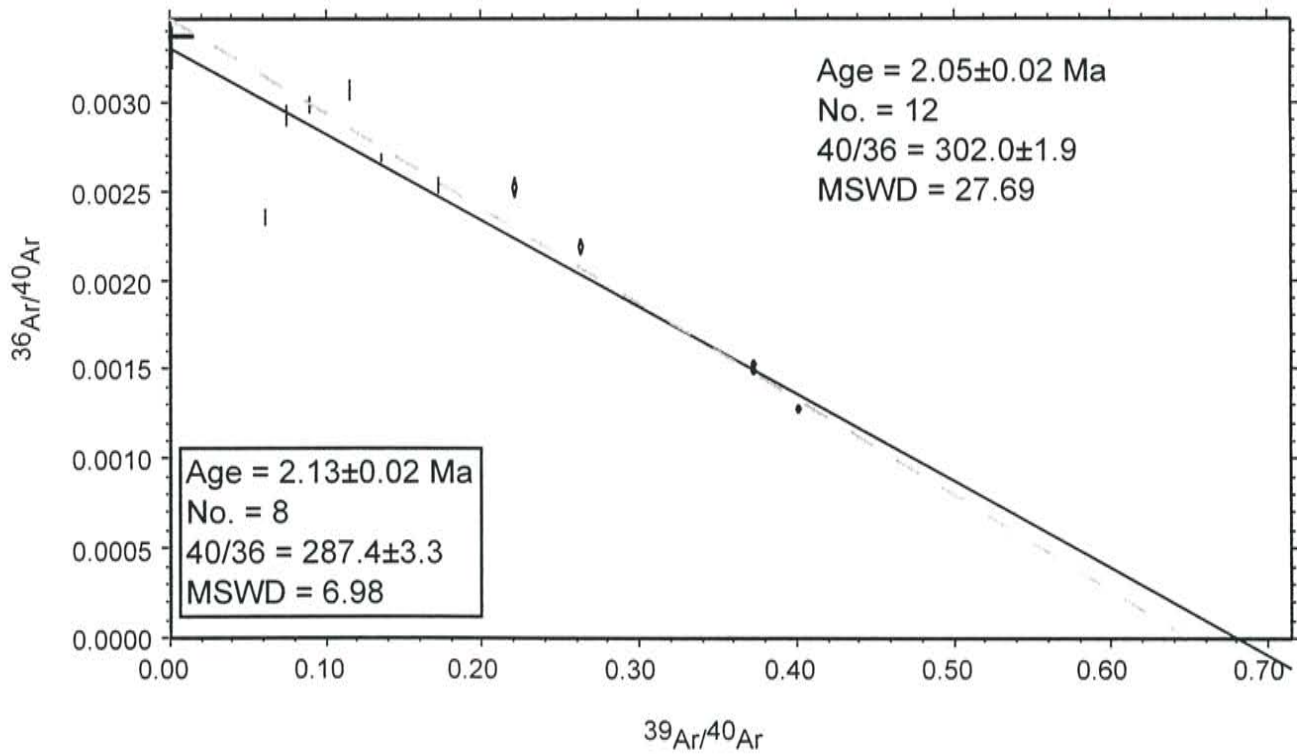
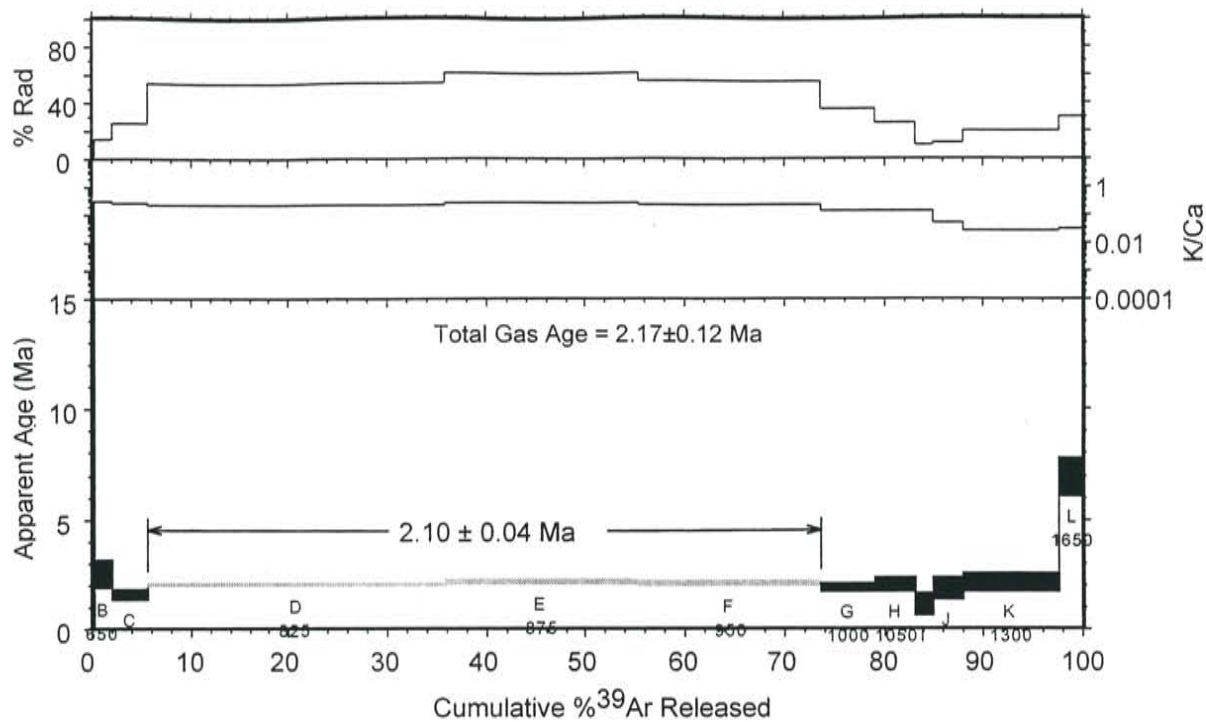
RA-079, Servilleta Basalt, Cerro Mojino, groundmass concentrate



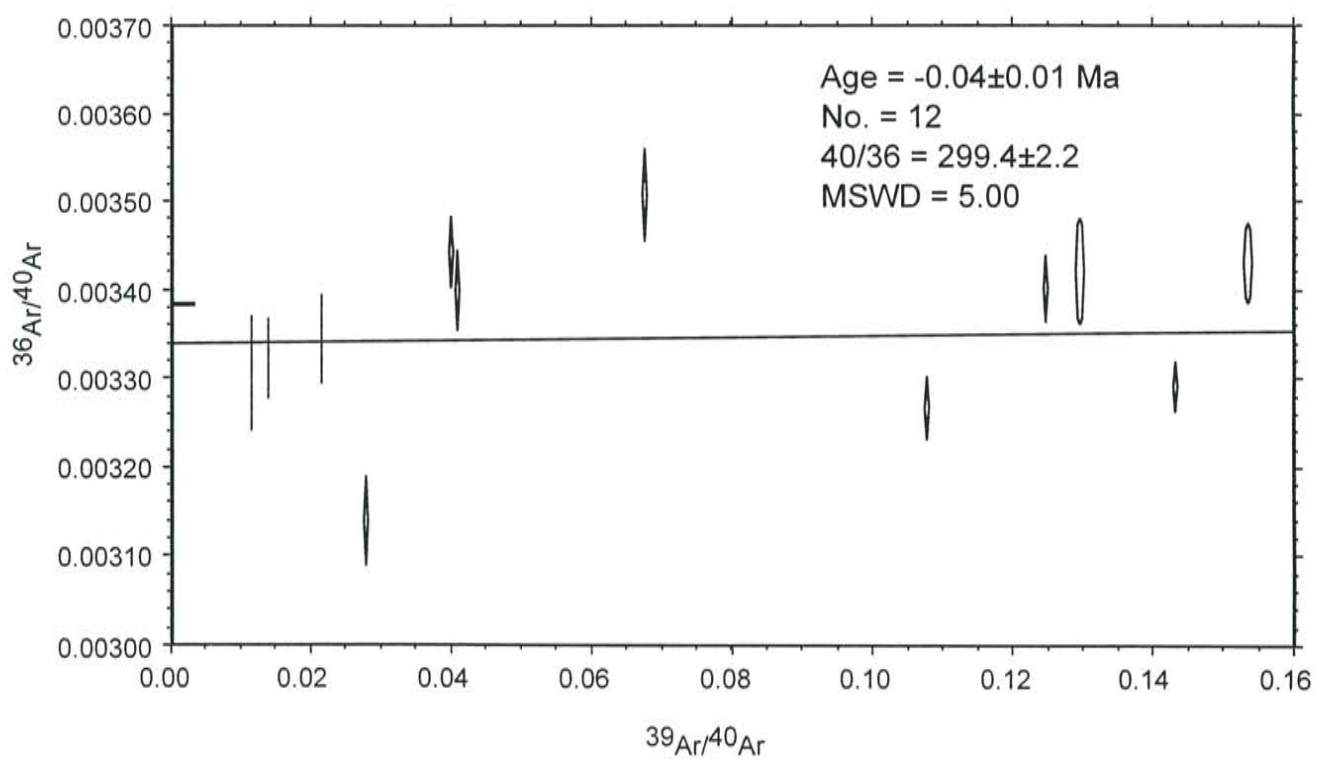
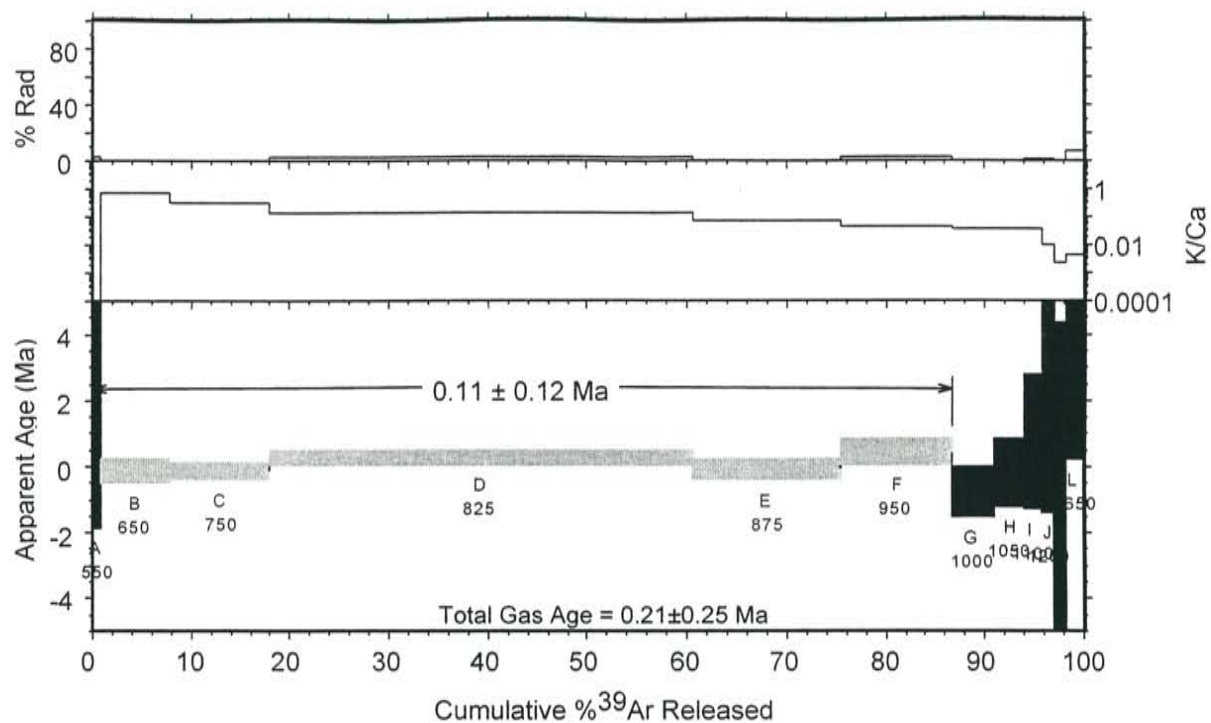
RA-080, Servilleta Basalt, Commanche Rim, groundmass concentrate



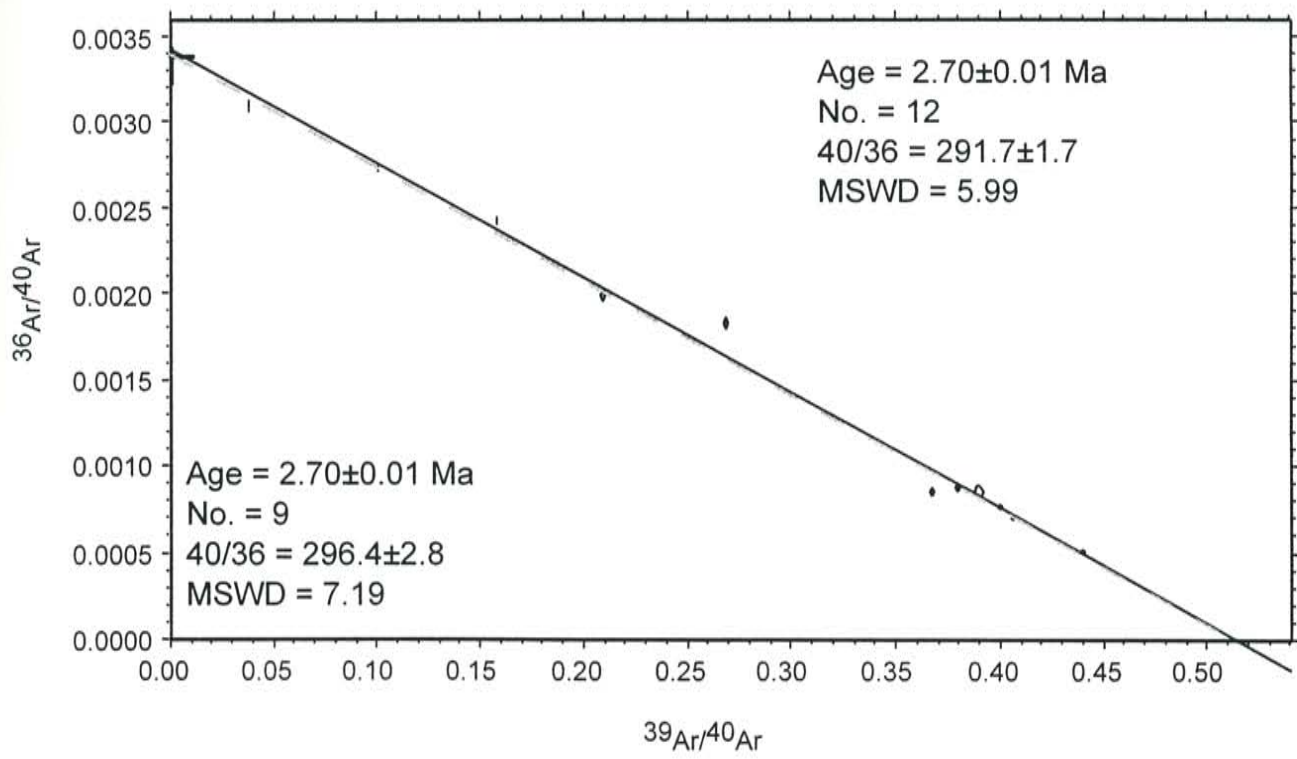
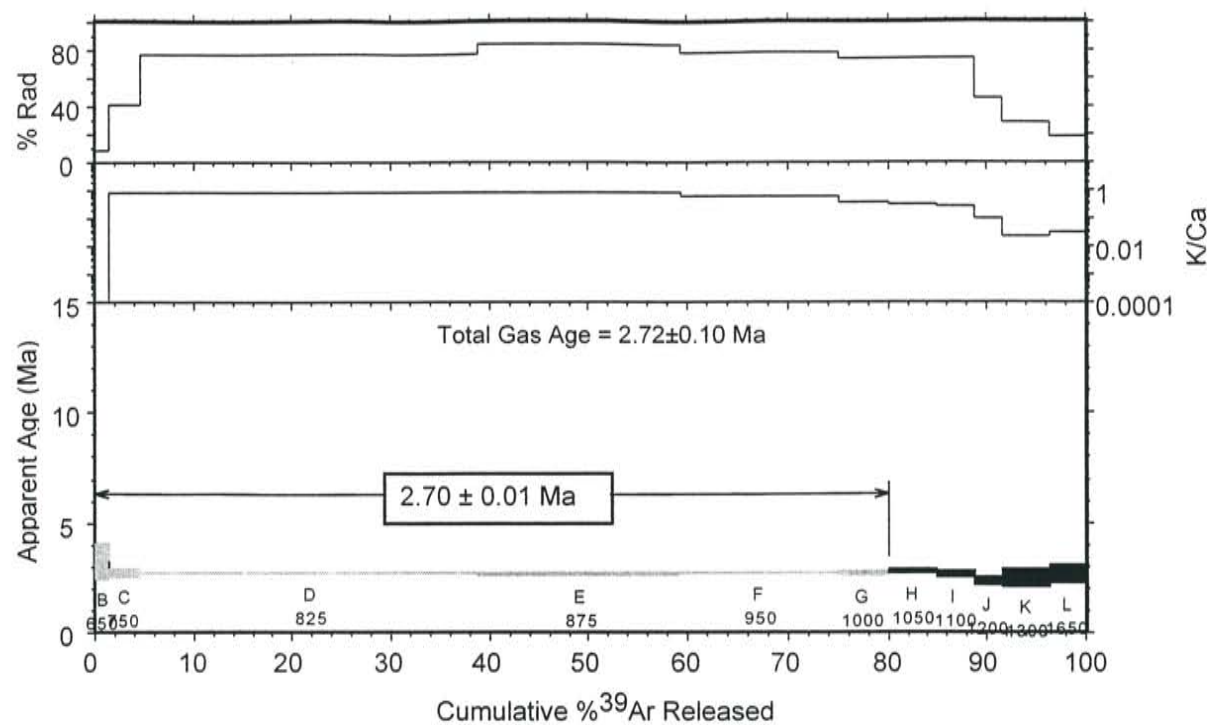
RA-082, pyroxene dacite, Ute Mtn., groundmass concentrate



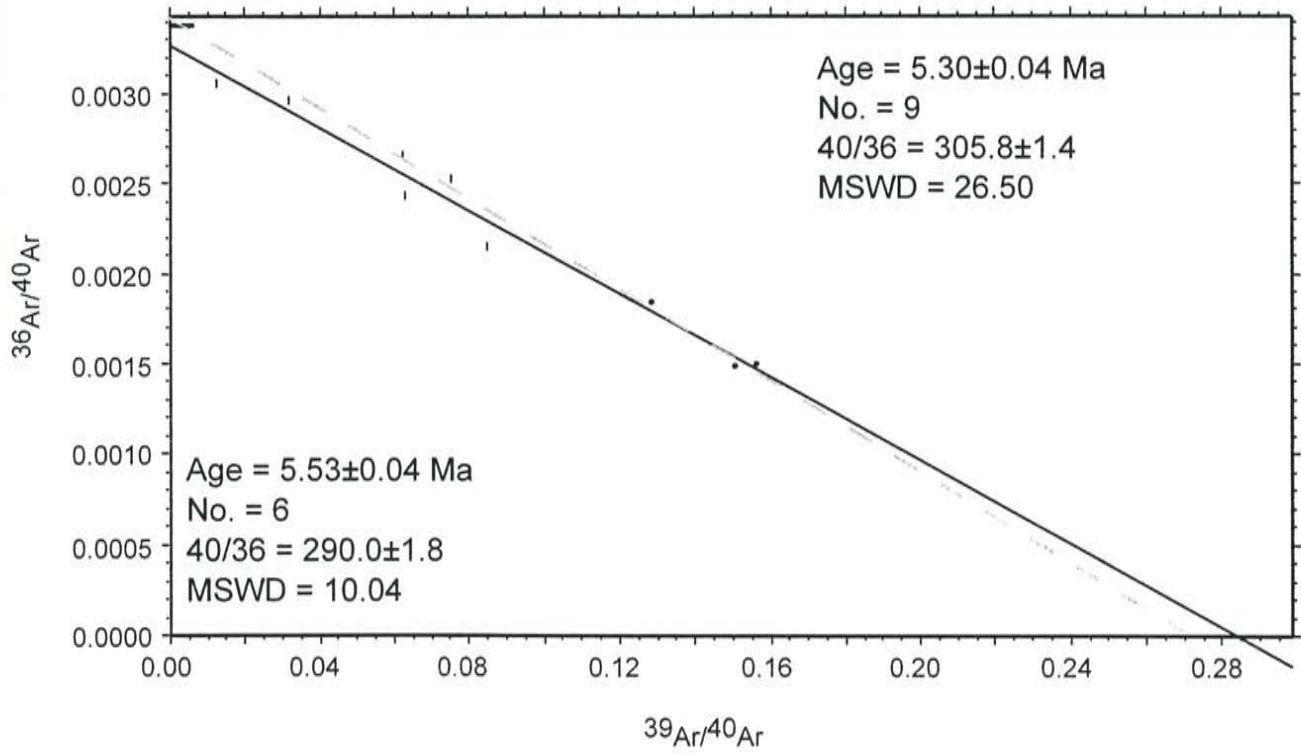
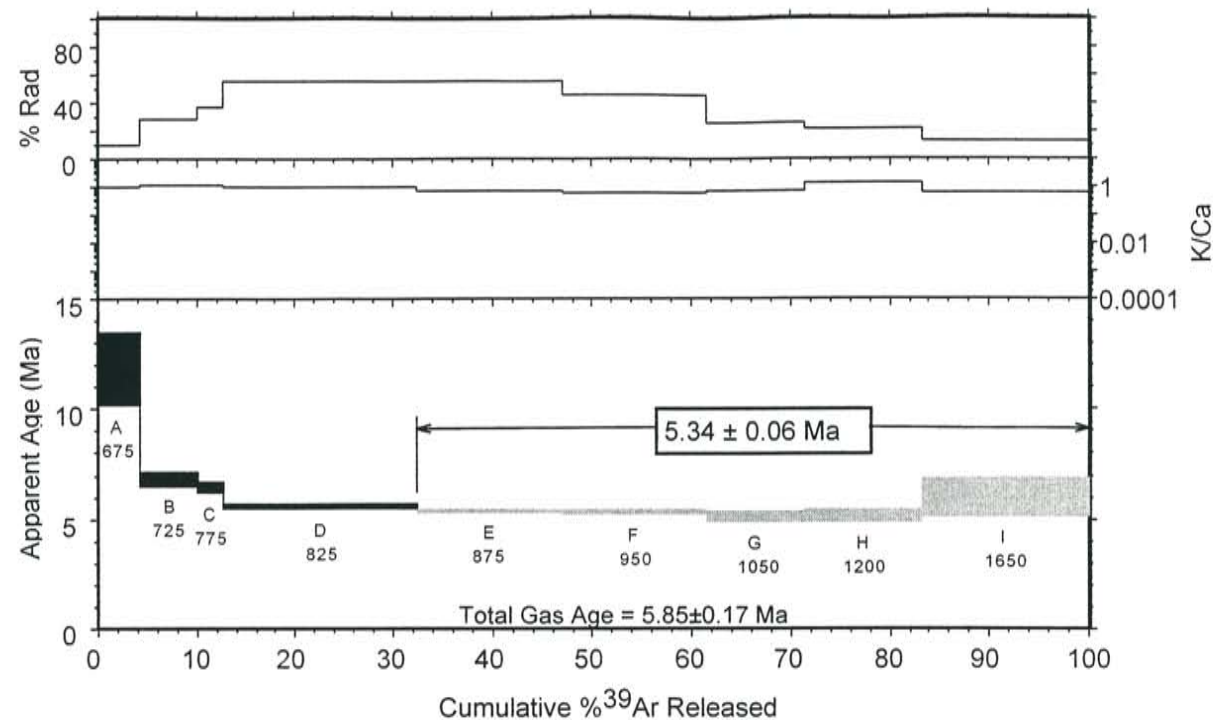
RA-083, pyroxene dacite, Ute Mtn., groundmass concentrate



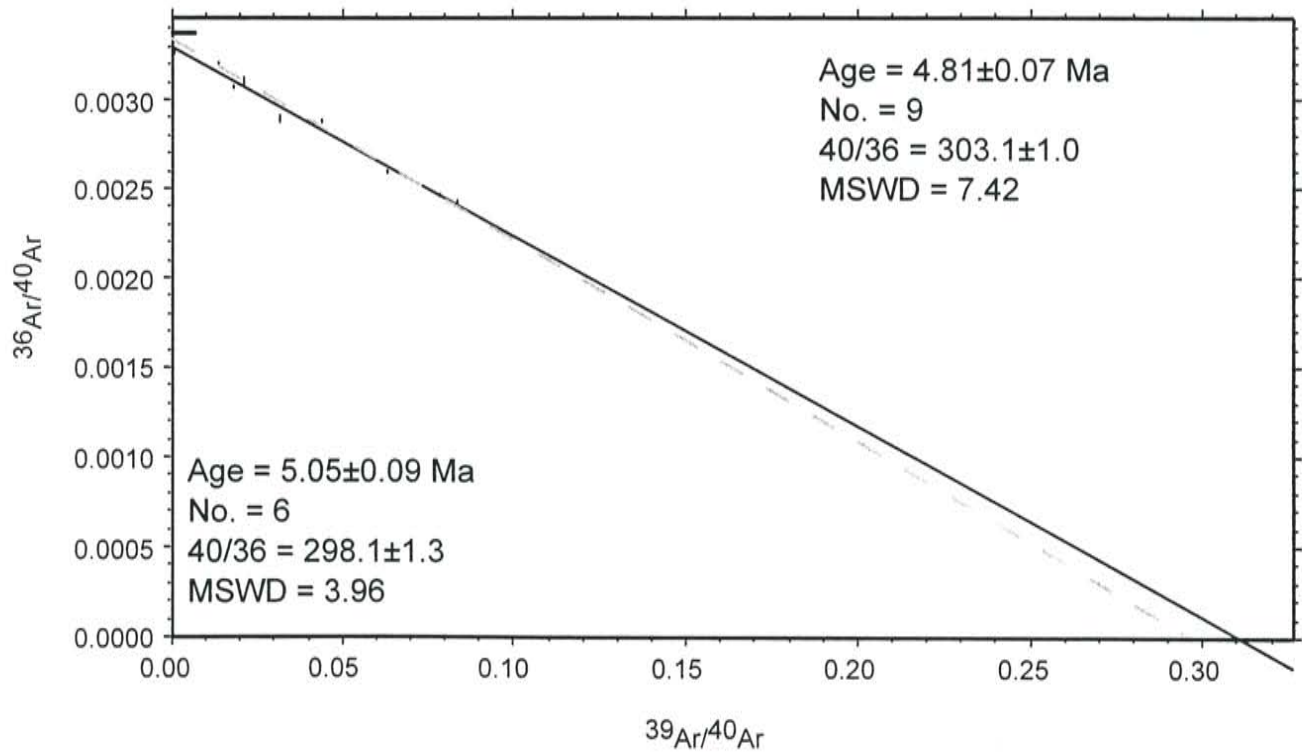
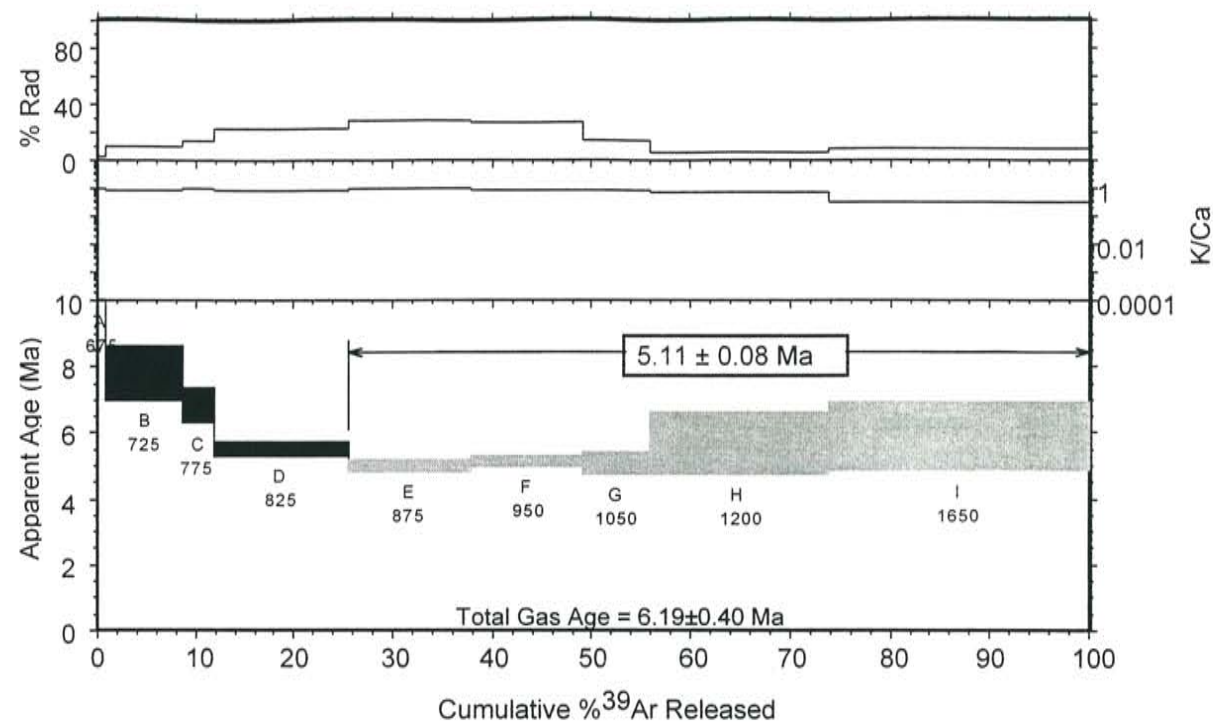
RA-084, pyroxene dacite, Ute Mtn., groundmass concentrate



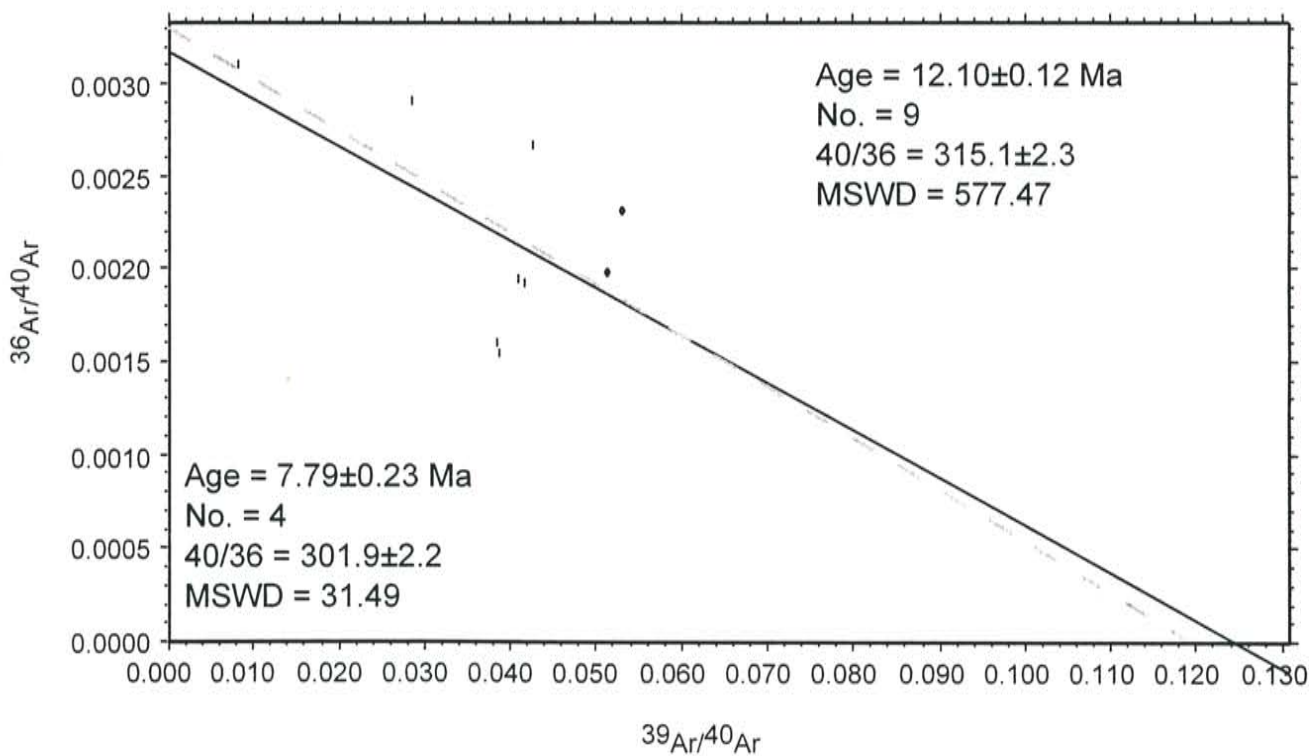
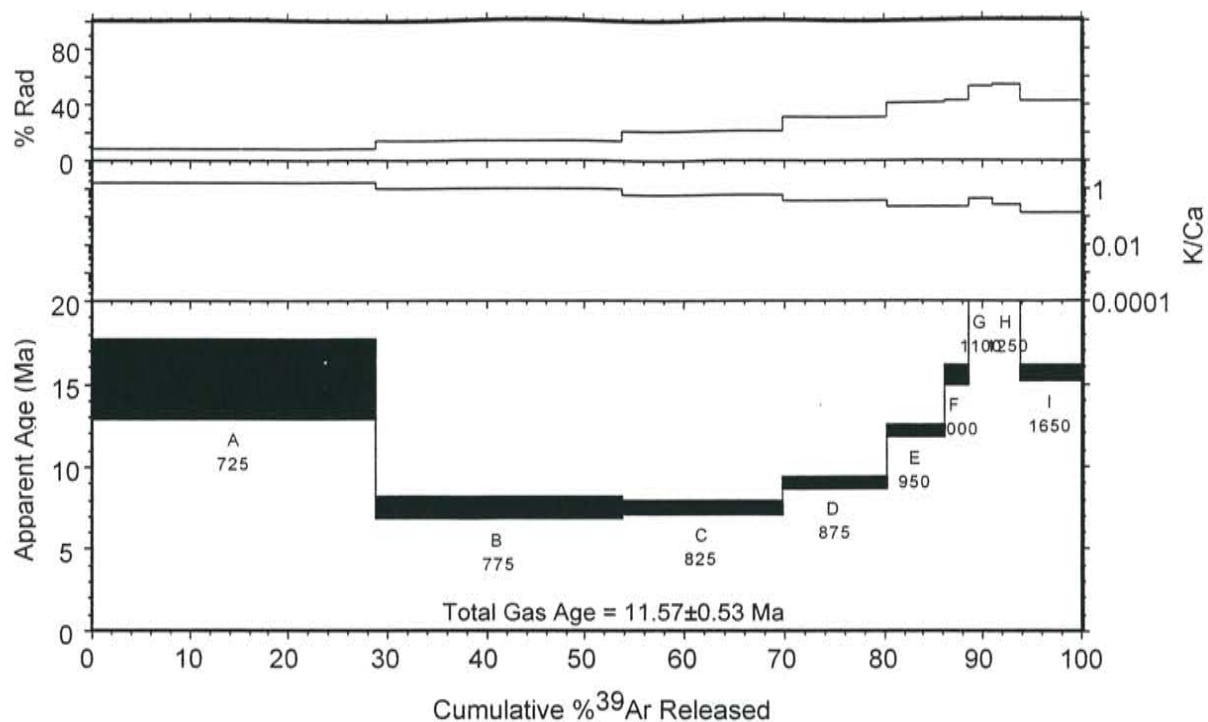
RA-085, pyroxene dacite, Guadalupe Mt., groundmass concentrate



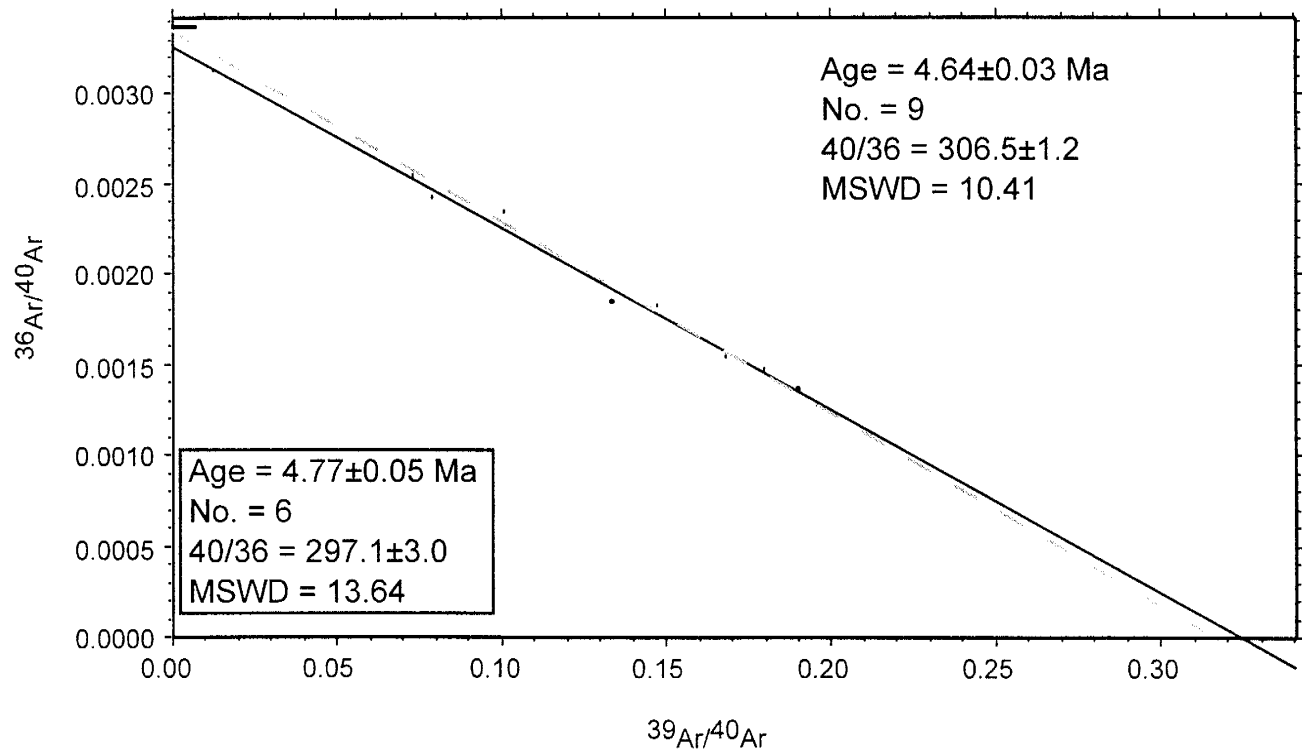
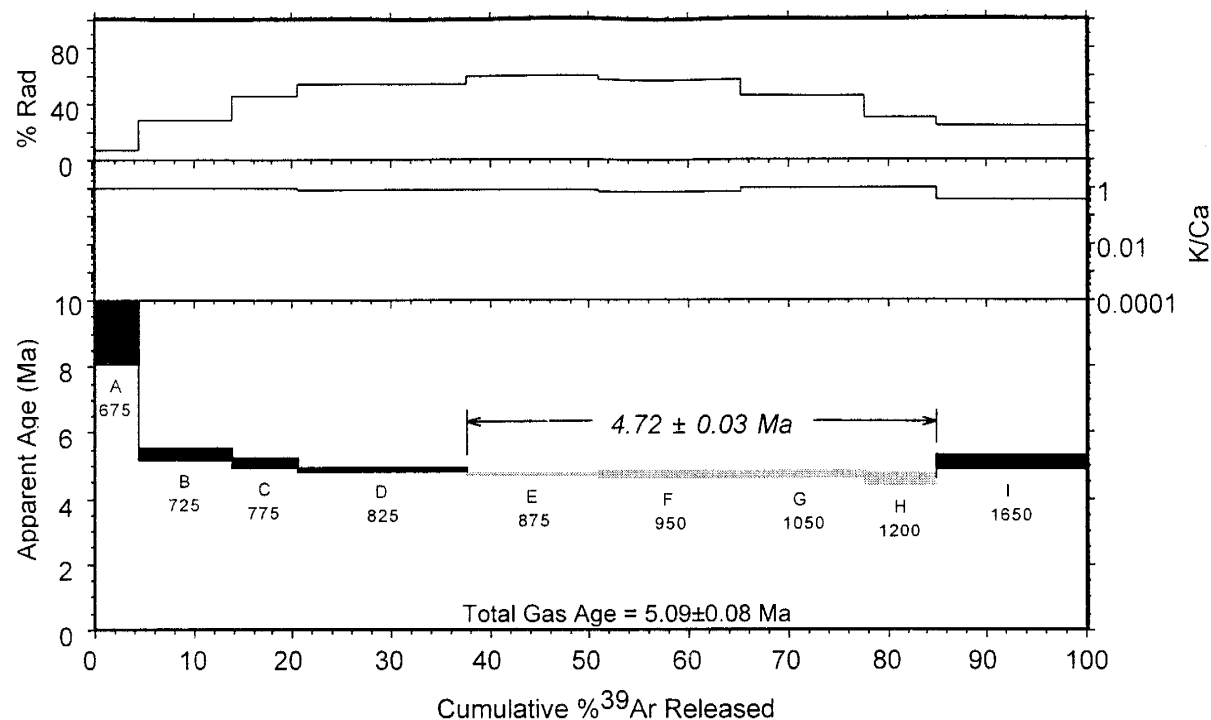
RA-086, pyroxene dacite, Guadelupe Mt., groundmass concentrate



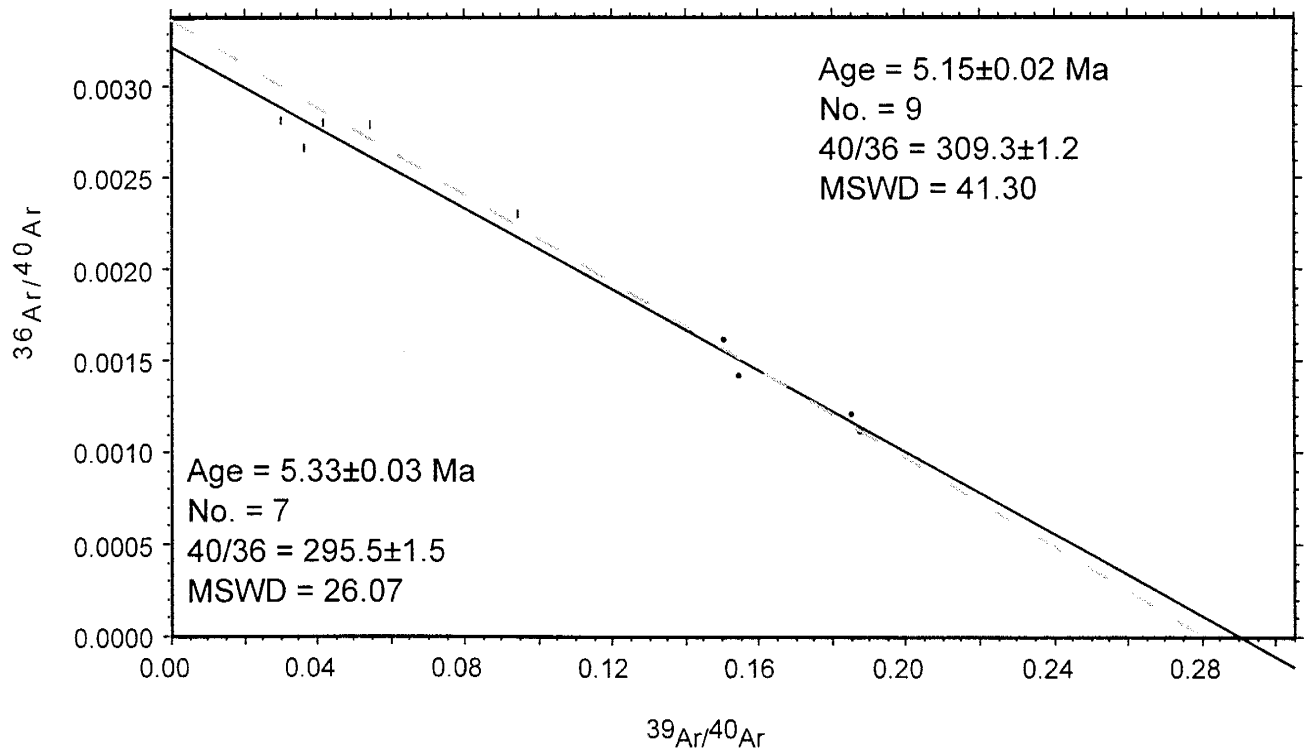
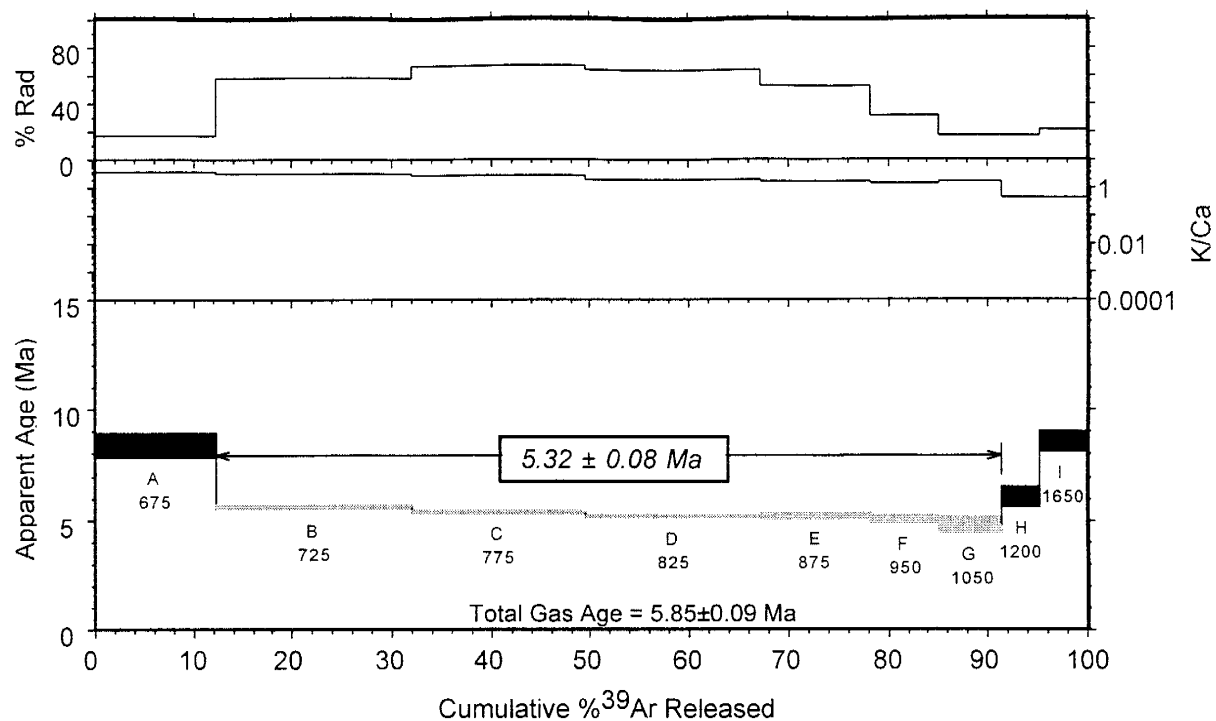
RA-087, pyroxene dacite, Guadelupe Mt., groundmass concentrate



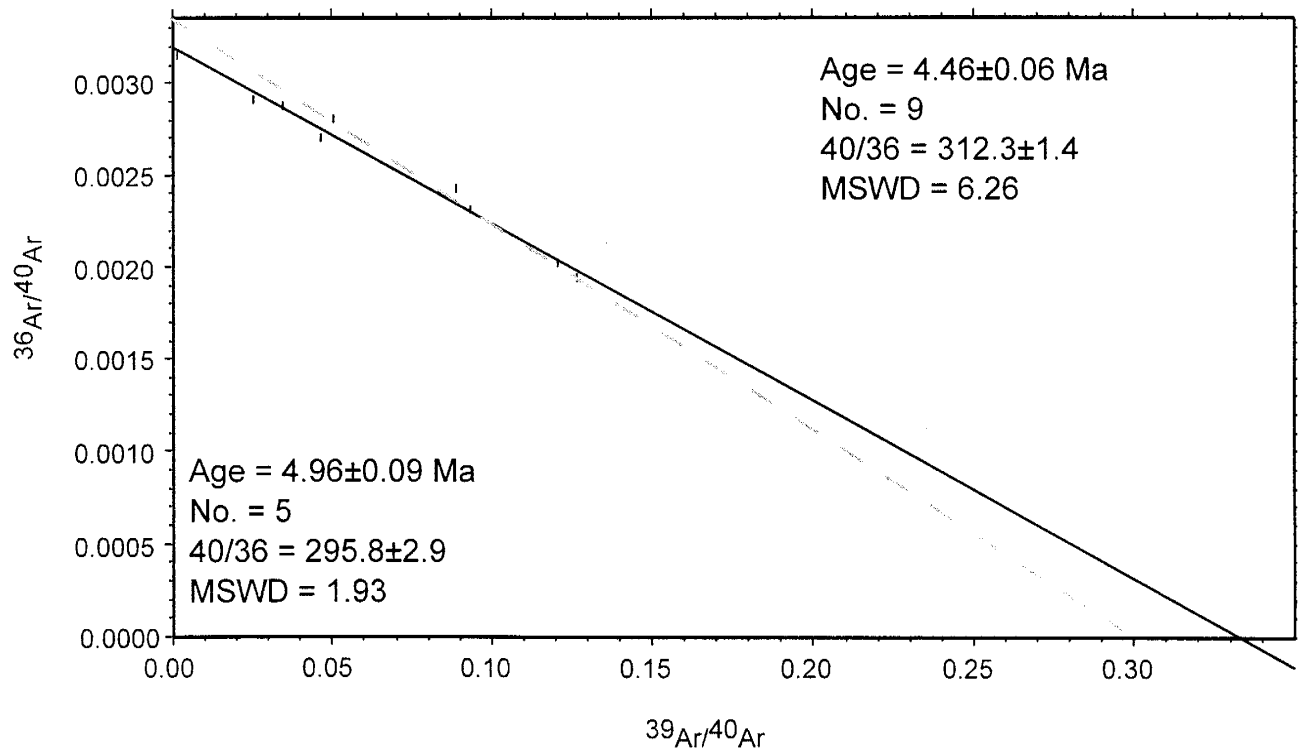
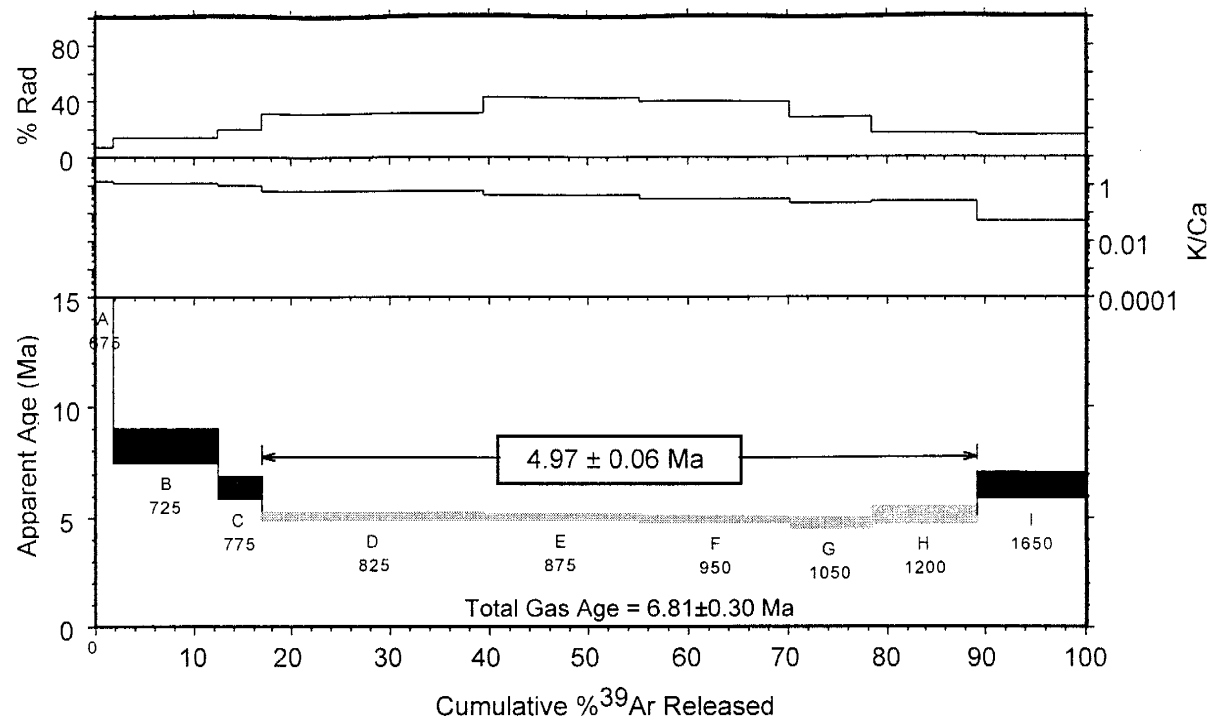
RA-088, pyroxene dacite, Cerro Negro roadcut, groundmass concentrate



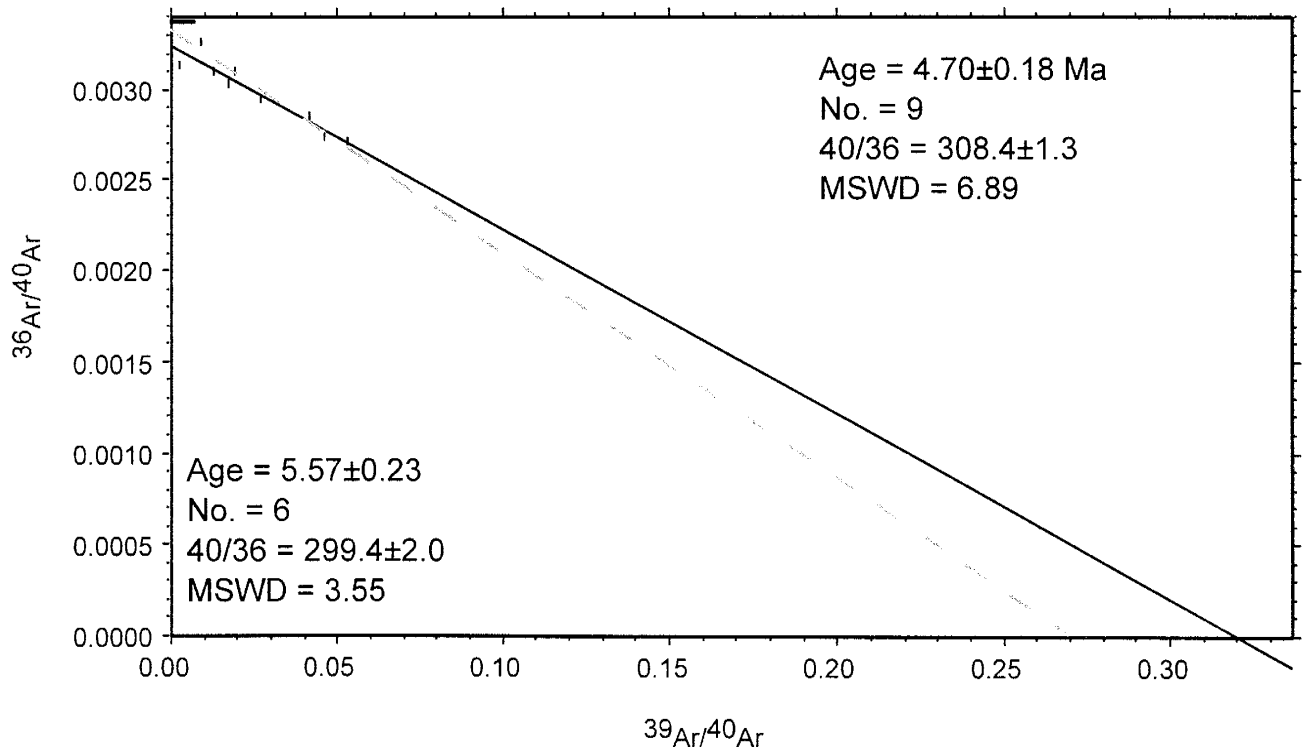
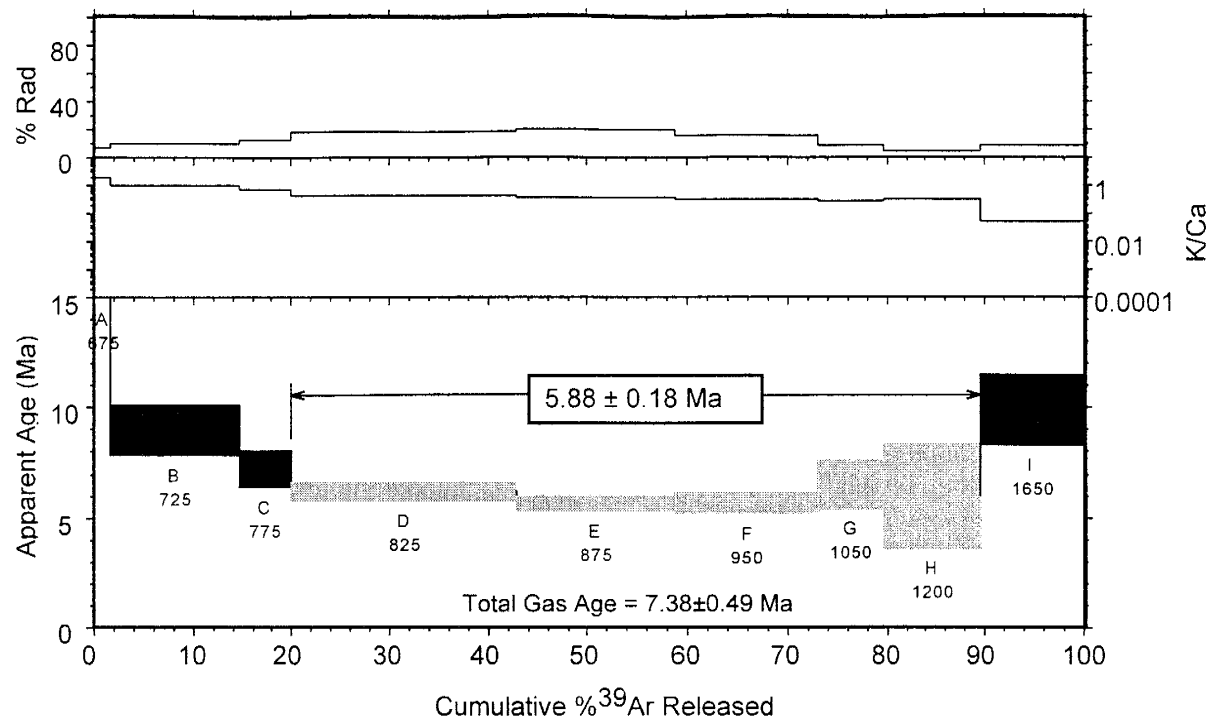
RA-089, quartz latite, Cerro Cheiflo, groundmass concentrate



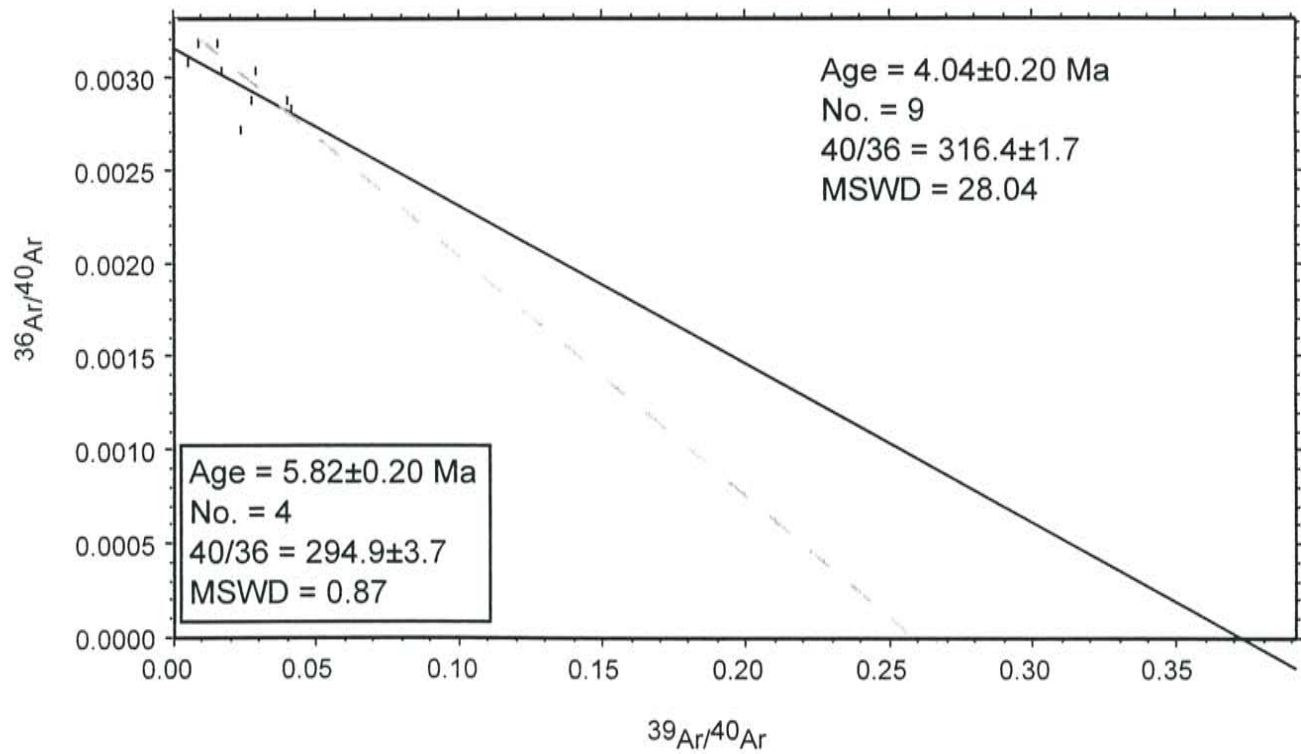
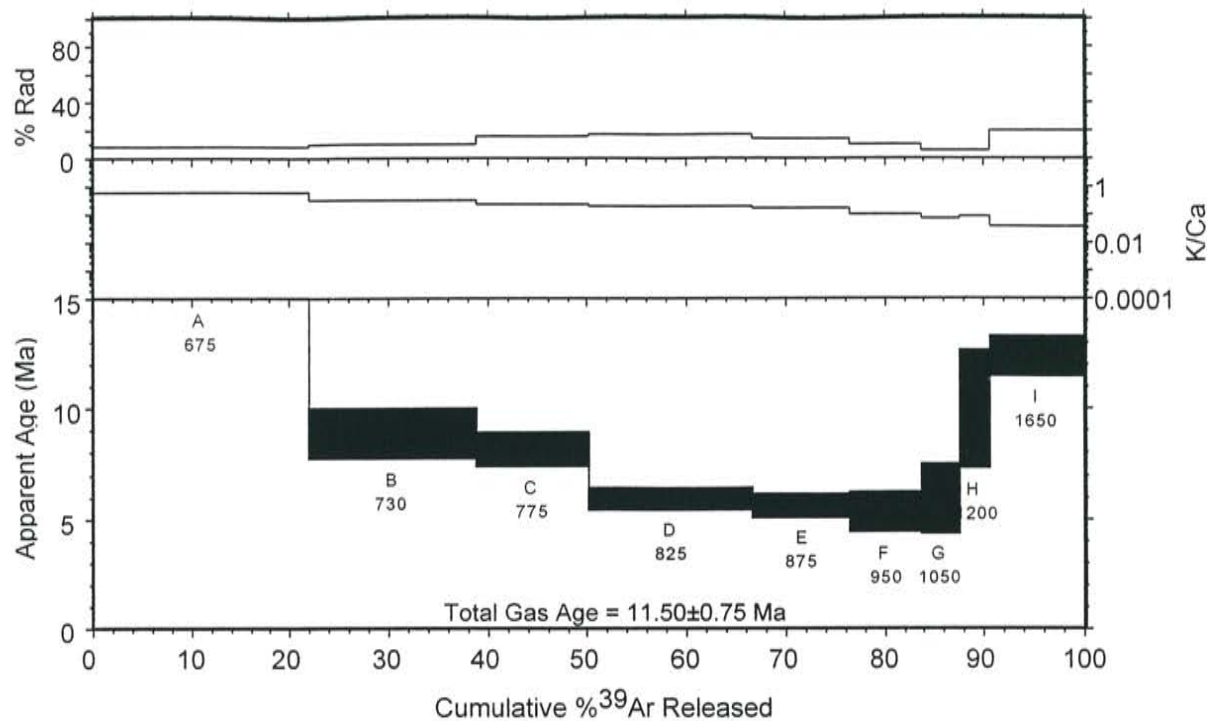
RA-090, olivine andesite, Cerro de la Olla, groundmass concentrate



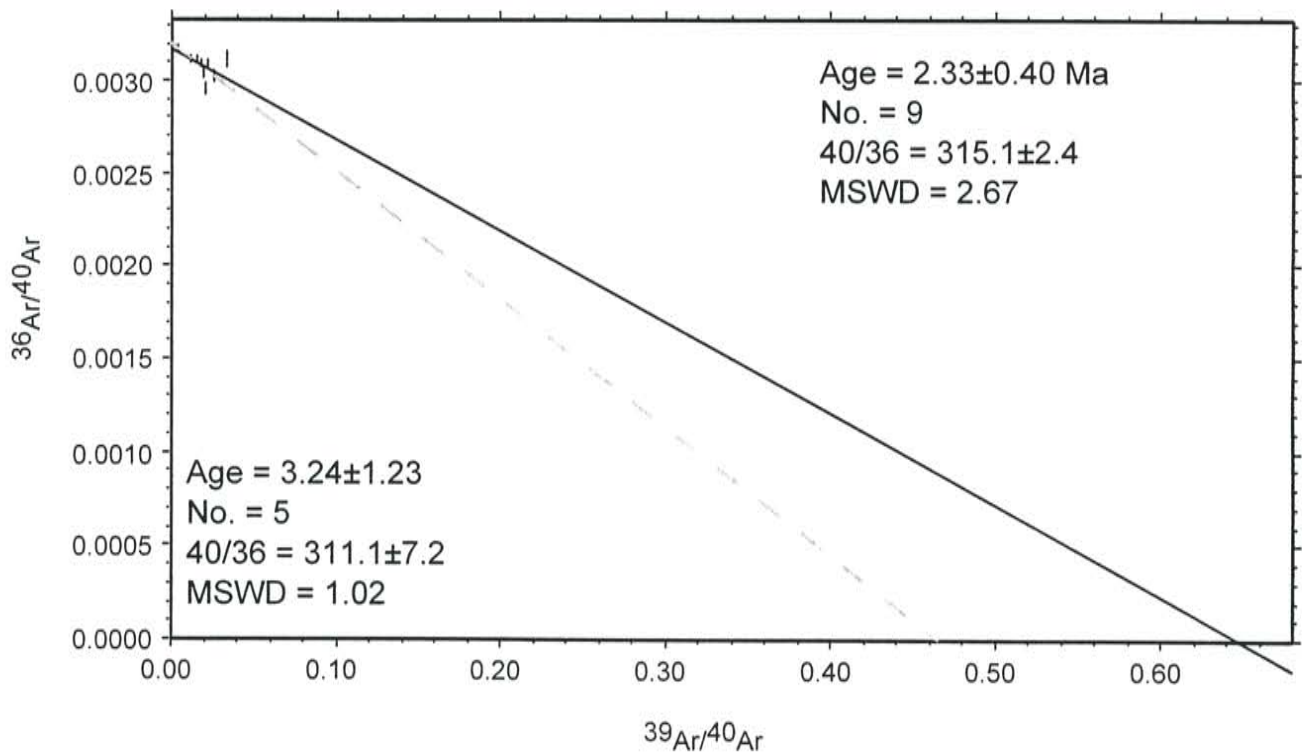
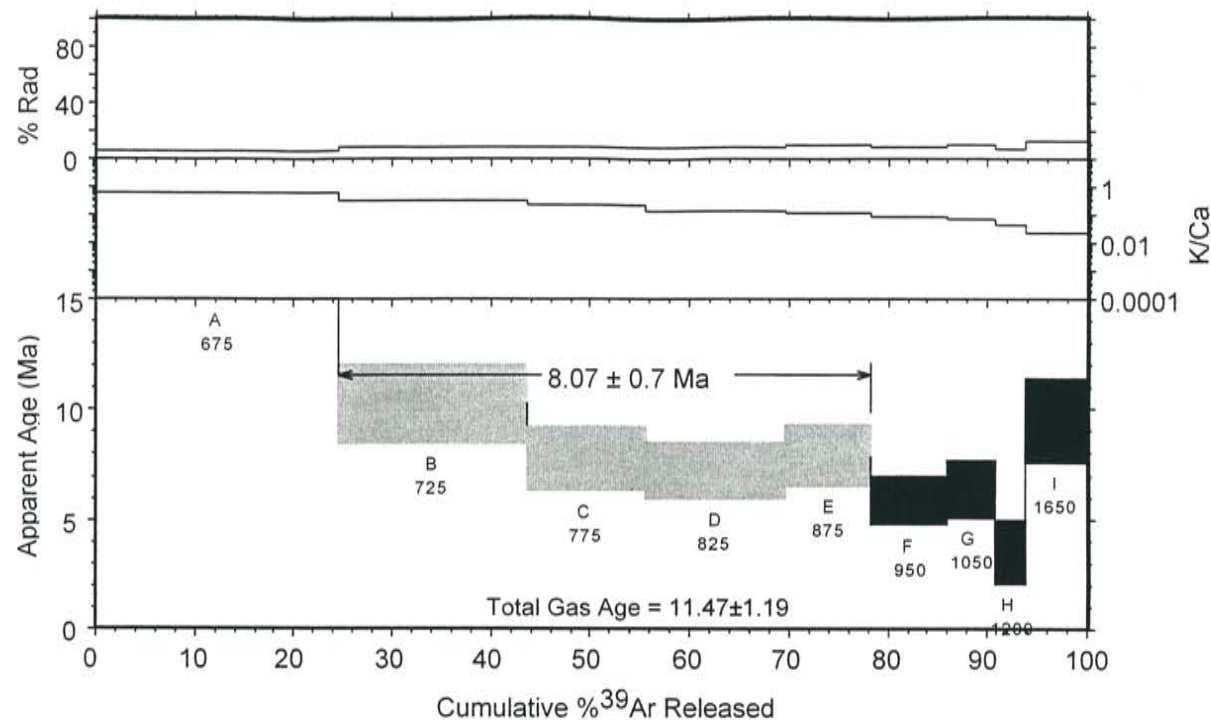
RA-091, olivine andesite, Cerro Montoso, groundmass concentrate



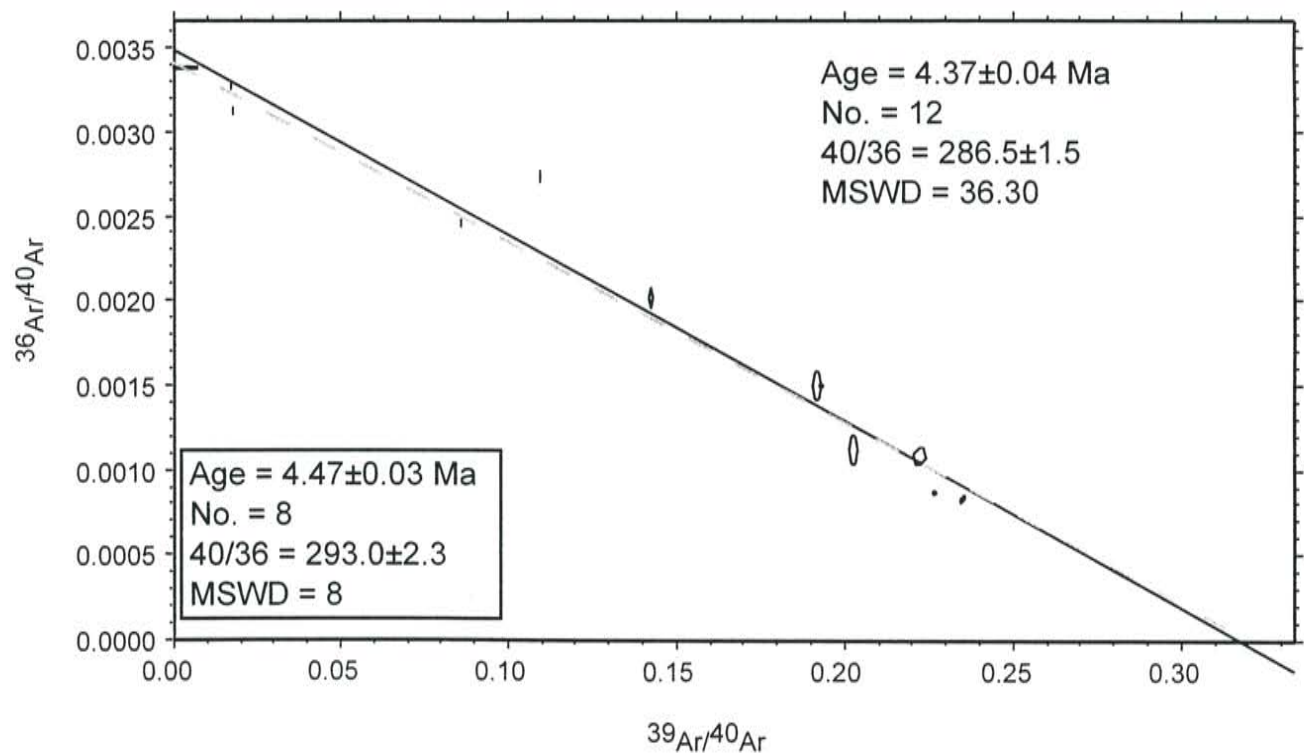
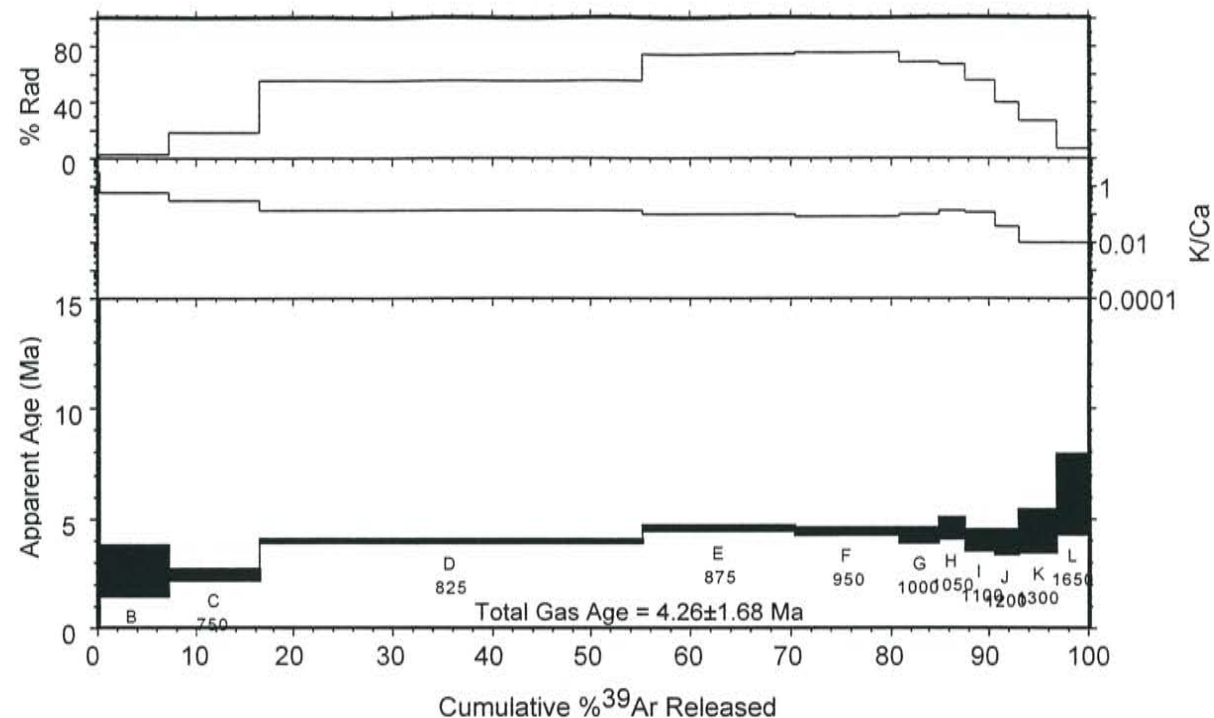
RA-092, basaltic andesite, Cerro Montoso area, groundmass concentrate



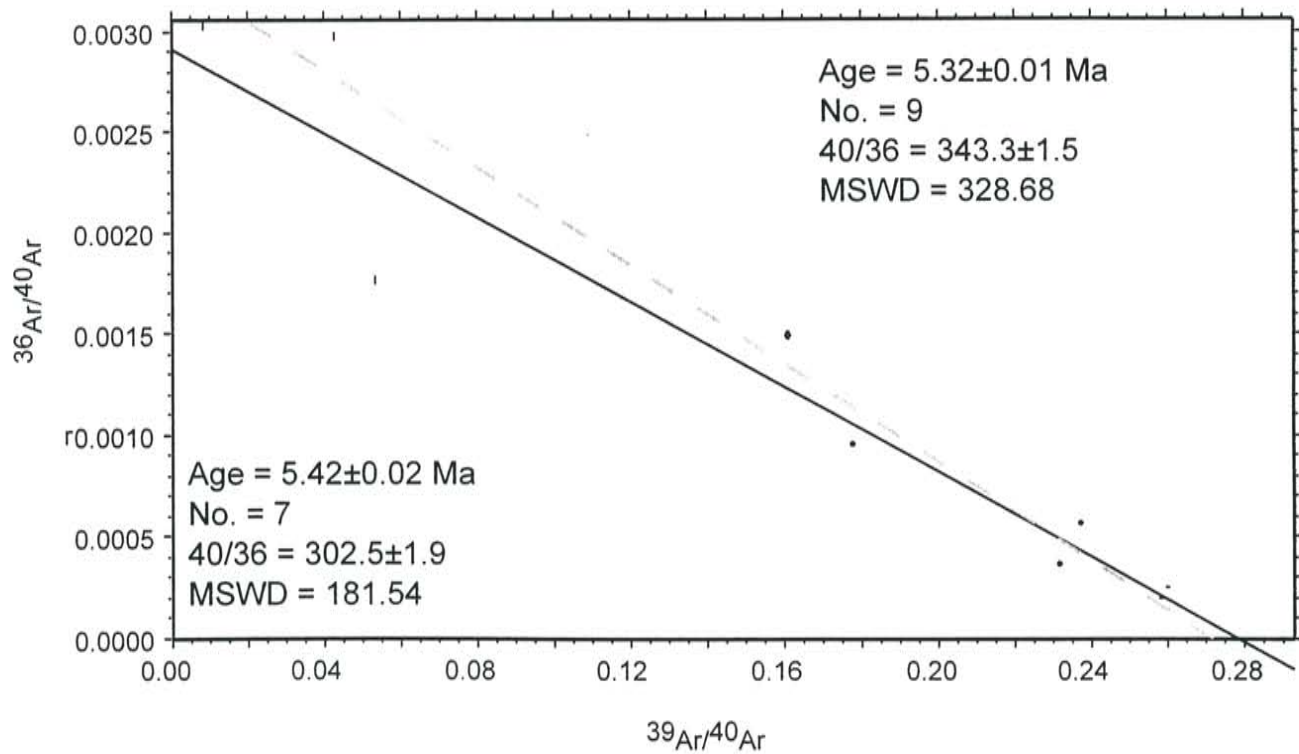
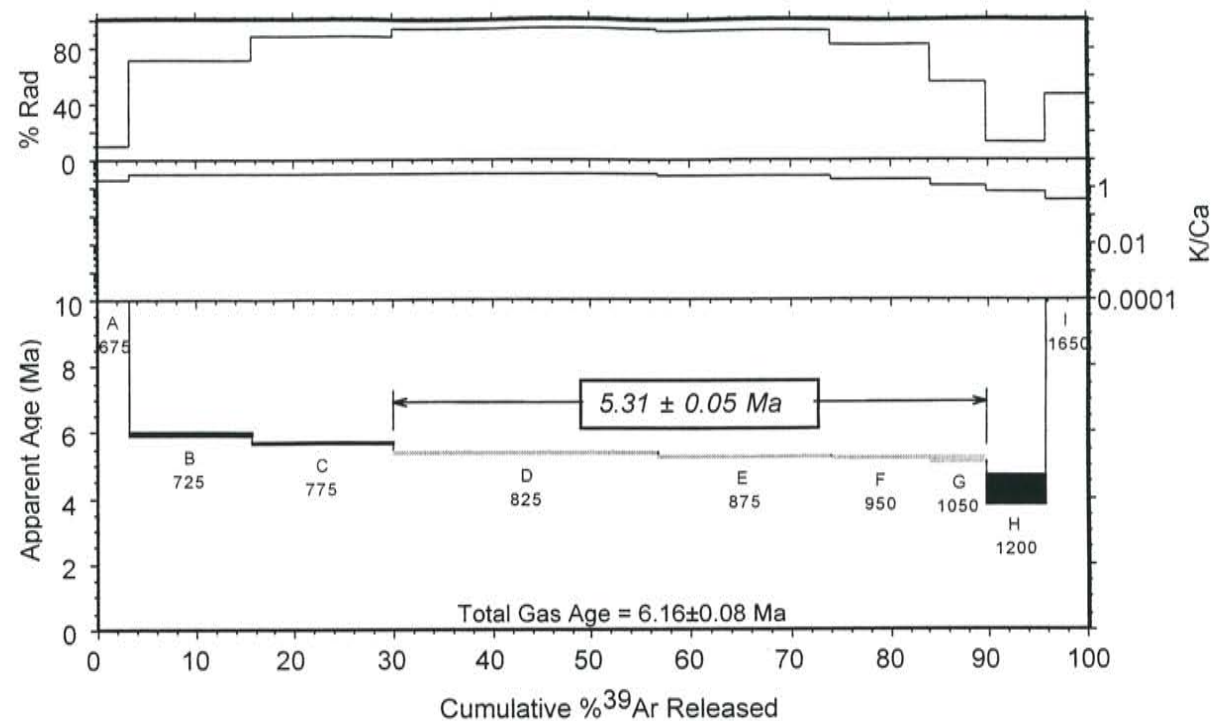
RA-093, basaltic andesite, Cerro Montosa area, groundmass concentrate



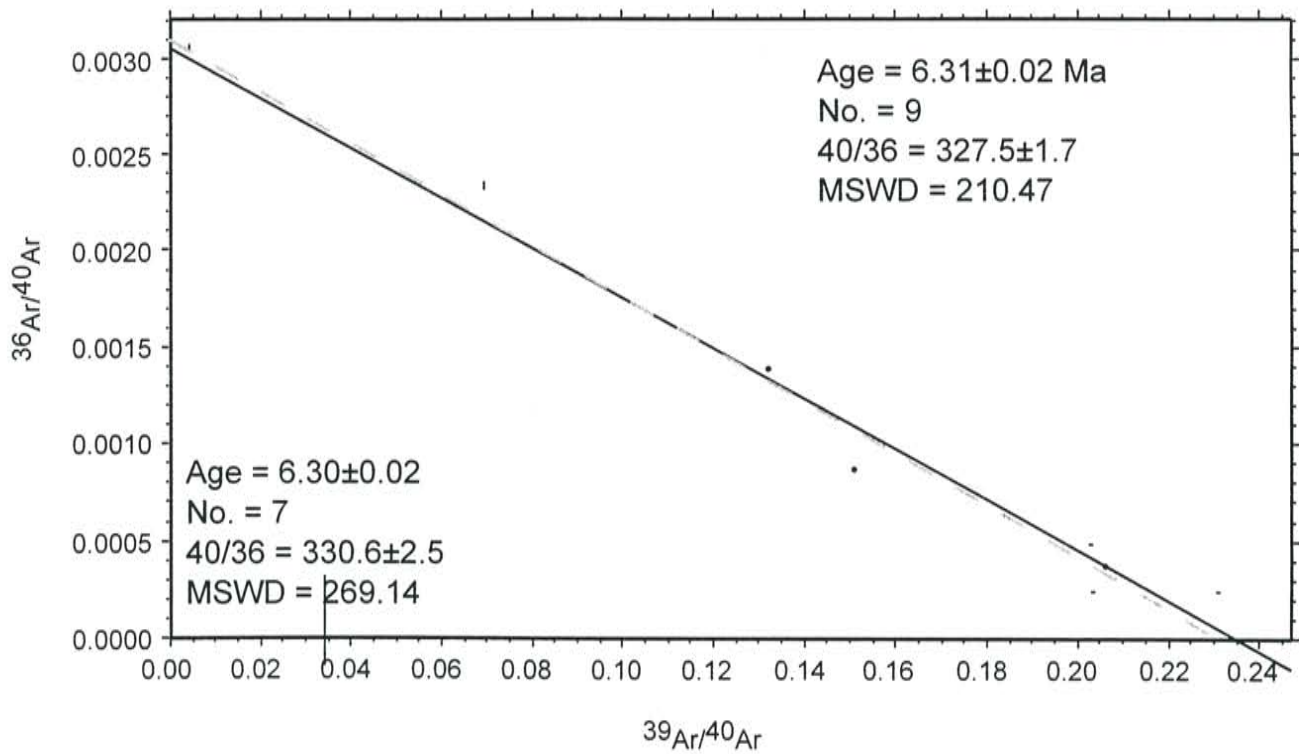
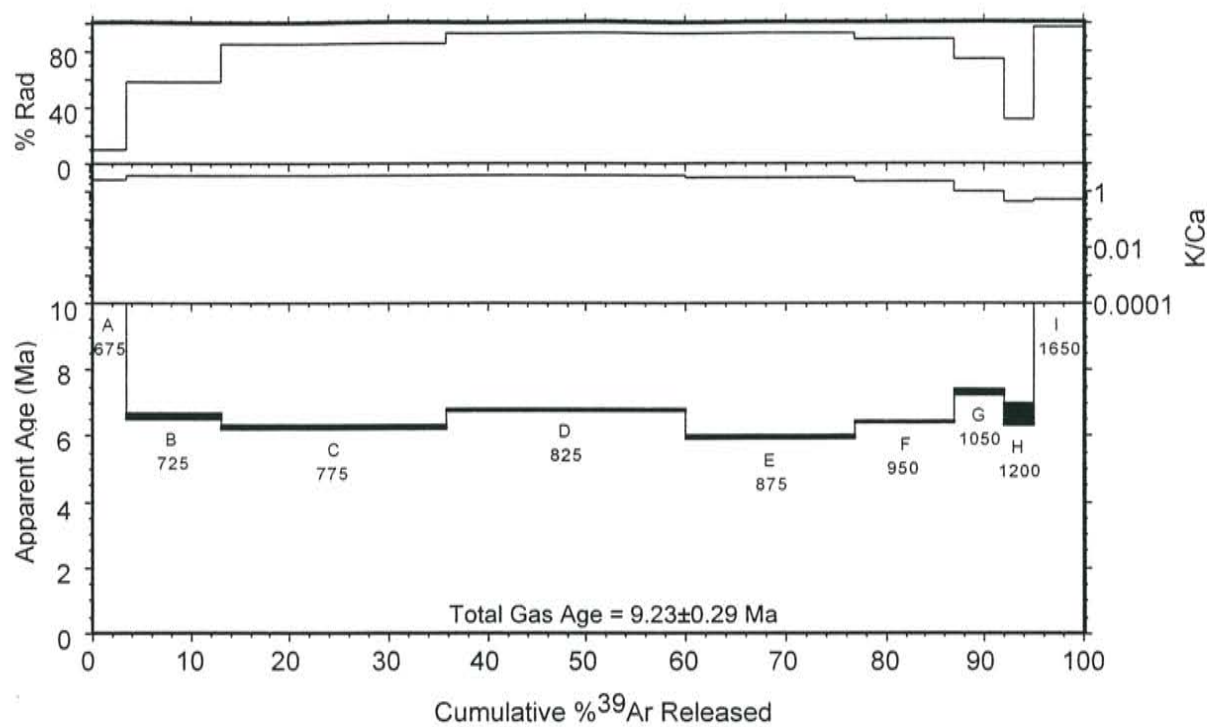
RA-102, basaltic andesite, Cerro Chiflo area, groundmass concentrate



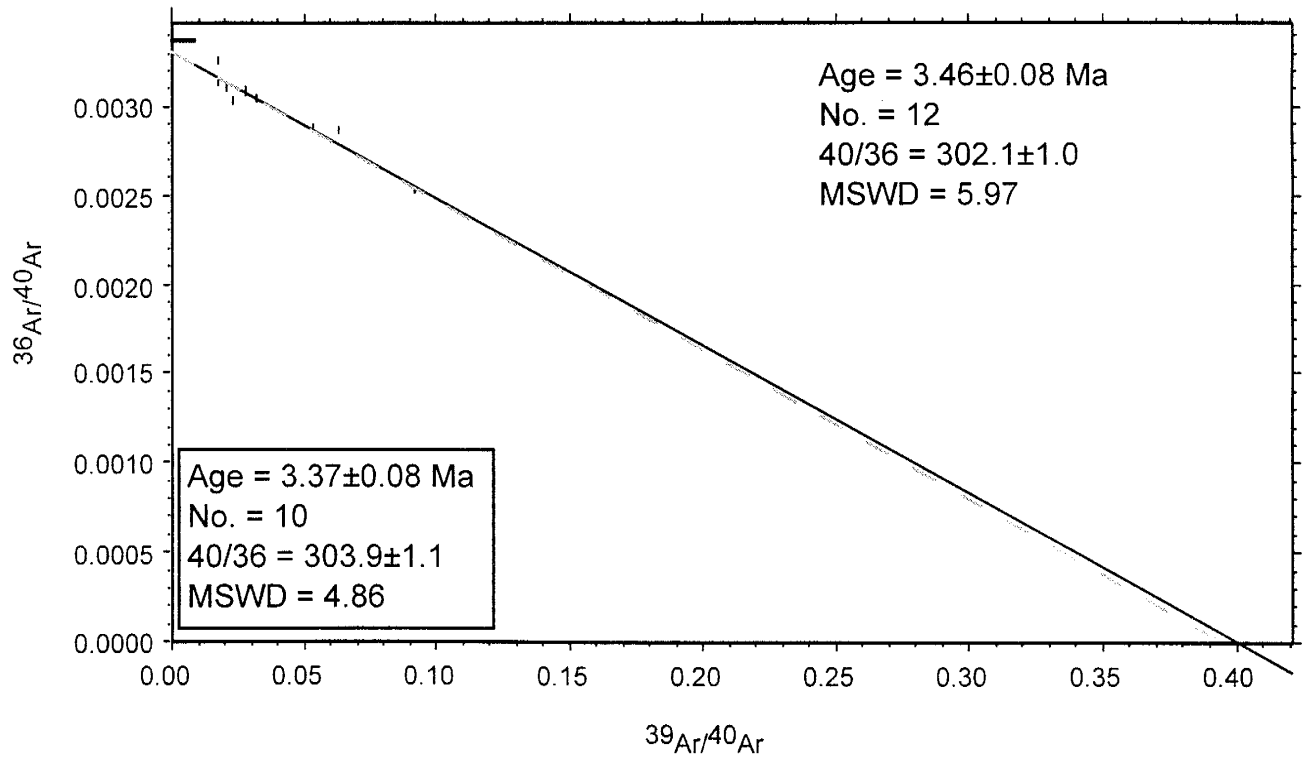
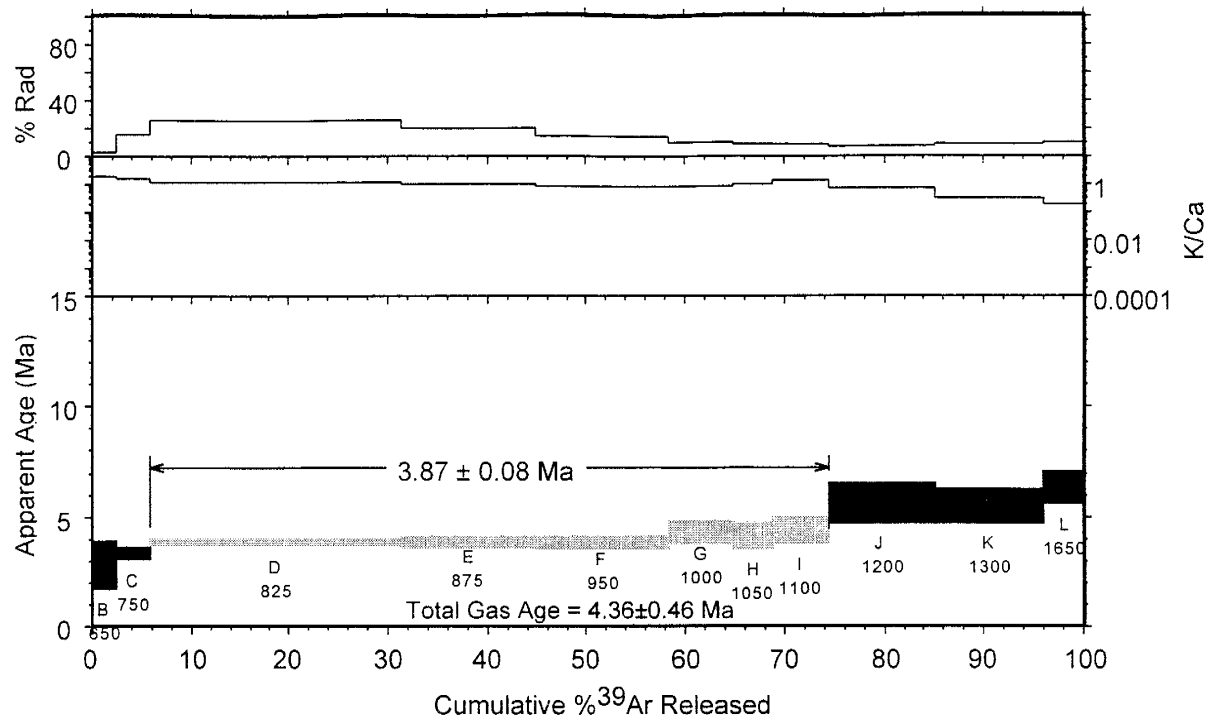
RA-103, quartz latite, Cerro Chiflo, groundmass concentrate



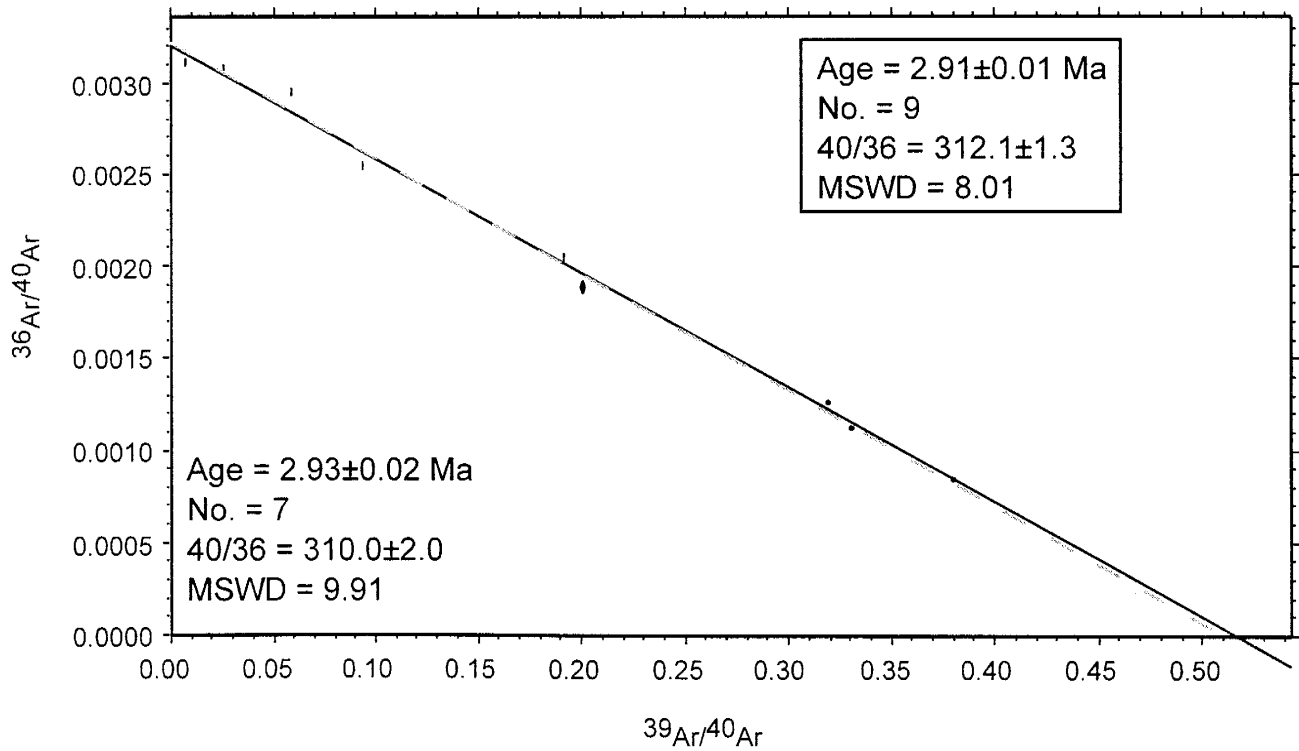
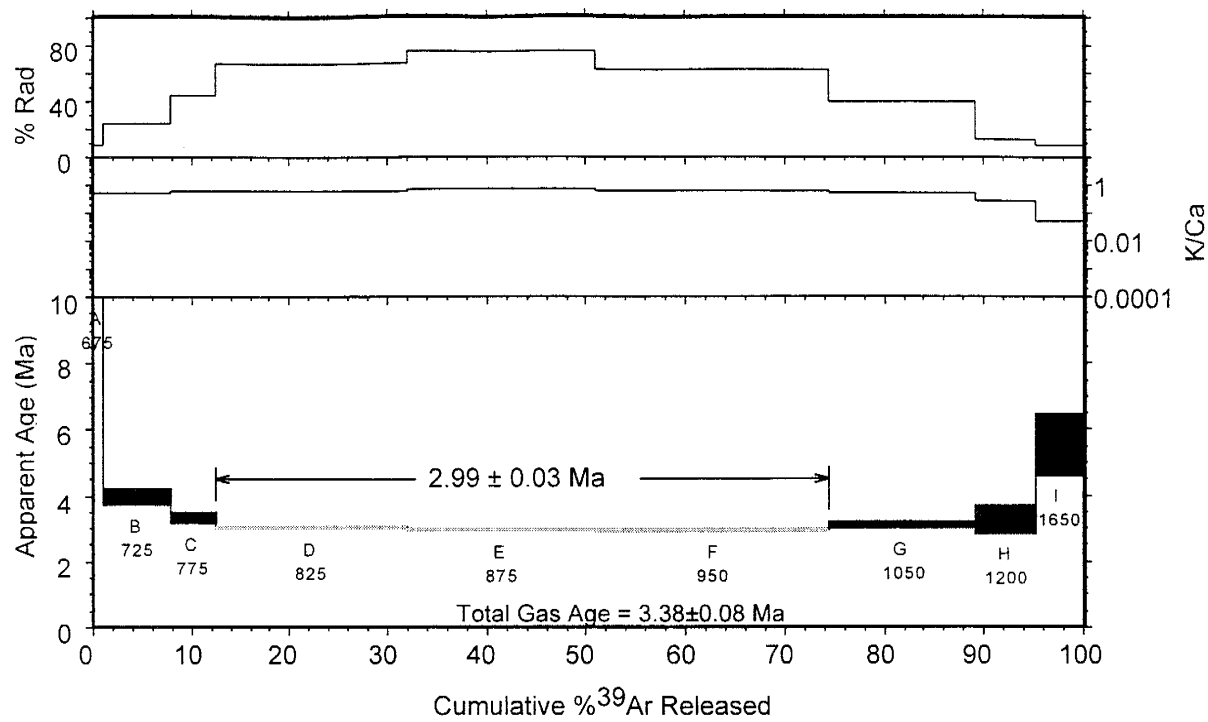
RA-104, quartz latite, Cerro Chiflo, groundmass concentrate



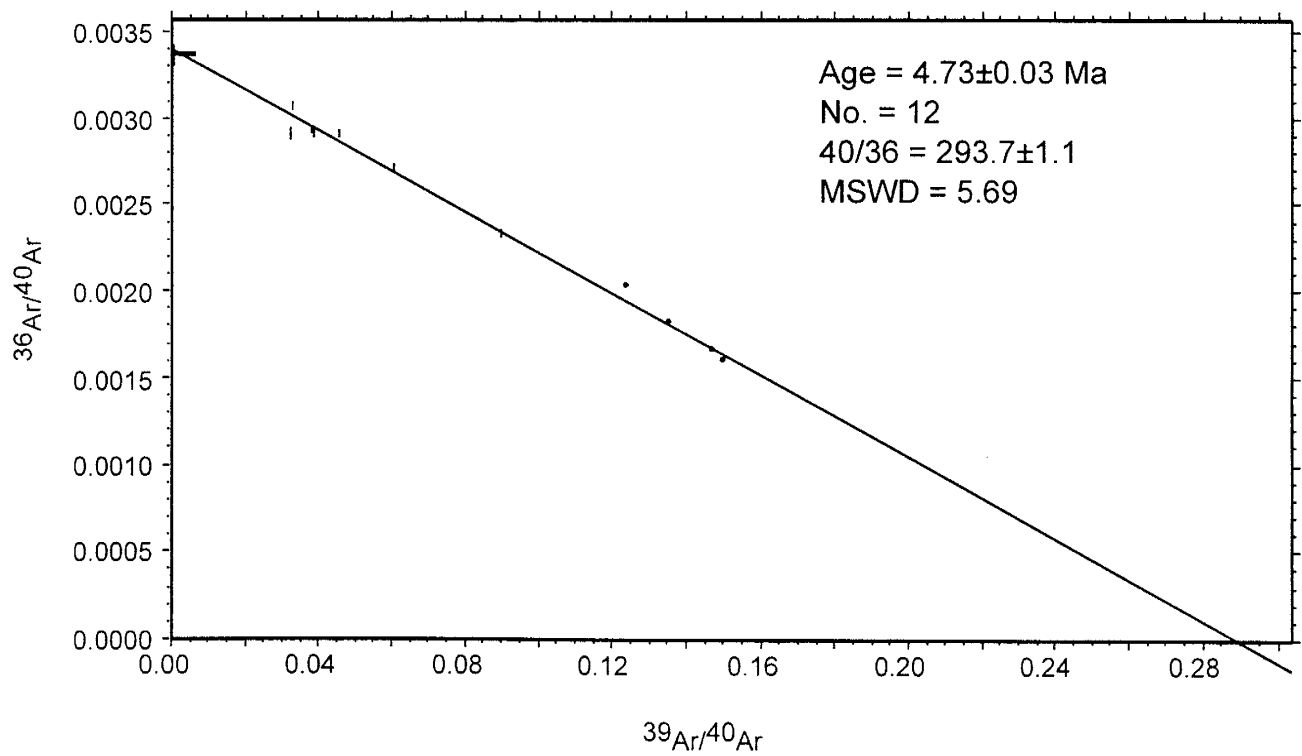
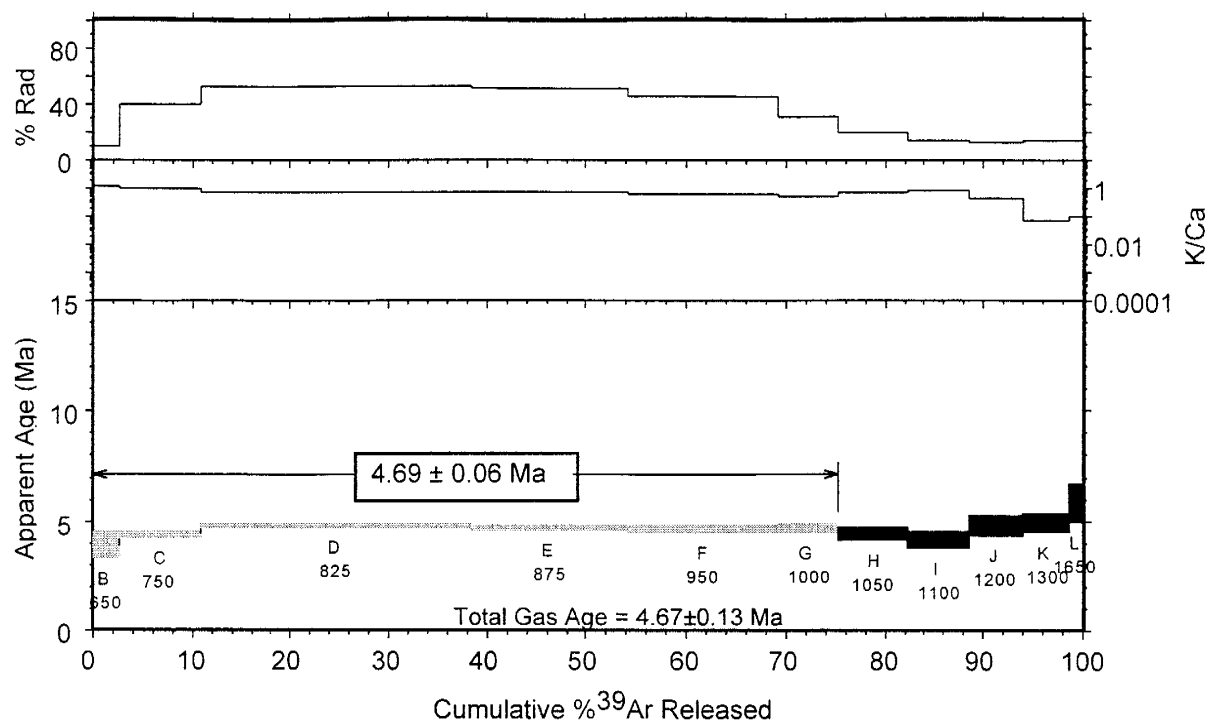
RA-107, basaltic andesite, No Aguia Peaks area, groundmass concentrate



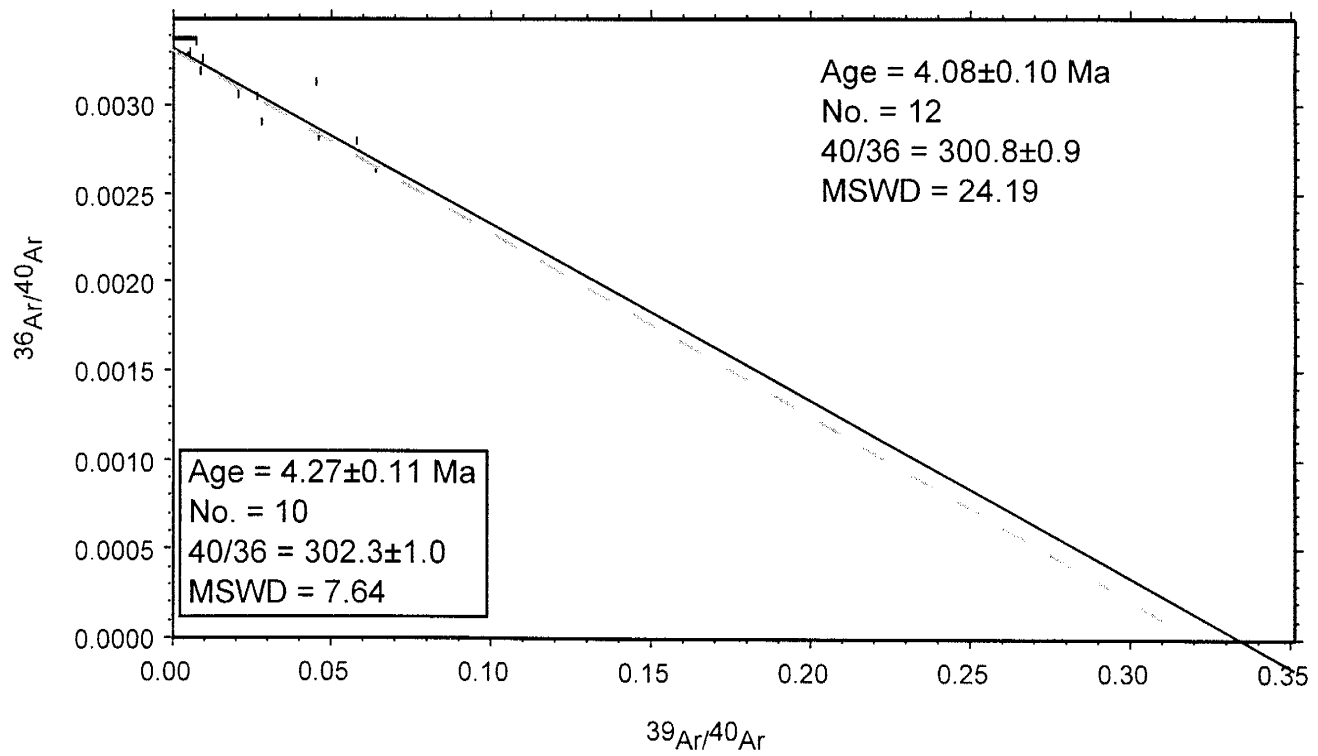
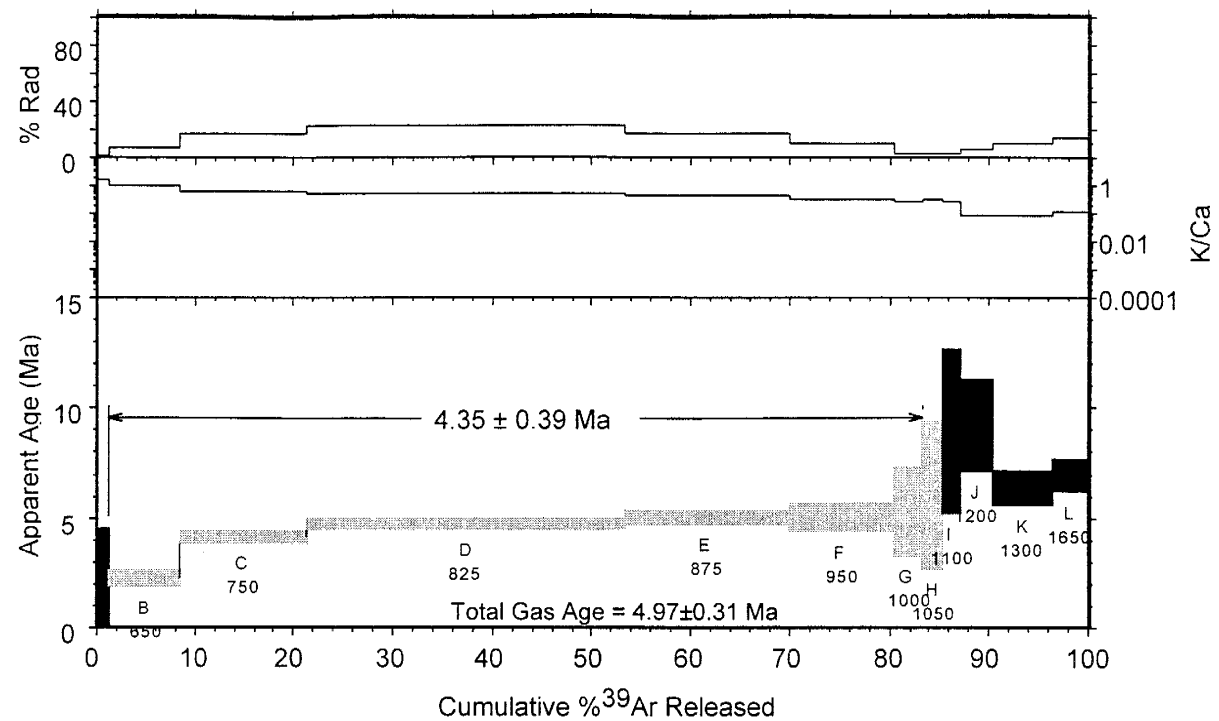
RA-109, basaltic andesite, Red Hill, groundmass concentrate



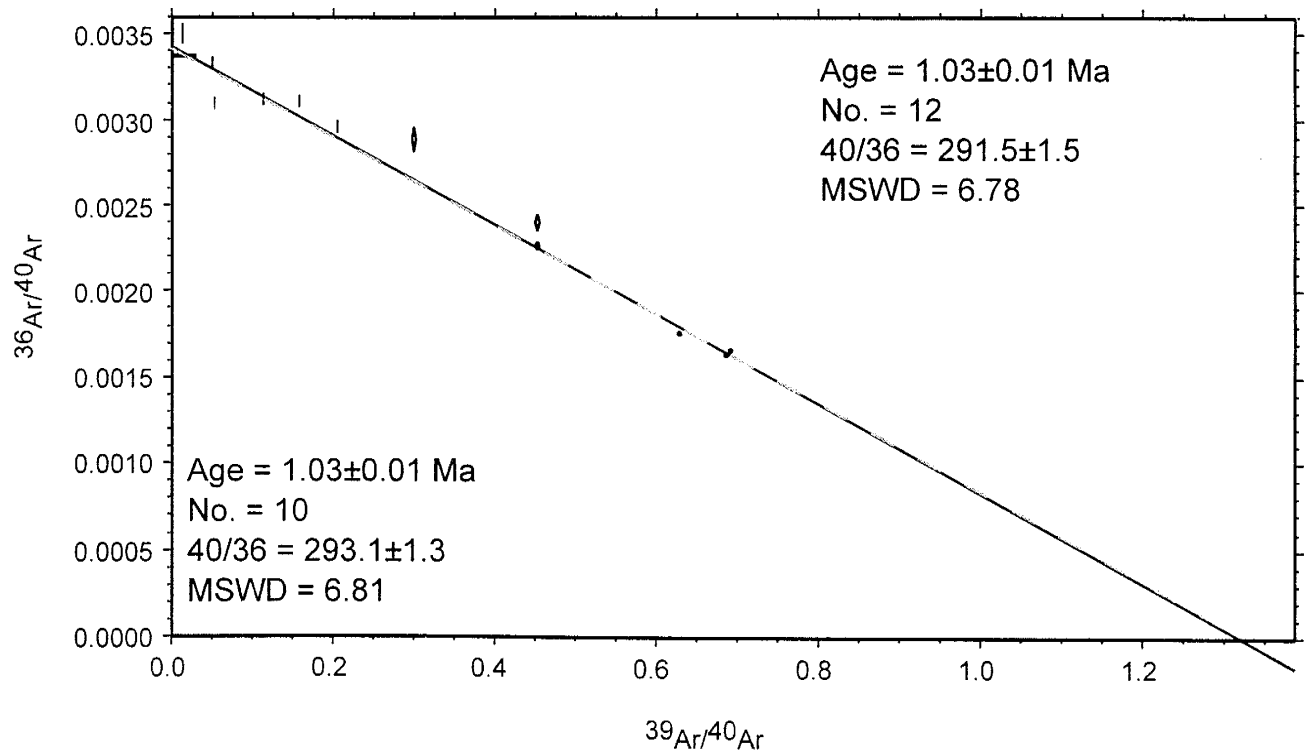
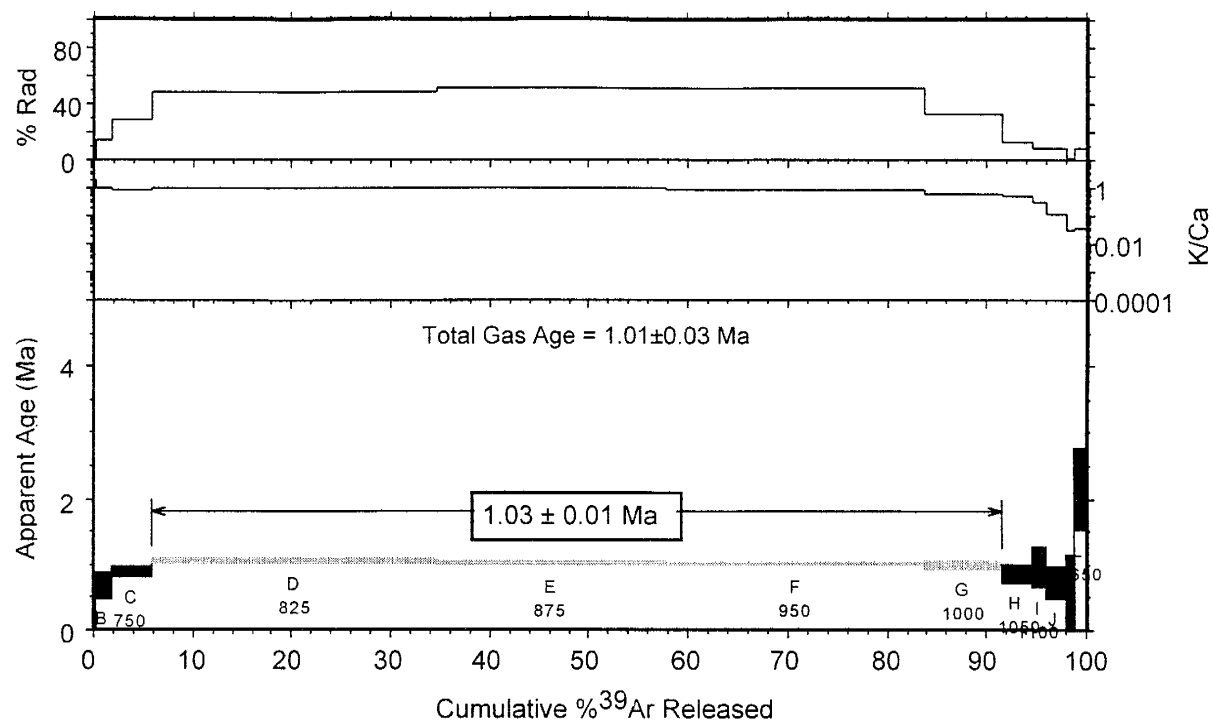
RA-112, pyroxene dacite, Servilleta Plaza cone, groundmass concentrate



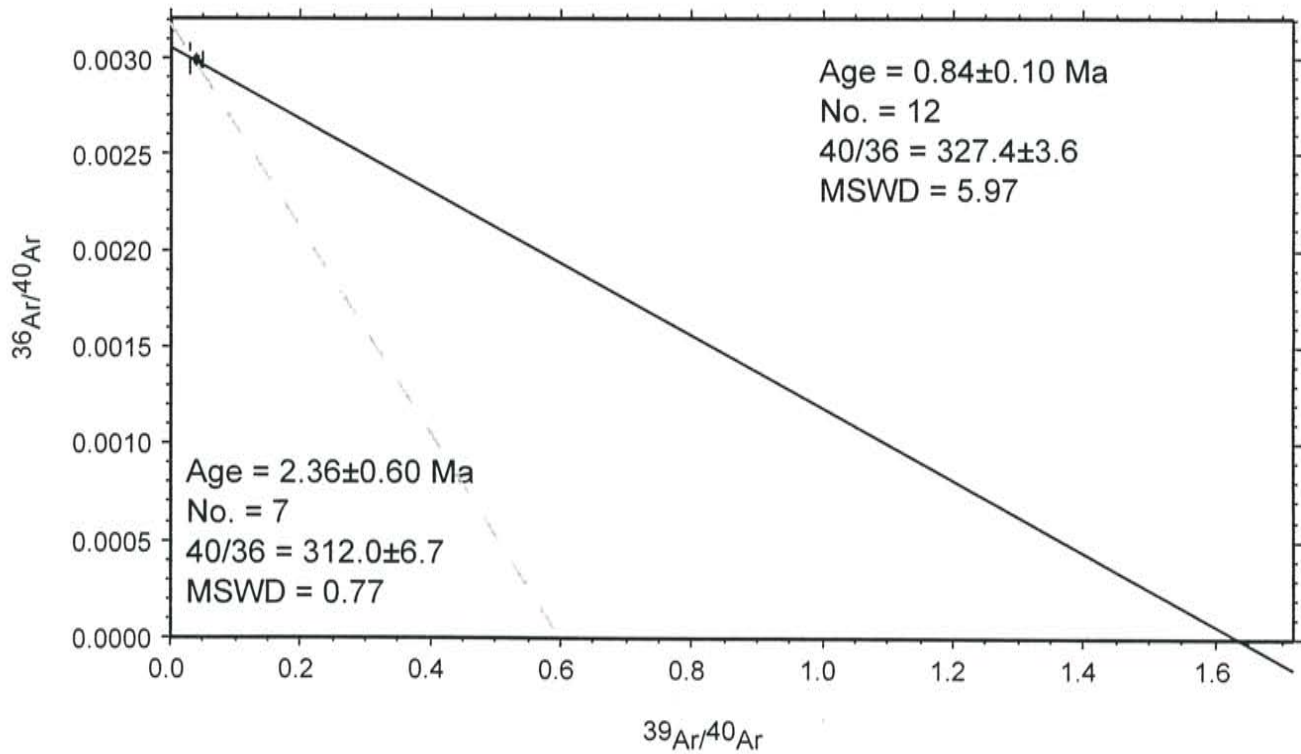
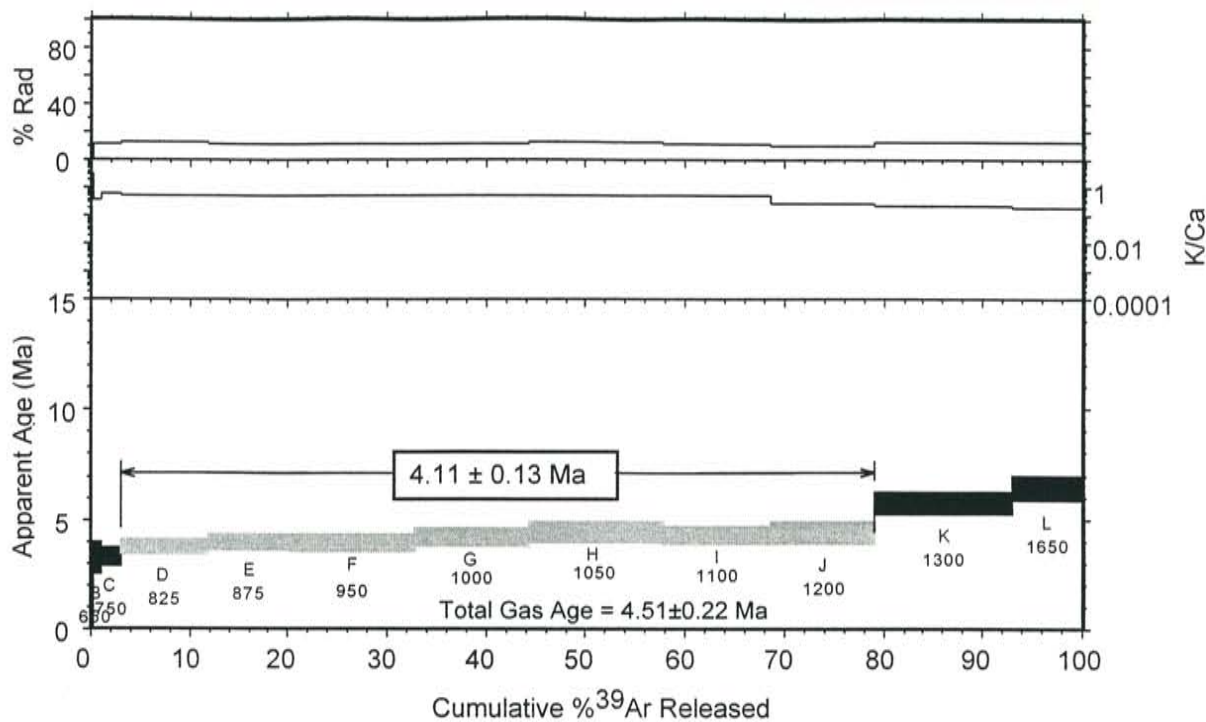
RA-113, pyroxene dacite, Servilleta Plaza cone, groundmass concentrate



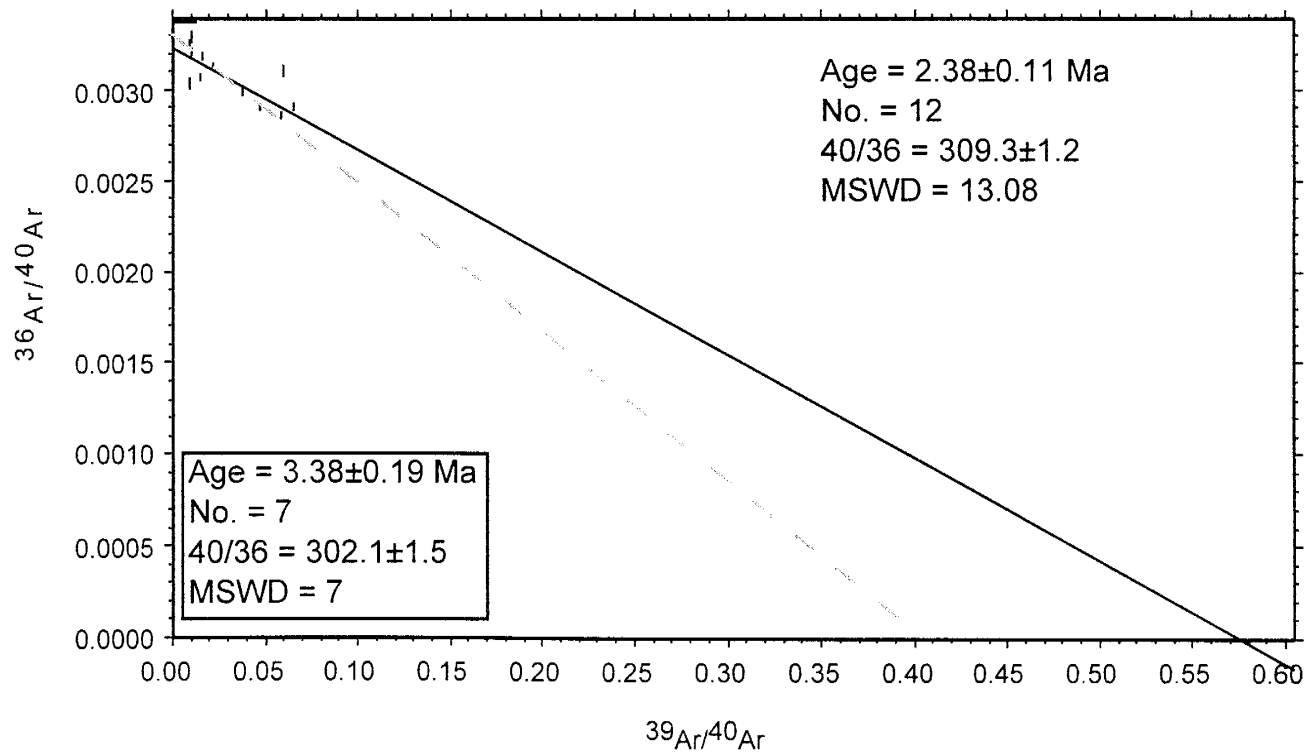
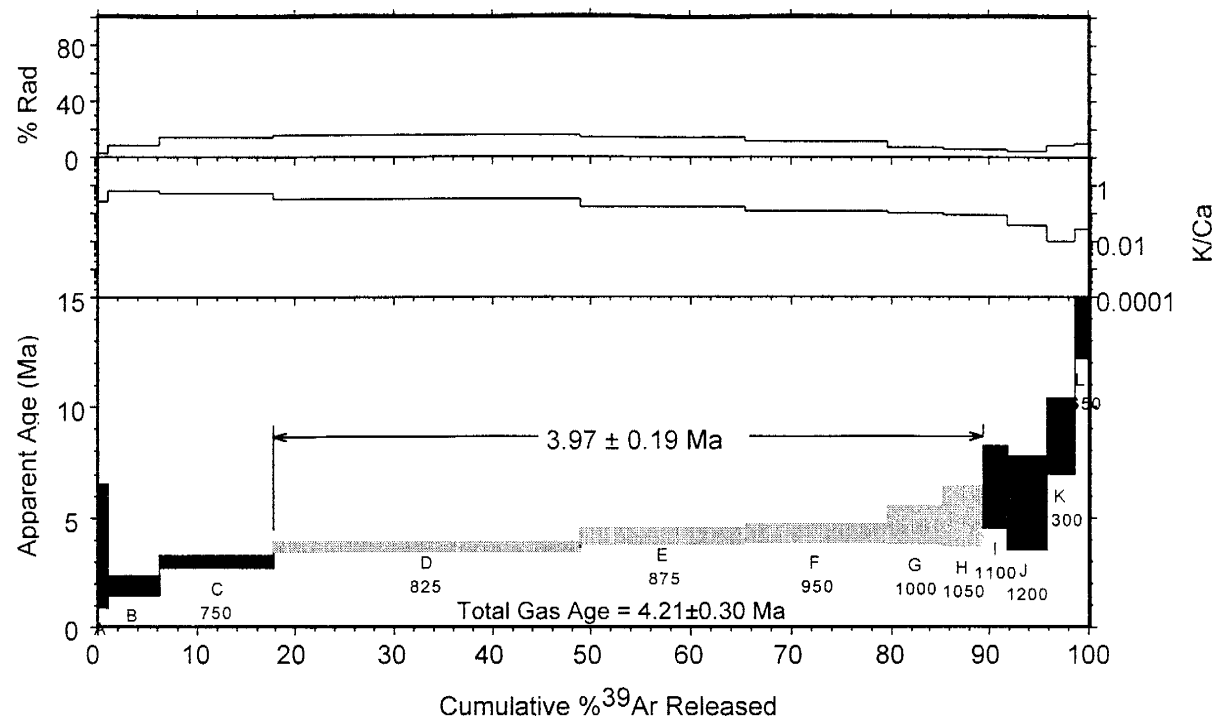
RA-114, basaltic andesite, Mesita vent, groundmass concentrate



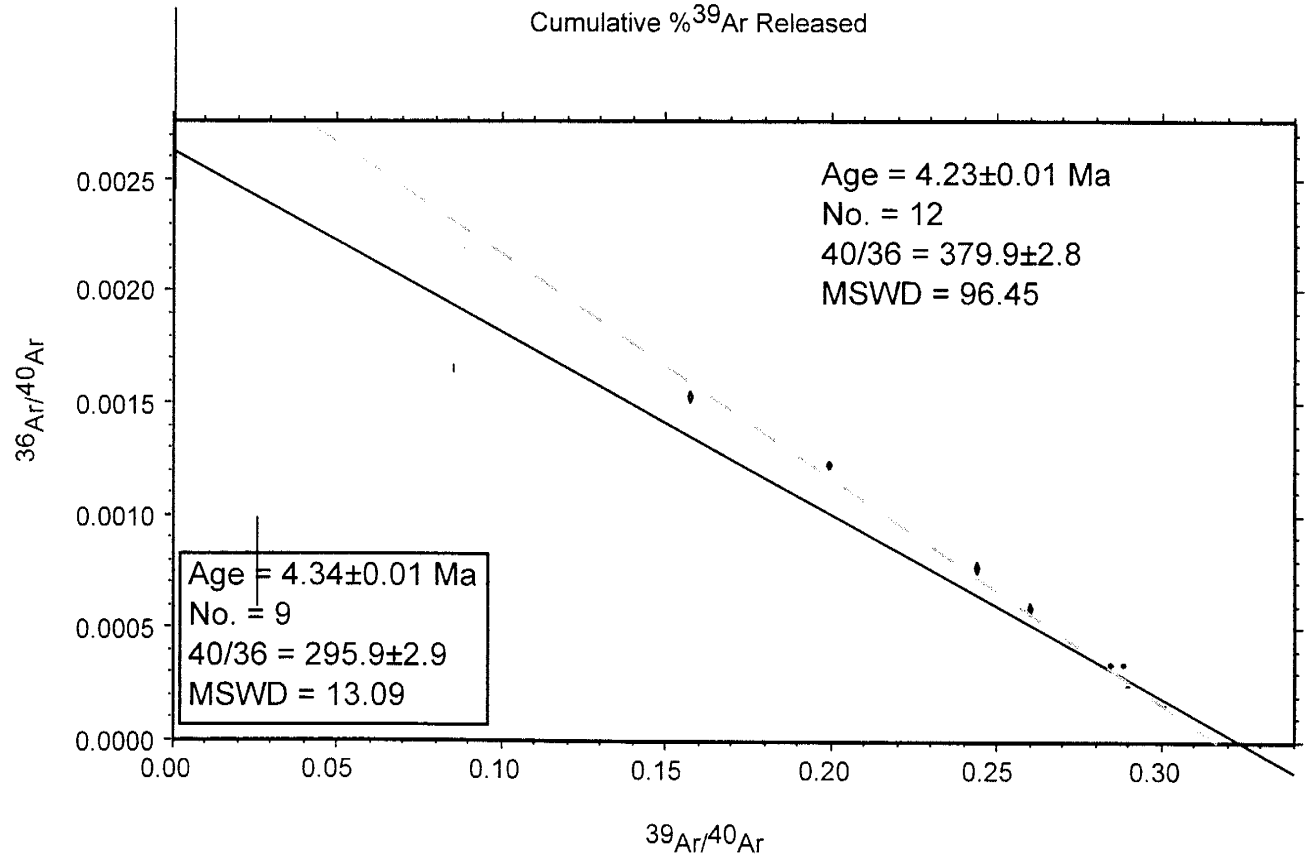
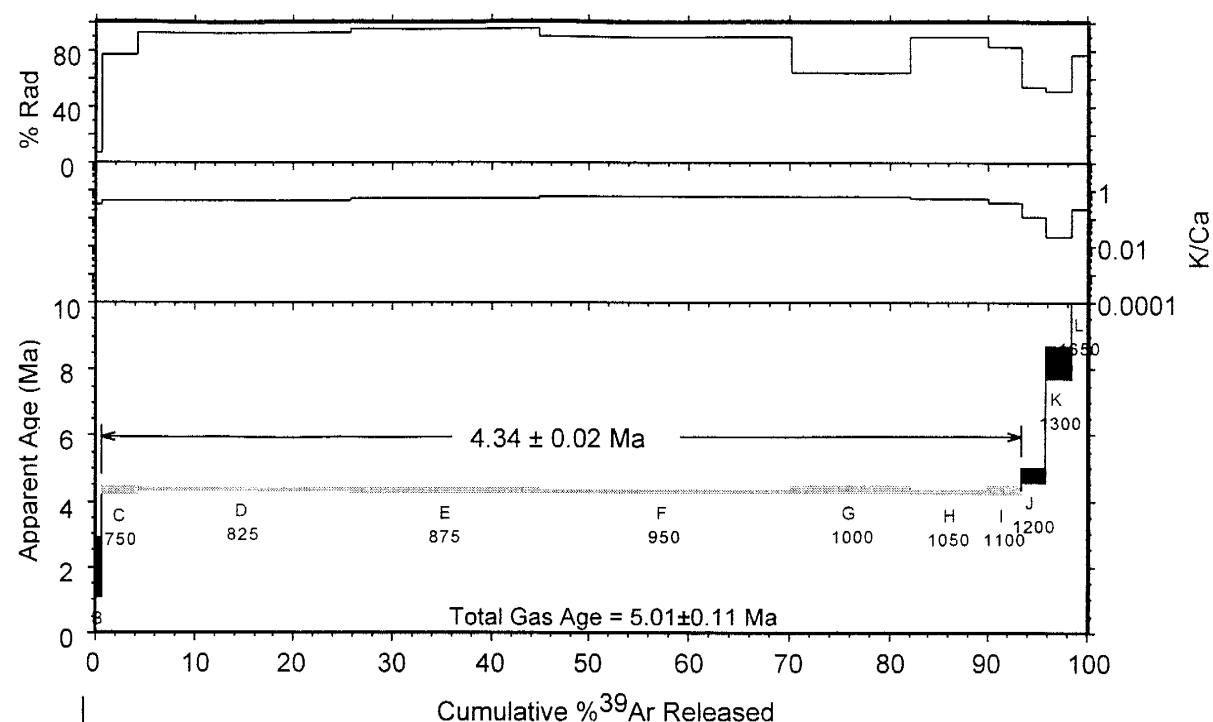
RA-115, pyroxene dacite, UCEM, groundmass concentrate



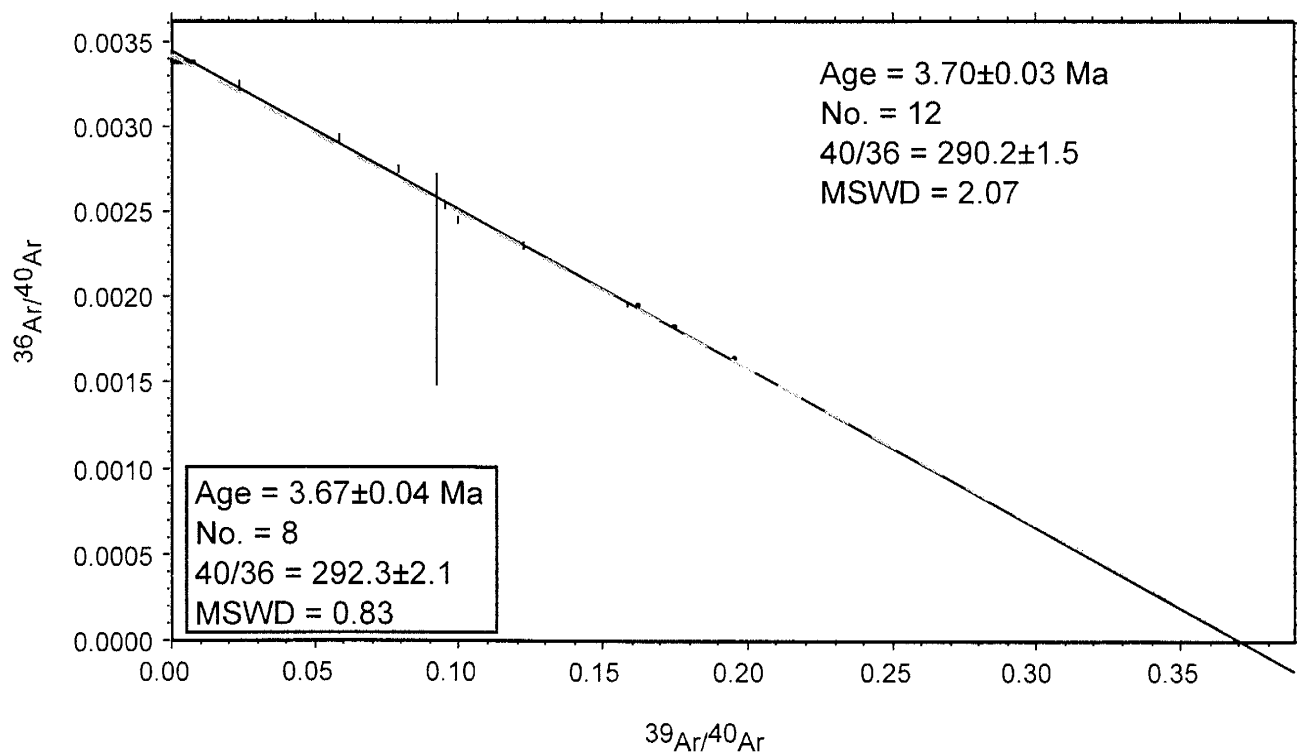
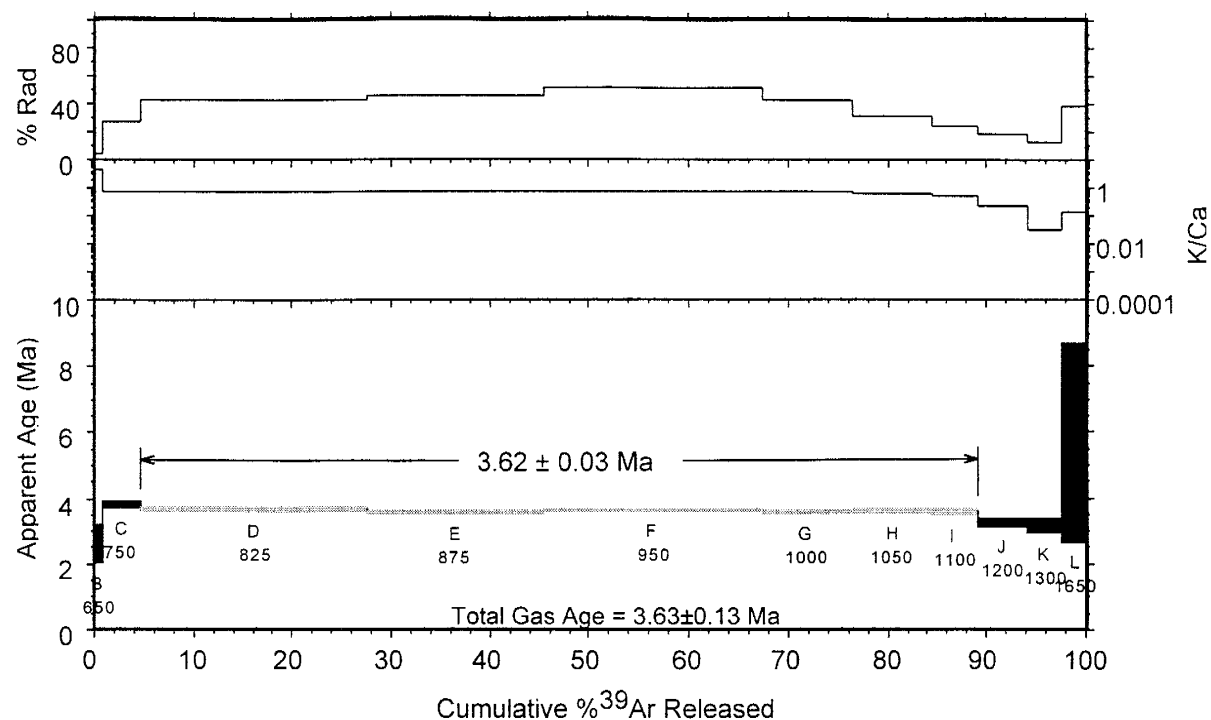
RA-116, Servilleta Basalt, NE of San Antonio Mt., groundmass concentrate



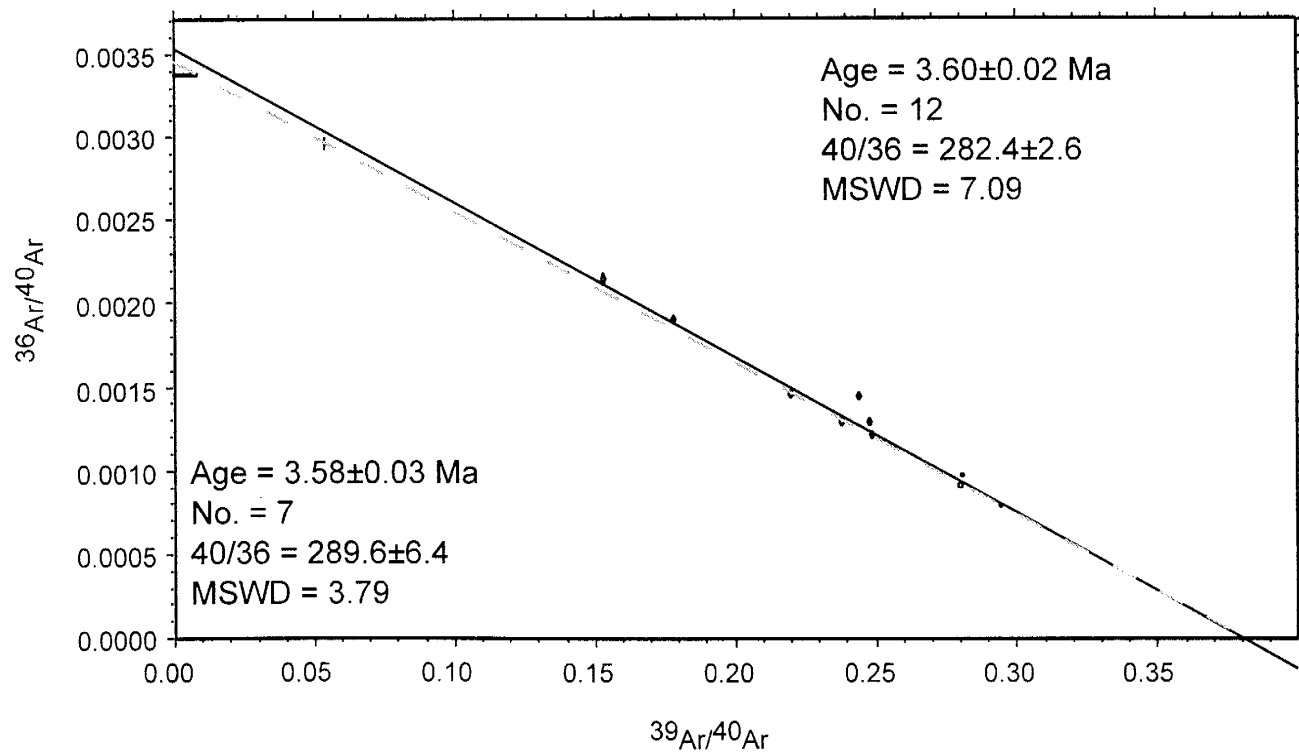
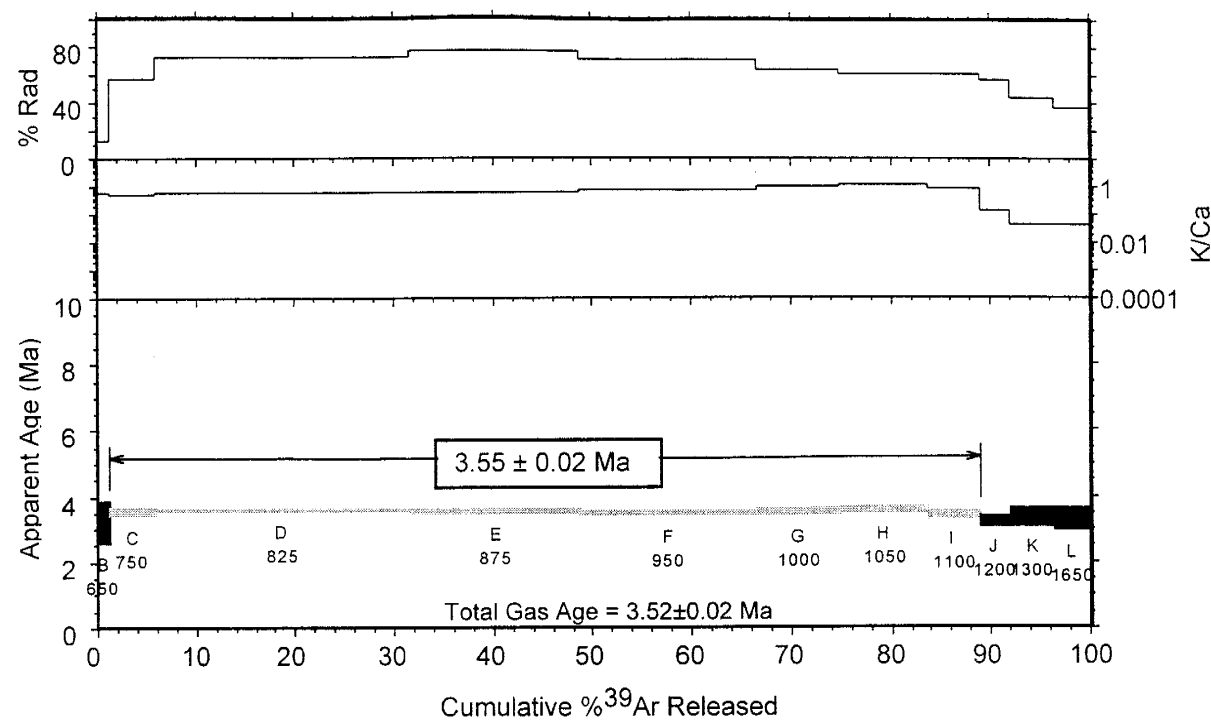
RA-117, Servilleta Basalt, Dunn Bridge, groundmass concentrate



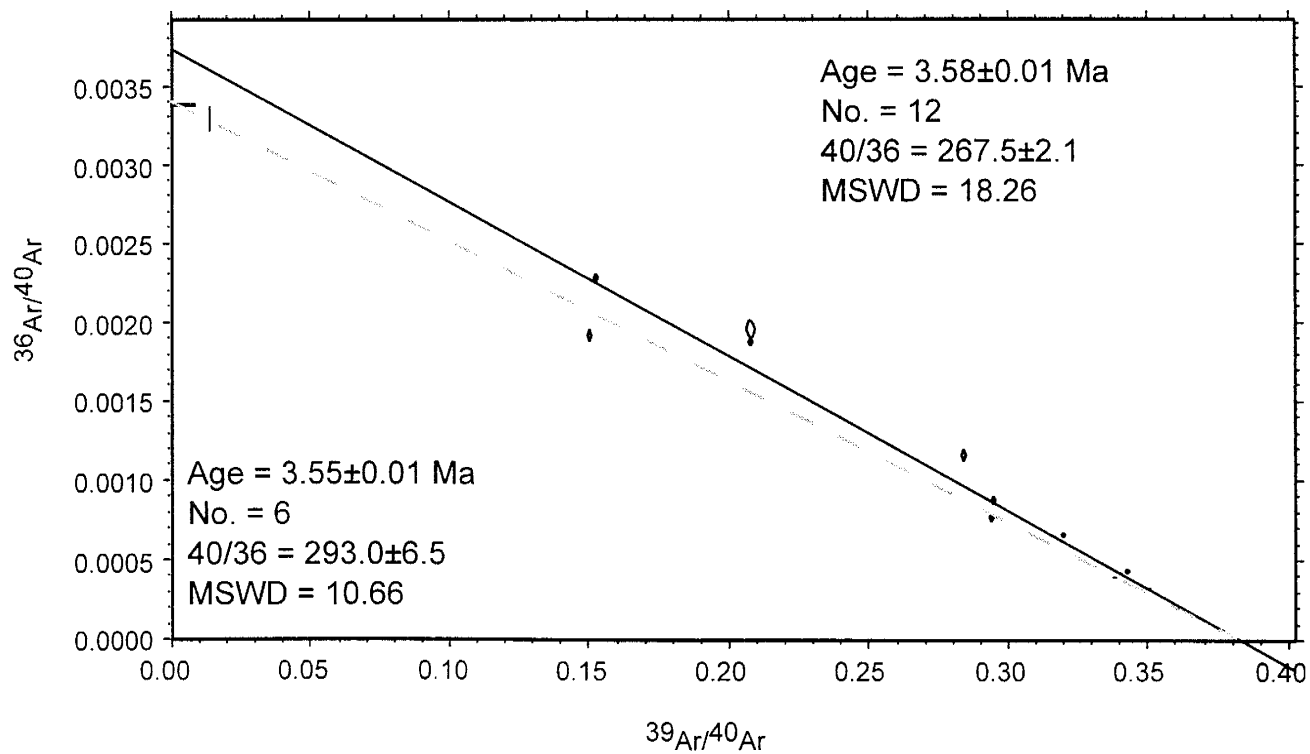
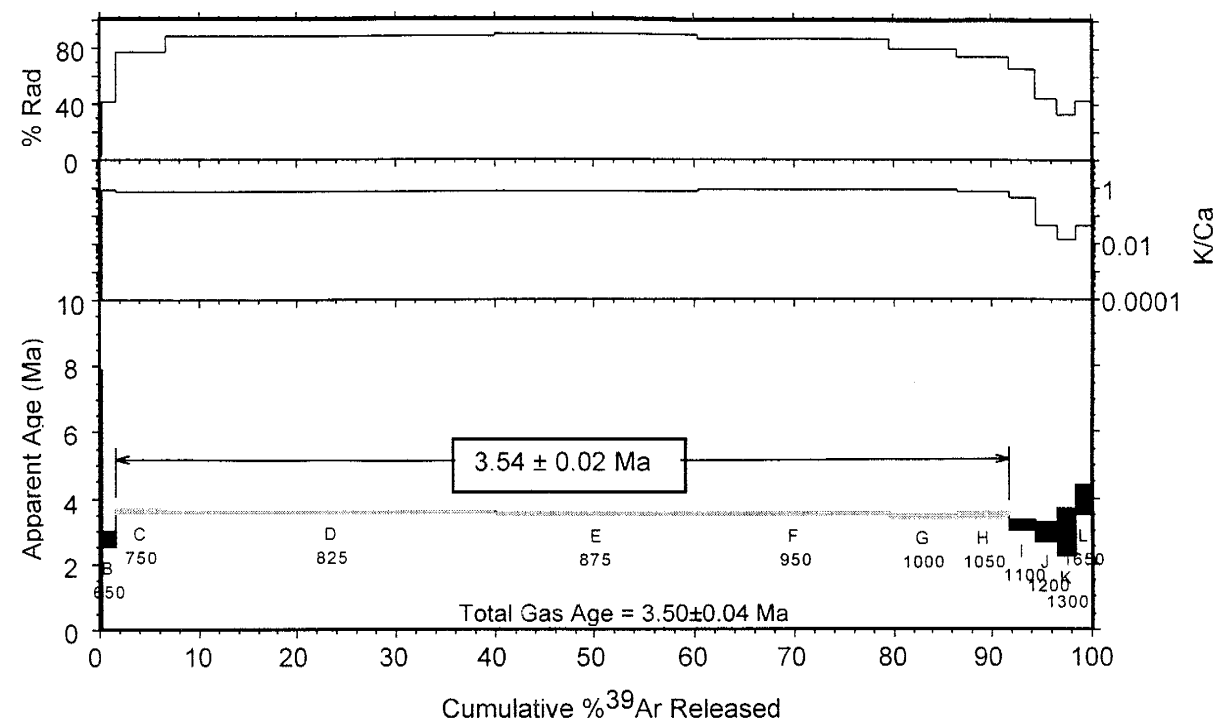
RA-118, Servilleta Basalt, Cerro del Aire area, groundmass concentrate



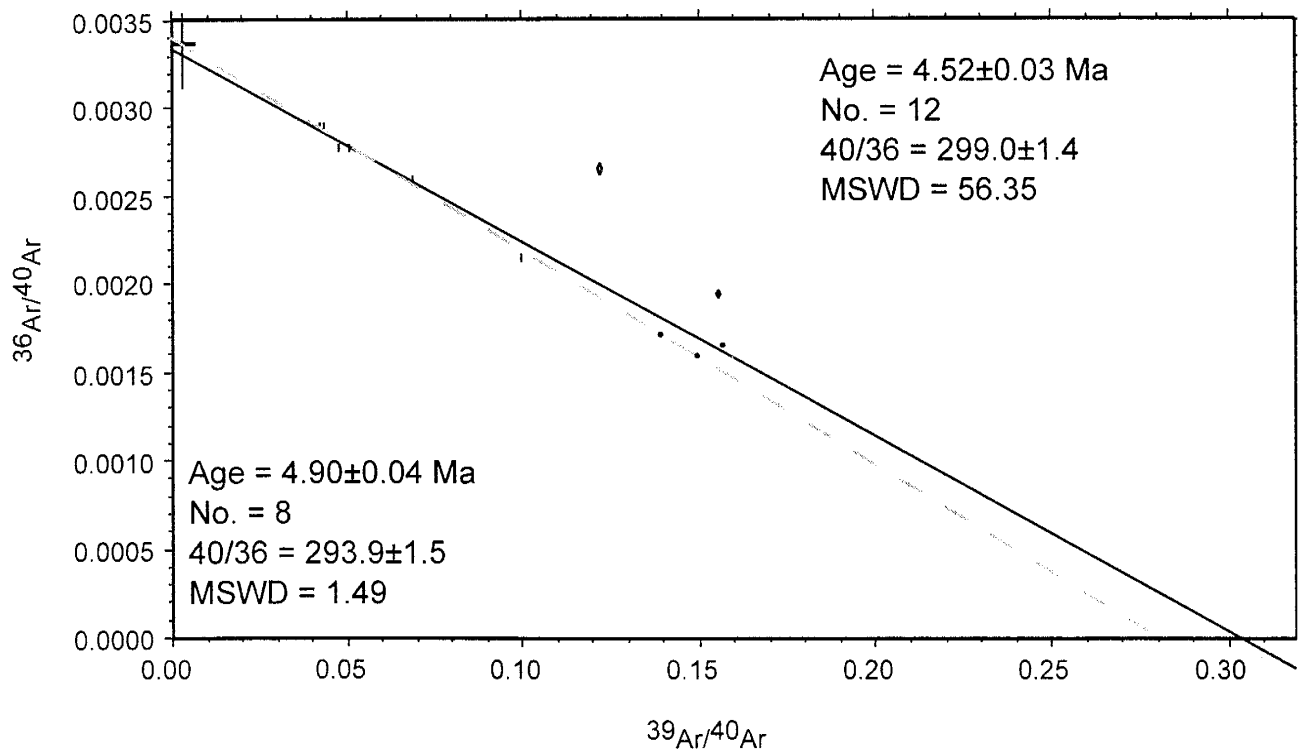
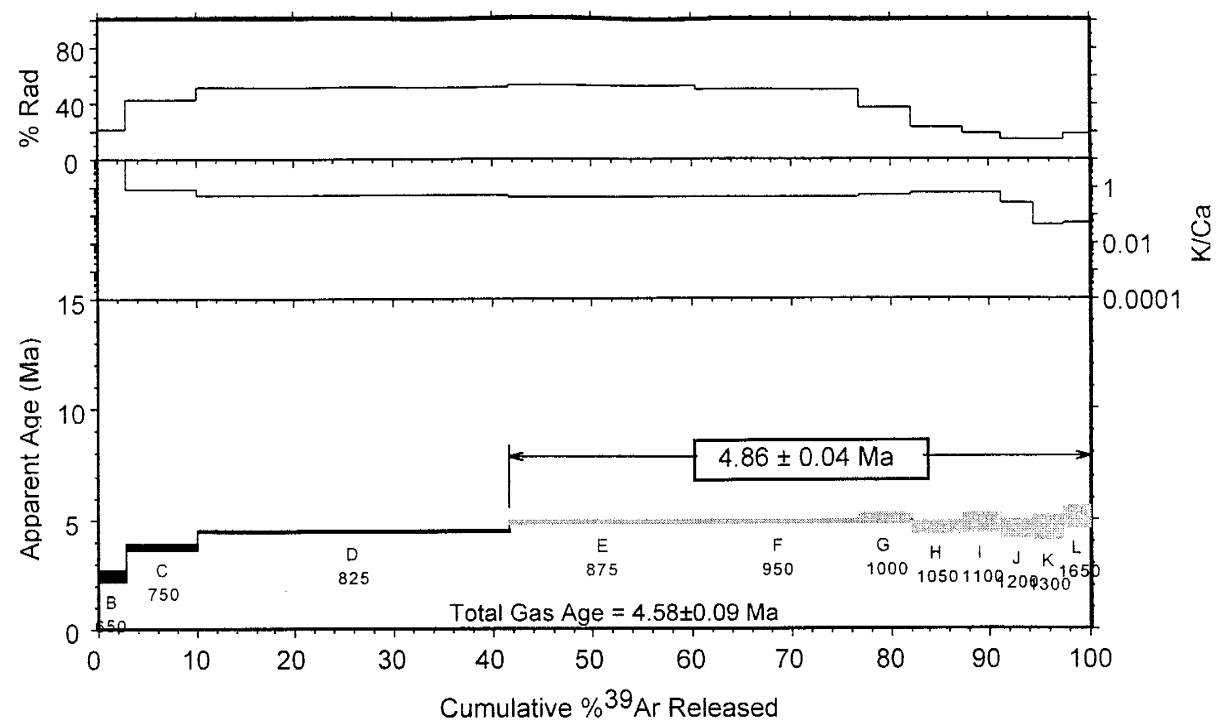
RA-119, Servilleta Basalt, Cerro del Aire area, groundmass concentrate



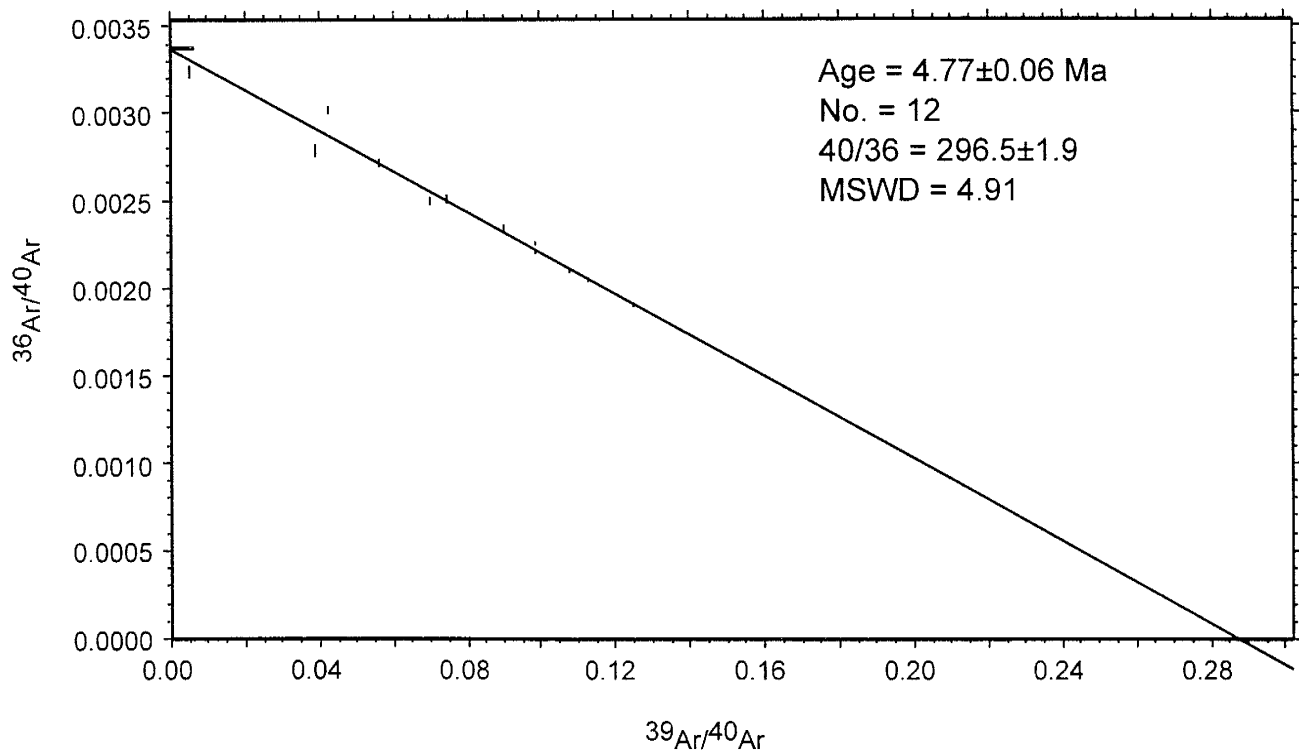
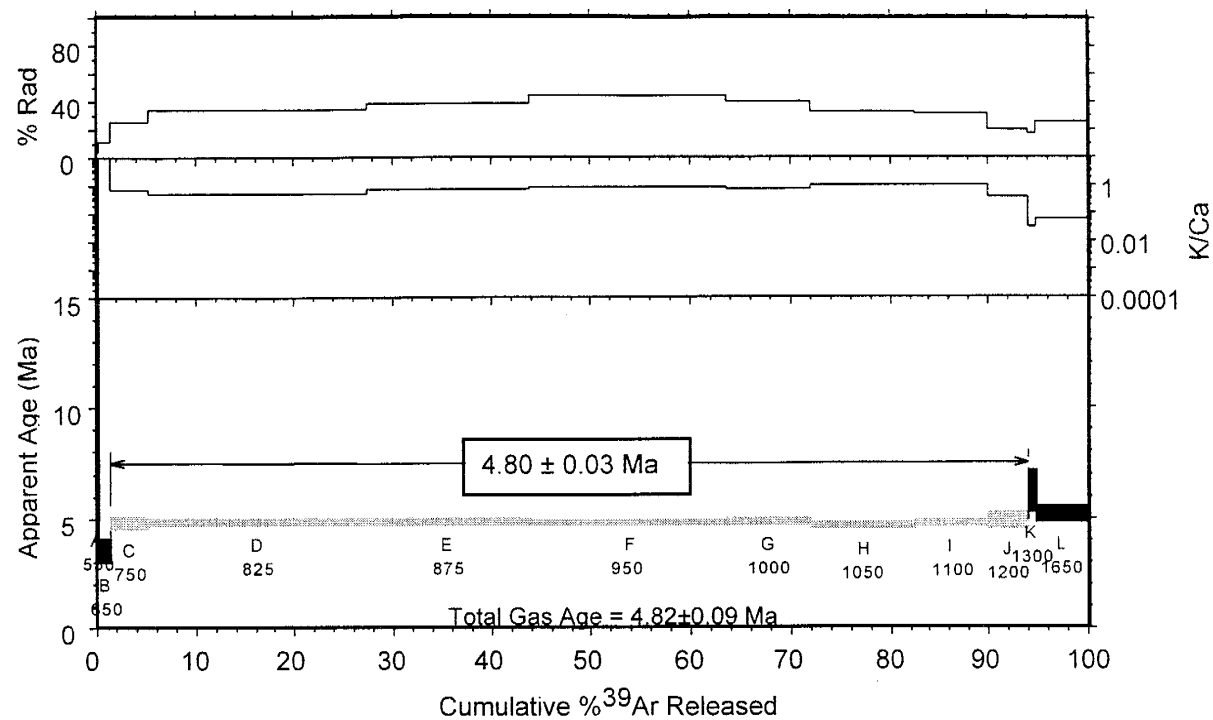
RA-120, Servilleta Basalt, Cerro del Aire area, groundmass concentrate



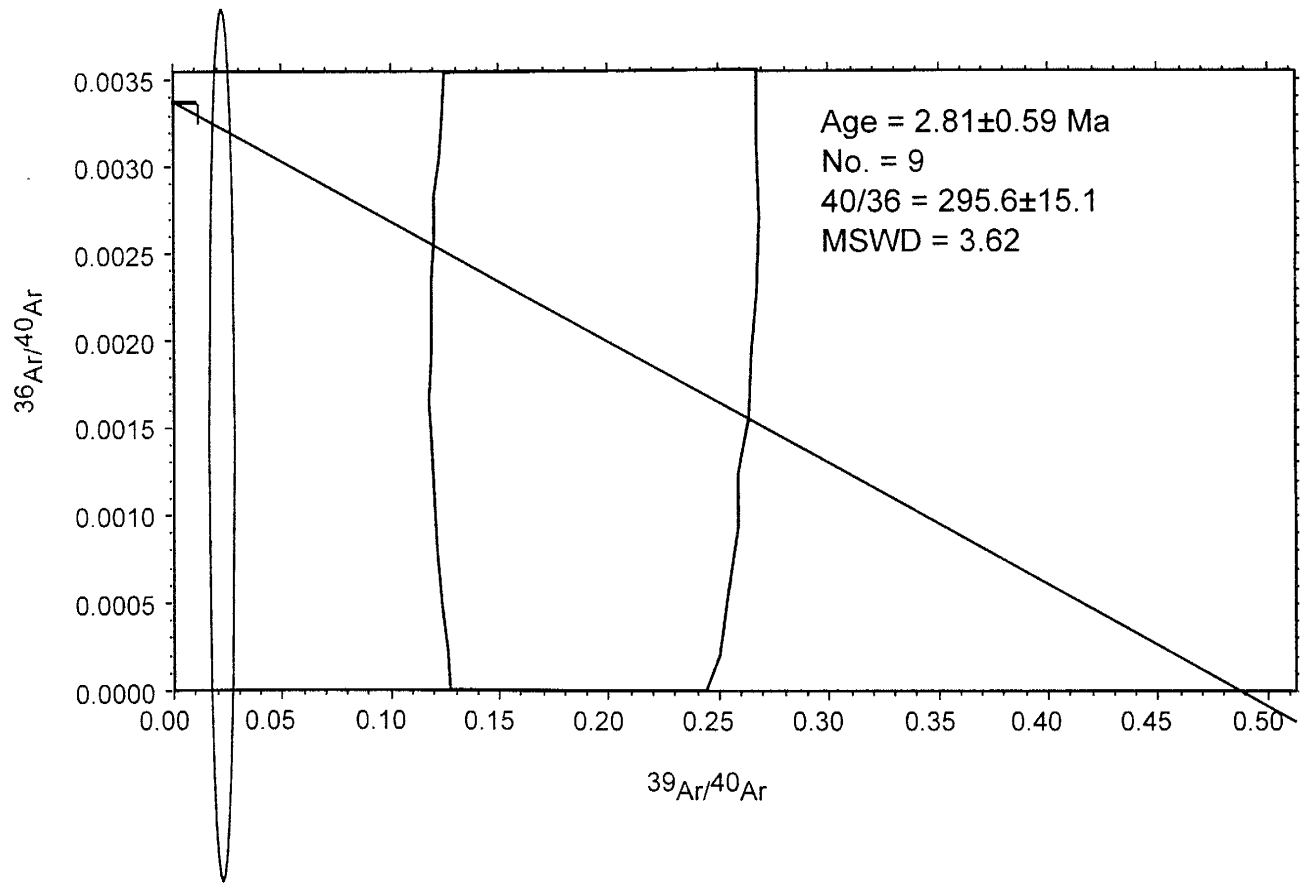
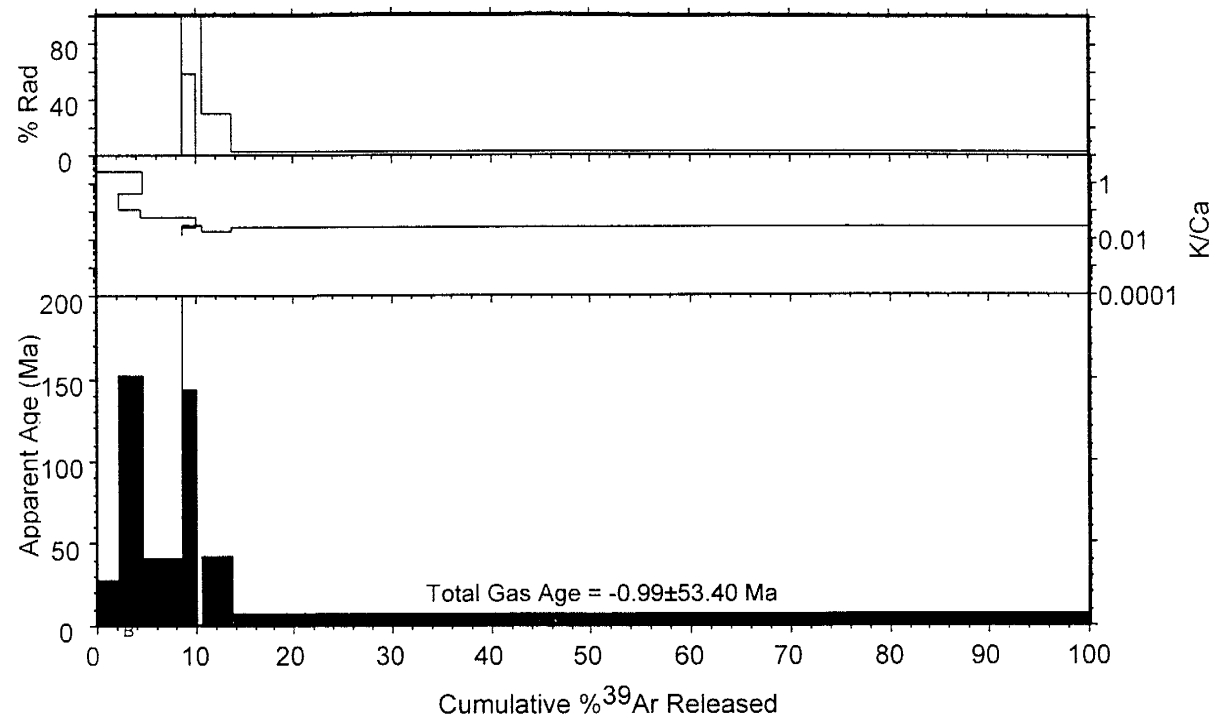
RA-121, olivine andesite, Cerros de los Taos, groundmass concentrate



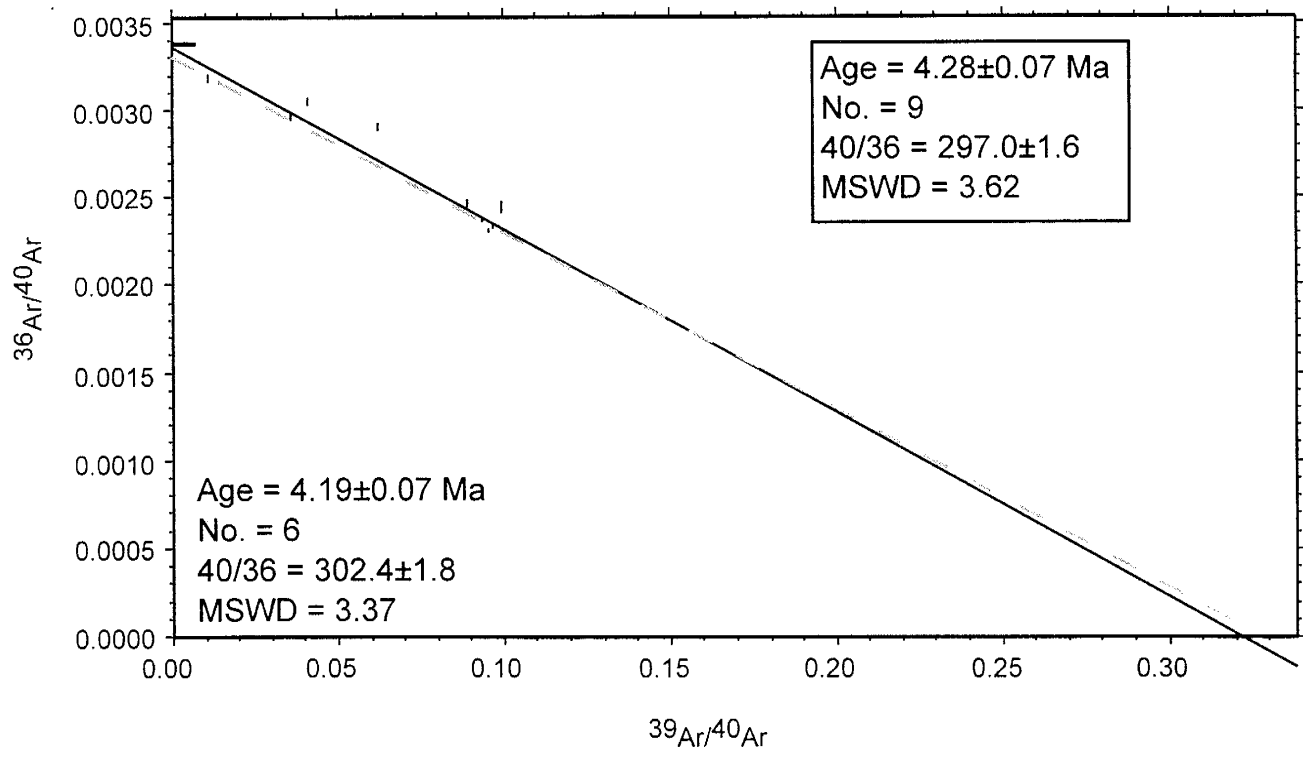
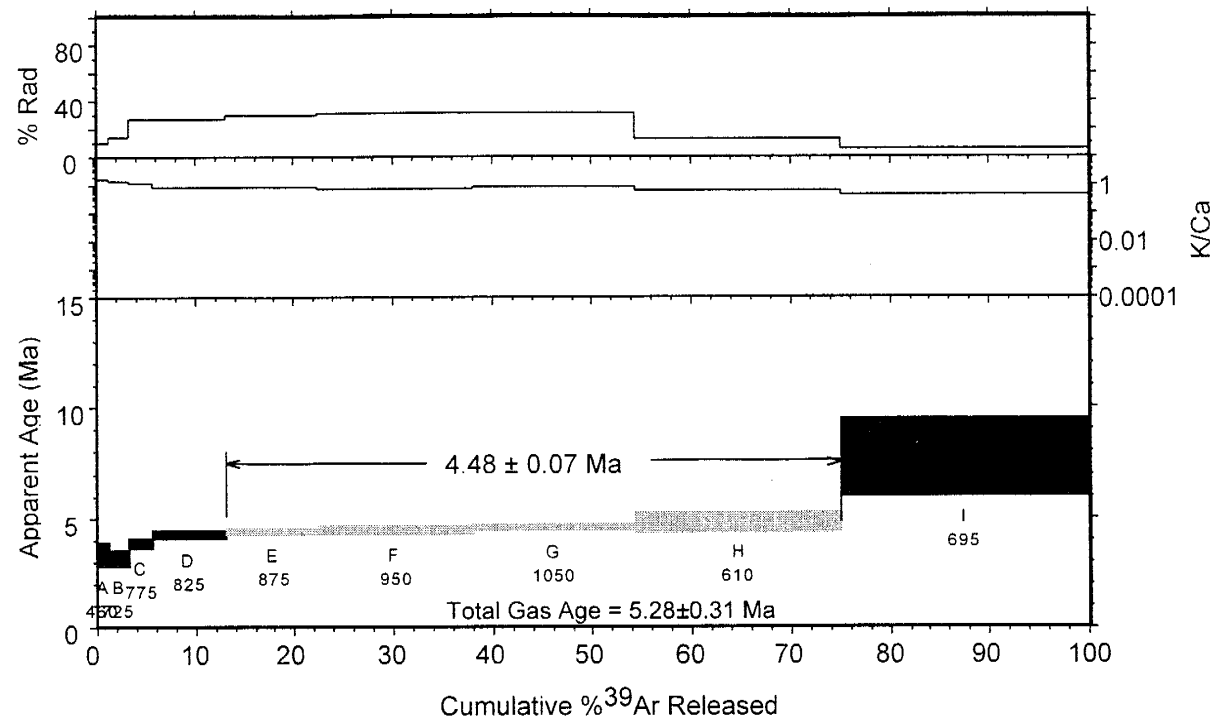
RA-122, olivine andesite, Cerro de los Taos, groundmass concentrate



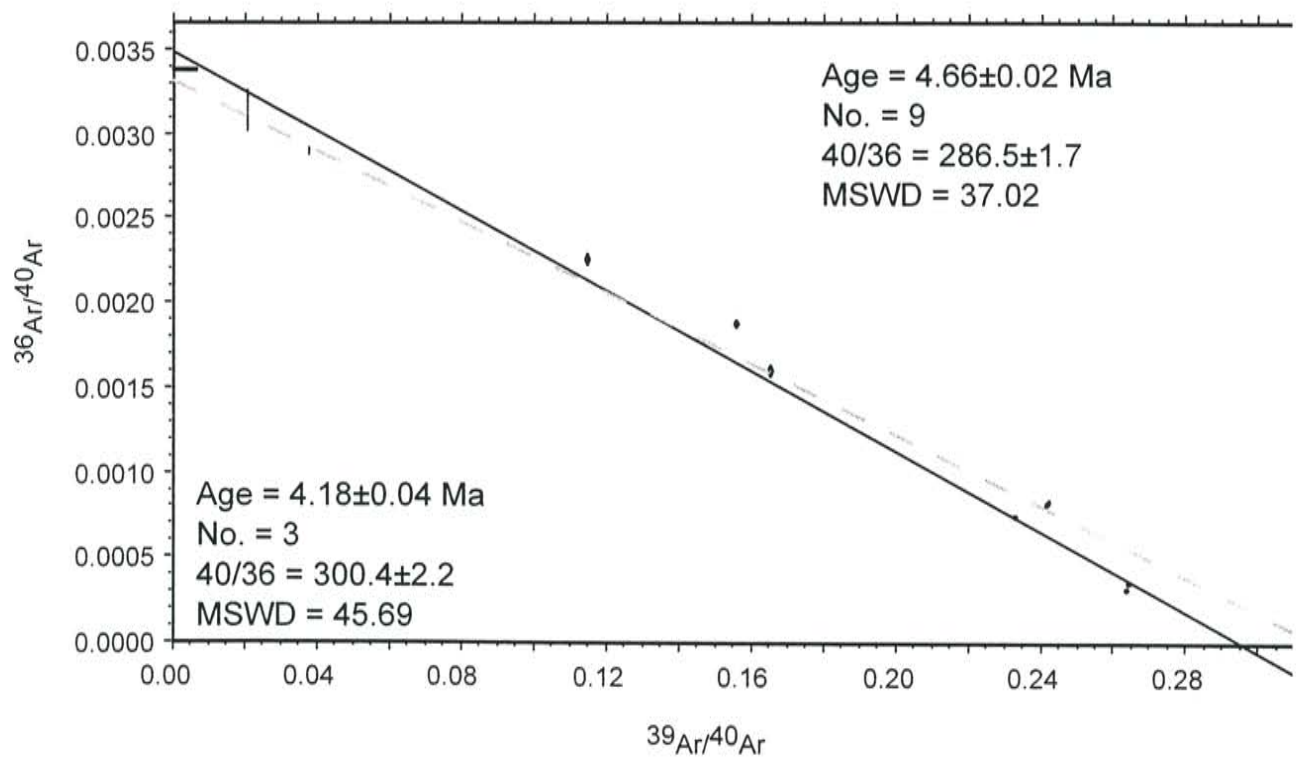
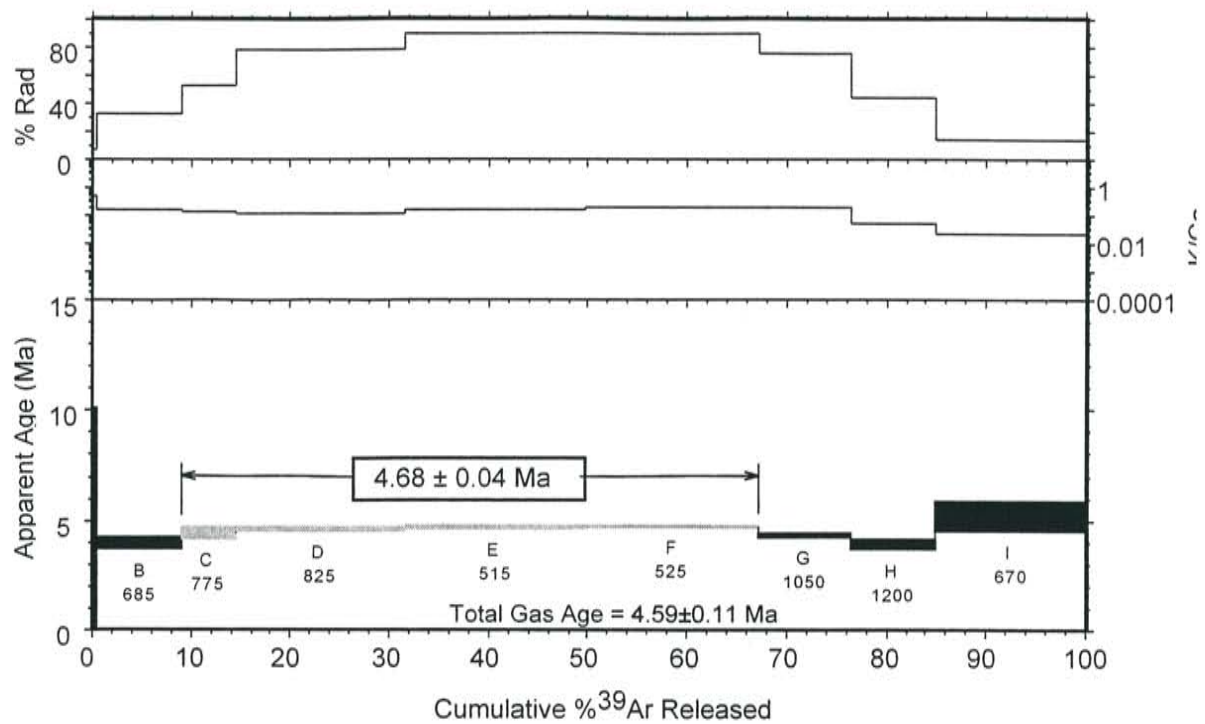
RA-123, olivine andesite, Cerro de los Taos, groundmass concentrate



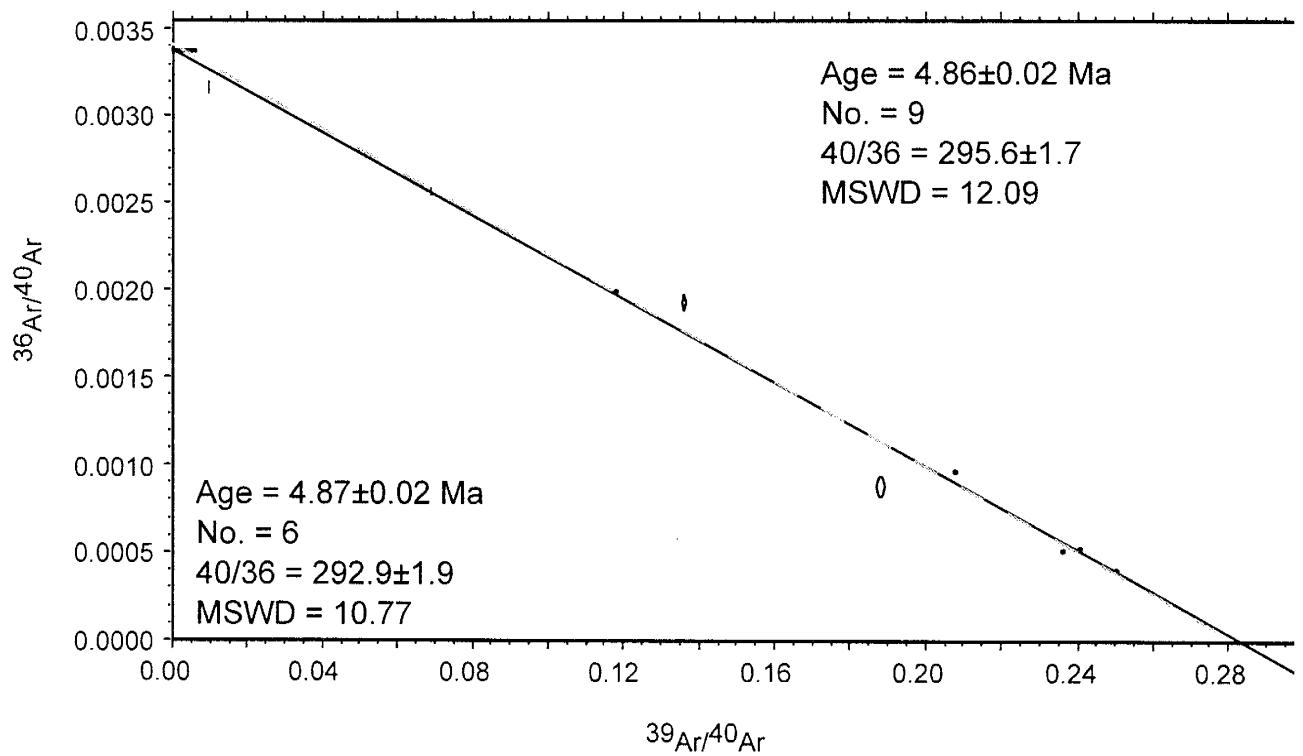
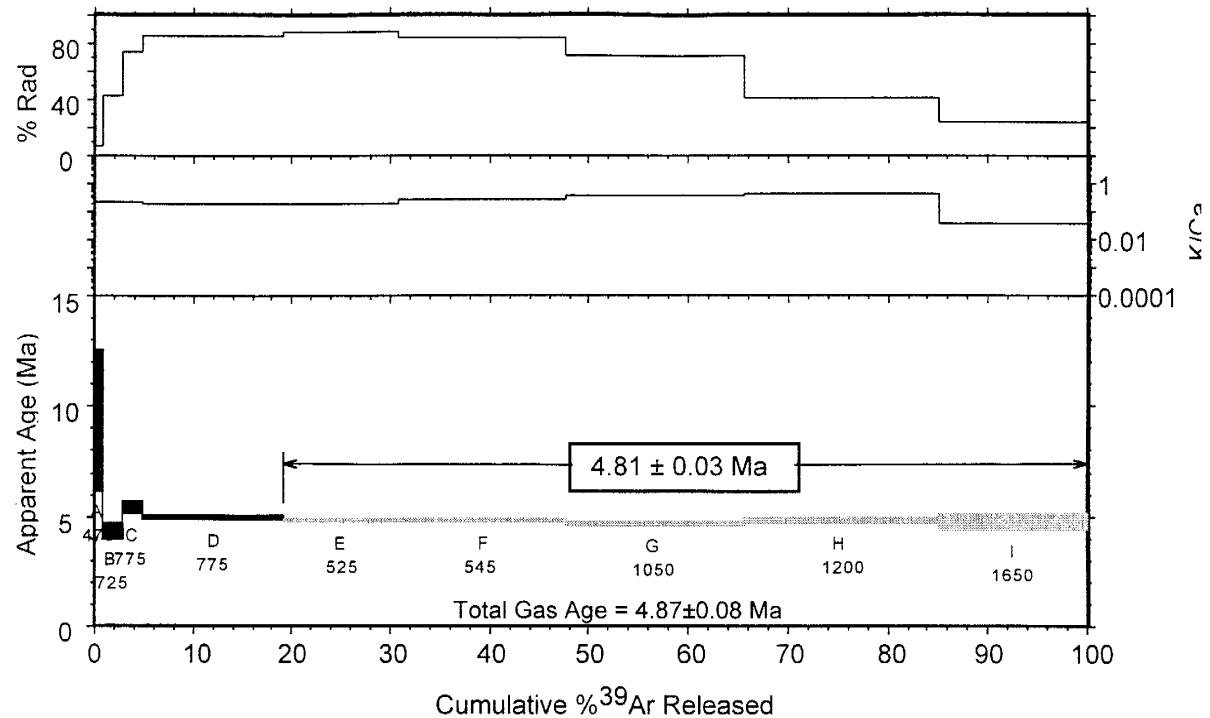
RA-128, pyroxene dacite, San Cristobol ranch, groundmass concentrate



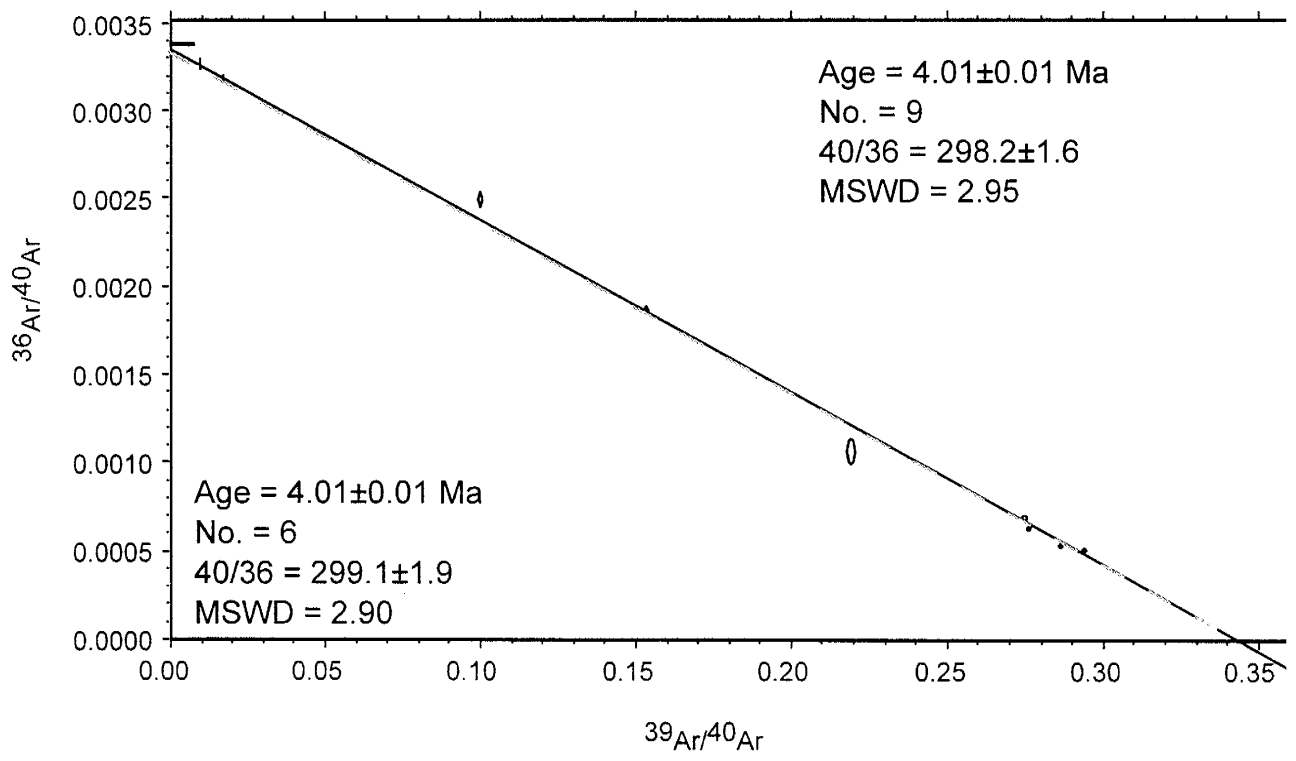
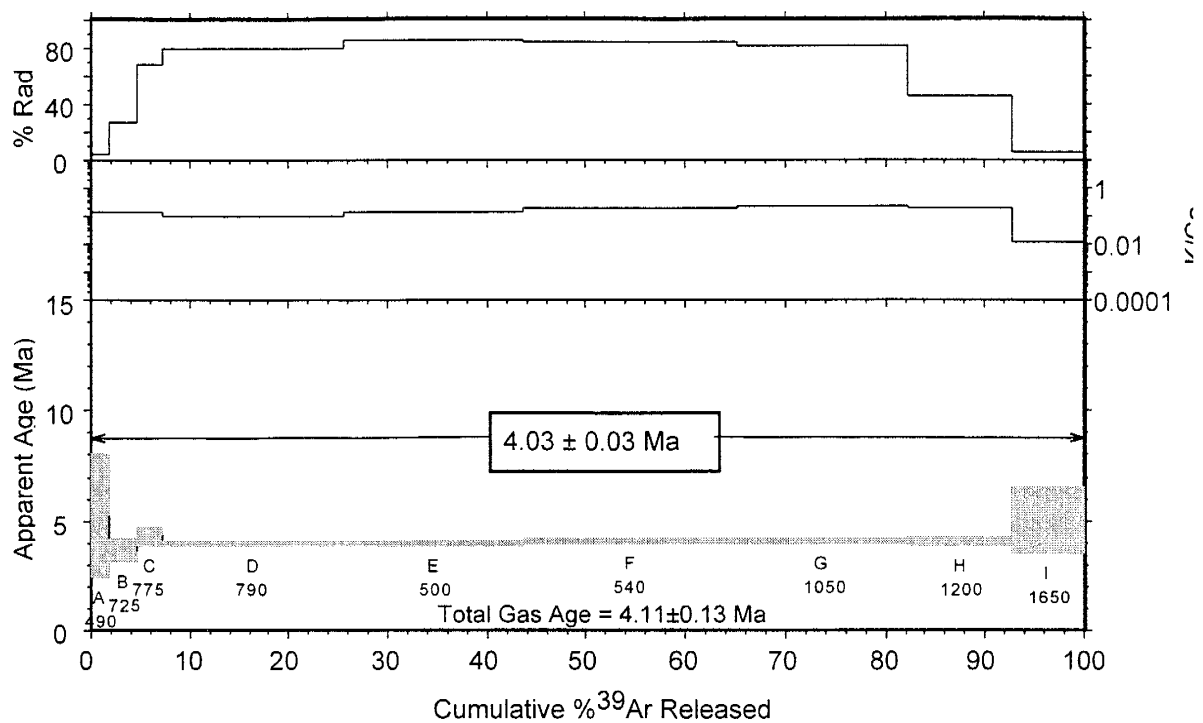
RA-129, Servilleta Basalt, Gorge bridge, groundmass concentrate



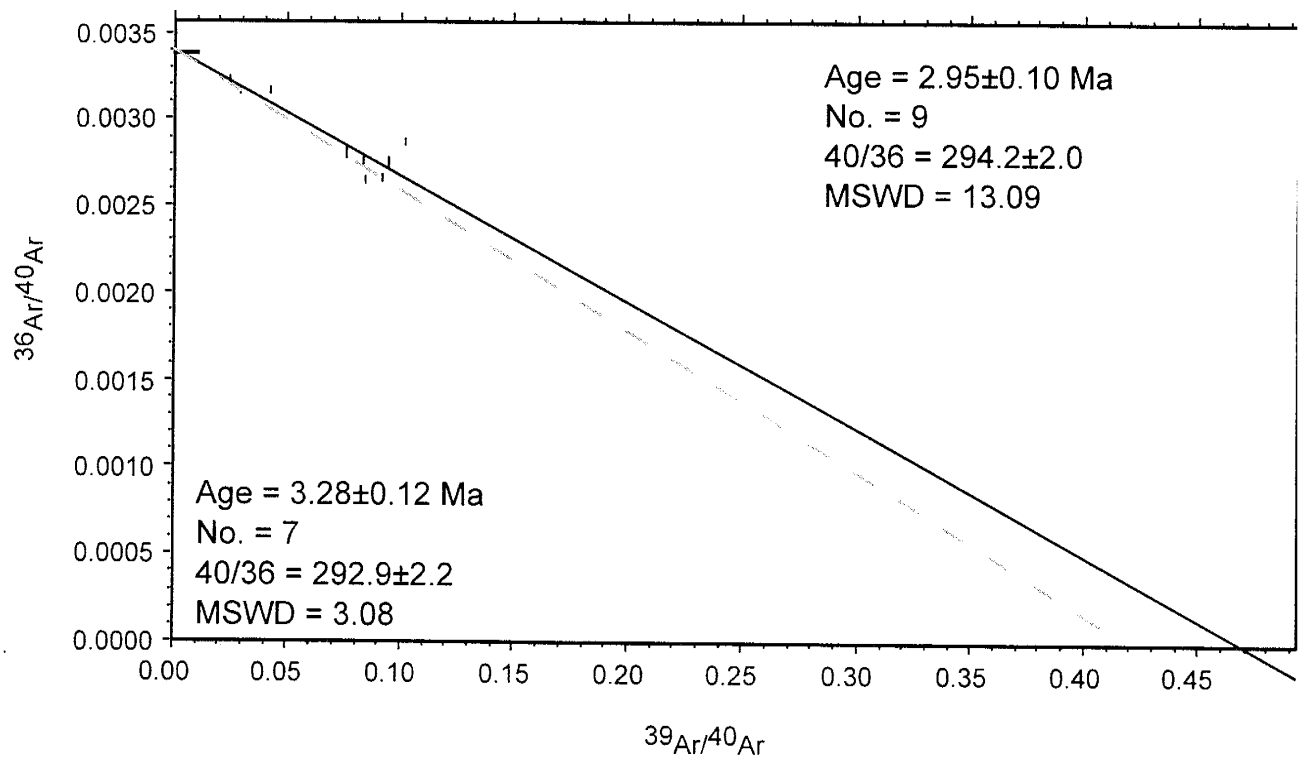
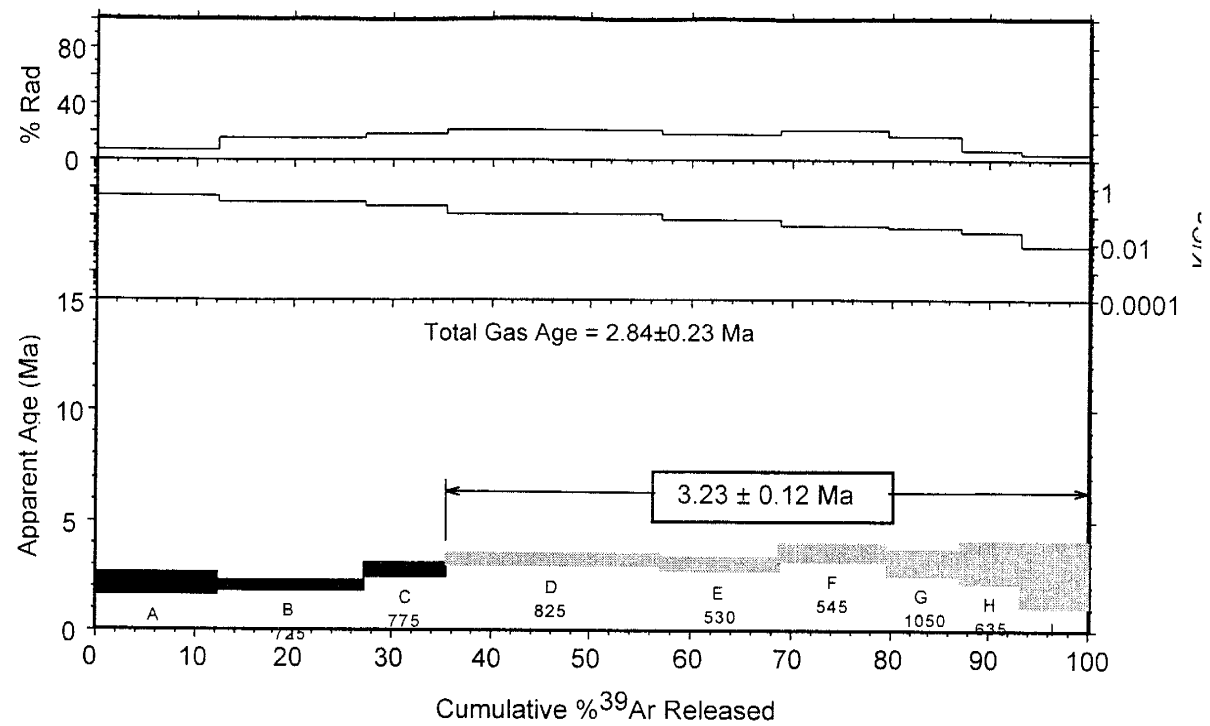
RA-131, Servilleta Basalt, Gorge bridge, groundmass concentrate



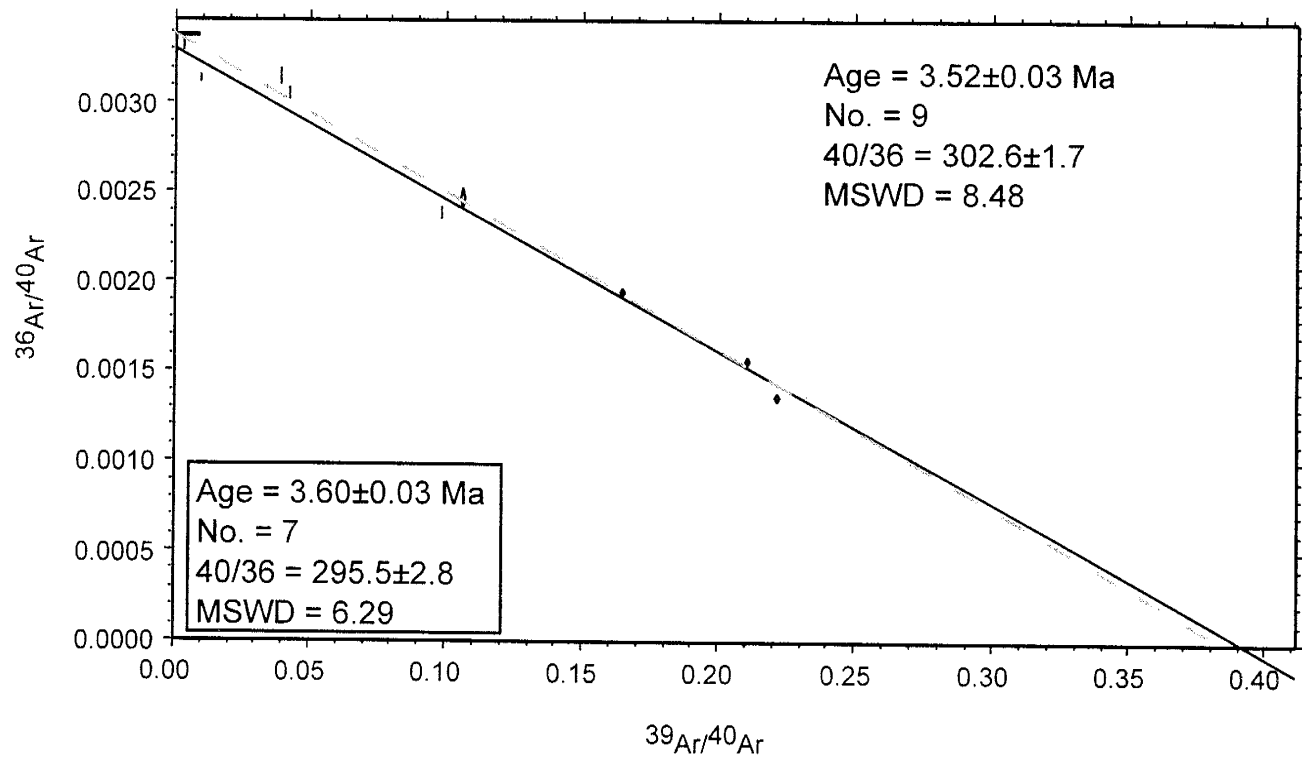
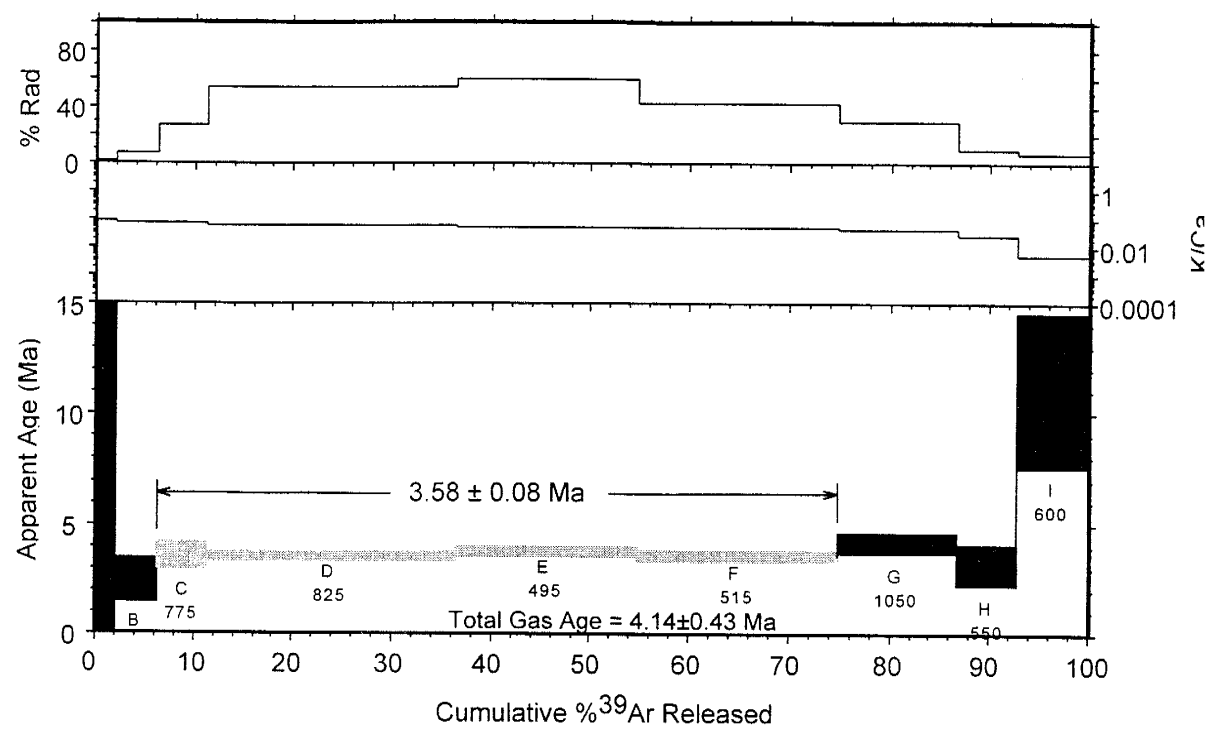
RA-132, Servilleta Basalt, Gorge bridge, groundmass concentrate



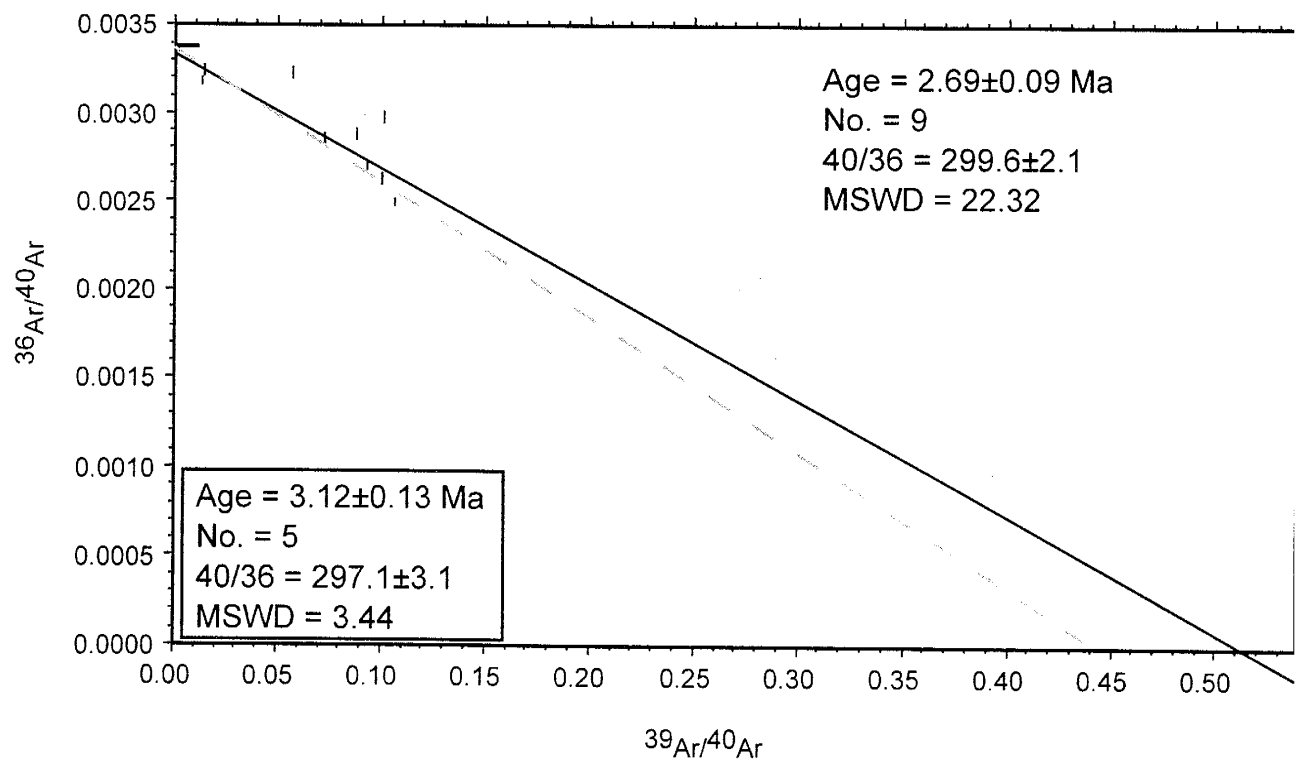
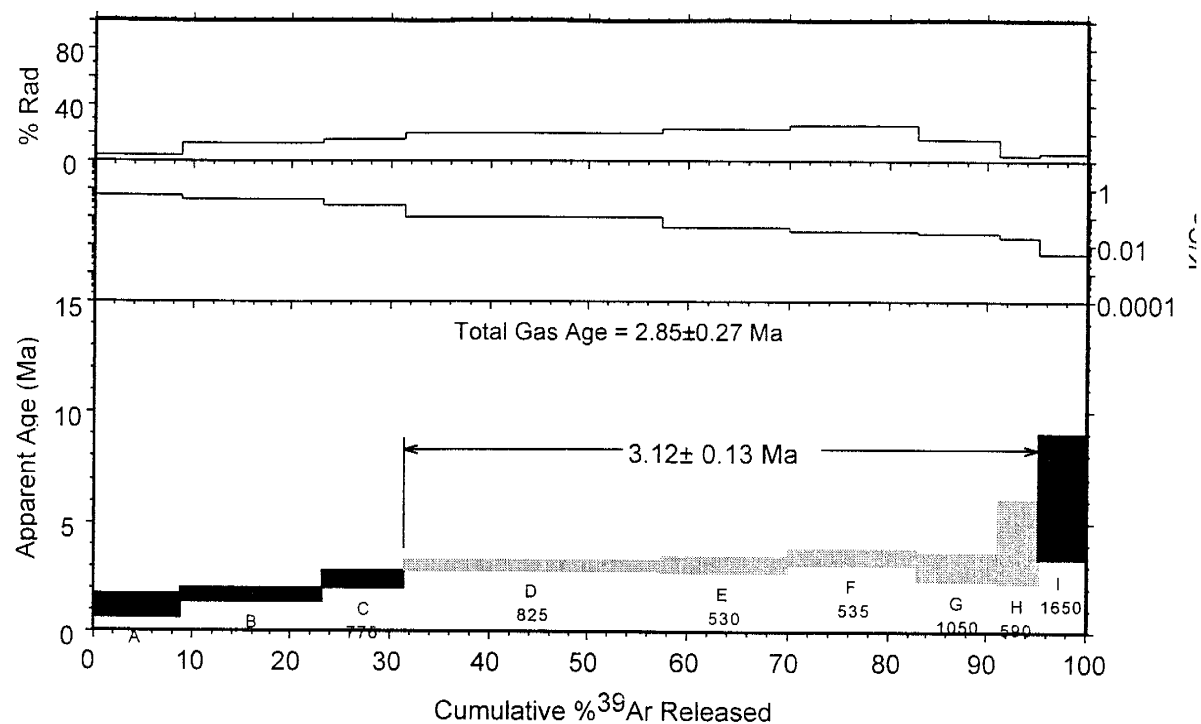
RA-133, Servilleta Basalt, Gorge bridge, groundmass concentrate



RA-135, Servilleta Basalt, Gorge Bridge, groundmass concentrate



RA-136, Servilleta Basalt, Gorge bridge, groundmass concentrate



This thesis is accepted on behalf of the faculty

of the institute by the following committee:

William C. McRae
Advisor

Philip R. Kyle
Charles E. Chapman

1/27/98

Date